KJPS Al-Kitab Journal for Pure Science
Vol.2 (2), ISSN: 2617-1260 (print), 2617-8141(online)
www.kjps.isnra.org

DOI: http://10.32441/kjps.02.02.p1

Cenomanian-Early Campanian Carbonate Reservoir Rocks of Northwestern Iraq: Diagenesis and Porosity Development

Mohamed A. Al-Haj[1], Ali I. Al-Juboury[1], Aboosh H. Al-Hadidy[2], Dalia K. Hassan[3]

[1]Department of Geology, College of Science, Mosul University, Mosul, Iraq

[2]North Oil Company, Kirkuk, Iraq

[3]Petroleum Engineering Department, Al-Kitab University, Kirkuk

alialjubory@yahoo.com, dalia.kamran9@gmail.com, dr_aboosh_hadid@yahoo.com, malhaj2006@yahoo.com

ABSTRACT

The present work focuses on the upper Cretaceous (Cenomanian-early Campanian) carbonate successions in selected wells from northwestern Iraq. These successions are represented by Gir Bir (Cenomanian-early Turonian), Wajna (late Santonian) and Mushorah (early Campanian) Formations. The succession has affected by early burial near-surface, unconformity-related and deep burial diagenesis represented by cementation, neomorphism, dolomitization, dedolomitization, silicification, authigenesis of glauconite and pyrite, compaction, micritization, solution and porosity formation. The common porosity types are intergranular, fenestral, intercrystalline, moldic, vuggy, channel and fracture. Three porosity zones (I, II, and III) are identified depending on variation in gamma ray which reflects their shale content. The upper part of zone (II) is highly porous and regarded on the main reservoir unit in the middle and upper parts of the Gir Bir Formation. Fracture and moldic and vuggy dissolution features in addition to karstic and fissure features are responsible for the porosity increase in the fractured reservoir unit.

Keywords: Carbonate Reservoir, Porosity, Diagenesis, Upper Cretaceous, Iraq.

KJPS Al-Kitab Journal for Pure Science
Vol.2 (2), ISSN: 2617-1260 (print), 2617-8141(online)
www.kjps.isnra.org

الصخور المكمنية الجيرية (السينوماني–الكامباني المبكر) في شمال غرب العراق: العمليات التحويرية وتطور المسامية

محمد احمد الحاج[1]، علي إسماعيل الجبوري[1]، عبوش حسين الحديدي[2]، داليا كامران حسن[3]
[1] قسم علوم الأرض، جامعة الموصل [2] شركة نفط الشمال، كركوك [3]قسم هندسة النفط، جامعة الكتاب، كركوك
alialjubory@yahoo.com, dalia.kamran9@gmail.com dr_aboosh_hadid@yahoo.com
malhaj2006@yahoo.com

الملخص

يتركز البحث الحالي على دراسة التعاقبات الجيرية بعمر الكريتاسي العلوي (السينوماني–الكامباني المبكر) في ابار مختارة من شمالي غرب العراق. تتمثل التعاقبات بالتكاوين جير بير (السينوماني–التوروني المبكر)، وجنة (السنتوني المتأخر) ومشورة (الكامباني المبكر). تأثرت التعاقبات قيد الدراسة بالعديد من العمليات التحويرية من قرب السطح والدفن الضحل والفن العميق متمثلة بالسمنتة والتشكل الجديد والدلمتة والديدلمتة والسلكتة والنشوء الموضعي للكلوكونايت والبايرايت. أنواع المسامية هي بين الحبيبات واللوزية وبين البلورية والقالبية والفجوية ومسامية المكسر. انطقة المسامية والتي تم تشخيصها بناءا على التغير في اشعه كاما والتي تعكس المحتوى الطيني هي (I,II.III). الجزء العلوي من النطاق المسامي (II) هو عالي المسامية ويعد المكمن الرئيسي في الجزئين الوسطي والعلوي من تكزين الجير بير وان مسامية المكسر والقالبية والفجوية هي من أهم مظاهر الاذابة في هذا التكوين فضلا عن ظواهر التشقق والكارست والمسؤوله عن زيادة المسامية في هذه الوحدة المكمنية.

الكلمات الدالة: المكمن الكاربوناتي، المسامية، العمليات التحويرية، الكريتاس يالعلوي، العراق.

1. Introduction

The Mesozoic carbonate system of the Arabian Plate is one of richest hydrocarbon provinces of the world. This is mostly due to combination of their large-scale dimensions and the presence of source and seal rocks within the same depositional system [1].

Iraq's largest hydrocarbon reserves are hosted in the Cretaceous sediments, particularly in the Mesopotamian Basin [2]. The Cretaceous succession in Iraq is up to 3000 m thick [3] and comprises megasequences AP8 and AP9 of Sharland et al., 2001, [4]

The Cretaceous succession has been extensively studied because it contains abundant reservoir intervals. It is the most productive interval in Iraq and contains about 80% of the country's oil reserves [2].

The present work focuses on the upper Cretaceous (Cenomanian-early Campanian) successions in selected wells from northwestern Iraq. These successions are represented by Gir Bir (Cenomanian-early Turonian), Wajna (late Santonian) and Mushorah (early Campanian) formations. Carbonate rocks of the Gir Bir Formation are represented by limestones (mostly recrystalized), marly limestone and fractured dolomite. Limestones (locally silicified), thinly laminated dolomite with occasional anhydrite nodules and fractured limestones form the main lithology of the Wajna Formation. Whereas, Limestone and marly limestone dominate the lithology of the Mushorah Formation. The Mushorah carbonates are based on conglomerate and brecciate bed, poorly sorted with subrounded-subangular rock fragments in a green marl matrix.

Several microfacies were distinguished in each formation, they were grouped into facies belts and the depositional environment were identified [5]. The Gir Bir carbonates were deposited in outer shelf, slope/shoal, rudist build-ups, back-reef/shoal and protected lagoons in a regressive shallowing upward sequence. Shallow marine environment with facies belts; supratidal, protected lagoons and outer lagoonal (shoal) are distinguished for the Wajna

KJPS Al-Kitab Journal for Pure Science
Vol.2 (2), ISSN: 2617-1260 (print), 2617-8141(online)
www.kjps.isnra.org

rocks. The succession of the Mushorah Formation is considered to be deposited in a relatively deep marine environments ranging from outer shelf to upper bathyal [5].

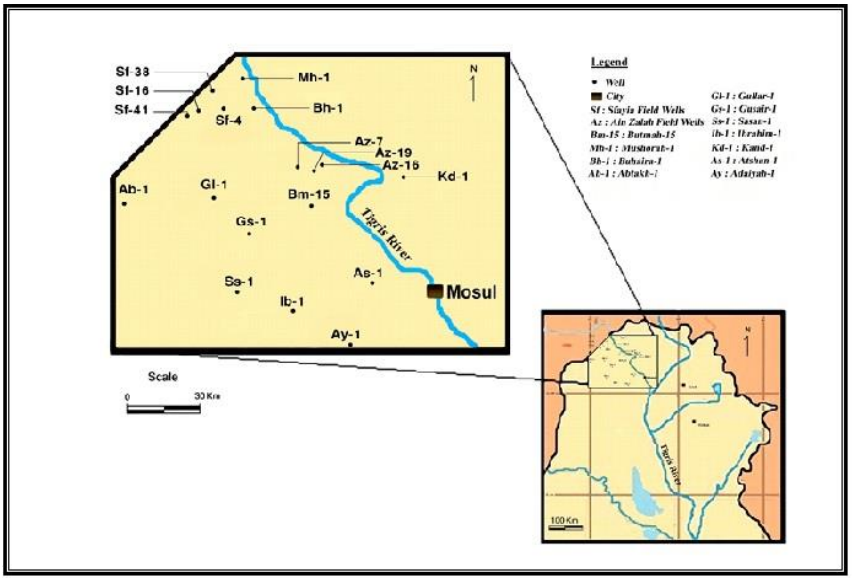

Fig. 1 Location map showing the studied wells from northwestern Iraq

The correlative rock successions in the north and eastern parts of Iraq were studied by Haddad and Ameen (2007), [6] who concluded that the Gulneri, Kometan and Mushorah formations (mid-Turonian- early Campanian) have been deposited in a flat-topped ramp that formed because of extensional tectonism.

The present work is conducted on several wells from northwestern (Figure 1) aiming to investigate the linking between diagenesis and porosity evolution of the studied formations.

2. Geologic Setting

The paleolatitudinal location of the Arabian Plate influenced Cretaceous stratigraphy in Iraq. Progressive northward drift placed the Arabian plate in equatorial tropical latitudes [7]. Carbonates rocks forming the main lithologies in the Cretaceous successions of Iraq and most of the Middle East region due to prevalence of warm equatorial climates [8].

KJPS Al-Kitab Journal for Pure Science
Vol.2 (2), ISSN: 2617-1260 (print), 2617-8141(online)
www.kjps.isnra.org

The upper Cretaceous successions in northwestern part of Iraq have been affected by several phases of tectonic movements [9], therefore, they are not completely documented from this part of the country. The study area was a part of the shelf during Cenomanian- early

Turonian and was separated from the main basin by the Mosul and Khleisia uplifts [10]. Prevailed warm and equatorial conditions on the Arabian Plate [11] promote the deposition of reefal and lagoonal facies of the Gir Bir Formation in the area. During Turonian- early Campanian, the area was still affected by uplifting with discontinuous and local subsidence that permit deposition of shallow lagoonal facies of the Wajna Formation. Transgression in the early Campanian led to deposition of shallow marine facies of the Mushorah Formation in the studied area.

According to Sharland et al. (2001), [4] , the studied formations present in two of the Arabian Plate Megasequences, Gir Bir Formation of the Cenomanian-early Turonian sequence which represents the upper part of the late Tithonian-early Turonian megasequence AP8 whereas, Wajna and Mushorah formations exist in the late Turonian-early Campanian sequence that represents the lower part of late Turonian-Danian AP9 megasequence. The studied formations and their correlative succession in other parts of Iraq and neighboring countries is illustrated in Figure (2).

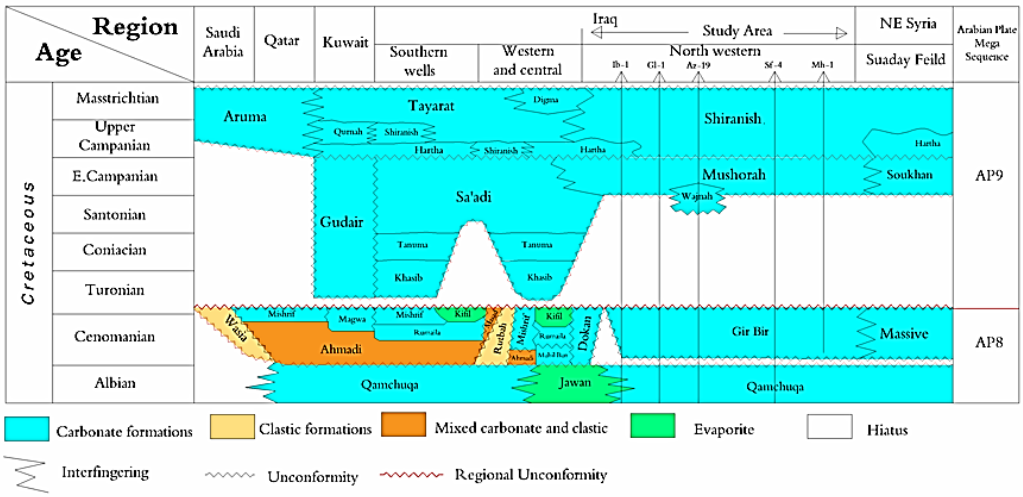

Fig. 2 Stratigraphic correlation of the studied formations within Iraq and some of the neighboring countries (modified from Al-Naqib, 1967), [12]

3. Materials and Methods

60 samples from the three studied formations Gir Bir, Wajna and Mushorah were investigated. Petrographic study is carried out for identification of the main components of the studied lithologies and to distinguish the main diagenetic events. Scanning electron microscopy is conducted at Steinman Institute of Bonn University, Germany and the Earth Sciences Department, Royall Holloway, University of London, UK for selected samples.

Pore types are identified according to Choquette and Pray (1970), [13] classification that based on the texture of rock matrix, visible pore structure, and typical petrophysical behavior that would be associated with the rock. The ages of the studied formations was considered according to biostratigraphic works of [14, 15].

For the study of porosity evolution, the studied successions are divided according to shale volume (V-Sh; [16]) into three porosity zones (A, B and C). Primary, total and effective porosities are measured from FDC, CNL and BHC logs of the three selected wells.

4. Results

Petrographic component

The main components of the studied carbonate successions are represented by skeletal and non-skeletal grains, micritic groundmass, sparry calcite cement and various types of pores (discussed separately).

The skeletal grains of the Gir Bir Formation are dominated by benthic foraminifera (Miliolids, Alveolina, and Orbitolina) and rudist while the non-skeletal constituents are represented by pelloids and lithoclasts. In the Wajna Formation, ostracoda, benthic foraminifera (Miliolids and Glomospira) and pelloids are the main constituents. Whereas, calcispheres, planktonic and benthic foraminifera and Inoceramus form the main constituents of the Mushorah Formation.

These components are distributed in a micritic groundmass that is composed mostly of calcite in addition to clay minerals that are dominated by kaolinite, illite,

palygorskite and glauconite [5]. The micritic groundmass has been affected by dolomitization and recrystallization. The sparry calcite cement is dominated in most of the studied carbonates either as intergranular cement or as filling of voids and fractures

.*Diagenetic processes*

Carbonates of the studied formations have been affected by both early-and late-stage diagenesis. The observed diagenetic events can be divided into constructive (isochemical and allochemical constructive diagenesis) and destructive diagenesis (sensu Milliman, 1974), [17]

Isochemical constructive events (without modifications in chemical composition of the rocks) are represented by cementation and neomophism. Cementation has led to occlusion of primary porosity in carbonates. The following cement types were recognized; blocky, syntaxial rim, drusy mosaic, radiaxial fibrous, fibrous and granular filling inter-and intragranular pores and fractures (Figure 3 A-H). These cements are believed to be of later diagenetic origin, although the mosaic cement may have formed during two or more phases

.Neomorphism is the dominant diagenetic event affecting on the carbonate rocks of the Gir Bir and the upper parts of the Wajna formations, whereas, it is slightly affected on the Mushorah carbonates. This process is divided into recrystallization and inversion (Figure 3 I-K).

Allochemical constructive events (that show some modification in chemical composition of the rocks) are represented by dolomitization, dedolomitization, silicification and authigenesis. Aphanotopic, fine-grained dolomite rhombs, floating and contact rhombs, spotted, sieve and sutured Mosaic dolomite textures were recognized (Figure 4 A-F) according to classification of Randazzo and Zachos (1984), [18].

Dolomitization has slightly enhanced the reservoir quality particularly with the formation secondary intercrystalline micropores. Dedolomitization is observed in poikilotopic, composite calcite rhombs and rhombic pores textures (Figure 4 G). This event is commonly recorded in the Mushorah Formation. Silicification in the form of

chert nodules and beds are sporadically exists in the lower part of the Mushorah Formation and in distinctive zones in the Gir Bir and Wajna formations. The process is diminished in the highly dolomitized beds and near stylolites rich in organic matter (Figure 4 H).

The authigenic minerals in the studied carbonates include glauconite and pyrite. Galuconite is observed as green rounded grains (Figure 4 I) in the upper part of the Mushorah Formation near the contact with Shiranish and Hartha formations and rarely occur in the lower and middle part of the formation. Pyrite occurs in various forms in all the studied formations. It exists either in planktonic foraminifera chambers or in calcispheres or in the pores of the micritic groundmass of the Mushorah Formation. Pyrite also found as euhedral cubics or in stylolites or in mollusca fragments of the the Gir Bir and Wajna formations (Figure 4 J)

.Destructive events include; compaction, micritization, bioturbation, dissolution and porosity formation (discussed separately).

Compaction generally decreases porosity due to the heavy sedimentary cover (>1000 m thickness) which gave the orientation property in their internal structure of the sediments [19]. The compaction has indirect relationship with the original primary cementation. It occurs in the studied carbonates in mechanical and chemical compaction. Mechanical compaction is observed by breakage in inoceramus shells (Figure 4 K) whereas, chemical compaction is recorded from various types of pressure solution or stylolitic textures (Figure 4 L and 5 A- B). Pressure solution has resulted in the formation of dissolution surfaces, clay seams, and stylolites Organic material and other relatively insoluble particles (dolomite rhombs, early calcite-cemented grains, and clay particles) commonly occur on the stylolite surfaces, indicating a late-diagenetic origin.

Micritization is an early diagenetic process that occurs in marine phreatic environments [20], and skeletal grains were micritized shortly after deposition due to fungi action and micritic envelops construction. In the present study, it seen in the successions of the Gir Bir and Wajna formations. Bioturbation is distinguished in mottled textures due to boring activities that lead to accumulation of organic matters

and give darker color for the bioturbated zones. It is recorded in distinctive areas where dolomitization and pyritization dominate (Figure 4 J).

Dissolution is a more effective diagenetic process than cementation in most of the reservoir beds that improved the carbonates porosity. This process acts to destroy the internal structures for the skeletal grains, leaving the micritic envelope to form the moldic porosity, vuggy porosity or enlarging the presenting vugs to form cavern porosity or channel porosity, and sometimes, there are open space structures due to the effect of the selective dissolution. In the present work, dissolution is recorded as karst and fissures in the upper part of the Gir Bir Formation where conglomerate and breccias dominate or in different forms throughout the studied carbonates (Figure 5 C).

Porosity types

The following types of the porosities have been distinguished according to Choquette and Pray (1970), [13]

1. Solution enhanced inter-granular that form as a result of dissolution of the cement between carbonate grains and this pores is enlarged by dissolution processes and cementation between grains is further removed (Figure 5 D).
2. Fenestral porosity which is formed as a result of dissolution of evaporite grains and organic matter and is commonly distinguished in the middle part of the Wajna Formation (Figure 5E). The aforementioned porosity types are considered as primary porosity types that have insignificant contribution to overall porosity.

The following types of porosity are considered as secondary porosities with most significant contributors to overall pore volume in the studied carbonates .

3. Intercrystallline: This type of pores are associated with recrystallized and/or dolomitized beds. It is observed between dolomite crystals in the Gir Bir and Mushorah formations (Figure 5F and 4E).

4. Moldic: Molds and incomplete molds are formed from the diagenetic dissolution of metastable grains. Moldic pores exhibit sharp and distinctive outlines of leached grains, while incomplete moldic pore boundaries are less distinctive and

adjacent to recrystallized remnants of the original grain. Moldic and incomplete moldic pores (Figure 5G) dominate the skeletal grains of most of the studied carbonates specially in the upper part of the Gir Bir Formation.

5. Vuggy: Vuggy pores occur as enlarged solution enhanced intra-matrix pores (Figure 5H and I). Pore outlines are irregular and pore shapes are typically blocky in nature. Vugs are fabric selective and do not resemble preexisting component grain shapes or sizes. Vugs may contribute to overall effective porosity when interconnected by sufficient intra-matrix porosity.
6. Channel: This porosity is distinguished as elongate vugs mostly filled with hydrocarbons in the upper parts of the Gir Bir and the lower part of the Mushorah formations (Figure 5J).
7. Fracture: It is the most effective and important secondary porosity generated by tectonic fracturing of the rocks and play as conduits for hydrocarbons in carbonate reservoirs. It is observed as an oblique fractures including sliken sides or as isolated or group of fractures (Figure 5 K and L) in various portions of the studied carbonates but commonly seen in the upper part of the Gir Bir Formation below the unconformity surface with the overlying Mushorah Formation.

KJPS Al-Kitab Journal for Pure Science
Vol.2 (2), ISSN: 2617-1260 (print), 2617-8141(online)
www.kjps.isnra.org

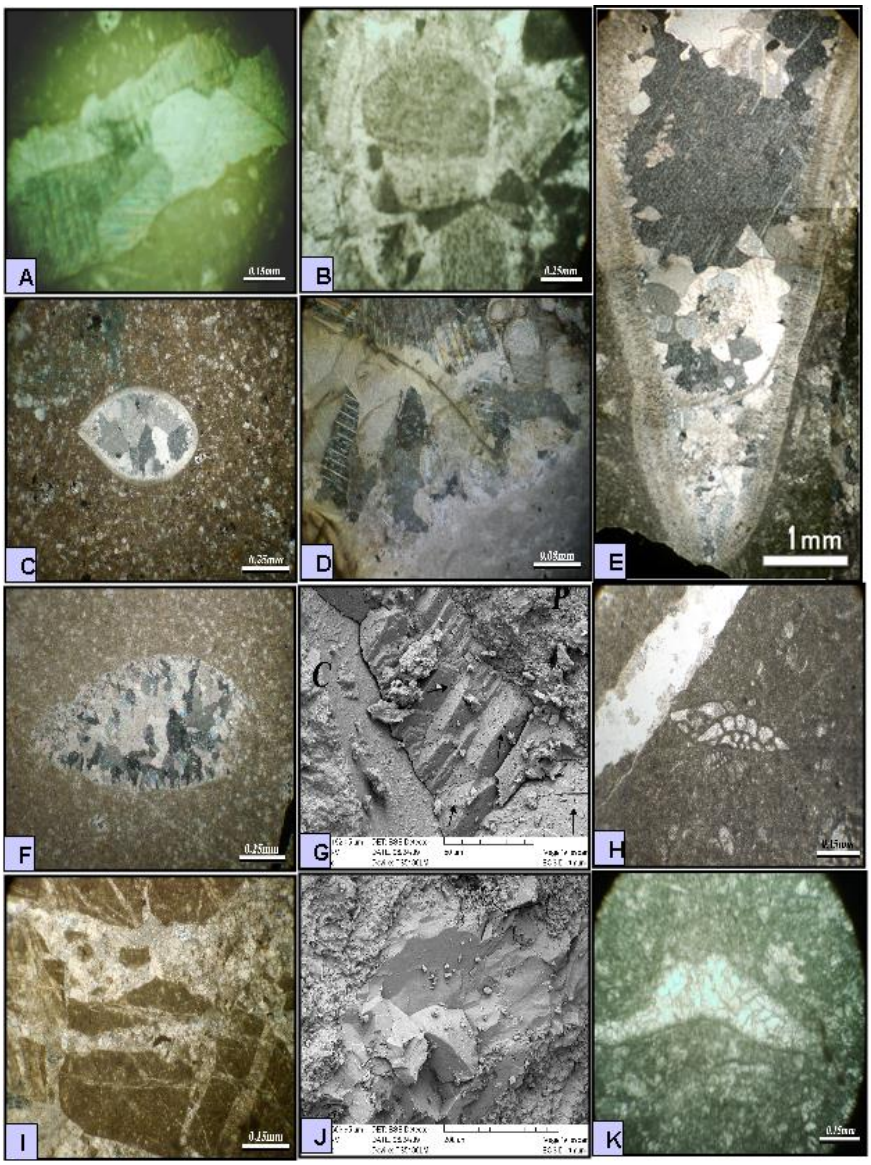

Fig. 3 Diagenetic features of the studied rocks, A, blocky cement in micritic groundmass, Gir Bir Formation. B, syntaxial rim cement around echinoderm fragment, Gir Bir Formation. C, fibrous cement in rim graded to drusy mosaic in center of ostracoda shell. Mushorah Formation. D, drusy mosaic cement in micritic groundmass, Gir Bir Formation. E, drusy cement in conical rudist shell, Gir Bir Formation. F, radaxial fibrous cement that develop to drusy cement in the center of a shell, Mushorah Formation. G, Scanning electron microscopic image (SEM) of radaxial fibrous cement with dissolution features and small pores (arrows), note calcispheres (C) and planktonic forams (P). Mushorah Formation. H, granular cement in Nezzazata benthic forams and vein filled with calcite, Gir Bir Formation. I, recrystallization of the micritic groundmass in the Mushorah Formation. J, SEM of recrystallization and microspar neomorphism, Gir Bir Formation. K, inversion of aragonite to calcite on a bioclast, Gir Bir Formation.

KJPS Al-Kitab Journal for Pure Science
Vol.2 (2), ISSN: 2617-1260 (print), 2617-8141(online)
www.kjps.isnra.org

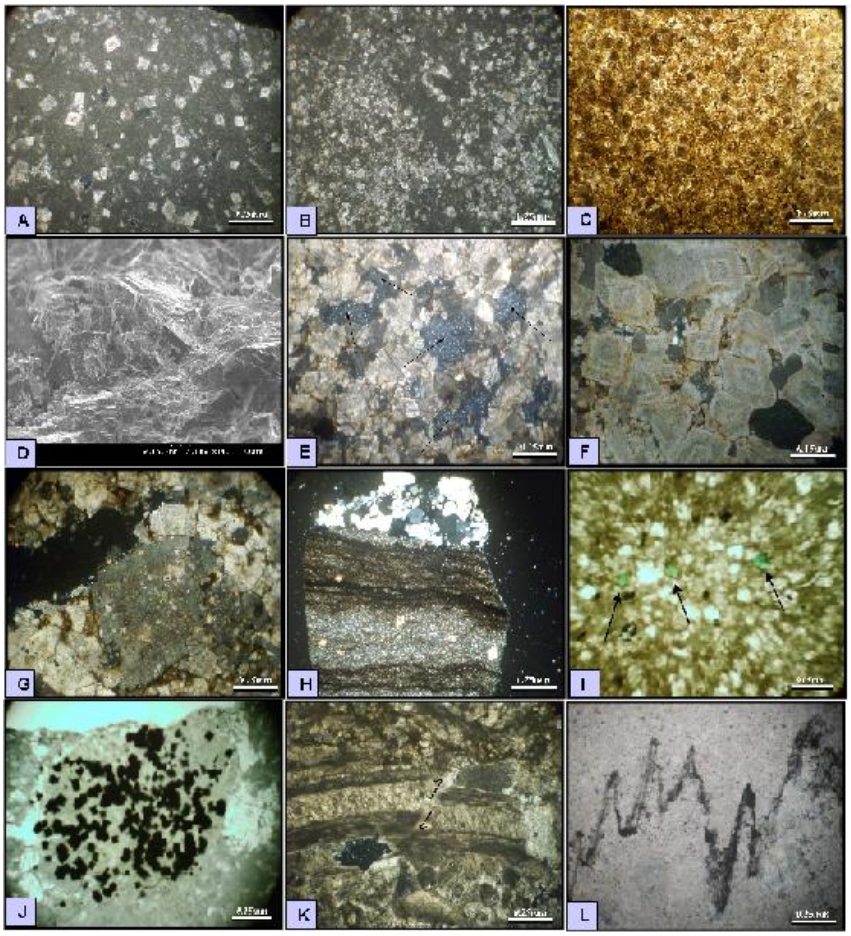

Fig. 4 Diagenetic features of the studied rocks. A, floating dolomite texture, Gir Bir Formation. B, contact rhomb fabric, Gir Bir Formation. C, drusy mosaic dolomite texture, Gir Bir Formation. D, SEM image of drusy mosaic dolomite texture, Gir Bir Formation. E, sieve mosaic texture with intercrystalline porosity (arrows), Mushorah Formation. F, zoned dolomite in contact rhomb structure, Gir Bir Formation. G, poikilotopic dedolomite texture, Mushorah Formation. H, silicification with growth of coarse quartz crystals, note inhabitation of silicification in the organic rich and dolomitized laminas (arrows refer to dolomite rhombs), Mushorah Formation. I, authigenic glauconite (arrows), Mushorah Formation. J, concentration of pyrite in bioturbated bed, Gir Bir Formation, K, mechanical compaction and breakage in Inoceramus shell, Mushorah Formation. L, low-amplitude stylolite filled with organic and clayey matters, Gir Bir Formation.

KJPS Al-Kitab Journal for Pure Science
Vol.2 (2), ISSN: 2617-1260 (print), 2617-8141(online)
www.kjps.isnra.org

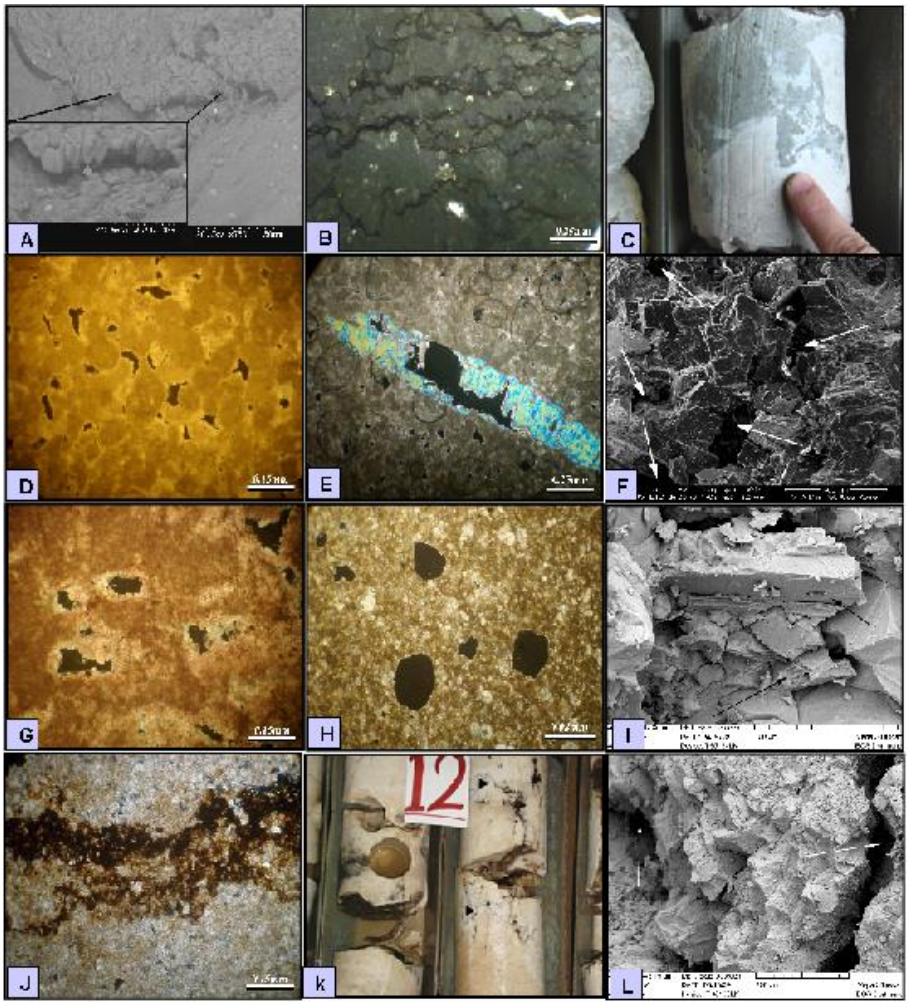

Fig. 5 Compaction features and porosity types in the studied rocks. A, SEM image of stylolite with enlarged view showing partial calcite growth in stylolite, Gir Bir Formation. B, irregular anastomosing stylolite, Gir Bir Formation. C, karstification in the upper surface of Gir Bir Formation, core sample. D, intergranular porosity in peloidal lime grainstone of Gir Bir Formation. E, fenestral porosity in lime mudstone that includes anhydrite nodules, Wajna Formation. F, SEM image of sieve mosaic dolomite with intercrystalline porosity (arrows), Mushorah Formation. G, moldic porosity after dissolution of skeletal grains and rimmed dolomite formation, Gir Bir Formation. H, vuggy porosity, Mushorah Formation. I, SEM image of differential dissolution in recrystallized limestone leaving micro-vuggy pores, Gir Bir Formation. J, channel porosity filled by organic matter, Mushorah Formation. K, high amplitude stylolite and fractures filled by hydrocarbons, core samples of Gir Bir Formation. L, micro-fracture porosity in SEM image of Gir Bir Formation.

KJPS Al-Kitab Journal for Pure Science
Vol.2 (2), ISSN: 2617-1260 (print), 2617-8141(online)
www.kjps.isnra.org

Porosity Evolution

The studied succession was divided into three zones (A, B, and C) depending on variations in Gamma ray, which reflects their shale content (Figure 6).

The A zone is recorded in well Bh-1 only and has a funnel shape (Figure 6) with 103 meter thick and high shale content. This zone is represented by stratigraphic sequence A and the TST from sequence B (the lower and middle parts of the Gir Bir Formation).

Zone B is of bell shape (Figure 6) and low content of shale. It has approximately 109 meter and appears in BH-1 well and continues in the upper parts of wells Sf-16 and 41. It is revealed that the upper part of zone (B) which coincides with (HST) of sequence (B) is highly porous and regarded on the main reservoir in the middle and upper parts of the Gir Bir Formation.

The funnel shape is also observed for the zone C (Figure 6) with high thickness in Sf-16 and 41 whereas, while it decreases to 34 meter thick in Bh-1 well. It has high shale content as compared with other zones and is represented by sequence C (Mushorah Formation).

The primary, total and effective porosities are calculated from the well logs (BHC, CNL, and FDC). The values are plotted with depth for selected wells (Figure 7) to show distribution of porosity with depth and to delineate the locations of the effective porosity that reflect the fluid direction and the reservoir zones in the studied successions.

In zone A, the total porosity is 2-15% (see Figure 7), the effective porosity is generally low, while primary porosity is high in some levels due to effect of dolomitization. This zone is composed of limestone and dolomitic limestone that are highly affected by recrystallization, in general, it is of poor reservoir characteristics.

The total porosity in the zone B range between 5-25% but increases in the upper part of the zone (in the upper surface of Gir Bir Formation). The primary porosity increases also in the upper part of the zone reaching 30% in Bh-1 well and 10% in Sf-16 and 41 wells (Figure 7). This increase may reflect the effect of fracture porosity [21], or it due to hydrocarbon effect [22].

A Fracturing and dissolution feature in the upper part of the Gir Bir Formation is the cause of increase in primary porosity. The upper part of zone B could be regarded as a

reservoir unit with total porosity (10-25%) and an effective porosity of 10% in addition to low shale content. This reservoir unit is of fracture reservoir type, which is formed of shallow marine facies with mud dominance.

In the zone C, the porosity is 3-5% with high shale content in the three studied wells except lower parts of the zone in Sf-41 where total porosity is relatively high (15%) and effective porosity of 10%. Core and petrographic investigations show that the studied rocks include intercrystalline porosity (Figures 4E and 5F) and saturated with hydrocarbons [5].

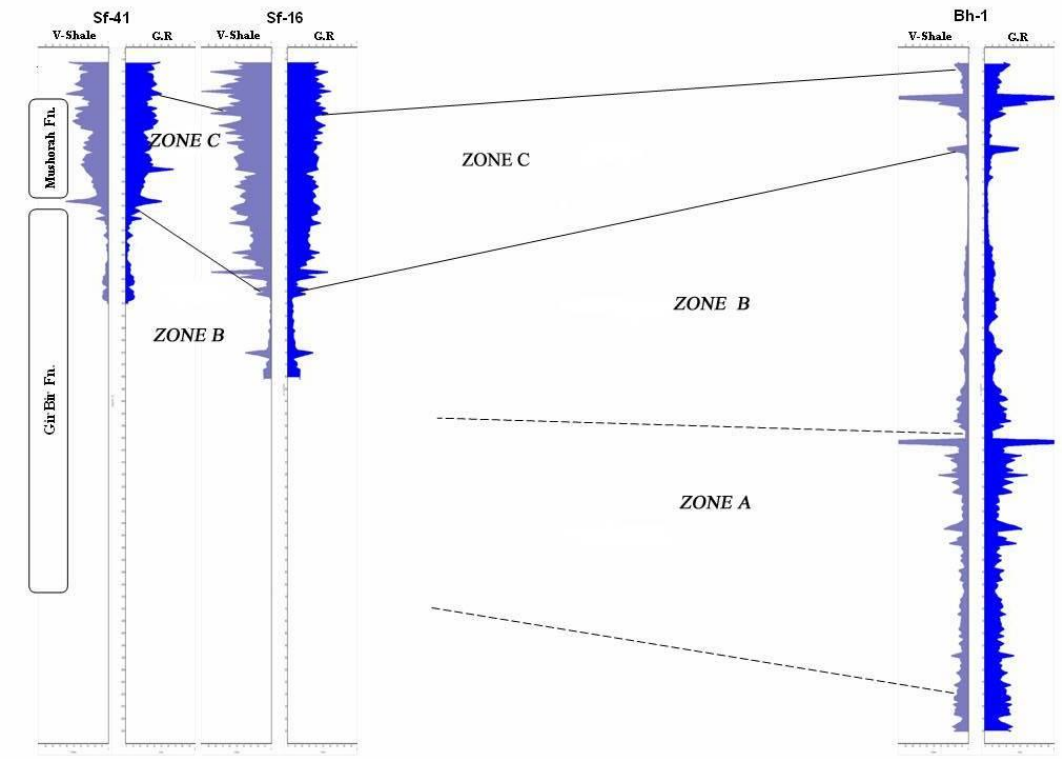

Fig. 6 Porosity zones based on gamma readings and shale volume.

KJPS Al-Kitab Journal for Pure Science
Vol.2 (2), ISSN: 2617-1260 (print), 2617-8141(online)
www.kjps.isnra.org

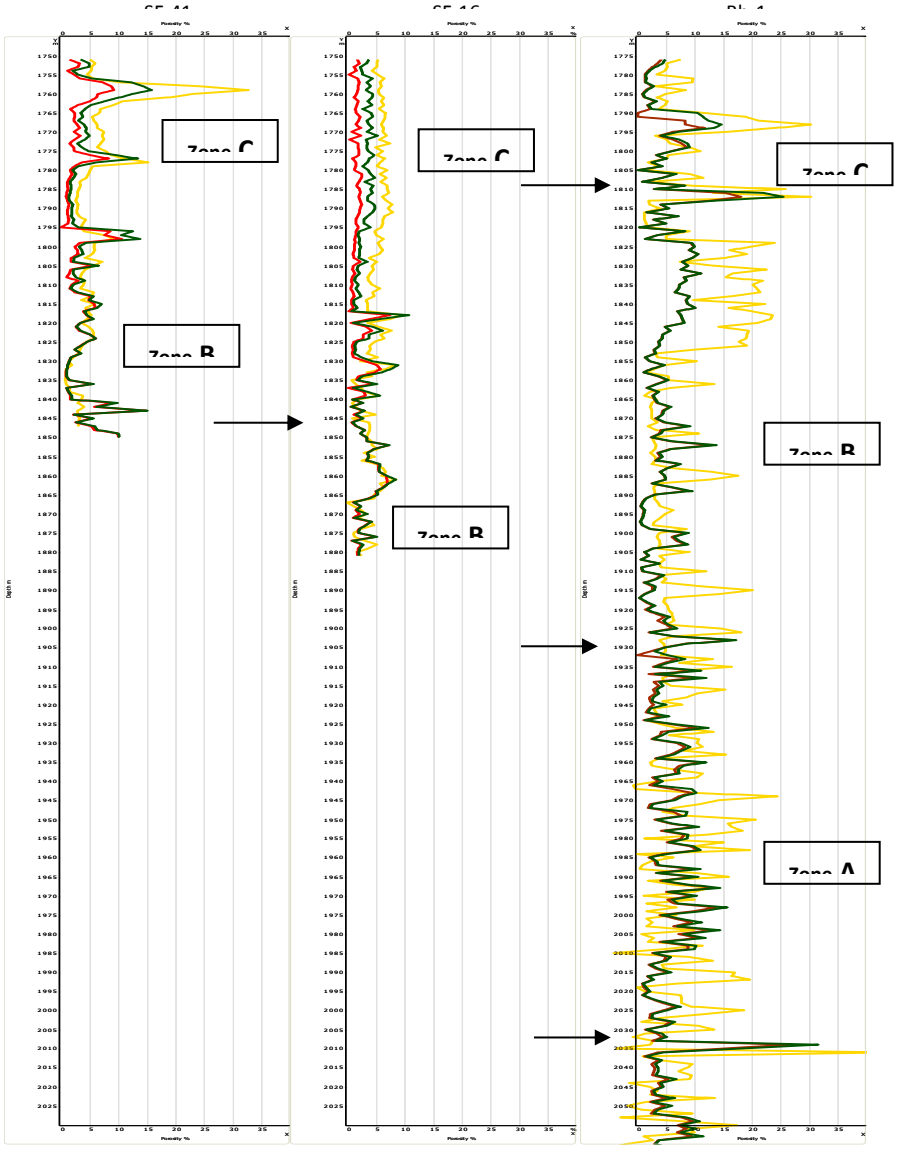

Fig. 7 Depth relation with total porosity (green), effective (red) and primary (yellow) in the wells Bh-1, Sf-16 and Sf-41.

5. Discussion and conclusions

The studied succession of the upper Cretaceous (Cenomanian-early Campanian) represented by Gir Bir, Wajna, and Mushorah formations of northwestern Iraq has affected

by three types of diagenetic stages; early burial, unconformity-related, and deep burial diagenesis .

Early diagenesis is represented by precipitation of fibrous cement on the inner rims of skeletal grains (primary porosity). Secondary porosity could be formed during this stage through dissolution of aragonite and calcite precipitation, which has unequal distribution leaving intergranular secondary porosity. In general, this stage has little effect on the studied rocks.

The unconformity-related diagenesis dominates in the upper parts of the Gir Bir Formation near the unconformity with Mushorah Formation where dissolution features are common as indicated from dissolution of rudist and bioclasts leaving vuggy and moldic porosity and other karstic and fissure structures. The effect of cementation on porosity is mostly limited during this stage. The absence of meniscus cement may refer to phreatic and vadose conditions, whereas, presence of syntaxial rim cement around echinoderm and common dissolution refer to the effect of meteoric water on the limestone of the Gir Bir Formation. This stage is considered as the main reservoir unit in the area under study.

In the deep burial diagenesis, various processes have affected on the studied rocks that decrease porosity such as cementation (mostly drusy mosaic and blocky), recrystallization and compaction (stylolite formation). Dolomitization enhanced the reservoir characteristics by formation of intercrystalline porosity as indicated from increasing of porosity in the lower part of the Gir Bir Formation (see Figures 6 and 7) and the lower part of the Mushorah Formation where dolomites and dolomitic limestone dominate.

The Gir Bir Formation is formed of shallowing upward succession. The reservoir characteristics are low in the lower part of the formation where slope and outer shelf environments dominate while they improve toward upper part of the formation where rudist build-ups and other bioclasts are common (Figure 7). Although the upper part was deposited in back reef shoal environment, it is regarded as the main reservoir in the studied succession due to fracturing and common vuggy and moldic porosities. Fracturing porosity is also dominated in the lagoonal facies of the correlative Mishrif Formation in the Arabian Gulf region [23].

Acknowledgment

The authors wish to thank the Northern Oil Company, Iraq for providing the data and supporting this research activity. Thanks also due to Georg Oleschinski (Steinmann Institute, Bonn, Germany) and Sharon Gibson (Royal Holloway of London University, UK) for help in scanning electron microscopy.

References

[1] R.J. Murris ***"Middle East stratigraphic evolution and oil habitat".*** AAPG Bull., 64, 597 (1980).

[2] J.A. Al-Sakini ***"Summary of the petroleum geology of Iraq and the Middle East".*** Northern Oil Company Press (Naft –Al-Shamal co.), Kikuk, Iraq (in Arabic), (1992).

[3] F.N. Saddoni and A.A.M. Aqrawi, Cretaceous sequence stratigraphy and petroleum potential of the Mesopotamian basin, Iraq. In: A. Alsharahn and B. Scott ***"Middle East Model of Jurassic-Cretaceous carbonate system"***, SEPM special publication (2000).

[4] P.R. Sharland, R. Archer, D. Casey, et al., 2001. ***"Arabian Plate Sequence Stratigrpahy",*** GeoArabia, Special Publication 2, Gulf Petrolik. Manama, Bahrain (2001).

[5] M.A.M. Al-Haj ***"Study of sedimentary basin evolution of cretaceous Cenomanian-early Campanian of northwestern Iraq".*** PhD thesis, Mosul University, Iraq (2011).

[6] S.N. Haddad and M.A. Ameen ***"Mid-Turonian-Early Campanian sequence stratigraphy of northeast Iraq"***. GeoArabia, Gulf PetroLink, Bahrain, 12, 2, 135 (2007).

[7] A.A.M. Aqrawi, J.C. Goff, A.D. Horbury and F.N. Sadooni ***"The Petroleum Geology of Iraq"***. Scientific Press, (2010).

[8] Z.R. Beydoun ***"Arabian hydrocarbon geology and potential, plate tectonic approach".*** AAPG, Bull., Studies in Geology (1991).

[9] T. Buday ***"The Regional Geology of Iraq, Stratigraphy and Paleogeography".*** Dar Al-Kutub publishing house, Mosul University. Mosul, Iraq (1980).

[10] M. Chatton and E. Hart ***"Review of the Cenomanian to Maestrichtian stratigrpahy in Iraq"***. Unpublished report, Iraq Petroleum Company, Palaeontological Department, Kirkuk (1961).

[11] W. Schlager and J. Philip, Cretaceous Carbonate platforms, In: R.N. Gisburg and B. Beaud ***"Cretaceous Resources, Events and Rhythmus"***. NATO ASC series 304, Kluwer Academic Publisher (1990).

[12] K.M. Al-Naqib ***"Geology of the Arabian Peninsula, southern west Iraq".*** United States Geological survey, Professional Paper, No. 560-G, (1967).

[13] P.W. Choquette and C.L. Pray ***"Geologic nomenclature and classification of porosity in sedimentary carbonate".*** AAPG. Bull., 22, 207 (1970).

[14] H.A.KH. Al-Jawari ***"Study of Upper Cretaceous at selected sections of Sfia wells, NW Iraq",*** MSc thesis, Baghdad University, Iraq (1989).

[15] M.E. Al-Esa and N.A. Fassola ***"Biostratigraphy of the Upper Cretaceous reservoir at Butmah field".*** Oil studies and Researches Journal, 2, 152 (2011).

[16] V.V. Larionov ***"Borehole Radiometry",*** Moscow, U.S.S.R. Nedra (1969).

[17] J.D. Milliman ***"Marine Carbonates",*** Springer Verlag, Berlin (1974).

[18] A.F. Randazzo and L.G. Zachos ***"Classification and description of dolomitic fabric of rocks from the Floridan Aquifer, U.S.A".*** Sedimentary Geology, 37,151 (1984).

[19] E. Flügel ***"Microfacies of Limestone",*** Christenson, K. (Translator), Springer-Verlag, Berlin (1982).

[20] E. Gischlor and A.J. Lomando ***"Recent sedimentology facies of isolated carbonate platforms, Belize-Yucatan System, Central America".*** Journal of Sedimentary Research, 6, 747 (1997).

[21] R.A. Nelson ***"Geologic Analysis of Naturally Fractured Reservoirs".*** Gulf Publishing, Houston (2001).

[22] D.W. Hilchie "***Applied Open Hole Log Interpretation"***. Golden, Colorado, Inc., (1978).

[23] T.P. Burchette and S.R. Britton Carbonate facies analysis in the exploration for hydrocarbons: a case study from the Cretaceous of the Middle East. In: P.J. Brenchley and B.P. Williams ***"Sedimentology, Recent Development and Applied Aspect".*** Blackwell, (1985).

KJPS Al-Kitab Journal for Pure Science
Vol.2 (2), ISSN: 2617-1260 (print), 2617-8141(online)
www.kjps.isnra.org

DOI: http://10.32441/kjps.02.02.p2

Efficient Performance Technical Selection of Positive Buck-Boost Converter

Ahmed K. Abbas[1], Abadal-Salam T. Hussain[2]

[1]Assistance Lecturer, University Headquarter – Anbar University, Anbar, Iraq
[2] Al-Kitab University, Biomedical Instrumentation engineering Technique Department, Alton Kupri, Kirkuk, Iraq
[1]ahmed_89@yahoo.com, [2]asth3@yahoo.com

ABSTRACT

The necessity for stable DC voltage in both removable and non-removable systems has been considerably desired recently. These systems have to be implemented efficiently in order to be responding rapidly based voltage variations. Under this act, the efficient power can extend the lifetime of the employed batteries in such systems. The presented efficiency can be realized with respect to buck and boost components that were implemented to generate what is called positive Buck-Boost converter circuits. The main functions of the positive Buck-Boost converter are identified by announcing the unchanged situation of output voltage polarity and indicating the level of the voltage rationally between the input and the output. It is worth mention, the positive Buck-Boost converter circuit was simulated based *Proteus* software, and the hardware components were connected in reality. Finally, the microcontroller type that employed in the proposed system is PIC_16F877A, which realizes the input voltage sensitively to generate Pulse Width Modulation (PWM) signals in order to feed the employed MOSFET element.

Keywords: Converter Circuits, Inverting and Non inverting Converters, Positive Buck and Boost Converters.

KJPS Al-Kitab Journal for Pure Science
Vol.2 (2), ISSN: 2617-1260 (print), 2617-8141(online)
www.kjps.isnra.org

تقنيات ألاداء الفائق لإختيار العاكس (الخافض – الرافع) الأيجابي

Ahmed K. Abbas[1], Abadal-Salam T. Hussain[2]
[1]Assistance Lecturer, University Headquarter – Anbar University, Anbar, Iraq
[2] Al-Kitab University, Computer Engineering Technology Department, Alton Kupri, Kirkuk, Iraq
[1]ahmed_89@yahoo.com,_[2]asth3@yahoo.com

الملخص

الحاجة إلى الجهد المستمر(DC) الثابت في كثير من الأنظمة التي يتغير فيها الجهد المستمر عندما يكون مصدرا للتغذيه او لايكون مصدرا في الآونة الأخيرة أصبحت مطلوبة بشكل كبير. لذلك تتطلب الحاجة الى مثل هكذا دائره الكترونيه لمثل هذه الأنظمة للعمل بكفاءة من أجل الاستجابة لتغيرات الجهد على أساس سريع. وبموجب هذا المتطلب ، يمكن للطاقة الفعالة أن تطيل عمر البطاريات المستخدمة في هذه الأنظمة مثلا ام المحافظه على أداءبكفائه عاليه. وكذلك يمكن أن تتحقق الكفاءة المتقدمة فيما يتعلق بالعواكس Back و Boost التي تم تنفيذها لتوليد ما يسمى تحويل دفعة Back و Boost إيجابية. الوظائف الرئيسية لمحول Back و Boost الإيجابي هي في حالة عدم تغيير قطبية الجهد الناتج ، والإشارة إلى مستوى الجهد بشكل رشيد بين المدخلات والمخرجات. ومن الجدير بالذكر ، تم محاكاة دائرة محسنة دفعة إيجابية على أساس برنامجProteus للتمثيل الرياضي ، وكذلك تم توصيل مكونات الأجهزة في الواقع الحقيق. وأخيرًا ، يكون نوع المتحكم الدقيق المستخدم في النظام المقترح هو PIC_16F877A ، الذي يحقق جهد الإدخال بحساسية لتوليد إشارات تعديل العرض النبضي (PWM) من أجل تغذية عنصر MOSFET المستخدم.

الكلمات الدالة: دائرة التحويل، المحول العاكس وغير العاكس، محول الخافض والرافع بالاتجاه الموجب

1. Introduction

The modern technologies have fascinated the universe by developing and enhancing the devices especially the portable devices that are massively needed nowadays. These portable devices need to be under the domination of great power providers. Lithium-ion batteries are considered the most applicable item in these devices. Hereby, the question is: how to design a power system capable of providing these devices by the required power in an efficient way

without wasting. That would be one of the applications of positive Buck-Boost converter that magnifies – reduce the input voltage based DC-DC conversion principle. There are many typologies were used for converting of DC-DC voltage. They have been commonly used in power supply applications for the majority of electronic systems. The most popular kind of converters are identified by [1, 2]:

1. Individual Buck converter.
2. Individual Boost converter.
3. Buck-Boost converter.

The basic principle of DC to DC positive Buck-Boost converter converts DC output voltages. The output voltage can be less than input, which is during Buck converter (step down), higher than the input during Boost converter (step-up) converter. It also could be same as the input. Recently, DC to DC converters is developed to be a popular subject matter, which has many requirements for best specification such as less costly, smaller size, lighter in weight and fewer power losses towards a highly efficient power conversion. Moreover, pulse width modulation (PWM) has been grown of DC electronic devices. Buck-Boost converter adapts an unstable input voltage into a fixed output voltage. The output voltage of the circuit can be dominated by utilizing a duty cycle.

1.1. DC-DC Converters

The basic typologies widely employed in DC-DC conversions are Buck converter, the Boost converter, and Buck-Boost converters. The Buck converter that is known as step-down the output voltage, regulates the output voltage to be less than the input. Besides, the Boost converter or what is called the step-up converter is utilized to regulate the output voltage, which could be higher - equal to the input voltage. Additionally, the Buck-Boost converter is used for both conversion issues, which could operate as a step-down and step up. There are a couple of different typologies of Buck-Boost converter in same circuit topology.

I. Buck-Boost inverting converter: The output voltage is reverse polarity.
II. Buck-Boost non-inverting converter: The output voltage is a similar polarity as the input voltage.

There are many different types of a single step up or step down DC-DC switching converters. For example of these converters topologies as Buck-Boost inverting converter, SEPIC- Single Ended Primary Inductance Converter, and Cuk converter that match the similar functionality. Nonetheless, some types of converters include drawback in terms as Buck-Boost inverting converter and Cuk converter where the output voltage is reversed in polarity [3].

On the other hands, the combination of positive Buck and Boost converter by a single circuit, which is by combining Buck and Boost converter circuits with independently controllable switches, which are a common choice for these types of applications requiring conversion capability. In this review paper, several different types of Buck-Boost with positive output voltage will be discussed. There are numerous approaches to provide a controlled the output voltage (without change polarity of the output voltage). The basic Buck-Boost inverting converter and Cuk converter are excluded, due to the output voltages that are reversed in polarity to the input.

In this review paper, the kind of Buck-Boost converter with a positive output voltage reviewed and analyzed by other researchers. In these days, the applications of DC-DC converters have been improved and expanded drastically since they commonly utilized as a part of sustainable power source frameworks, for example, fuel cells, hybrid electric vehicles, battery chargers, and solar systems [4, 5]. The hybrid energy such as solar energy and wind energy are categorized as varied voltage due to the fact that solar power is

dependent on sunlight and the wind energy depends on the wind. For that reason, DC-DC converter is used to regulate the output voltage to step-up or step-down the output voltage to supplied steady levels, the range of the input voltage is a between (6-18) V and need to get 12V output at steady.

1.2. Single Ended Primary Inductor Converter (SEPIC)

SEPIC is certainly the simplest circuit is a kind of DC-DC converter, the electrical power potential voltage at the output could be higher, lower or same as the input voltage. The SEPIC is regulated by the duty cycle [6]. A SEPIC converter generally is the same as a classic of Buck-Boost inverting converter. However, SEPIC has an advantage of getting Non-inverted output voltage, which can be identified as the output voltage that is similar to polarity voltage [7]. The conventional SEPIC converter has two inductors, two capacitances, one switching and one diode as shown in Fig. 1.

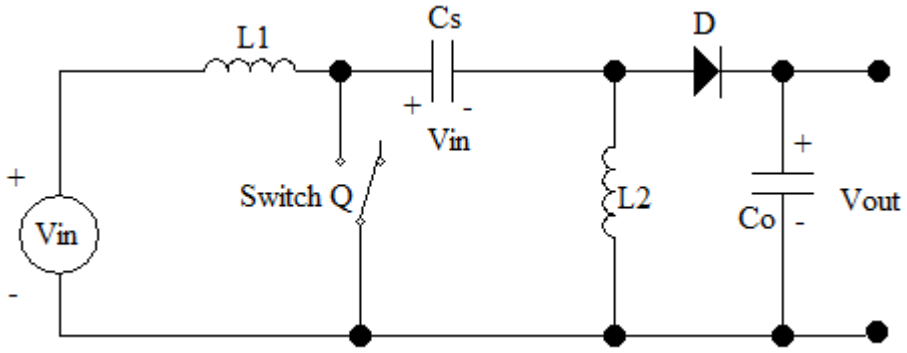

Fig. 1 SEPIC circuit diagram

It is clearly understood that the (switch Q) is connected parallel with the input voltage, and $L2$ is joined together in parallel to the load. Capacitance Co is connected in parallel with switch Q and the resonant inductor $L1$ is connected

in series with Cs [8]. The operation of SEPIC has happened during two states. When switch Q is closed, the current of I_{L1} is increased in a positive direction and the I_{L2} is increasing in the negative direction. The energy power required to raise I_{L2}, which is come from the input supply. When the switch is closed the voltage of V_{CS} is roughly equal to V_{IN}, the voltage V_{L2} is also roughly to V_{IN}. Thus, the capacitor V_{CS} provides the power to improve the magnitude field of the current in I_{L2} for growing the energy stored in I_{L2}. Additionally, the diode works as a reverse as open circuit [9]. When (switch Q) is open, the current I_{CS} becomes equal to I_{L1} because the inductors do not enable on immediate changes in the current. I_{L2} keeps in the negative path, in reality, it certainly not reverses path. $I_{L2}$and I_{L1} leads to increase the current delivered to the load [10]. There are some researchers were discussed about the model of SEPIC converters [11, 12, 13], which was the extremely popular Buck-Boost converter. However, it needs additional components. SEPIC, used a couple of inductors and capacitors. Thus, including occupy extra space lead to be increasing the size and the price. Extra components lead to increase the losses, and the efficacy of converter will be lower. However, the SEPIC include some advantages which the output voltage is actually having a similar polarity of the input voltage. Additionally, it could be regulated fixed output voltage regardless of the input voltage is lower or higher than the required.

1.3. Combination Circuit Converters

There are two types of the most popular combination converters, which is Boost-Buck converter and Buck-Boost converter. The characteristics of the proposed converters are obtained by connection a couple of general converters with positive output voltage [5]. At the first type of converter, which is Boost-Buck converter, the Boost converter stage could

be located at the first then Buck converter is connected by series with it. At second the type of Buck-Boost converter, the Buck converter could be located at the first stage and followed by the Boost converter. Both of converters will be explained, discussed and compared.

1.4. Positive Boost-Buck Converter

The topology that achieved by separated devices includes two DC-DC converters. In these types of converter, the output voltage could be greater or smaller than the input voltage. The output voltage of Boost-Buck converter is a positive. During a Buck or a Boost converter, 2 switches are turned on and off per every period [14, 15]. This type of circuit is required two inductors, a couple of MOSFETs, two diodes and two capacitors as shown in Fig. 2.

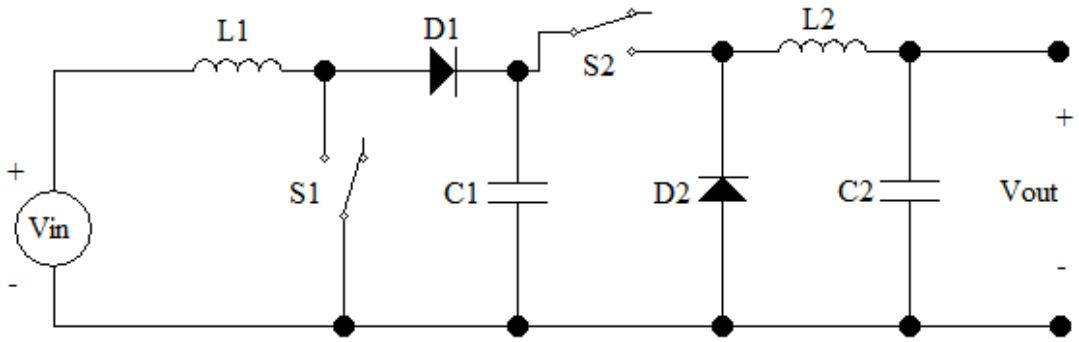

Fig. 2 Circuit of positive Boost-Buck converter

In spite of the fact that the circuit works with respect to drive the two switches concurrently, as well as Pulse Width Modulation (PWM) control is used to drive S1 and S2. When the Boost function is needed, the S1 is driven by PWM and S2 is adjusted through the output voltage as shown in Figure 2. Besides that when the Buck function is required as a (Vin>Vout) MOSFET S2 will be operated by controlled PWM while S1 hold off [8].

The researchers were combined a circuit of positive Boost-Buck converter by used two switches to regulate the output voltage. This work was applied by using two DC-DC converters that are combined Boost converter and followed by Buck converter [16, 17]. The advantage of this converter was the output voltage always-positive direction. Whereas the limitations of this converter are, the losses are high, which leads to lowers on efficiency

KJPS Al-Kitab Journal for Pure Science
Vol.2 (2), ISSN: 2617-1260 (print), 2617-8141(online)
www.kjps.isnra.org

because the amount of the components as twice of capacitors, inductors, and compensation network required for both of controllers is more. More equipment, additional space is engaged, which leads to increase [18, 19] the cost. Furthermore, the control system of the two PWM loop is difficulty according to [20].

1.5. Positive Buck-Boost Converter

This converter circuit has similar functions previous circuit of positive Boost-Buck converter, which is explained before and shown in Figure 2. In this case, of positive Buck-Boost converter is basically a combination of a Buck section converter concatenated by the Boost section. This topology has two MOSFETs switches, two diodes one output capacitor and one inductor [21] as shown in Fig. 3.

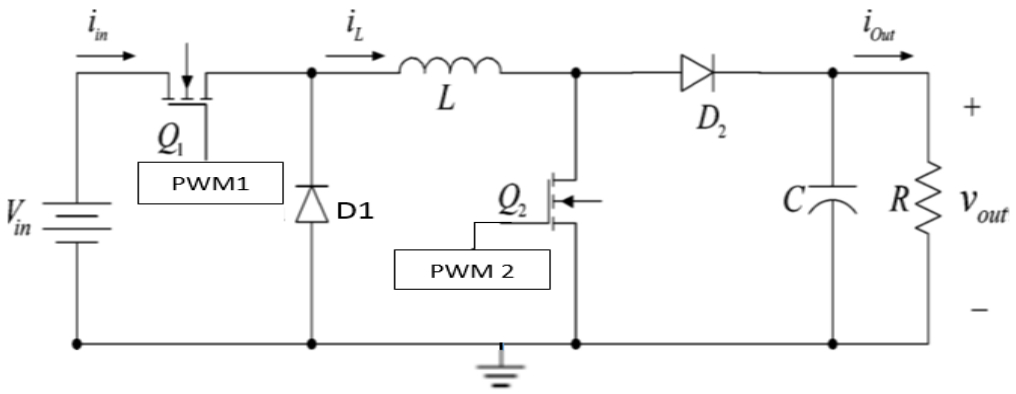

Fig. 3 A circuit of positive Buck-Boost converter [19]

In addition this circuit of positive Buck-Boost converter or what is called Buck-Boost Non-inverting converter could be used as step-up or step-down DC-DC converters [22], it is permitted to connect a Buck with Boost converter in one topology to lead a single inductor in order to be employed with high fulfillment in Buck-Boost converter [23, 24]. This type of converter could be used as a Buck converter only by controlling switch Q1, diode D1, Q2 will be turned OFF and D2 will be conducted. Besides, it could work like a Boost converter by dominating switch Q2 and diode D2, during the Q1 conducts, While D1 not conducts.

The operation of Buck converter occurs in two cases, the first case when MOSFET of Buck converter S1 is closed and the second case when S1 is opened. In the first case, the current flow through the source Vin from the inductor to the load that charges the inductor by rising the magnetic field, when the Diode of Buck converter D1 is reverse bias. Simultaneously, the current flow from the inductor, causes energy amplification. When V_{out} reached to the required value, switch S1 opens and diode D1 turns ON in the second case of the operation in Buck converter. When the MOSFET1 (S1) is open, the inductor works as the main source to preserve the current over the load resistor. The current goes on streaming over the inductor from the diode D1 and waits for magnetic field break down operation and the inductor discharges. Before discharge operation, D1 is opened, S1 is closed, and the period is repeated.

The operation of the Boost converter also occurs in two cases. As well as, in Buck converter. During the first case, the MOSFET2 S2 is closed. The current through the switch MOSFET2 S2 conducts, therefore current flows between the positive and negative source terminals throughout the inductor, which can store electrical energy by generating a magnetic field. There is certainly no current streaming in the other parts of the circuit as diode D2 or capacitor C. The MOSFET is quickly turned OFF (during S2 open). It causes a drop in current and eventually derives the inductor to generate a back electromagnetic field (e.m.f), in a reversed polarity with respect the voltage across the inductor. While on period, to continue current streaming which leads to a couple of voltages, the given supply voltage V_{in} and the generated back (e.m.f). The higher voltage comes from voltage supply and inductor. There is absolutely no current through the MOSFET 2. Lastly, the current through D2 charges up the capacitor to V supply +VL with a small forward voltage drop across D2, then supplied to the load.

In the work of researchers [3, 24, 25] an identification technique was presented for soft transitions in positive Buck-Boost converter. The circuit is chosen because it has an individual inductor, which is used for both of converters, Buck and Boost. It is a well-known decision for applications requiring bidirectional conversion capability, high efficiency and less component stressed. The researchers found reduced conduction losses and decreased inductor stress as compared to the Boost converter. In Addition, the characteristic of this

arrangement includes the capacity to select the output DC voltage. Moreover, the researchers in [19, 26] stated the perfect techniques requires an exchange among the costs, lesser output noise and lesser ripple factor. This type of converter techniques could regulate the output voltage into lower, higher or equivalent voltage. The extra benefit of the converter circuit is the output voltage of the converter in a positive direction.

2. Positive Buck-Boost Technique Implementation

The models of different converter topologies are discussed in this review paper. The operation of different circuits of Buck-Boot converters, which were supplied positive output voltage, were explained in details. The advantages and disadvantages in the converters, was addressed. The techniques theory of combination of DC-DC converters was presented. The SEPTIC is a simple circuit, however not considered functional. A converter topology named positive Buck-Boost converters, which can work with both converter (step-down), and (step-up) was chosen, because it has, many advantages compared with another type of Buck-Boost converter. The main difference between configurations converters that have explained the positive Buck-Boost converter was utilized less number of components electrical devices compared with other converters. The circuit of positive Buck-Boost converter has been simulated by Proteus simulation software and fabrication in hardware to get the result as shown in Fig. 4, 5.

KJPS Al-Kitab Journal for Pure Science
Vol.2 (2), ISSN: 2617-1260 (print), 2617-8141(online)
www.kjps.isnra.org

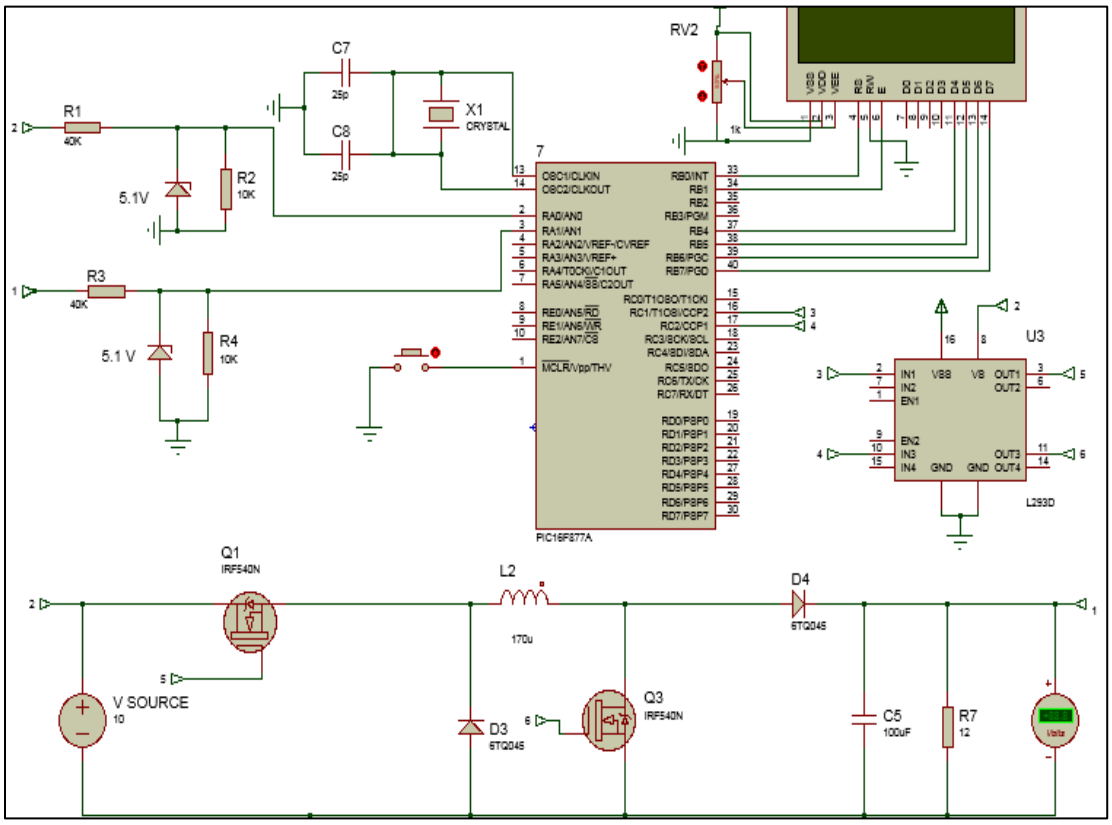

Fig. 4 Design circuit connection of positive Buck-Boost Converter

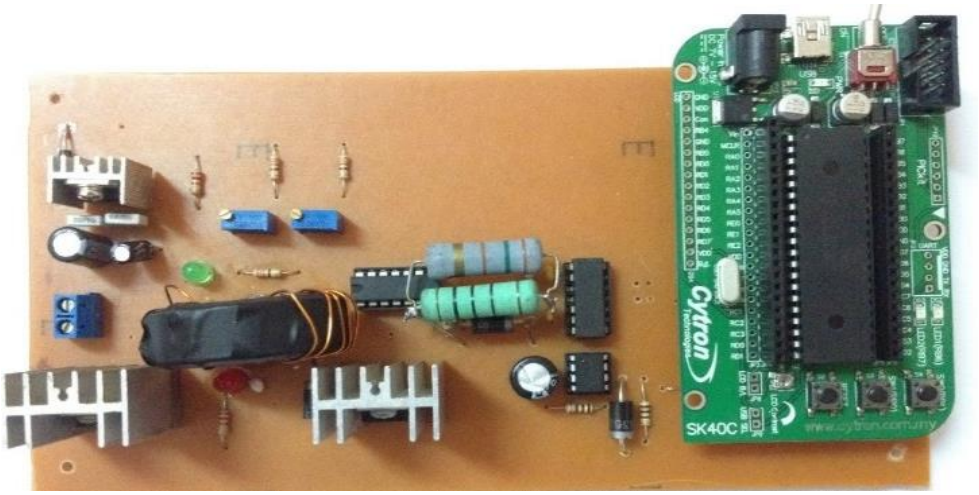

Fig. 5 Hardware implementation of positive Buck-Boost converter.

KJPS Al-Kitab Journal for Pure Science
Vol.2 (2), ISSN: 2617-1260 (print), 2617-8141(online)
www.kjps.isnra.org

3. Results And Discussions

3.1. PWM Waveform Result

PIC Microcontroller (16F877A) generates PWM waveform, which is the frequency that has been used is 50 KHz. The duty cycles of PWM are not constant. It is dependent on the input voltage supply. Fig. 6 shows the PWM waveform in software simulation during different duty cycle value.

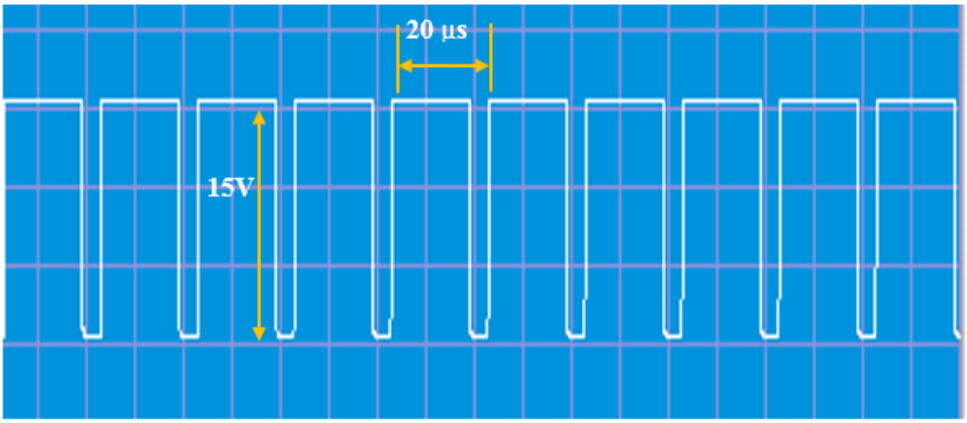

Fig.6 PWM on simulation software at 80% of the duty cycle.

3.2. The result of Buck Converter Simulation

Consequently, the following results were obtained from the simulation. The outcomes were found in accordance with the result than expected. The output voltage is the main part of this project. The output of Buck circuit is always lower than the input. The input voltage is not constant which is a variable. The range of input voltage for Buck converter is from 13-18 and the output is 12VDC. Table 1 shows a several different input value through Buck converter. Despite the input voltage is varied, the output voltage still virtually regulated at approximately 12VDC. The difference of the duty cycle as the assignment of the output voltage is shown in Table 1, which exposes a linear relationship between the duty cycle and the Vout/Vin ratio for a larger scope of output voltages.

KJPS Al-Kitab Journal for Pure Science
Vol.2 (2), ISSN: 2617-1260 (print), 2617-8141(online)
www.kjps.isnra.org

Table 1 Output voltage during Buck converter on simulation.

V_{in}	V_{out}	Duty Cycle (%)
13	11.97	93.2
14	12.08	85.7
15	12.02	80
16	12.04	75
17	12.05	70.5
18	12.05	66

3.3. The result of Boost Converter Simulation

Table 2 shows the output voltage through the Boost converter, which indicates that the output voltage is greater than the input. Table 2 shows the indicates a fairly constant output of approximately 12 VDC. Even the input voltage for Boost converter is varied from 6V to 11V, the output voltage remained virtually at 12VDC.

Table 2 Output voltage during Boost converter on simulation.

V_{in}	V_{out}	Duty Cycle (%)
6	12.16	50
7	11.99	41.6
8	12.07	33.3
9	11.96	25
10	11.98	16.6
11	11.98	8.3

KJPS Al-Kitab Journal for Pure Science
Vol.2 (2), ISSN: 2617-1260 (print), 2617-8141(online)
www.kjps.isnra.org

4. Hardware Implementation Result

4.1. The result of Buck Converter on Experimental

The results of Buck converter were presented in Table 3. The input voltage of this project was a variable with a range from 13V to 18V. The output voltages of Buck converter was roughly constant at 12V. The correlation between the output voltage and the duty cycle is a positive relationship, which that means; when the duty cycle increased the output will be increased.

Table 3 Output voltage during Buck converter on hardware.

V_{in}	V_{out}	Duty Cycle (%)
13	11.85	92.3
14	11.83	85.7
15	11.90	80
16	11.88	75
17	11.86	70.5
18	11.92	66

4.2. The result of Boost Converter on Experimental

The results from the Boost converter were presented in Table 4. The Boost converter is an operation with a different input voltage also and the output voltage was kept at around 12V. The relationship between the output voltage and the duty cycle is a positive relationship also, which that means; when the duty cycle increased the output will be increased.

Table 4 Output voltages during Boost converter on hardware.

V_{in}	V_{out}	*Duty Cycle (%)*
6	11.87	50
7	11.93	41.6
8	12	33.3
9	11.93	25
10	11.95	16.6
11	11.9	8.3

From the results, there are two sections; simulation software results and hardware implementation. The values of Buck converter and Boost converter from the simulation software were almost the same as the value of the experimental fabrication result. The result values from the simulation were quite high compared with the values from hardware fabrication. The hardware implementation has higher losses because of the electrical power losses such as conduction losses and switching losses. Conduction losses were those voltage drops and currents of the elements that happen when the MOSFET is conducting. Switching losses were included in both of equipment as MOSFETs and diodes. The frequency of switching was high, the switching operations change quickly. This includes rise time and fall time for each switching change. Besides what was mentioned, the components sometimes, do not give the exact value that required because of other effects as temperature. The accuracy voltage for experimental are not very different and still under the limit.

5. Conclusions

The analysis has been done for the control signals. PWM waveform generated by using PIC Microcontroller 16F877A to drive the MOSFETs. PWM waveform connected to the gate driver provides a greater amplitude of the waveform. The converter was checked and tested with variable input voltages. The circuit has achieved output voltage at 12VDC that means the Buck-Boost DC-DC converter circuit was able to step-up or step-down the output

voltage. The output voltage could be controlled by fixing at 12V even though the input voltage keeps changing from 6V to 18V. The important part for this circuit was achieved by working without changing the polarity of the output voltage. This kind of converter has found more compact, with high efficiency. Analog - Digital Converter ADC on the PIC16F877A was used to sense the input voltage to generate the PWM as required. From the data collected of the input and output power, it has been found the overall efficiency of positive Buck-Boost converter is 82%.

Acknowledgment

I would like to express my thanks and gratitude to our Al-Kitab University College, providing for us the chance to explore life and allow us to explore and apply new techniques and innovations that we have got.

References

[1]. Chakraborty, A., Khaligh, A., Emadi, A., & Pfaelzer, A. (2006, June). ***Digital combination of buck and boost converters to control a positive buck-boost converter.*** In Power Electronics Specialists Conference, 2006. PESC'06. 37th IEEE (pp. 1-6). IEEE.

[2]. Yao, K., & Lee, F. C. (2002). ***A novel resonant gate driver for high-frequency synchronous buck converter***s. Power Electronics, IEEE Transactions on, 17(2), 180-186.

[3]. Chen, J., Maksimovi C, D., & Erickson, R. (2001). ***Buck-boost PWM converters having two independently controlled switches***. In Power Electronics Specialists Conference, 2001. PESC. 2001 IEEE 32nd Annual (Vol. 2, pp. 736-741). IEEE.

[4]. Restrepo, C., Calvente, J., Cid-Pastor, A., Aroudi, A. E., &Giral, R. (2011). ***A noninverting buck-boost DC-DC switching converter with high efficiency and wide bandwidth***. Power Electronics, IEEE Transactions on, 26(9), 2490-2503.

[5]. Erickson, R. W. (1997, May). ***Some topologies of high-quality rectifiers***. In the Proc. of the First International Conference on Energy, Power, and Motion Control.

[6]. Chiang, S. J., Shieh, H. J., & Chen, M. C. (2009). ***Modeling and control of PV charger system with SEPIC converter***. Industrial Electronics, IEEE Transactions on, 56(11), 4344-4353.

[7]. Dongbing Zhang. (2013). ***Designing A SEPIC Converter*** This page was last modified on 21 November 2014, at 16:41. https://en.wiki2.org/wiki/Single-ended_primary-inductor_converter.

[8]. Mullett, C (2013). ***DC-DC Converter for Driving High-Intensity Light-Emitting Diodes with the SEPIC Circuit***. Application Note AND8138/D, available from ON Semiconductor (www. onsemi. com).

[9]. Venkatanarayanan, S., & Saravanan, M. (2014). ***Design and Implementation Of Low-Cost Sepic Photovoltaic System For Constant Voltage***. Journal of Theoretical & Applied Information Technology, 63(3).

[10]. Chiang, S. J., Shieh, H. J., & Chen, M. C. (2009). ***Modeling and control of PV charger system with SEPIC converter. Industrial Electronics***, IEEE Transactions on, 56(11), 4344-4353.

[11]. Wei, C. L., Chen, C. H., Wu, K. C., &Ko, I. T. (2012). ***Design of an average-current-mode noninverting buck-boost DC-DC converter with reduced switching and conduction losses***. Power Electronics, IEEE Transactions on, 27(12), 4934-4943.

[12]. Adar, D., Rahav, G., & Ben-Yaakov, S. (1997, June). ***A unified behavioral average model of SEPIC converters with coupled inductors.*** In Power Electronics Specialists Conference, 1997. PESC'97 Record. 28th Annual IEEE (Vol. 1, pp. 441-446). IEEE.

[13]. Moussa, W. M. (1995, March). ***Modeling and performance evaluation of a DC/DC SEPIC converter***. In Applied Power Electronics Conference and Exposition, 1995. APEC'95. Conference Proceedings 1995. Tenth Annual (pp. 702-706). IEEE.

[14]. Xiong, Y., Sun, S., Jia, H., Shea, P., &Shen, Z. J. (2009). ***New physical insights into power MOSFET switching losses***. Power Electronics, IEEE Transactions on, 24(2), 525-531.

[15]. Eberle, W., Zhang, Z., Liu, Y. F., &Sen, P. C. (2009). ***A practical switching loss model for buck voltage regulators. Power Electronics***, IEEE Transactions on, 24(3), 700-713.

[16]. Wai, R. J., & Shih, L. C. (2011). ***Design of voltage tracking control for a DC-DC boost converter via a total sliding-mode technique***. Industrial Electronics, IEEE Transactions on, 58(6), 2502-2511.

[17]. Lee, Y. J., Khaligh, A., Chakraborty, A., & Emadi, A. (2009). ***Digital combination of buck and boost converters to control a positive buck-boost converter and improve the output transients***. Power Electronics, IEEE Transactions on, 24(5), 1267-1279.

[18]. Mao, H., & Thottuvelil, V. J. (2000). ***Switching controller for a buck+boostconverter and method of operation***. U.S. Patent No. 6,037,755. Washington, DC: U.S. Patent and Trademark Office.

[19]. Chen, J., Maksimovic, D., & Erickson, R. W. (2006). ***Analysis and design of a low-stress buck-boost converter in universal-input PFC applications***. Power Electronics, IEEE Transactions on, 21(2), 320-329.

[20]. Dwelley, D. M., & Barcelo, T. W. (2000). ***Control circuit and method for maintaining high efficiency in a buck-boost switching regulator***. U.S. Patent No. 6,166,527. Washington, DC: U.S. Patent and Trademark Office.

[21]. Duran, E., Sidrach-de-Cardona, M., Galan, J., & Andujar, J. M. (2008, June). ***Comparative analysis of buck-boost converters used to obtain I–V characteristic curves of photovoltaic modules.*** In Power Electronics Specialists Conference, 2008. PESC 2008. IEEE (pp. 2036-2042). IEEE.

[22]. Kondrath, N., & Kazimierczuk, M. K. (2012). ***Comparison of wide-and high-frequency duty-ratio-to-inductor-current transfer functions of DC-DC PWM buck converter in CCM***. Industrial Electronics, IEEE Transactions on, 59(1), 641-643.

[23]. Huang, P. C., Wu, W. Q., Ho, H. H., & Chen, K. H. (2010). ***Hybrid buck-boost feedforward and reduced average inductor current techniques in fast line transient and high-efficiency buck-boost converter***. Power Electronics, IEEE Transactions on, 25(3), 719-730.

[24]. Lee, Y. J., Khaligh, A., & Emadi, A. (2009). ***A compensation technique for smooth transitions in a noninverting buck-boost converter***. Power Electronics, IEEE Transactions on, 24(4), 1002-1015.

[25]. Chen, J., Maksimovi C, D., & Erickson, R. (2001). ***Buck-boost PWM converters having two independently controlled switches***. In Power Electronics Specialists Conference, 2001. PESC. 2001 IEEE 32nd Annual (Vol. 2, pp. 736-741). IEEE.

[26]. Nanda k. k, & Giri R. (2013). ***A Positive Buck-Boost Converter Controlled By Digital Combination Of Buck And Boost Converters To Improve The Output Transients***" Vol.2, No.2, Pages: 139-148Special Issue of NCRTECE 2013 - 8-9 February.

KJPS Al-Kitab Journal for Pure Science
Vol.2 (2), ISSN: 2617-1260 (print), 2617-8141(online)
www.kjps.isnra.org

DOI: http://10.32441/kjps.02.02.p3

An Enhancement of Simultaneous Localization and Mapping Model Using Artificial Neural Networks

Musa. A.Hameed,
Department of Control of petroleum systems, College of Petroleum & Minerals Engineering, Tikrit University, Salahaldeen, Iraq.
mousa_hameed@yahoo.com,

ABSTRACT

This paper presents a model of Environment Representation Architecture for Intelligent Robot. The model consists of a vehicle, an environment, and landmarks. The proposed method is based on using SLAM based on ANN, back propagation algorithm, to be trained on predefined datasets on some environment. In this paper dun Using Artificial Neural on the Simultaneous Localization and Mapping enhances the obtained maps of the robot. Limitation of this paper to test the proposed system, different maps with different datasets are required, however, these datasets, need expensive sensors, vehicles and GPS receivers to be built. Use this information to build their decisions. The systematic error was solved by the proposed approach using ANN, depends only on the initial values that were used during the training phase, it considers previous landmarks in order to build the next route, but on the other hand, it does not accumulate the previous error.

Keywords: Simultaneous Localization and Mapping (SLAM), Artificial Neural Network (ANN).

.

KJPS Al-Kitab Journal for Pure Science
Vol.2 (2), ISSN: 2617-1260 (print), 2617-8141(online)
www.kjps.isnra.org

تعزيز خوارزمية التوطين ورسم الخرائط في ان واحد باستخدام الشبكات العصبية الاصطناعية

موسى عبدالله حميد

قسم سيطرة المنظومات النفطية، كلية هندسة النفط والمعادن، جامعة تكريت، صلاح الدين، العراق.

Mousa_hameed@yahoo.com

الملخص

يقدم هذا البحث نموذج لهيكلية تمثيل البيئة للروبوت الذكي باستخدام الشبكات العصبية الاصطناعية. النموذج يتكون من سيارة، بيئة ومعالم. الطريقة المقترحة هي مبنية على استخدام التوطين ورسم الخرائط في وقت واحد بالاعتماد على الشبكات العصبونية الذكية، خوارزمية الانتشار الخلفي، ليتم تعليمها على مجموعات البيانات المعرفة مسبقا لنفس البيئة. في هذا البحث تم استخدام الشبكات العصبونية الذكية والتوطين ورسم الخرائط في وقت واحد لتطوير الخريطة المبنية للبيئة عن طريق الروبوت. المحددات في هذا البحث تكمن في فحص النظام المقترح. خرائط مختلفة مع مجموعات بيانات مختلفة مطلوبة، هذه المجموعات من البيانات تحتاج مجسات غالية الثمن مركبة وأجهزة استقبال واحداثيات ليتم بناؤها. تم حل الخطأ المنهجي من خلال النهج المقترح باستخدام الشبكات العصبية الاصطناعية، بالاعتماد فقط على القيم الأولية التي استخدمت خلال مرحلة التدريب، بالنظر للمعالم السابقة من أجل بناء الطريق التالي، لتجنب عدم تراكم الاخطاء السابقة.

الكلمات الدالة: خوارزمية التوطين ورسم الخرائ في ان واحد، الشبكات العصبية الاصطناعية.

1. Introduction

Many natural systems of most creatures in the world are very rich topics for the scientific researchers, since that a simple individual behavior can cooperate to create a system able to solve a real complex problem and perform very sophisticated tasks [1] "SLAM has been performed theoretically in different forms; it is also implemented in different domains, such as, indoor, outdoor and underwater environments. Probabilistic SLAM problem was first proposed at the IEEE Robotics and Automation Conference on 1986. Many researchers had been working on applying estimation-theoretic methods to environment mapping and

localization problems. A few years later a new statistical method was established by Smith, Cheesman and Durrant-White" [2]. "This statistical based for measuring the relationships between landmarks in addition to manipulating geometric uncertainty. They showed in their work that there must be a high degree of correlation between the estimation of different landmark locations in the map, which grows with successive observations".

Zhan et al [3], "focused on visual methods to find solutions to this problem, using sensor fusion navigation, resulted in enhancing the landmark representation of the environment, other researches based on visual methods allowed a mobile robot to move through an unknown environment taking relative observations of landmarks" [4] [5]. "The high correlation between the estimates of these landmarks was due to the margin of error in the estimated vehicle location" [6].

"The landmarks positions in addition to the vehicle situations shape a full solution to the localization and mapping combined problem. However, a huge state vector required to be implemented scaling the number of landmarks in the map. Thus, the researchers considered the complexity of the mapping problem computations only, regardless of its convergence, they focused their attention on a sequence of approximations to the solution of the localization and mapping problem. Their method considered minimizing the high correlation between the landmarks, resulted in reducing the usage of the filter to a series of decupled landmark to vehicle filter" [7] [8].

"SLAM problem structure and the results of the convergence was first presented. Recently, several kinds of research and approaches were proposed on the theory of convergence, such as [9] [10] [11]. Also on localization and mapping", such as [12] [13] [14] [15] [16] [17], "working on indoor, outdoor and underwater environments" [18].

Modeling of environment for use in robotic systems has, in fact, become a major focus of contemporary autonomous robotic research. There are many researchers have done research in this area, but are considering the specific environment and this research considering the general environment. There are problems related to the development of a model for general environments, such as; How to build a robotic system capable of building map proximity

form the original environment by identifying the characteristics of the environment and work in any environment. How to identify the relationships between required information for a robot related to an environment with the robot tasks. Simultaneous Localization and Mapping (SLAM) algorithm, is an algorithm used by robots for map building, this work will be based on SLAM algorithm calculations to produce the mapped datasets and landmark. On the other hand, Artificial Neural Network (ANN) algorithms are very important for modern systems, which it can be trained and work without pre-requests. While SLAM requires pre-requests in order to build the robots landmarks and map. The proposed system in this work uses ANN to allow the robots to build its own map without pre-requests. Moreover, ANN enhances SLAM and allows the robot to map any environment.

2. Methodology

The proposed model for the environment representation architecture consists of five parts; these are Organize Object in environment, landmark, localization, algorithm SLAM, and Apply of ANN form the environment, as seen in figure 1.

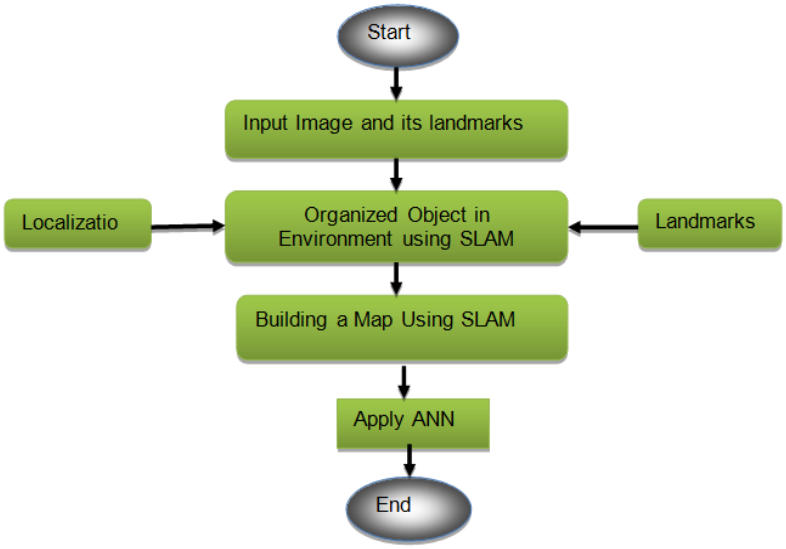

Figure 1: Flow chart of Development Representation an Environment for Robot

2.1 The Environment

In this paper will be considered one types of environment that is static. The static environment is the environment that does not change and can be easily dealt with by an intelligent agent [20].

Using SLAM for construction of a map for the environment for a priori data or put the update on a given map in a known environment using vehicle without forgetting to keep its track of the position [20].

In the following subsections are the brief descriptions for SLAM objectives, building a map and locating the vehicle simultaneously.

SLAM makes a vehicle capable to move in an environment with an unknown location, moreover [21]. It allows the vehicle to map this environment simultaneously, and use this map to calculate vehicle location. Figure 2 presents how to do SLAM using internal representations for the positions of landmarks (map) and the vehicle parameters, always takes the zero starting position.

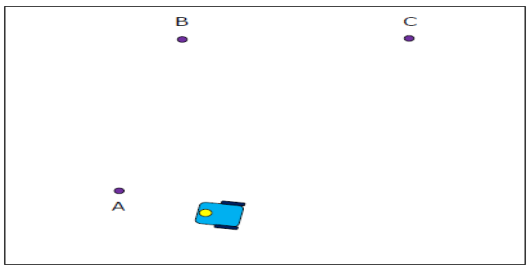

Figure 2: SLAM Behavior [23]

Localization and mapping are coupled, each has a relationship with the other For this reason, been getting better results [23].

2.2 Modeling Vehicle Coordinated System

To position the used vehicle several parameters as shown in Figure 4. "In Figure 4 explain vehicle navigation in the environment, that means the robot's ability to determine the

position in the environment and then to plan a path towards goal location. Navigation can be defined as the combination of the three fundamental competencies: localization, path planning, map-building. Robot localization denotes the robot's ability to determine its position and orientation in the environment. Path planning is effectively an extension of localization, in that it requires the determination of the robot's current position and a position of a goal location. Map building can be in the shape of a metric map or any way. In this study use, steering control alpha is defined in vehicle coordinate frame; the laser sensor is located in the front of the vehicle and returns range and bearing related to objects at distances of up to 50 meters, high-intensity reflection can be obtained by placing high reflectivity beacons in the area of operation".

In this study use "steering control alpha is defined in vehicle coordinate frame as shown in Figure 4; the laser sensor is located in the front of the vehicle and returns range and bearing related to objects at distances of up to 50 meters, high-intensity reflection can be obtained by placing high reflectivity beacons in the area of operation".

"The landmarks are labeled as Bi(i=1..n) and measured with respect to the vehicle coordinates (x_1, y_1), that is $z(k)$ = (r, b, I), where r is the distance from the beacon to the laser, b is the sensor bearing measured with respect to the vehicle coordinate frame and I is the intensity information".

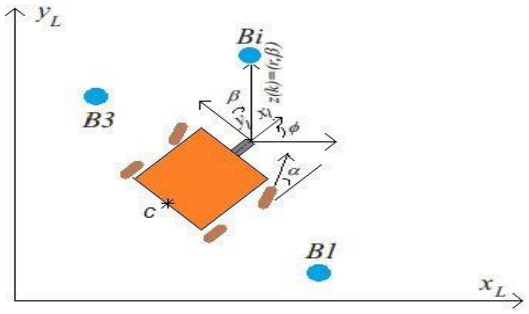

Figure 3: Vehicle Coordinated System

Figure 5 shows the kinematic parameters of the vehicle. This figure does not change (fixed) explains measurements between the landmarks of the environment and the landmarks of the vehicle and between measurements components of the vehicle.

KJPS Al-Kitab Journal for Pure Science
Vol.2 (2), ISSN: 2617-1260 (print), 2617-8141(online)
www.kjps.isnra.org

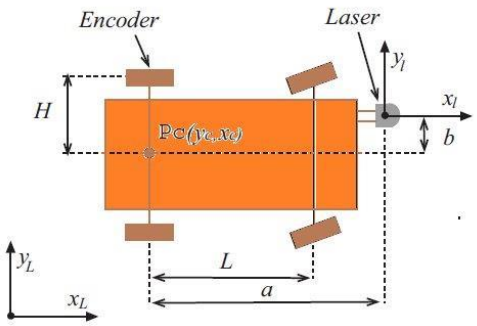

Figure 4 Kinematics parameters

"Suppose that the vehicle is controlled through the vehicle velocity Vc and the steering angle α. Then to predict the trajectory of the back axle center C, the below equation should be followed. Because the laser is located in the front of the vehicle, the translation of the center of the back axle, the transformation data is defined by the orientation angle, the velocity is generated by the encoder and translated to the center of the axle".

2.4 Artificial Neural Networks

A neural network "consists of a set of neurons connected together by weighted connections. It is characterized mainly by the type of units used and by its topology. There are two types of specific neurons in a network: neurons receiving input data from the outside world (the situation) and the output neurons providing the result of the performed treatment (the evaluation)"[26].

2.4.1 Architecture of ANN

Input layer represents the raw information that is fed into the network that consists of 16 layers. This part of the network is never changing its values. Every single input to the network is duplicated and sends down to the nodes in the hidden layer. Hidden Layer accepts data from the input layer. It uses input values and modules them using some weighted value, this new value is then sent to the output layer but it will also be modified by some weight from the connection between hidden and the output layer. Output layer consist of 16 layer process information received from the hidden layer and produces an output [26].

KJPS Al-Kitab Journal for Pure Science
Vol.2 (2), ISSN: 2617-1260 (print), 2617-8141(online)
www.kjps.isnra.org

2.5 Back Propagation (BP) Algorithm

One of the most popular NN algorithms is "backpropagation algorithm. Claimed that BP algorithm could be broken down to four main steps. After choosing the weights of the network randomly, the backpropagation algorithm is used to compute the necessary corrections. The basic formula for BP algorithm". "The algorithm can be decomposed in the following four steps"[27]:

- Feed-forward computation.
- Backpropagation to the output layer.
- Backpropagation to the hidden layer.

3. Implementation of the Model to Build Map

The evaluated of this algorithm by using MATLAB® R2013a. The systematic error found in Nebot's work was solved by the proposed approach, because, using ANN, depends only on the initial values that were used during the training phase, it considers previous landmarks in order to build the next route, but it does not accumulate the previous error.

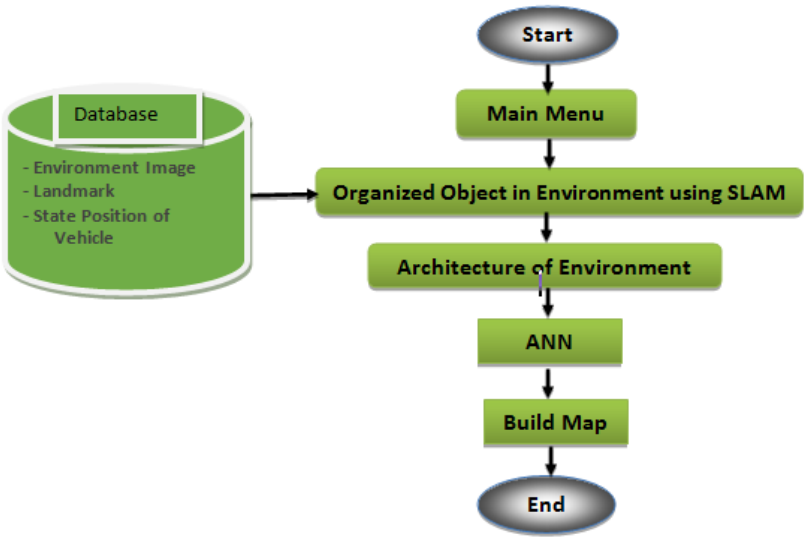

Figure 5: a Flow chart for Implementation the model to build a map

4. Results and Discussion

The navigation system was tested with a utility vehicle retrofitted with the described sensors. The utility car used for the experiment is shown in Figure 9.

Figure 6: Utility car used for the experiments (Nebot 2000)

In the experiment," using the dataset contains the true landmarks and GPS coordinates for his map were taken from Drexel Autonomous System Lab datasets, which were scanned using a SICK scanner (Drexel), in this study used the vehicle model and sensor pose, mentioned earlier". The "stars in the map represent potential natural landmarks and the "circles" are the artificial reflective beacons. Although this environment is very rich with respect to the number of natural landmarks, the data association becomes very difficult since most of the landmarks are very close together". The evaluation of the model was using MATLAB® R2013a. After explaining the proposed approach and methodology, in addition to the experiment and evaluation of this approach, in the next section, the result showing for SLAM and ANN as seen in figure 7,8:

KJPS Al-Kitab Journal for Pure Science
Vol.2 (2), ISSN: 2617-1260 (print), 2617-8141(online)
www.kjps.isnra.org

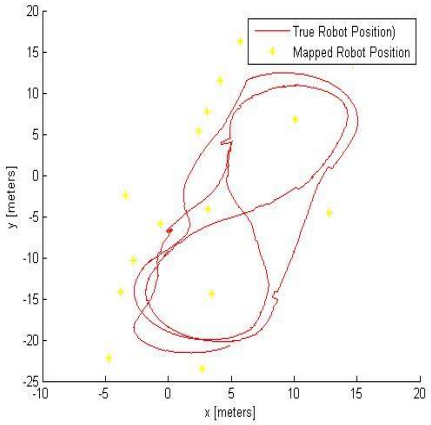

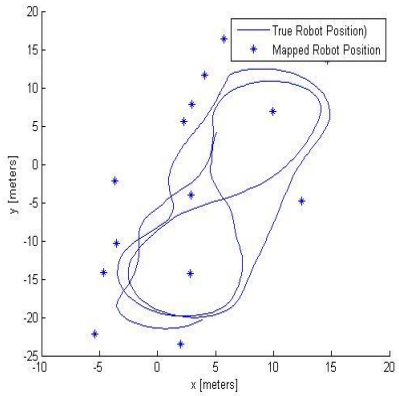

Figure 7: The Result Map from ANN **Figure 8: Building Map Using SLAM**

To improve results and reduce the error in the artificial neural network by giving you a number of examples of (input) in order to give better results and working principle of this artificial neural network

The resulted map is shown in the below Figure 9.

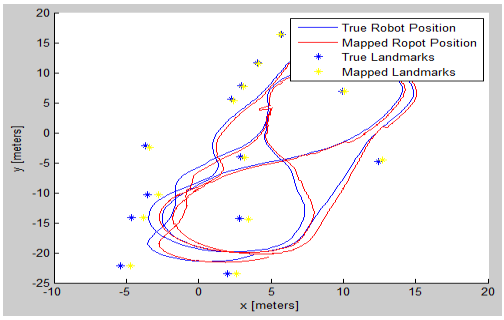

Figure 9: True and Robot Maps

As it is shown in Figure 5 above, you have reached a relatively good result in mapping the landmarks and the environment, the robot followed the same direction, but with small error margin.

The ANN error histogram is shown in the below Figure 10.

KJPS Al-Kitab Journal for Pure Science
Vol.2 (2), ISSN: 2617-1260 (print), 2617-8141(online)
www.kjps.isnra.org

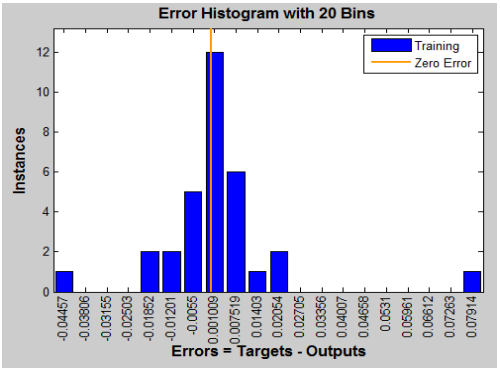

Figure 10: ANN Model Error Histogram

The performance plot is shown in Figure 11, below.

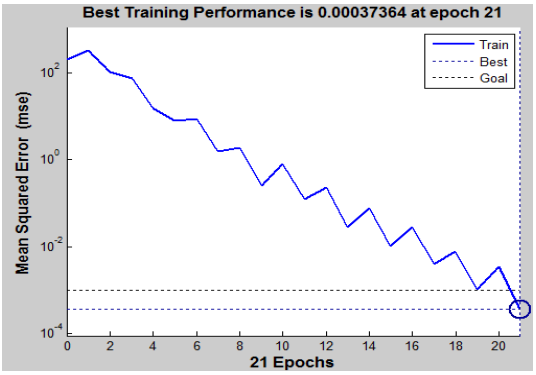

Figure 11: Performance Plot

From the error histogram and the plots above, "it is noticed that good results of landmarks mapping are reached, which is very close to the true landmarks position. Based on that, very good results of environment mapping have been obtained, as shown in Figure 9 above; the model mapped line is very close to the true line".

It can be noticed from the figures above, that very good results in comparison to the previous works are reached, some of them discussed previously. Using Artificial Neural Network (ANN) enhanced the accuracy of the map, which is noticed in figure 8 where the mapped landmarks and routes are almost the same. Moreover, using ANN enhanced the speed of

map building which is a very important achievement especially in real-time applications, or in robots that use this information to build their decisions.

The systematic error found in Nebot's work (Nebot 2000), "was solved by the proposed approach, because, using ANN, depends only on the initial values that were used during the training phase, it considers previous landmarks in order to build the next route, but on the other hand, it does not accumulate the previous error. The table show of the compression between the work of SLAM and ANN".

4.1The Developed Application

In this section, work is enhanced SLAM algorithm based on ANN. In this method, using Back-propagation ANN to make the robot estimate the locations of landmarks accurately.

In this algorithm "used the equations of the SLAM landmark equations to train a neural network; a landmark dataset is also used from Drexel Autonomous System Lab datasets, which were scanned using a SICK scanner (Drexel)" as seen below:

The original landmark ⟶ SLAM algorithm ⟶ result of SLAM (build map using

(Input) SLAM)

In this works has been trained the ANN on the SLAM landmark equation results as seen below:

The result of SLAM ⟶ operation ANN ⟶ result of ANN (build map using ANN)

(Input)

The evaluated of this algorithm by using MATLAB® R2013a. The systematic error found in Nebot's work was solved by the proposed approach, because, using ANN, depends only on the initial values that were used during the training phase, it considers previous landmarks in order to build the next route, but it does not accumulate the previous error.

5. Conclusions

The proposed solution for this book concerns the localization of a vehicle and an environmental mapping simultaneously. The design of this algorithm, in addition to the modeling aspects, is presented with an implementation of it. Modeling SLAM using landmarks does not require any landmarks surveying.

References

[1]. Hussein H. Owaied, Suhaib I Al-Ghazi, ***"Developing Cognitive Map from Blueprint Map"***, Trent of Applied Sciences Research, Issue 6, No. 8, pp 848-862 (2011).

[2]. H.F. Durrant-Whyte. ***"Uncertain geometry in robotics".*** *IEEE Trans. Robotics and Automation*, 4(1):23{31, (1988).

[3]. Zhang, Xinzheng, Ahmad B. Rad, and Yiu-Kwong Wong. ***"Sensor fusion of monocular cameras and laser rangefinders for line-based simultaneous localization and mapping (SLAM) tasks in autonomous mobile robots."*** Sensors 12.1, 429-452 (2012).

[4]. Engelhard, Nikolas, et al. ***"Real-time 3D visual SLAM with a hand-held RGB-D camera."*** Proc. of the RGB-D Workshop on 3D Perception in Robotics at the European Robotics Forum, Vasteras, Sweden. Vol. 2011. 2011.

[5]. Gil, Arturo, et al. ***"A comparative evaluation of interest point detectors and local descriptors for visual SLAM"***, Machine Vision and Applications 21.6 (2010): 905-920.

[6]. J.J. Leonard and H.F. Durrant-Whyte. "***Simultaneous map building and localization for an autonomous mobile robot***". In Proc. IEEE Int. Workshop on Intelligent Robots and Systems (IROS), pages 1442{1447, Osaka, Japan, 1991.

[7]. Sola, Joan, et al. ***"Impact of landmark parametrization on monocular EKF-SLAM with points and lines."*** International journal of computer vision 97.3 (2012): 339-368.

[8]. Carrillo, Henry, Ian Reid, and José A. Castellanos. ***"On the comparison of uncertainty criteria for active SLAM"***, Robotics and Automation (ICRA), 2012 IEEE International Conference on. IEEE, 2012.

[9]. H. Durrant-Whyte, D. Rye, and E. Nebot. ***"Localisation of automatic guided vehicles"***. In G. Giralt and G. Hirzinger, editors, Robotics Research: The 7th International Symposium (ISRR'95), pages 613{625. Springer Verlag, 1996.

[10]. Cheein, Fernando A. Aunt, and Ricardo Carelli. ***"Analysis of different feature selection criteria based on a covariance convergence perspective for a SLAM algorithm"*** Sensors (Basel, Switzerland) 11.1 (2011): 62.

[11]. Dissanayake, Gamini, et al. ***"Convergence comparison of least squares based bearing-only SLAM algorithms using different landmark parametrizations."*** (2012).

[12]. Benini, A., et al. ***"Adaptive extended Kalman filter for indoor/outdoor localization using an 802.15. 4a wireless network***." Proceedings of the 5th European Conference on Mobile Robots ECMR. 2011.

[13]. Kümmerle, Rainer, et al. ***"Large scale graph-based SLAM using aerial images as prior information"***, Autonomous Robots 30.1 (2011): 25-39.

[14]. McDonald, John, et al. ***"6-DOF multi-session visual SLAM using anchor nodes"***, European Conference on Mobile Robotics, Orbero, Sweden. Vol. 13. 2011.

[15]. Lee, Yong-Ju, Jae-Bok Song, and Ji-Hoon Choi. ***"Performance Improvement of Iterative Closest Point-Based Outdoor SLAM by Rotation Invariant Descriptors of Salient Regions"***, Journal of Intelligent & Robotic Systems (2012): 1-12.

[16]. Mei, Christopher, et al. ***"Hidden view synthesis using real-time visual SLAM for simplifying video surveillance analysis"***, Robotics and Automation (ICRA), 2011 IEEE International Conference on. IEEE, 2011.

[17]. Stachniss, Cyrill, Stefan Williams, and José Neira. ***"Editorial: Visual navigation and mapping outdoors",*** Journal of Field Robotics 27.5 (2010): 509-510.

[18]. Lee, Yong-Ju, Joong-Tae Park, and Jae-Bok Song. ***"Three-dimensional outdoor SLAM Using rotation invariant descriptors of salient regions"***, Control, Automation and Systems (ICCAS), 2011 11th International Conference on. IEEE, 2011.

[19]. M.W.M.G. Dissanayake, P.Newman, H.F. Durrant-Whyte, S. Clark, and M.Csobra. ***"An experimental and theoretical investigation into simultaneous localization and map building (SLAM)".*** In Proc. 6th International Symposium on Experimental Robotics, Pages 171-180, Sydney, Australia, March 1999.

[20]. Berns, Karsten, and Ewald von Puttkamer. ***"Simultaneous localization and mapping (SLAM)"***, Autonomous Land Vehicles. Vieweg+ Teubner, 2009. 146-172.

[21]. Chin, Wei Hong, and Chu Kiong Loo. ***"Topological Gaussian ARAM for Simultaneous Localization and Mapping (SLAM)"***, Micro-NanoMechatronics and Human Science (MHS), 2012 International Symposium on. IEEE, 2012.

[22]. Margarita Chli, ***"Simultaneous Localization And Mapping",*** AUTONOMOUS SYSTEMS LAB, (2011).

[23]. Drexel Autonomous System Lab (DASL). ***"Simultaneous Localization and Mapping (SLAM)"***, Drexel University (2011).

[24]. Nebot Eduardo, Jose Guivant and Stephan Baiker " ***Autonomous Navigation and Map building Using Laser Range Sensors in Outdoor Applications***", Journal of robotics systems, Vol 17, No 10, October, (2000).

[25]. Mirza Cilimkovic, "***Neural Networks and Back Propagation Algorithm, Institute of Technology",*** (2009)

[26]. Raul Rojas, ***"Neural Networks: A Systematic Introduction"***, (2005).

KJPS Al-Kitab Journal for Pure Science
Vol.2 (2), ISSN: 2617-1260 (print), 2617-8141(online)
www.kjps.isnra.org

DOI: http://10.32441/kjps.02.02.p4

Candida spp Complications in Acute Myeloid Leukemia Patients in Erbil City

***Payman A.Hamsaeed [1], Amera M. Muhammad [2]**

[1] Biology Department , College of Education , Salahaddin University , Erbil, Iraq.

Pathological analysis Department, College of Science, Knowledge University, Erbil, Iraq.

[2] Biology Department, College of Science, Mosul University, Mosul, Iraq.

1paymanakram@yahoo.com, 2 umnashwa@yahoo.com

ABSTRACT

This study has been carried out in Erbil City -Iraq, 30 patients were diagnosis by flow cytometry as AML which they were admitted to Nanakaly Hospital for Blood Disease and submitted to chemotherapy. Number of adults/children 22 (73.3%) / 8 (26.7%), female / male 13 (43.3%) / 17(56.7%). Only 20 (66.7%) patients were smoker. The highest number was subtyping M4 10 (33.3%) patients, followed by M1 7(23.3%), M3 6(20%), M2 were 3(10%) patients. M5 and M6 were 2 (6.7%). Ten candida spp isolates before induction phase chemotherapy show 9(90%) C.albicans, 1(10%) C. lusitaniae, and from 32 isolates after induction phase chemotherapy, 17(53.1%) C.albicans, 7(21.9%) C. lusitaniae, and 8(25%) C.famata. According to the site of infection, before starting chemotherapy 8(88.9%) C. albicans isolates were in the oral cavity and 1(11.1%) on the skin, while C. lusitaniae was 1 (100%) in oral cavity only. While after chemotherapy 12(70.6%) C.albicans in the oral cavity and 5(29.4%) on the skin, C. lusitaniae was 2 (28.6%) in the oral cavity and 5(71.4%) on the skin, while all C. famata was 8 (100%) on the skin.

The immunophenotype shows that the number and percentage of patients which the myeloid cells expressed cyMPO was 27(90) with mean percentage of positivity 59.38, while all patients expressed CD33 and CD13 on their blast cell 30(100) with a mean percentage of positivity 59.81 and 30.83 respectively.

Keywords: Blood cancer, flow cytometry, *candida spp*, chemotherapy.

KJPS Al-Kitab Journal for Pure Science
Vol.2 (2), ISSN: 2617-1260 (print), 2617-8141(online)
www.kjps.isnra.org

تعقيدات فطر *Candida spp.* في مرضى سرطانِ الدم المايلودي الحاد في مدينة أربيل

* بيمان اكرم حمه سعيد [1] ،اميرة محمود محمد [2]

[1] قسم البايولوجي، كلية التربية ، جامعة صلاح الدين ، اربيل ، العراق/ قسم التحليلات المرضية ، كلية العلوم ، جامعة نولج ، اربيل

[2] قسم البايولوجي، كلية العلوم ، جامعة موصل, موصل ، العراق.

[1]paymanakram@yahoo.com, [2] umnashwa@yahoo.com

الملخص

أجريت هذه الدراسةِ في محافظةِ أربيل , العراق. تم تشخيص 30 مريض بواسطة جهاز cytometry flow مصاب بسرطانِ الدمِّ من نوع AML والذين أُدخلوا إلى مستشفى نانةكةلي لامراضِ الدمِّ وخضعوا للعلاج الكيمياوي. عدد المرضى بالغين/اطفال 22 (73.3 %) / 8 (26.7 %) ، عدد الأناث/ الذكورِ كَانَ 13 (43.3 %) / 17 (56.7 %). فقط 20 (66.7 %) مرضى كَانوامن المدخّنينَ.ان العددَ الأعلى من المرضى كَانتْ 4 10M(33.3%) مريض، تَليها 7M1 (23.3)، 6 M3(20%) و2 M كانت 3 (10 %) .كُلّ من مرضى 5 M و6 M كَانتْ 2 (6.7 %). عشرة عزلات فطرَ Candida spp قَبْلَ العلاج الكيمياوي كانّت 9 (90 %) عزلة C albicans،و1(10%)عزلة C. lusitaniae، ومِنْ 32 عزلة وبعد العلاج الكيمياوي 17 (53.1 %) عزلة كَانَت C. albicans، 7(21.9%) كَانَ C. lusitaniae، و8 (25 %) كَانَ C. famata. طبقاً لموقعِ العدوى، قبل بَدْء العلاج الكيمياوي 8 (88.9 %) C. albicans في التجويفِ الفمي و1 (11.1 %) على الجلدِ، بينما C. lusitaniae كَانَ 1 (100 %) في التجويفِ الفمي فقط. بعد العلاج الكيمياوي 12 (70.6 %) C. albicans في التجويفِ الفمي و5 (29.4 %) على الجلدِ، C. lusitaniae كَانَ 2 (28.6 %) في التجويفِ الفمي و5 (71.4 %) على الجلدِ، بينما كُلّ C. famata كَانَ 8 (100 %) على الجلدِ.

KJPS Al-Kitab Journal for Pure Science
Vol.2 (2), ISSN: 2617-1260 (print), 2617-8141(online)
www.kjps.isnra.org

بينت التنميط المناعي immunophenotype بأنّ العددَ والنسبة المئويةَ مِنْ المرضى الذي اظهرت خلايا myeloid cyMPO كَانتْ 27 (90 %) وكانت معدل النسبة المئويةِ للإيجابيةِ 59.38، بينما اظهر CD33و 13 CDعلى خليةِ السرطانية لجميع المرضى 30 (100 %) وكانت معدل النسبة المئويةِ للإيجابيةِ 59.81 و30.83 على التوالي

الكلمات الدالة: سرطان الدم ،فلوسايتوميتر ،*candida spp*.، العلاج الكيميائي .

1. Introduction

Blood cancer or leukemia is a type of blood or bone marrow (BM) cancer characterized by an abnormal increase of cells called "blasts" [1]. All hematopoietic neoplasms can be classified to acute and chronic leukemia. Acute leukemia which is characterized by a rapid and uncontrolled proliferation of hematopoietic precursor cells, with a loss of maturation and differentiation was classified to acute lymphoid leukemia (ALL) and acute myeloid leukemia (AML) [2][3]. AML is a hematological malignancy resulting from the proliferation of a clone of myeloid stem cells that show defective or absent maturation. The French-American-British (FAB) classification system divided AML into 8 subtypes(M0- M7) based on the type of cell from which leukemia developed and the degree of its maturity [4][5]. The AML occurs at all ages, but it is predominantly a disease of adults. The incidence rises progressively with age, reaching 12.6 per 100,000 in adult ≥65 years. Approximately 85% of acute leukemia in adults are AML, compared to 15% of acute leukemia in children [6].

In AML the blast cells often differ from more mature cells by expressing markers of immaturity and lacking antigens expressed by more mature cells. Immunophenotype by flow cytometry is most useful in identifying myeloid lineage and distinguishing between AML and ALL. Myeloid lineage–associated markers include CD13, CD15, and CD33.CD7 is often found on AMLs (M0 and M1) [7].

Infectious complications Infections are an important cause of morbidity and mortality in leukemia patients, which are at high risk of infection, likely related to the intensity of their induction phase chemotherapy resulting in repeated episodes of prolonged and profound

neutropenia. Infections also prolong hospitalization, compromise chemotherapy delivery, affect the quality of life, and increase health care utilization. Furthermore, protracted empiric and therapeutic use of broad-spectrum antibiotics may contribute to the evolution of resistant microbiologic flora (Lange *et al*., 2004). Fungal infections with *Candida albicans C. tropicalis C. krusei C. glabrata* are a threat to patients who have prolonged neutropenia [8].

Systemic fungal infections including those by *C. albicans* have emerged as important causes of morbidity and mortality in immunocompromised patients. Nosocomial candidemia occurs predominately in patients who have hematological malignancies and/or have undergone stem cell transplantation and is associated with a high mortality rate [9]. In addition, hospital-acquired infections by *C. albicans* have become a cause of major health concerns. Patients with AML developed cervical lymphadenitis and chronic disseminated infection due *to C. albicans* [10]. *C.albicans* appendicitis was reported in a neutropenic patient after induction chemotherapy [11]. *Candida lusitaniae* was first identified as a human pathogen in 1979. There has been a marked increase in the number of recognized cases of candidemia due to this organism in the last two decades, bone marrow transplantation and high dose cytoreductive chemotherapy have both been identified as risk factors for infections with this organism [12]. *Candida Famata* is a hemiascomycetous yeast commonly found in natural substrates and in cheese [13]. It has been described in human infections [14][15]. *C. famata* has been reported in the patient undergoing chemotherapy for Hodgkin's disease and caused bloodstream infections [16][17].

2. Material and Methods

A- Patients

This study included 30 newly diagnosed blood cancer patients type AML before treatment and after the first induction phase chemotherapy, they admitted to the" Nanacally Hospital for Blood Disease" in Erbil province A questionnaire form was provided to each patient which included age, sex, family degree, education level, smoking, residence (geographical area).

B- Sample collection

1-Bone marrow aspiration

Two ml bone marrow samples (BM) were collected aseptically in collaboration with senior hematopathologists at Nanakaly Hospital. (BM) from patients with newly diagnosed blood cancer were studied with flow cytometry FC500 with a battery of monoclonal antibodies. For the FC evaluation, the BM was diluted with phosphate buffered saline (PBS) to maintain cells *in vitro* for brief periods. The immunophenotyping staining procedures are:

A-Surface membrane staining of the blast cells

1- The combination of fluorochrome-conjugated antibodies for each panel designed for an FC study was added to 12×75 mm plastic test tubes supplied by Beckman Coulter.

2- Then 100 µL of single-cell BM suspension was pipetted into the tubes and incubated at room temperature (18-25°C) for 15-20 minutes in the dark.

3- Two ml VersaLysisR lysing solution was added to each tube to destroy RBCs in the sample. The samples were gently vortexed and incubated for 10 minutes in the dark at room temperature.

4- The mixture was then centrifuged for 5 minutes at 150 rpm and the supernatant discarded.

5- The cell pellet was washed by re-adding 2 ml of PBS to each tube and centrifuged at 150 rpm for 5 minutes. The supernatant was discarded and the cell pellet resuspended with 0.5 ml of PBS to each tube. The sample will be ready for FC study within 2 hours.

b- Intracytoplasmic and nuclear staining procedures

1- Hundred µl of reagent 1IntraPrepR (fixative reagent) was added to a 50µl BM sample to fix the cells. The specimen was then incubated for 15 minutes in the dark.

2- Four ml PBS solution was added and centrifuged for 5 minutes at 300 rpm, and then the supernatant was discarded.

3- Hundred µl of reagent 2 (IntraPrepR permeabilization solution) was added to the separated cell pellet and incubated for 5 minutes in the dark. This procedure creates holes in the cytoplasmic and nuclear membrane that allowed monoclonal antibodies (MoAbs) to enter the internal structures of the cell.

4- The fluorescent-conjugated monoclonal antibodies for cytoplasmic and nuclear antigen detection were added and allowed to incubate for 15-20 minutes in the dark. In this step, antibodies diffuse into the interior of the cell.

5- Four ml PBS solution was added for washing. After 5 minutes centrifugation at 300 rpm, the cell pellet was suspended in 0.5 to 1 ml PBS. The sample was ready for FC study. After FC was completed, the cases were given a blast lineage assignment as myeloid or lymphoid classification based upon antigen expression.

2- Skin and abscess swabs

The swab tip was moistened with normal saline and was rotated in the center of the skin or abscess for 30 seconds. Then the swab was placed in the appropriate container and cultured on Sabuorate agar media.

3- Oral cavity swabs

The cotton tip of the swab was typically rubbed on the inside of the oral cavity for several seconds then placed into a sterile container to cultured on Sabuorate agar media.

Skin or abscess swabs and oral cavity swabs were streaked on Sabouraud agar plates gently. plates were incubated at 25°C for 5-7days and identified by VITEK 2 directly in which a sterile swab on applicator stick was used to transfer a sufficient number of pure culture and to suspend the microorganism in 3 ml of sterile saline (aqueous 0.45% to 0.50% NaCl, pH 4.5 to 7.0) in a 12 x 75 mm clear plastic polystyrene test tube. The turbidity was measured using a turbidity meter (Denis Chek™). Suspension turbidities used for card

inoculation (McFarland Turbidity Range) for fungi were 1.80 - 2.20. For Card Sealing and Incubation, the inoculated cards were passed by a mechanism, which cut off the transfer tube and seals the card prior to loading into the carousel incubator. Identification levels of unknown biopattern were compared to the database of reactions for each taxon, and a numerical probability calculation was performed. Various qualitative levels of identification were assigned based on the numerical probability calculation. The different levels were Excellence 96-99%, Very good 93 -95%.

3. Results and Discussion

Table1 shows the distribution of patients according to some risk factors. Most of the AML patients were adults 22 (73.3) and children were 8 (26.7). Another study on the prevalence of acute leukemia among a group of Iraqi patients with acute leukemia registered and treated in Oncology Department attached to the Al-Yarmuk Teaching Hospital and Child Central Hospital in Baghdad were showed that the incidence with AML in adults was 27.5% (Mohammad *et al*., 2009). The result shows that the number of female to male patients was 13 (43.3)/17(56.7). In another study included 115 Iraqi patients with AML, there were 63 males and 52 females with a median age of 35 years [18]. Prevalence and comparison of male and female patients with different types of leukemia during 2001-2010 in the multiethnic population of North Karnataka, there were 122,000 males 78,000 female in AML [19]. [20] found 8/22 females to male in AML patients. [21] found 14 females and 25 males AML patients. Most of the patients were without family relationship 15 (50%). Most of AML patients10 (33.3) were of a bachelor level. 20 (66.7) of AML patients were a cigarette smoker. This result agrees with [22] who found that among the 161 males and 119 females with AML, 101 (36.1%) had never smoked and 179 (63.9%) were ever smokers.

KJPS Al-Kitab Journal for Pure Science
Vol.2 (2), ISSN: 2617-1260 (print), 2617-8141(online)
www.kjps.isnra.org

Table 1 showed the distribution of patients according to some risk factors.

Risk factors	AML	
	N	%
Child(≤ 18 years)	8	26.7
Adult(>18 years)	22	73.3
Male	17	56.7
Female	13	43.3
Family relationship		
First degree	7	23.3
Second degree	6	20.0
Third degree	2	6.7
None	15	50.0
Education level		
Primary	2	6.7
Secondary	6	20
Diploma	5	16.7
Bachelor	10	33.3
None	7	23.3
Smoking		
Non smoker	10	33.3
Smoker	20	66.7
Total	30	100%

Exposure to ionizing radiation such as the atomic bombings of Hiroshima and Nagasaki had an increased rate of AML [23]. Alkylating agents and inhibitors of DNA topoisomerase II enzyme, increase the risk of leukemia both in children and adults. The disease occurs mostly as AML, in some cases also as ALL [24][25]. The chemical classes most commonly associated with childhood leukemia are hydrocarbons and pesticides. The most widely recognized hydrocarbon is benzene which has a strong relationship with leukemia [26]. On the other hand, [27] suggested a link between pesticides exposure and childhood leukemia. Chronic exposure to certain chemicals such as benzene, embalming fluids, ethylene oxides, and herbicides also appears to be at increased risk [28]. Workers exposed to benzene were found to have increased levels of cytogenetic abnormalities associated with AML [29]. Smoking has been increased risk of developing AML

especially in those persons aged 60–75 [30]. Smoking increases the risk of AML blood cancer and causes around 6% of all leukemia cases in the United Kingdom [31].

Table2 describes the immunophenotype or the CD marker of AML leukemia. The number and percentage of patients which the myeloid cells expressed cyMPO 27(90) with mean percentage of positivity 59.38,while all patients expressed CD33 and CD13 on their blast cell 30(100) with mean percentage of positivity 59.81 and 30.83 respectively, while CD 117,CD15, CD34, CD64, CD36 and CD14 positivity were 21(70), 13(43.33), 8(26.67), 10(33.33), 11(36.67) and 11(36.67) respectively, with mean percentage of positivity 48.33, 24.66, 45.11, 56.22, 43.14 and 23. Fig.1 shows the passivity of AML case to some CD markers by flow cytometry.

Table 2 Immunophenotype and CD marker of AML leukemia.

CD marker of AML Leukemia	N(%) of positive case	Mean of positivity	Rang of positivity	conjugated fluorochromes
cyMPO	27(90)	59.38	24-92	FITC
CD 33	30(100)	59.81	21-94	FITC
CD 13	30(100)	30.83	20-45	PC5
CD 117	21(70)	48.33	20-70	PE
CD 15	13(43.33)	24.66	20-30	PC5
CD 34	8(26.67)	45.11	20- 69	ECD
CD 64	10(33.33)	56.22	25-90	PE
CD 36	11(36.67)	43.14	20-88	FITC
CD14	11(36.67)	23	21-25	ECD

Acute Myeloid Leukemia without maturation (M1) subtype usually presents with blasts expressing cyMPO and one or more of myeloid-associated antigens such as CD13, CD33, and CD117. CD34 is positive in approximately 70% of cases. There is generally no expression of markers associated with granulocytic maturation such as CD15 and CD65 or monocytic markers such as CD14 and CD64. In AML with maturation (M2) the blast cells usually express one or more of the myeloid-associated antigens (CD13, CD33, and CD15). There is often an expression of CD34 and/or CD117, which may be present only in a fraction of blasts. Monocytic markers such as CD14 and CD64 are usually absent. While in acute promyelocytic leukemia (M3) the FC immunophenotyping shows a lack of expression of CD34, with positive CD33, cytoplasmic MPO, and variable expression of CD13. CD15 is typically absent [32].Acute Myelomonocytic Leukemia

KJPS Al-Kitab Journal for Pure Science
Vol.2 (2), ISSN: 2617-1260 (print), 2617-8141(online)
www.kjps.isnra.org

(M4) generally show several populations of blasts variably an expressing myeloid antigens CD13, CD33, and CD15; and others expressing markers characteristic of monocytic differentiation such as CD14and CD36, CD64[33].

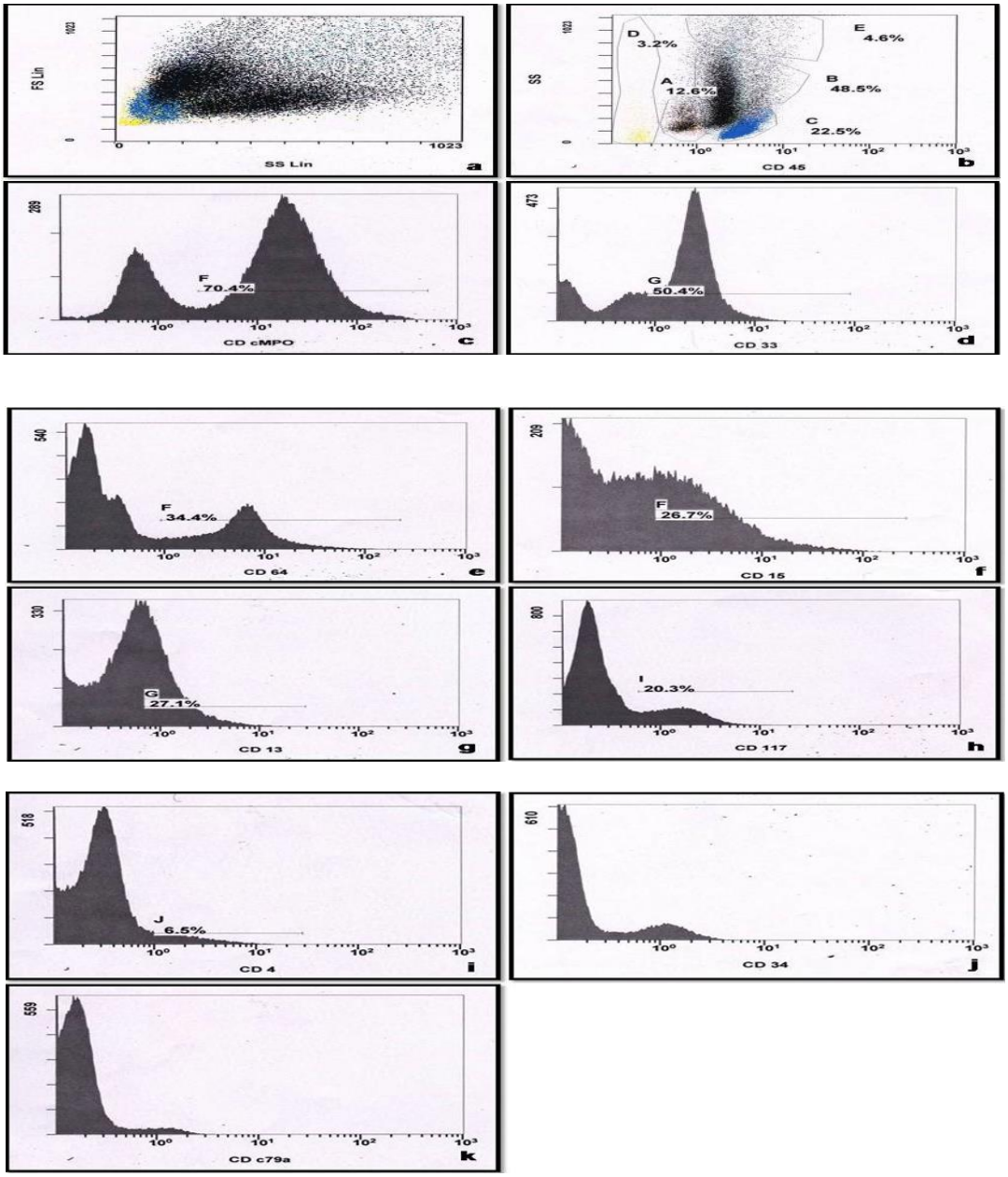

Fig. 1 Immunophenotype and CD marker of AML patients .(a)FS.Forward Scatter ,SS. Side Scatter distribution of the blast cells.(b) is CD45 and SSC,(c) is CD cMPO ,(d) is CD13,(e) is CD64,(f) is CD15, (g) is CD13 ,(h) is CD117 were positive .(i),(j) and (k) for CD4,CD34 and CD79 were negative.

Fig. 2 showed that the highest number was M4 10 (33.3%) patients, followed by M1 7(23.3%), M3 6(20%), M2 was accounted for 3(10%) of all AML patients. M5 and M6 were 2 (6.7%) patients which are the lowest number of AML subtypes. While there was no case of M0 and M7 in this study.

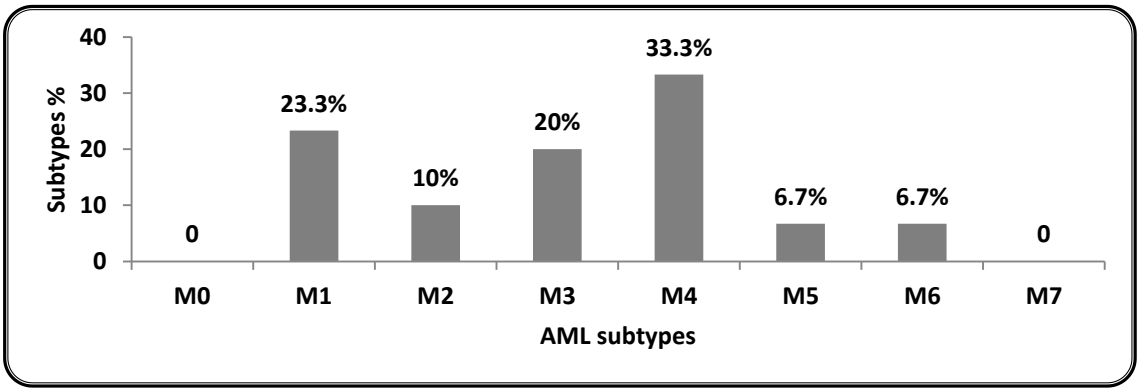

Fig.2 The percentages of AML subtype according to FAB classification.

A study done by [34] supports the results of our study. They found that the percentage of patients with M4 was the most frequent subtype 40%. Of the overall 1686 evaluable cases, 400 (23.7%) were diagnosed AML-M4 [35]. Numeric differences between the AML subtypes showed that M4 number was 68/300 which was the second number after M2 (73), while M1 49, M3 22, M0 18, M5 12, M6 7 and M7 6, although 45 cases were unclassified [36]. Other researchers demonstrated that the most common subtype was M1 (35%) followed by M3, M4, M2, M6 31%, 15%, 15%, and 4%, respectively. None of the patients were diagnosed as M5, M7 or M0 subtype [37].

Identification of several cytogenetic subgroups of AML, characterized by more or less distinct and specific clinical and morphologic features, has proved its great importance in the classification, understanding, and clinical management of this complex and heterogeneous disorder [38]. According to FAB classification patient with inversion (16) and translocation (16;16), translocations of chromosome 16 have been identified in AML subtype M4, and translocation (8;21) occurs most commonly in subtypes M1 and M3, and M4 has a high correlation with t(15;17) while M2 has a correlation with t(8;21). High frequency of M4, M1 and M3 subtype in our study may be related to environmental predisposing factors such as carcinogen in weather, diet, soil and industrial products as a

KJPS Al-Kitab Journal for Pure Science
Vol.2 (2), ISSN: 2617-1260 (print), 2617-8141(online)
www.kjps.isnra.org

second event for the subsequent development of these subtypes, in addition to the genetic alteration to the occurrence of these subtypes in our community [39].

Table 3 shows distribution of total 10 *candida spp* isolates before induction phase chemotherapy shows that 9(90%)isolates were C.albicans,1(10%) was *C. lusitaniae*, and from 32 isolates after induction phase chemotherapy,17(53.1%) isolates were C.albicans, 7(21.9%) was *C. lusitaniae*,and 8(25%) was *C.famata*. According to the site of infection, before starting chemotherapy 8(88.9%) *C. albicans* isolates were in the oral cavity and 1(11.1%) on the skin, while *C. lusitaniae* was 1 (100%) in oral cavity only. While after induction phase chemotherapy 12(70.6%) *C.albicans* in the oral cavity and 5(29.4%) on the skin, *C. lusitaniae* was 2 (28.6%) in the oral cavity and 5(71.4%) on the skin, while all *C. famata* was 8 (100%) on the skin.

Table 3 Distribution of *Candida Spp*. isolates before and after chemotherapy according to the site of infection.

Blood cancer type	*Candida albicans*				*Candida lusitaniae*				*Candida famata*				Total			
	Before															
	Oral cavity		Skin		Oral cavity		Skin		Oral cavity		Skin		Oral cavity		Skin	
	N	%	N	%	N	%	N	%	N	%	N	%	N	%	N	%
AML	8	88.9	1	100	1	0	0	0	0	0	0	0	9	90	1	10
Total	8		1		1		0		0		0		10(100)			
	After															
Blood cancer type	Oral cavity		Skin		Oral cavity		Skin		Oral cavity		Skin		Oral cavity		Skin	
	N	%	N	%	N	%	N	%	N	%	N	%	N	%	N	%
AML	12	70.6	5	29.4	2	28.6	5	71.4	0	0	8	100	14	43.7	18	56.3
Total	17(53.1)				7(21.9)				8(25)				32(100)			

Candida spp. is the most common cause of invasive fungal infection in humans. *Candida* infection in immunocompromised hosts was frequently life-threatening [40]. Fungal infections were also observed in AML patients by [41]. *C. albicans*, other *Candida spp. Aspergillus, Fusarium*, and Mucor species were reported in the skin of Children with acute leukemia by [42]. There were 16 isolates of *Candida, C. albicans* 13 and other *Candida spp.* was 3. Nineteen of 22 fungal isolates were detected in the induction phase of chemotherapy as compared to 3 in the intensification/consolidation phase versus none in the maintenance chemotherapy [43]. The epidemiology of fungal infections in patients with hematologic malignancies was described by [44] who found candidemia in patients with hematologic malignancies. [45] represent to appendicitis in a neutropenic patient by *C. albicans* after induction chemotherapy.

Conclusions

Most of patients AML were adults in our community and M4 subtype was more prevalent when compared to another subtype. The number of Candida spp isolates increased after induction phase chemotherapy. The immunophenotype shows that most patients' myeloid cells expressed cyMPO.

References

[1] Jean, T., Dennerll, P., and Davis, E, " **Medical Terminology: A Programmed Systems Approach "10th** ed., Spiral-bound (2009).

[2] Tkachuk, D.C. and Jan, V. H, **"Wintrobes Atlas of clinical Hematology"**, Lippincott William and Wilkins USA (2007).

[3] Provan, D., and Gribben, J.G, **"Molecular Hematology**" 3rd edition. Singapore. Wiley-Blackwell (2010).

[4] Deschler. B. and Michael, L" **Acute myeloid leukemia: epidemiology and etiology",** Cancer, 107 (9), 112-118 (2006).

[5] American Cancer Society **"How is Acute Myeloid Leukemia (AML) Classified? 2010"**

[6] Aquino, VM. " **Acute myelogenous leukemia"**, Curr. Probl. Pediatr. Adolesc Health Care, 32 (2),50-58(2002).

[7] Craig, F.E. and Foon, K.A, **"Flow cytometric immunophenotyping for hematologic neoplasms"**, Blood, 111 (8), 71-74 (2008).

[8] Chow, J.K., Golan, Y., Ruthazer, R., Karchmer, A.W., Carmeli, Y., and Lichtenberg, D.A, **" Risk factors for albicans and non-albicans candidemia in the intensive care unit"** , Crit.Care. Med, 36, 1993–1998 (2008).

[9] Krcmery, V., Barnes, A.J, **"Non-albicans *Candida spp*. causing fungemia: pathogenicity and antifungal resistance"**, J .Hosp. Infect, 50 (4), 243-60 (2002) .

[10] Alsan, M.M., Nicolas, C. I., Sarah, P. H., Danny, A. M. J., Daniel, J. D., and Lindsey, R. B., **"*Candida albicans* cervical lymphadenitis in patients who have acute myeloid leukemia",** Clin. Lymphoma, Myeloma, and Leukemia, 11(4), 375-377(2011).

[11] Elio, C.a, Ilaria, C., and Riccardo, H, **" Guidelines for the management bacterial and fungal infections during chemotherapy for pediatric acute leukemia or solid tumors: what is available in 2010? "**, Pediatr.Reports 3, 7-9 (2011).

[12] Wingard, J.R, **"Importance of Candida species other than C. albicans as pathogens in oncology patients",** Clin. Infect. Dis, 20, 115-125(1995).

[13] Barnett, J. A., Payne, R. W. and Yarrow, D, **" Yeasts: characteristics an Identification",** 3rd ed., Cambridge, University Press, Cambridge (2000).

[14] Wagner, D. A., Sander, H., Bertz, J. F., and Kern, W. V, **" Breakthrough invasive infection due to *Debaryomyces hansenii* (teleomorph *Candida famata*) and *Scopulariopsis brevicaulis* in a stem cell transplant patient receiving liposomal amphotericin B and caspofungin for suspected aspergillosis"** , Infection, 33, 397-400 (2005) .

[15] Gupta, A., Mi, H. Wroe, C. Jaques, B. and Talbot, D, **" Fatal *Candida famata* peritonitis complicating sclerosing peritonitis in a peritoneal dialysis patient"**, Nephrol. Dial. Transplant, 21 , 2036-2037 (2006) .

[16] Elkamouni. Y, Lmimouni, B., Doghmi K., and Elouenass, M, **" *Candida famata* candidemia in an immunosuppressed patient: report of a case with literature review"**, Ann. Biol.Clin , 69 (5),609-611 (2011).

[17] Beyda, N.D, Chuang, SH., Alam, M.J., Shah D.N, McCaskey, L., Garey, K.W, **"Treatment of Candida famata bloodstream infections: case series and review of the literature"**, J Antimicrob Chemother, 68 (2), 438-443 (2013).

[18]Alwan, A.F., Zedan, J. Z., and Omar, S. S**, " Acute myeloid leukemia: clinical features and follow-up of 115 Iraqi patients admitted to Baghdad Teaching Hospital"**, Tikrit Med.J, 15 (1), 1-8(2009).

[19] Modak, H., Salamandra, S., Kulkarni , G. S. ,Kadako, S. V. ,Hiremath, B. R. Patil, U.H, and Pramod, B. G, **" Prevalence and Risk of Leukemia in the Multi-ethnic**

Population of North Karnataka" , Asian Pacific J. of Cancer Prevention, 12(12), 671-675 (2011) .

[20] Ishfaq, M. A., Muhammad, A., Muhammad, N., Khan, M., Saeed, Q.,Sara, Z.,Abdul, M.,, Mahwish A., Mahmood Husain, Q., Adeel, C.,Mohammed Hussain A.,and Mahmood, R, **" Molecular Characterization of FLT3 Mutations in Acute Leukemia Patients "** , Asian Pacific J. Can. Preve, l 13, 4581-4585 (2012).

[21]Al-Mawali, A., David, G., and Ian, L**," Characteristics and Prognosis of Adult Acute Myeloid Leukemia with internal tandem Duplication in the FLT3 Gene"**, Oman Med. J, 28(6), 432-440(2013).

[22] Varadarajan, R., Andrea, S. L., Andrew, J. y., Laurie, A. F., Sheila, N. J. S., Annemarie, W. B., Maurice, B., Maria, R. B., Eunice, S. W., and Meir, W, **"Smoking adversely affects survival in acute myeloid leukemia patients " ,** Int. J. Cancer,130, 1451–1458 (2012).

[23] Yoshinaga, S., Mabuchi, K., Sigurdson, A., Doody, M., and Ron, E, **" risks among radiologists and radiologic technologists: a review of epidemiologic studies"**, Radiology,233 (2), 313-321 (2004).

[24] Pui, C.H., Ribeiro, R.C., and Hancock, M.L, **" Acute myeloid leukemia in children treated with epipodophyllotoxins for acute lymphoblastic leukemia"**, N. Engl .J.Med, 325,1682-1687 (1991).

[25] Greaves, M. F, **" Aetiology of acute leukemia"**, Lancet,349, 344-349 (1997).

[26] Glass, D.C, **" Leukemia risk associated with low – level benzene exposure"** Epidemiology, 14,596-577 (2003).

[27] Zahm, S.H., and Ward, M.H, **" Pesticides and childhood cancer"**, Environ. Health Perspect, 106, 893-908(1998).

[28] Austin, H., Delzell, E., Cole, P**, " Benzene and leukemia. A review of the literature and a risk assessment"**, Am. J. Epidemiol, 127 (3),419-439(1988).

[29] Zhang, L., Rothman, N., and Wang, Y**, " Increased aneusomy and long arm deletion of chromosomes 5 and 7 in the lymphocytes of Chinese workers exposed to benzene",** Carcinogenesis, 19, 1955-1961 (1998).

[30] Pogoda, J.M, Preston-Martin, S., Nichols, P.W., and Ross, R.K, **" Smoking and risk of acute myeloid leukemia: results from a Los Angeles county case-control study"**, Am. J .Epidemiol, 155, 546–553 (2002) .

[31] Parkin, D.M., Boyd, L., and Walker, L.C**, " The fraction of cancer attributable to lifestyle and environmental factors in the UK in 2010"**, Br .J. Cancer, 105 (Suppl 2), S77-81 (2011).

[32] Heerema-McKenney, A. and Arber, D.A, **" Acute Myeloid Leukemia",** Hematol. Oncol. Clin. North America, 23, 633-54 (2009).

[33] Abdullah, D.A, " **Flow Cytometric Profiles ofAcute Leukemia: a comparative study of morphologic and immunophenotyping diagnoses"**Ph.D. Thesis, Hawler Medical University(2010).

[34] Robert, G.T., Spence, D.G., Padmos, M.A., Sheth, K.V., Clink, H., and Ernst, P, " **Morphological, immunophenotypic and cytogenetic pattern of adult acute myeloid leukemia in Saudi Arabia"**, Leuk.Res, 16, 181-190 (1992).

[35] Pulsoni, A., Simona, I., Massimo, B. M., Andrea, C., Nicola ,C., Francesco, D.R., Paola, F., Franco, L., Vincenzo ,L., Marco ,M., Filippo ,M., Angela M., Luca ,M., Lorella ,M., Giovanna ,M., Salvo, M., Giorgina, S., Caterina, G.V., Adriano ,.V, Giuseppe, L., Robin ,F., Franco ,M., and Livio, P, " **M4 acute myeloid leukemia: the role of eosinophilia and cytogenetics in treatment response and survival"**, Gimema Experi. Haematol,93 (7) , 1025-1032 (2008).

[36] Daniel, A. A., Anthony, S. S., Nora, H. C., David, I., Stephen, J. F., and Marilyn, L. S, " **Prognostic impact of acute myeloid leukemia classification. importance of detection of recurring cytogenetic abnormalities and multilineage dysplasia on survival",** Am. J .Clin. Pathol, 119, 672-680 (2003).

[37]Asif, N., Khalid, H., and Nuzhat, Y, " **Acute myeloblastic leukemia in children",** International J.Pathol, 9 (2), 67-70(2011).

[38] Burnett, A.K, **"Tailoring the treatment of acute myeloid leukemia"** Curr Opin. Hematol, 6,247–253 (1999).

[39] Morikawa, J., Kim, S., Nishii, K., Ueno, S., and Suh, E**, " Identification of signature genes by microarray for acute myeloid leukemia without maturation and acute promyelocytic leukemia with t (15; 17) (q22; q12)"**, Int. J .Oncology, 23, 617-625 (2003).

[40] Pappas, P.G., Kauffman, C.A., and Andes, D, " **Clinical practice guidelines for the management of candidiasis: 2009 update by the Infectious Diseases Society of America"** , Clin. Infect. Dis , 48, 503-535 (2009) .

[41] Caira, M., Girmenia, C., and Fadda, R.M**, "Invasive fungal infections in patients with acute myeloid leukemia and in those submitted to allogeneic hemopoietic stem cell transplant: who is at highest risk?" ,** Eur. J Haematol,81, 242- 243 (2008).

[42] Sung, L., Beverly, J., Lange, B., Gerbing, T. A., and James F, **"Microbiologically documented infections and infection-related mortality in children with acute myeloid leukemia"**, Blood, 110 (10), 3532-3539 (2007).

[43]Bakhshi, S., Padmanjali, K. S. and Arya, L. S, " **Infection in childhood acute lymphoblastic leukemia: An Analysis of 222 Febrile Neutropenic Episodes"**, Pediatr.Hematol.Oncol, 25, 385-392 (2008).

[44] Sipsas, N.V., Lewis R.E., and Tarrant, J, " **Candidemia in patients with hematologic malignancies in the era of new antifungal agents (2001-2007): stable incidence**

but changing epidemiology of a still frequently lethal infection", Cancer, 115 (20),4745-4752 (2009).

[45] Rohtesh, S. Mehta, M., and David, C, " ***C. albicans*** **appendicitis in a neutropenic patient after induction chemotherapy",** Comm. Oncol, 10(8),244-246 (2013).

KJPS Al-Kitab Journal for Pure Science
Vol.2 (2), ISSN: 2617-1260 (print), 2617-8141(online)
www.kjps.isnra.org

DOI: http://10.32441/kjps.02.02.p5

Environmental Pollution of Cellular Mobile Base Station in Populated Areas

Asst.Prof.Dr. Adheed Hasan Sallomi[1], Assist.Lect. Radhi Isa Sahan[2]
[1,2]Faculty of Engineering-Al Mustansiriya University
[1]adalameed@yahoo.com

ABSTRACT

Cellular mobile communication technology has grown exponentially in the last decade resulting in large number of base stations in areas at which people are living or working. All over the world, the electromagnetic pollution produced from cellular base stations erected in residential areas and its effect on the environment and human body is a problem that has been concerning the society for many years.

This paper, introduces the effects of electromagnetic energy emitted by cellular base stations on the biological systems of the human body. The induced electromagnetic fields (EMF), and specific absorption rate (SAR) were calculated in close proximity to cellular mobile base stations.

The calculated values of SAR were compared with the most commonly used international limits. The results show that the electromagnetic radiation (EMR) exposure levels at a distance of several meters from the base station towers can cause hazardous effects to the public.

Keywords: Electromagnetic radiation (EMR), Electromagnetic pollution, Cellular mobile communication systems, SAR, Mobile effects on human health.

KJPS Al-Kitab Journal for Pure Science
Vol.2 (2), ISSN: 2617-1260 (print), 2617-8141(online)
www.kjps.isnra.org

التلوث البيئي لمحطات الهاتف الخلوي النقال في المناطق السكنية

ا.م.د. عضيد حسن سلومي [1] ، م.م. راضي صالح صحن [2]

[1,2] قسم الهندسة الكهربائية، كلية الهندسة، الجامعة المستنصرية، بغداد، العراق.

[1]adalameed@yahoo.com

الملخص

تطورت تكنولوجيا الهاتف الخليوي النقال بشكل متزايد في العقد الأخير مما نتج عنه محطات أكثر في المناطق التي يسكن أو يعمل فيها الناس. في كل أرجاء العالم ، الإشعاعات الكهرومغناطيسية المنبعثة من محطات القاعدة الخلوية المنصوبة في المناطق السكنية وتأثيراتها على البيئة و جسم الإنسان وتمثل مشكلة مقلقة للمجتمع منذ عدة سنوات.

يعرض هذا البحث تأثيرات الطاقة الكهرومغناطيسية المنبعثة من محطات القاعدة الخليوية على الأجهزة الحيوية لجسم الإنسان . تم احتساب كثافة القدرة، المجالات الكهرومغناطيسية المحتثة ومعدل الامتصاص النوعي في المناطق القريبة من محطات الهاتف النقال . تمت مقارنة معدل الامتصاص النوعي المحتسبة بالمعايير الدولية الأكثر استخداما وقد بينت النتائج بان مستوى التعرض للمجالات الكهرومغناطيسية عند بضعة أمتار من محطات القاعدة ممكن أن يسبب تأثيرات خطيرة على عامة الناس.

1. Introduction

The Global System for Mobile communications (GSM) are second-generation (2G) systems were adopted in many countries all over the world. Base station antennas transmit in the frequency range of 935 to 960 MHz (GSM-900), 1810 to 1880 MHz (GSM-1800). 3G cellular system has been adopted in many countries, in which base station antennas transmit in the frequency range of 2110-2170 MHz [1] [2].

Base station antennas are usually mounted on the roofs of buildings or on free-standing masts, and down-tilted, so that the signals are directed towards ground level.

Cellular mobile communication system operates via base stations, and each base station covers a limited region(cell) [3]. The widespread use of cellular phones requires more base stations to provide good coverage, as sitting base stations far from the user will result in poor quality link, and causes the phones to increase their output power to sustain the connection. Therefore, many base stations were erected in areas of high population density.

The presence of base station towers in residential areas is certainly discomforting and a cause of serious concern regarding the potential hazardous effects on people, particularly for those living or working in the vicinity of these base stations [2] [4].

Exposure of the general public to non-ionizing radiations from mobile base stations, TV /radio broadcasting transmitters, and other wireless networks is almost continuous. Exposure guidelines are always based on the thermal effects of the radio frequency (RF) energy which can be evaluated in terms of specific absorption rate (SAR), and RF field intensities [4].

The objective of this paper is to develop a simplified theoretical method to assess the effect of RF radiation on people living nearby GSM base station, depending on the prediction of the induced electric field around the base station transmitting antenna, calculation of the penetrated electric field and (SAR) inside the human body tissues. Finally, compliance of the calculated values of SAR has been evaluated with the guidelines given by the most known authorities.

2. Material And Methods

a. RF Field – Power Density Variation

As the human body consists of 70% liquid, the main effect of exposure to microwave is the heating of body tissues in a way that is similar to cooking in microwave ovens, leading to increase in body temperature. The effect of microwave (MW) radiations on biological systems depends on the radiation frequency, power level, dielectric constant, conductivity of the tissue, and exposure time[3] [5].

KJPS Al-Kitab Journal for Pure Science
Vol.2 (2), ISSN: 2617-1260 (print), 2617-8141(online)
www.kjps.isnra.org

Radiation from base station in the far-field region is usually defined by the power density, or field intensities. The power density (S) and field components in air are relating by the equations [6]:

$$S = \frac{E_o^2\ \varepsilon_o\ c_o}{2} = \frac{P_t\ G_t}{4\pi r^2} \quad (1)$$

$$E_o = \sqrt{\frac{2}{4\pi\varepsilon_o c_o}} \cdot \frac{\sqrt{P_t\ G_t}}{r} = 7.74\ \frac{\sqrt{P_t\ G_t}}{r} \quad (2)$$

Where E_o is the electric field intensity in free space, P_t is the transmitted power, G_t is the transmitting antenna gain, r is the distance between the RF source and the exposed point, ε_o is the free space permittivity, and c_o is the radio wave speed.

The geometry illustrated in Figure 1, shown below will be used to determine the power density on each point of the exposed body that receives the RF power from the base station as a monopole antenna.

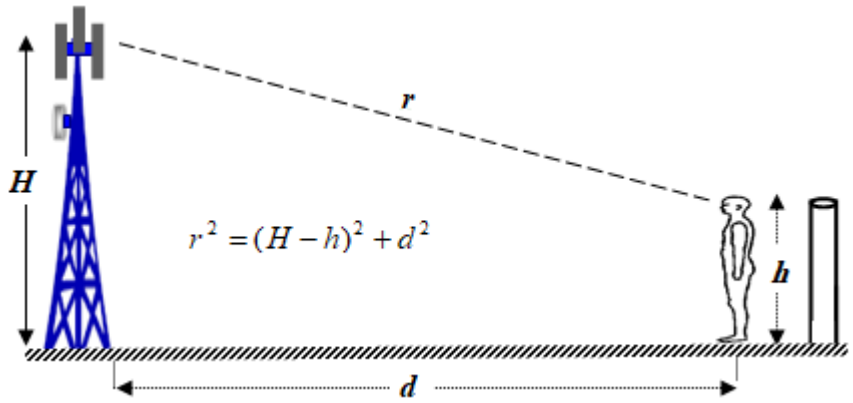

Fig. 1: Power Density and Electric Field Calculations Geometry.

b. Penetration Depth Estimation

When electromagnetic radiations are penetrated inside the human body, the incident power density will be reduced by a factor of e^{-2}. The depth at which the induced field is reduced to 1/e (about 0.367) compared to its magnitude at the surface of any material is

called the (skin depth). Therefore, the field (E_i) at a depth distance, z, due to the incident field E_o, on the surface is given as [5]

$$E_i = E_o\, e^{-z/\delta} \tag{3}$$

where δ, is the skin depth in any material that can be given by [7]:

$$\delta = \frac{1}{\omega}\sqrt{\frac{2}{\mu\varepsilon}}\left[\sqrt{1+\left(\frac{\sigma}{\omega\varepsilon}\right)^2}-1\right]^{-0.5} \tag{4}$$

$$\omega = 2\pi f, \quad \mu = \mu_o\,\mu_r, \quad \varepsilon = \varepsilon_o\,\varepsilon_r \tag{5}$$

where ω is the angular frequency, f is the frequency, σ is the conductivity, μ is the permeability, μ_o is the permeability of vacuum, μ_r is the relative permeability, ε is the permittivity, ε_o is permittivity of vacuum, and ε_r is the relative permittivity.

c. SAR Calculation

When a human body is exposed to electromagnetic radiations, it absorbs radiation and results in heating of biological tissue. The amount of heat required to change a unit mass of a substance by one unit of temperature is called the specific heat; its unit is J/(kg.K) or J/(kg.ºC). The average specific heat that has been used for the human body is 3470 J/(kg.ºC). Hence, the relationship between heat quantity absorbed by the human body, and temperature change is given as [8] [5]

$$\Delta Q = 3470\, m\,(\Delta T) \tag{6}$$

where Q is the heat energy absorbed or dissipated in joule (J), m is the mass of the substance(kg), ΔT is the change in temperature(ºC).

Exposure to RF energy can be determined by the Specific Absorption Rate (SAR) that is a measure of the absorbed power per mass of tissue when exposed to radiofrequency measured in watts per kilogram (W/kg). SAR is the time derivative of the incremental energy absorbed by or dissipated in an incremental mass (∂m) contained in a volume element (∂V) of a density (ρ). Therefore, SAR is given as [8] [9]

KJPS Al-Kitab Journal for Pure Science
Vol.2 (2), ISSN: 2617-1260 (print), 2617-8141(online)
www.kjps.isnra.org

$$SAR = \frac{\partial}{\partial t}\left(\frac{\Delta Q}{\partial m}\right) = \frac{\partial}{\partial t}\left(\frac{\Delta Q}{\rho \partial V}\right) \quad (7)$$

$$SAR = \frac{1}{t}\left(3470\,\Delta T\right) = \frac{3470\,\Delta T}{t} \quad (8)$$

$$SAR = \frac{\sigma\, E_i^2}{2\rho} \quad (9)$$

where E_i is the field inside that material (induced in tissue) (V/m), and ρ is the tissue density (kg/m^3). This relation implies that the SAR value of tissue depends on the intensity of the internal electric field, and tissue properties that are presented in Table 1.

Table 1 The Human Head-Body Tissue Properties [10].

Frequency (MHz)	**Head** (**μ** = μ_o, **ρ** = 1000 kg/m^3)		**Body** (**μ** = μ_o, **ρ** = 1000 kg/m^3)	
	σ S/m	**σ** S/m	ε_r	ε_r
835	41.5	0.90	55.2	0.97
900	41.5	0.98	55.0	1.05
915	41.5	0.98	55.0	1.06
1000-2000	40.0	1.40	53.2	1.52

d. RF Exposure Standards

Many international authorities provide protection for the public exposed to RF and microwave radiations through setting the permitted maximum exposure (PME) levels. The most respected standard levels are those recommended by the International Commission on Non-Ionizing Radiation Protection (ICNIRP), and those developed by American National Standards Institute and the Institute of Electrical and Electronics Engineers (ANSI/IEEE) [4].

According to the ICNIRP, the admissible power density limit in W/m2 for the public in the frequency range between (400-2000 MHz) can be calculated as ($f\,(MHz)/200$) [3][5].

KJPS Al-Kitab Journal for Pure Science
Vol.2 (2), ISSN: 2617-1260 (print), 2617-8141(online)
www.kjps.isnra.org

The ANSI/IEEE standard C95.1-1992 RF Safety Guideline suggests that the admissible power density limit in W/m2 for the public in the frequency range between (400-2000 MHz) can be calculated as ($f(MHz)/150$) [8][12].

3. Results And Dıscussıon

Most of the cellular base station radiates a power of 20 watt, through an antenna of 18dBi gain (63.095), therefore, the maximum power density (S) will be in an area near the base station antenna, and is inversely proportional to the square of the distance (r) as can be noticed from equation 1. For different heights of base station antenna (H), the power density (S) in W/m^2 is plotted for different exposed body heights (h) when it is located at different distances (d) from the radiating source. Figure 2, shows that the power density has no considerable variation with the height of the exposed body while it decreases as the distance (d) and transmitting antenna height (H) is increased. Therefore, increasing the base station antenna height can be used as one of the main technique for RF pollution reduction. Furthermore, the power density at a distance of 30 m from the base station doesn't exceed 0.9 W/m^2 which is below the permissible limits.

KJPS Al-Kitab Journal for Pure Science
Vol.2 (2), ISSN: 2617-1260 (print), 2617-8141(online)
www.kjps.isnra.org

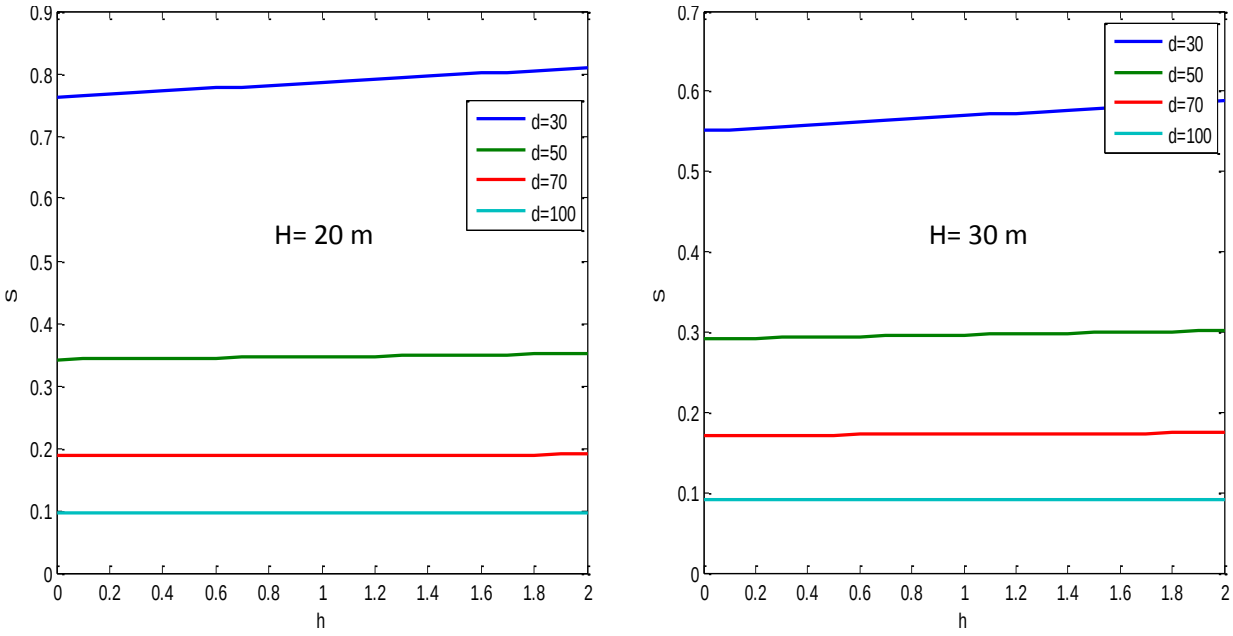

Figure 2: Power Density Variation with Exposed Body Height and Distance

The median transmits frequency of GSM-900 and GSM-1800 can be calculated to be 947.5 MHz and 1845 MHz respectively. The depth by which the electric field caused by base station radiation penetrates human body can be calculated by using equation (4) with the help of the human biological tissue characteristics given in Table 1. The penetration depth for GSM-900 was calculated to be 3.77 cm for a human body, and 3.57 cm in a human head. The penetration depth for GSM-1800 was calculated to be 2.57 cm for a human body, and 2.43 cm for a human head.

The variation of the induced field inside the human tissues is calculated by applying equation 3. Figure 3 illustrates the variation of the electric field inside the human body for different distances from GSM-900 and GSM-1800 base stations, and for different depth distances (z). It can be noticed that as depth distance increased, the field will be decreased, and the induced field in human body exposed to GSM-900 radiations is more than that

KJPS Al-Kitab Journal for Pure Science
Vol.2 (2), ISSN: 2617-1260 (print), 2617-8141(online)
www.kjps.isnra.org

induced due to the effect of GSM-1800 base station radiation at the same depth distance when the effective radiated powers are equal.

Figure 4, shows the variation of the electric field inside the human head and body due to the radiation emitted by GSM-900 and GSM-1800 base stations respectively at 1 cm depth distance. From Figure 4, it can be seen that the induced field in the human body is more than that induced in the human head because the human body has more penetration depth due to higher conductivity and permittivity. Furthermore, the induced electric field due to GSM-900 base station radiation is more that of GSM-1800 base station radiation, because of higher frequency results in less penetration depth.

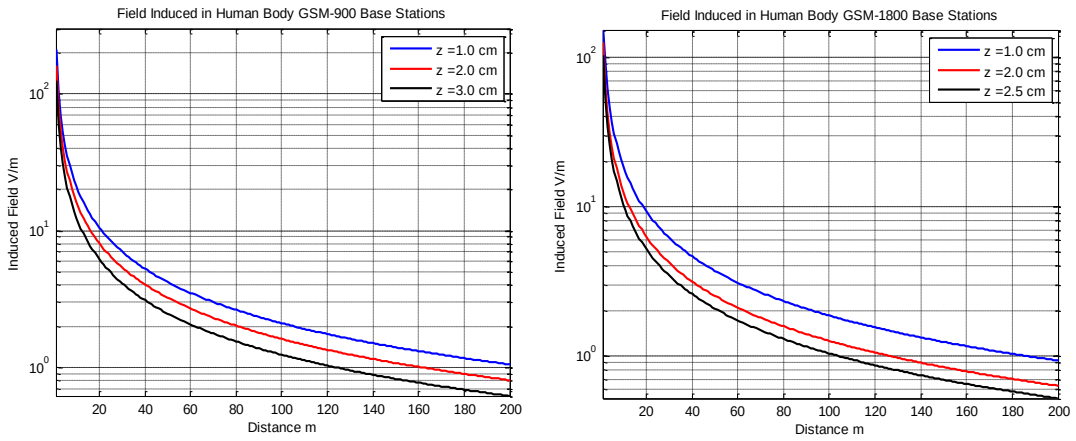

Figure 3. Induced Field inside Human Body For GSM Base Stations

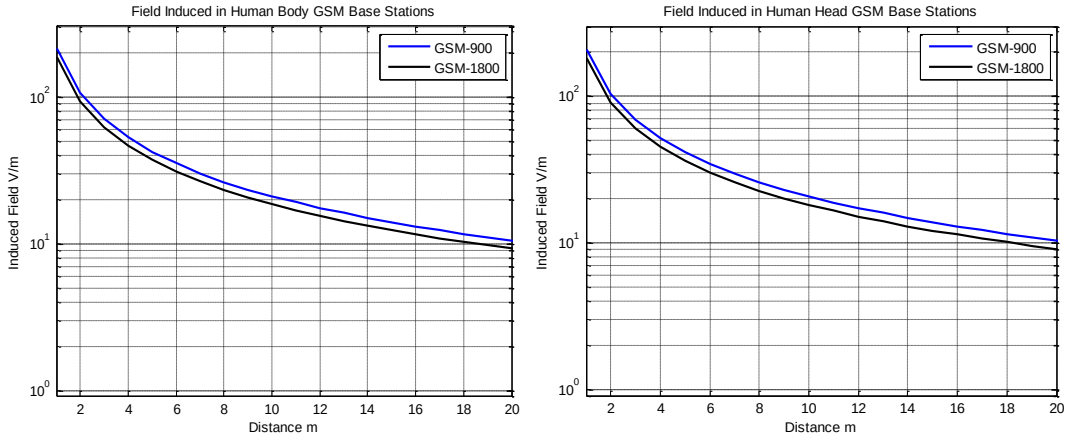

Figure 4. Field-Induced in Human Body-Head over 1 cm Penetration Distance

KJPS Al-Kitab Journal for Pure Science
Vol.2 (2), ISSN: 2617-1260 (print), 2617-8141(online)
www.kjps.isnra.org

By using equation 9, and Table 1, the value of SAR in the human body and head were calculated for different distances from the base station tower at different depth distances. The calculated values of SAR due to GSM-900 and GSM-1800 base stations are given in Tables 2, and 3 respectively.

From these tables, it can be noticed that the amount of the absorbed RF energy decreases rapidly with increasing distance from the base station antenna. As a result, the level of exposure to radio waves at ground level is very low compared to the level close to the base station antenna. The values of SAR at a distance of 5 meters away from the GSM base station is below the safe value of SAR set by international agencies(less than 1.6 W/kg), and this implies that it is unsafe to be at a distance less than 5 meters from the base station tower for the recommended exposure time.

Table 2 The Calculated Values of SAR for GSM-900 Base Stations.

Distance from Base Station (m)	SAR in Human Body (W/kg) Depth Distance (z)			SAR in Human Head (W/kg) Depth Distance (z)		
	1.0 cm	2.0 cm	2.0 cm	1.0 cm	2.0 cm	3.0 cm
0.5	94.28	94.28	55.993	111.973	84.618	63.945
1.0	23.57	23.57	13.998	27.9934	21.154	15.986
2.0	5.89	5.89	3.4995	6.9983	5.2886	3.9965
3.0	2.61	2.61	1.555	3.1103	2.3504	1.776
4.0	1.47	1.47	0.874	1.749	1.3006	0.9991
5.0	0.94	0.94	0.5599	1.1197	0.8461	0.6394
6.0	0.65	0.65	0.3888	0.7775	0.5876	0.4440
7.0	0.485	0.485	0.285	0.5712	0.4317	0.326
8.0	0.36	0.36	0.2187	0.4373	0.3305	0.2497
9.0	0.29	0.29	0.1728	0.3455	0.2611	0.1973
10	0.23	0.23	0.1399	0.2799	0.2115	0.1598

KJPS Al-Kitab Journal for Pure Science
Vol.2 (2), ISSN: 2617-1260 (print), 2617-8141(online)
www.kjps.isnra.org

Table 3 The Calculated Values of SAR for GSM-1800 Base Stations.

Distance from Base Station (m)	SAR in Human Body (W/kg) Depth Distance (z)		SAR in Human Head (W/kg) Depth Distance (z)	
	1.0 cm	2.0 cm	1.0 cm	2.0 cm
0.5	105.33	48.460	140.264	92.944
1.0	26.333	12.115	35.066	23.236
2.0	6.583	3.028	8.7665	5.809
3.0	2.925	1.346	3.8962	2.5817
4.0	1.645	0.7517	2.1915	1.4522
5.0	1.053	0.4846	1.4026	0.9294
6.0	0.7314	0.3365	0.9740	0.6454
7.0	0.5374	0.2472	0.7156	0.474
8.0	0.4114	0.1892	0.5478	0.3630
9.0	0.3250	0.1495	0.4329	0.2868
10	0.2633	0.1211	0.3506	0.2323

According to the ICNIRP, the admissible power density for GSM-900 base stations will be equal to (4.737 W/m^2). For the case of 20 W transmitted power through an antenna of (18 dBi) gain, the safety distance can be calculated as:

$$S = \frac{f(MHz)}{200} = \frac{947.5}{200} = \frac{P_t G_t}{4\pi r^2} = 4.737\ W/m^2 \Rightarrow r = \sqrt{\frac{P_t G_t}{4\pi S}} = \sqrt{\frac{20 \times 63.095}{4\pi \times 4.737}} = 4.6\ m$$

At this distance, and for 0.01m depth distance; the value of SAR can be calculated to be 1.139 W/kg which is less than the limit has set by many organizations that are 1.6 W/kg for the whole body.

With the use of the ANSI/IEEE standard, the admissible power density for GSM-900 base stations will be equal to (6.316 W/m^2). For the case of 20W transmitted power through an antenna of (18 dBi) gain, the safety distance can be calculated as:

$$S = \frac{f(MHz)}{150} = \frac{947.5}{150} = \frac{P_t G_t}{4\pi r^2} = 6.316\ W/m^2 \Rightarrow r = \sqrt{\frac{P_t G_t}{4\pi S}} = \sqrt{\frac{20 \times 63.095}{4\pi \times 6.316}} = 3.987\ m$$

At this distance, and for 0.01 m penetration distance; the value of SAR can be calculated to be 1.482 W/kg which is also less than 1.6 W/kg.

These results show that the calculated values of SAR agree with the power density standard limits have set by many international agencies.

4. Conclusions

The values of SAR inside the human body tissues due to exposure to non- ionizing radiation can be evaluated using a simplified theoretical approach to assess the effect of RF radiation on people living nearby GSM cellular base stations. Theoretical results show that when cellular base stations are mounted on houses rooftops, it is possible that a person at a distance less than 5.0 m or very close to the base station could be exposed to high RF levels greater than the maximum permissible exposure (MPE) limits. Hence, exposure levels exceeding the safety limits are likely to be found very close to and directly in front of the base station antennas, and at this hazardous distance, access should be limited, and should not be reached by the public.

Comparing the calculated values of SAR with ICNIRP, and ANSI/IEEE exposure limits, an idea for the compliance distance where the radiation level is safe for public exposures was estimated.

References

[1] Garg, Vijay K., "***Wireless Communications and Networking***", Morgan Kaufmann Publishers, USA, First Edition, 2007.

[2] Girish, Kumar, ***"Report on Cell Tower radiation ",*** IIT Bombay, December, 2010.www.ee.iitb.ac.in

[3] Seyfi, Levent, ***"Assessment of Electromagnetic Radiation with Respect to Base Station Types"***, International Journal of Information and Electronics Engineering, Vol.5, No.3, May 2015, pp.176-179.

[4] Aziz, Jabir S., ***"Analysis of Biological Effects of Microwave Energy and Safe Distance Calculations"***, Journal of Al-Rafidain Un, for Science, No.25, 2009, pp.1-8.

[5] ***"Health Effects From Radiofrequency Electromagnetic Fields"***; Report of the independent advisory group of on non-ionising radiation, Documents of the health protection agency, April 2012.

[6] Kitchen, Ronald, "RF and Microwave Radiation Safety Handbook", Second edition, Reed Educational and Professional Publishing Ltd, 2001.

[7] Kumar, Sandeep, Pathak, P, ***"Effect of Electromagnetic Radiation from Mobile Phones Towers on Human Body"***, Indian Journal of Radio & Space Physics, Vol. 40, No. 1, December 2011, pp. 340-342.

[8] Seybold, John S., ***"Introduction to RF Propagation"***, John Wiley & Sons, Inc., New Jersey, First Edition, 2005.

[9] Karunarathna, M.A., and Dayawansa, I.J, ***"Energy Absorption by the Human Body from RF and Microwave Emissions in Sri Lanka"***, Sri Lankan Journal of Physics, Vol.7 (2006), PP 35-47.

[10] Abdelati, Mohammed, ***"Electromagnetic Radiation from Mobile Base stations at Gaza"***, Journal of The Islamic University of Gaza (Natural Sciences Series) Vol.13, No.2, 2005, PP 129-146.

[11] ***"Evaluating Compliance with FCC Guidelines for Human Exposure to Radiofrequency Electromagnetic Fields"***, Additional Information for Evaluating Compliance of Mobile and Portable Devices with FCC Limits for Human Exposure to Radiofrequency Emissions, Supplement C, June 2001.

[12] Kamo, Bexhet, Miho, Rozeta, and others, ***" Estimation of Peak Power Density in the Vicinity of Cellular Base Stations, FM, UHF and WiMAX Antennas"***, International Journal of Engineering & Technology IJET-IJENS Vol. 11, No. 2, 2011, pp. 58-64.

KJPS Al-Kitab Journal for Pure Science
Vol.2 (2), ISSN: 2617-1260 (print), 2617-8141(online)
www.kjps.isnra.org

DOI: http://10.32441/kjps.02.02.p6

Cellular Networks Pollution Reduction

Asst.Prof.Dr. AdheedHasanSallomi[1], Asst.Prof. Dr. Musa Hadi Wali[2]
[1]Faculty of Engineering-Al Mustansiriya University,[2]Faculty of Engineering-University of Al-Qadisiyah
[1]adalameed@yahoo.com, [2]musa.h.wali@qu.edu.iq

ABSTRACT

The potential of adaptive antennas to optimize the wireless network performance make it one of the promising technologies that can face the increased demand for wireless communications services with the limited available bandwidth. Adaptive antennas have the ability to steer their main lobe in the direction of interest and placing nulls in the direction of interference. This can result in co-channel interference minimization, maximizing Signal to Interference Ratio (SIR) and then improve the receiver sensitivity.

In this paper, the base-station sensitivity improvement and its effect on the mobile transmit power were investigated at different scenarios. Results show that using adaptive antenna yields in RF pollution reduction.

Keywords: RF pollution reduction; cellular communication networks; SIR.

KJPS Al-Kitab Journal for Pure Science
Vol.2 (2), ISSN: 2617-1260 (print), 2617-8141(online)
www.kjps.isnra.org

الحد من تلوث الشبكات الخلوية

ا.م.د. عضيد حسن سلومي[1] , ا.م.د. موسى هادي والي[2]

[1]كلية الهندسة – الجامعة المستنصرية , [2]كلية الهندسة – جامعة القادسية

المستخلص

إمكانيات الهوائي التكيفي في الحصول على أقصى أداء للشبكات اللاسلكية جعلته واحد من وسائل التكنولوجيا الواعدة التي يمكن أن تواجه الطلب المتزايد على خدمات الاتصالات اللاسلكية ضمن الحزمة المحدودة العرض. يمتلك الهوائي التكيفي القابلية على تدوير فصوصه الرئيسية بالاتجاه المطلوب ووضع الأصفار باتجاه مصدر التداخل. ينتج عن ذلك تقليل التداخل بين الخلايا التي تعمل بنفس القنوات, زيادة نسبة الإشارة الى الضوضاء و من ثم تحسين حساسية المستقبل.

في هذا البحث, تحسين حساسية محطة القاعدة وتأثيرها في القدرة المرسلة من الهاتف النقّال تم اختبارها بسيناريوهات مختلفة. بينت النتائج المعروضة بان استعمال الهوائي التكيفي ينتج عنه تقليل التلوث الراديوي.

1. Introduction

Base stations in conventional cellular communication networks use either omnidirectional antennas or sectored antennas. In these networks, most of the power is radiated in other directions than toward the desired user as there is no information about mobile units (users) locations. The power radiated in other directions can be regarded as a waste of power, and experienced as interference by users in co-cells, i.e. those cells using the same set of radio channels [1] [2].

Widespread utilization of cellular mobile communications services results in the concentration of more base stations installed in populated and commercial areas to provide good coverage. Cellular base stations use directional antennas to transmit through several carrier frequencies, resulting in a power of several kilowatts may be transmitted in the main beam direction. This increases the public concern about the effects of electromagnetic

radiation on the exposed biological tissues and may result in many electromagnetic compatibility (EMC) problems [3].

This study concentrates on the benefits regarding the RF radiation reduction obtained through the use of adaptive antennas.

The paper is organized as follows: A brief concept of the adaptive antenna system and its benefit is described in Section II. Section III describes the mathematical derivation of the signal to noise ratio (SNR). The impact of RF radiation reduction on RF pollution mitigation is given by simulation in section IV. Conclusions and future work are mentioned in Section V.

2. Adaptive Antenna Technology

The adaptive antenna is an array of antennas with a digital signal processing unit. The whole system can be viewed as a single antenna with a flexible radiation pattern that dynamically varies in response to the radio environment. The transmitted signal is directed toward the intended or the desired user, and nulls are placed in the direction of interferers [1-3]. The signals received at the array elements are multiplied by the complex weights and then summed up to obtain the desired radiation pattern. The complex weights that are determined by the processing unit are continuously adjusted by the signal processing unit which uses the available properties of the desired signal to calculate the weights [4]. Utilizing the initial information about the signal characteristics such as a direction of arrival (DOA), adaptive algorithms can adjust the array weights dynamically with respect to signal environment and perform the desired radiation pattern [5]. Uniform linear array with N antenna elements is assumed to receive uncorrelated signals from K sources. The input signal vector x(t)can be expressed as:

$$x(t) = \sum_{k=1}^{K} a(\theta_k)\, S_k(t) + n(t) \qquad (1)$$

KJPS Al-Kitab Journal for Pure Science
Vol.2 (2), ISSN: 2617-1260 (print), 2617-8141(online)
www.kjps.isnra.org

where$_k$(t) is K ×1 vector concerning to the k-th source located at direction θ_k from the array, a (θ_k) is the N×1 steering vector of the array for the direction of θ_k that can be written as:

$$a(\theta_k) = [1 \quad e^{-j\beta dsin\theta_k} e^{-j2\beta dsin\theta_k} \quad \dots \quad e^{-j(N-1)\beta dsin\theta_k}] \qquad (2)$$

where is the inter-element spacing that is assumed to be equal to (λ/2), and β=2π/λ.

The array output y(t) can be generated through the adjustment of the complex weight vectors as shown in Figure 1.

$$y(t) = \sum_{m=1}^{N} x(t)\, w^H(t) \qquad (3)$$

where (w^H)denotes the transposition of the complex conjugate vector.

Many algorithms are used in many papers such as [4], [5], and [6] to determine and update the uplink weight vectors for performing beamforming on the received signals. In this study, Normalized Least Mean Square (NLMS) algorithm is employed due to its reliable results in stability.

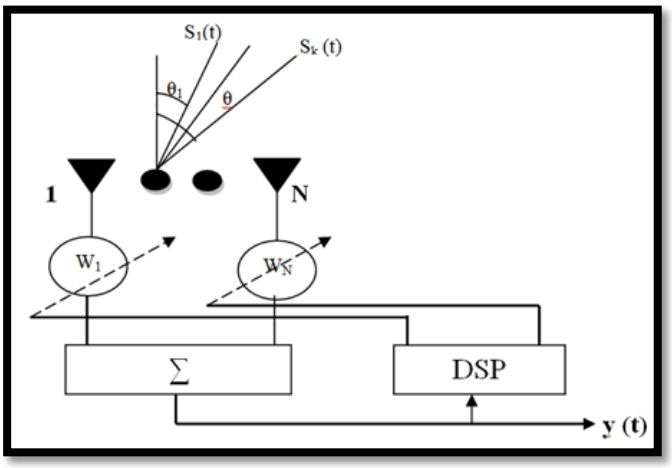

Fig. 1: Adaptive Antenna Construction.

KJPS Al-Kitab Journal for Pure Science
Vol.2 (2), ISSN: 2617-1260 (print), 2617-8141(online)
www.kjps.isnra.org

3. Derivation of Signal to Noise Ratio (SNR)

The output at each antenna element in the adaptive array is phase shifted by multiplication with the weight coefficients, and these outputs will be positively combined to increase the signal amplitude increases N times.

In the uplink, the amplitude of the received signal from the i-th user at any cell and the noise at the base station will be given as:

$$\text{Signal received by basestation} = \sum_{m=1}^{N} r_m = N_r$$

$$Noise = n = n_1 + n_2 + n_3 + \cdots + n_N = N_n$$

$$SNR = \frac{(Nr)^2}{Nn^2} = \frac{N^2 r^2}{Nn^2}$$

$$= N\frac{r^2}{n^2} \qquad (4)$$

In the worst-case scenario when the signal power and noise power are the same (r=n), the signal to noise ratio (SNR) can be given as:

$$SNR = N \qquad (5)$$

The base station receiver sensitivity S can be given in terms of the carrier power C, and the total interference I_t as ($S = C/I_t$)

Adaptive antenna usage at the base station can be characterized by a reduction in C/I ratio or the sensitivity required by the receiver. If the receiver sensitivity is reduced from S1to S2, a capacity increase of (β) and a power reduction of (δ) can be obtained, as follows [3]:

$$S_1 = \frac{C}{I_t} = \frac{C}{I_{MAI} + n}$$

KJPS Al-Kitab Journal for Pure Science
Vol.2 (2), ISSN: 2617-1260 (print), 2617-8141(online)
www.kjps.isnra.org

where C is the carrier power, It is the sum of multiple access interference (I_{MAI}) from the same cell (intra-cell) and other cells (inter-cell), and n is the noise power.

$$S_2 = \frac{\delta\ C}{(1-\alpha)\ I_t\ + \beta\ \delta\ \alpha I_t} \Longrightarrow \frac{S_1}{S_2} = \frac{C}{I_t} \cdot \frac{(1-\alpha)\ I_t\ + \beta\ \delta\ \alpha I_t}{\delta\ C}$$

$$\delta = \frac{1-\alpha}{(S_1/S_2) - \beta\alpha} \qquad (6)$$

where α is the cell load that is equal to the ratio of active users to the maximum allowable number of users expressed in terms of percentage of capacity.

A.Receiver Sensitivity Improvement

As can be noticed from equation 6, the use of adaptive antenna has the ability to decrease the base station receiver sensitivity by a magnitude that is equivalent to the additional diversity gain obtained in up-link without capacity extension. Figure 2 shows the obtained power reduction (α) due to adaptive antenna usage at different load factors. It can be seen that in a 40% loaded system, a 6.0 dB receiver sensitivity improvement could lead to a 7.75 dB power reduction. The same receiver sensitivity could lead to about 9.27 dB in 60% loaded system, and 12.0 dB in 80% loaded system. This can allow the receiver to receive a weaker signal from the cell phones and can be translated into cellphone battery life extension and radiated power density reduction around the head of the cell phone user.

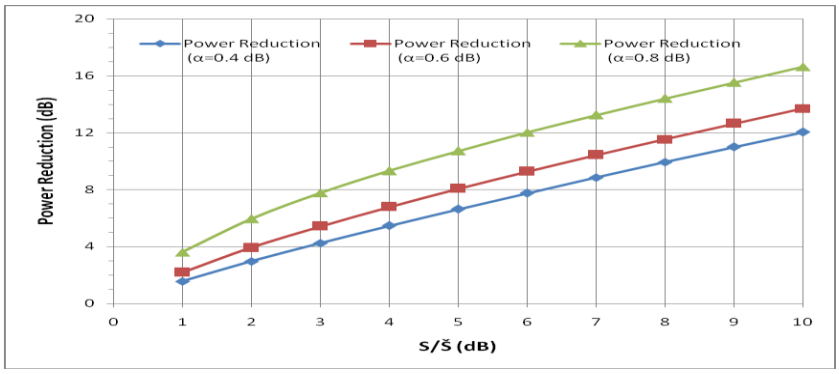

Figure 2: Power Reduction Effects on Receiver Sensitivity

The adaptive antenna with ten elements at the base station would need (1/10) the power transmitted by the cell phone to produce the equivalent radiation of a single antenna base station. On the other hand, when the power transmitted by the mobile phone remains the same as the adaptive antenna array of N elements at the base station, the cost of the amplifier required at the base station will reduce.

Therefore, the use of adaptive antenna has the ability to decrease the base station receiver sensitivity by a magnitude that is equivalent to the additional diversity gain obtained. This can allow the receiver to receive a weaker signal from the cell phones, and this can be translated into cell phone battery life extension and capacity improvement.

B. RF Pollution Reduction

Keeping the size of the area covered by a base station, the adaptive antenna can be used to reduce the actual power transmitted by the base station. Replacing an antenna with a gain of (G_1) by another antenna with a gain of (G_2) allows reducing the actual transmitting power from (P_1) to (P_2), with the same effective transmitted power (ERP).

$$(ERP)_1 = P_1 G_1 \quad , \quad (ERP)_2 = P_2 G_2$$

$$P_2 = P_1 \frac{G_1}{G_2} = P_1 \frac{G_1}{N G_1} = P_1 \frac{1}{N} \qquad (7)$$

Equation (8) implies that the transmitted power of the base station can be reduced by a factor of (1/N).

The power density (P_d) at any distanced from the base station antenna can be given as:

$$P_d = \frac{P G}{4 \pi d^2} \qquad (8)$$

Where P is the power transmitted by the base station through an antenna with a gain of G is an antenna gain.

KJPS Al-Kitab Journal for Pure Science
Vol.2 (2), ISSN: 2617-1260 (print), 2617-8141(online)
www.kjps.isnra.org

$$(P_d)_1 = \frac{P_1 G_1}{4\pi d^2} \quad ,(P_d)_2 = \frac{P_2 G_2}{4\pi d^2}$$

$$\frac{(P_d)_2}{(P_d)_1} = \frac{1}{N} \tag{9}$$

This implies that the exposer of any object to the electromagnetic radiation emitted by the base station antenna will be reduced by (1/N).

Figure 3 shows the power density against the number of antenna elements used at the base station when a power of ten watts is transmitted through an antenna of 18 dBi gain. It can be noticed that the power density at a distance of 20m from the base station antenna is equal to 1.255mW/cm^2 when one antenna is used, while it decreases to 0.627mW/cm^2 when an array of two elements is used, a value of 0.313 mW/cm^2 with a base station of four elements, the use of eight elements array produces a 0.016mW/cm^2, and a 16-elements array gives 0.785 µw/cm^2.

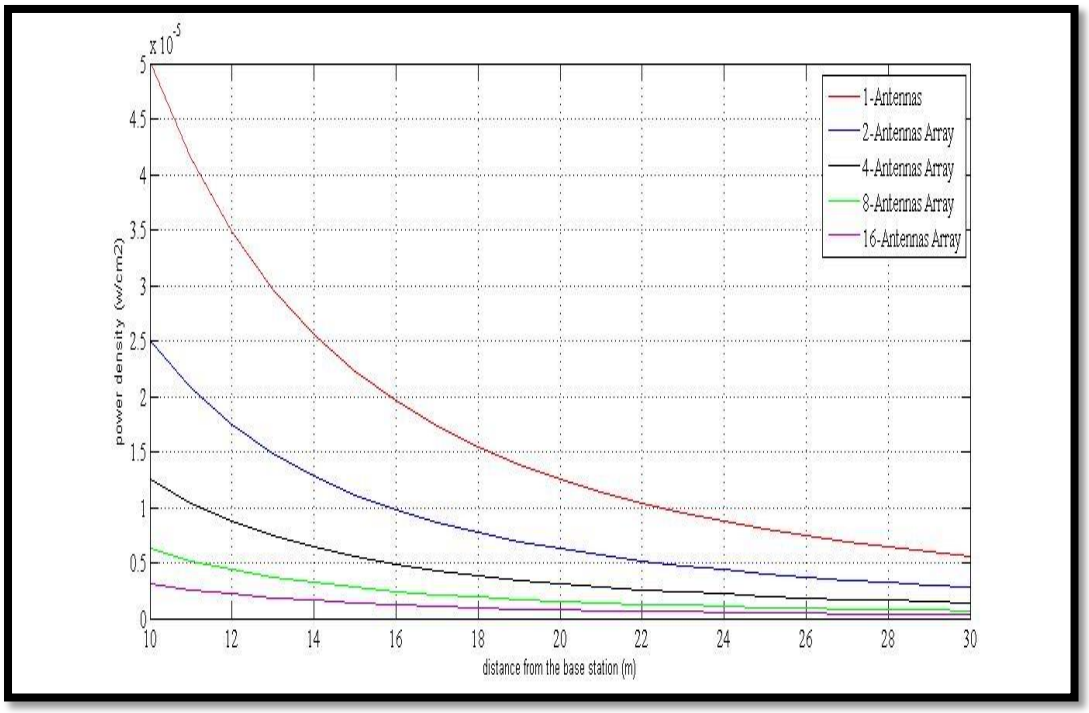

Figure 3: Power density vs adaptive array elements

KJPS Al-Kitab Journal for Pure Science
Vol.2 (2), ISSN: 2617-1260 (print), 2617-8141(online)
www.kjps.isnra.org

C.Base Stations Density Reduction

With adaptive antenna application, the excessive gain that is equivalent to the number of antenna array *N*will increase the highest allowable path loss level. With the adaptive antenna, the maximum path loss will be achieved at a distance (d_2) that is greater than the distance (d_1) obtained with the use of the single antenna element.

$$P_r(d) = P_t\ G_t\ G_r\ \frac{h_b^{\,2}\ h_m^{\,2}}{d^4}$$

$$path\ loss = \frac{P_r}{P_t} = P_L(d) = G_t\ G_r\ \frac{h_b^{\,2}\ h_m^{\,2}}{d^4}$$

$$[P_L(d_1)]_{dB} = G_t + G_r + 20\log(h_b\ h_m) - 40\log(d_1)$$

$$[P_L(d_1)]_{dB} = G_t + 10\log(M_m) + G_r + 20\log(h_b\ h_m) - 40\log(d_2)$$

For range extension without power reduction: $[P_L(d_1)]_{dB} = [P_L(d_1)]_{dB}$

$$G_t + 10\log(N_m) + G_r + 20\log(h_b\ h_m) - 40\log(d_2) = G_t + 20\log(h_b\ h_m) - 40\log(d_1)$$

$$10\log(N_m) = -40\log(d_1) + 40\log(d_2)$$

$$10\log(N_m) = 40\log(d_2/d_1)$$

$$(d_2/d_1) = Range\ Extension = \sqrt[4]{N} = N^{1/4}$$

Assuming circular cell, the area covered by a base station with a single antenna will be $(\pi\ d_1^{\,2})$, the area covered by a base station with an adaptive array will be $(\pi\ d_2^{\,2})$, and the coverage extension will be

$$Coverage\ Extension = \frac{\pi\ (d_2)^2}{\pi\ (d_1)^2} = \left(N^{\frac{1}{4}}\right)^2 = \sqrt{N} \qquad (10)$$

If the total area required to be covered by the cellular network is assumed to be *A* and the system base stations are distributed uniformly, the required base station for full coverage

KJPS Al-Kitab Journal for Pure Science
Vol.2 (2), ISSN: 2617-1260 (print), 2617-8141(online)
www.kjps.isnra.org

will be reduced by $(A/\pi\, d_1^{\,2})$ with single antenna base station against $(A/\pi\, d_2^{\,2})$ with the use of the adaptive antenna. This will reduce the required number of base stations.

$$Base\ Station\ reduction = \frac{A/\pi\, d_2^{\,2}}{A/\pi\, d_1^{\,2}} = 1/\sqrt{N} \tag{11}$$

This means that the required number of the base station will be reduced $(1/\sqrt{N})$, and this, in turn, will reduce the number of electromagnetic radiation sources.

D.Frequency Reuse Efficiency Improvement

The interference is one of the main limiting factors in cellular network capacity. The frequency reuse efficiency *f* has defined the ratio of the other-cell interference power I_{oc} to the same-cell interference power I_{sc}. Interference level reduction can increase the maximum number of supportable users in a cellular system.

$$f = \frac{I_{OC}}{I_{SC}} \tag{12}$$

Assuming omnidirectional base stations network of a total coverage area of a radius *R*, and the users are uniformly distributed in each network cell. The distance between any user at any cell and the serving base station denoted r_u. The power received by mobile at distance r_u from its serving base station will represent the user contribution in same cell interference (I_{sc}). It can be given as

$$P_{ru} = P_t\ K\ (r_u)^{-\gamma} = I_{sc} \tag{13}$$

where *K* is a constant that depends on the antenna heights, the antenna gains, and the operating frequency, γ is the power exponent value, P_{ru} is the power received by the mobile phone, and P_t is the power transmitted by the serving base station. Each elementary surface ($z\ dzd\theta$) at a distance *z* from the desired user contains ($\rho BSzdzd\theta$) base stations which contribute in other cell interference as shown in Figure 6.

$$I_{oc} = \int_0^{2\pi} \int_{2R_c}^{R} \rho_{BS} P_t\ K\ z^{-\gamma}\ z\ dz\ d\theta \tag{14}$$

KJPS Al-Kitab Journal for Pure Science
Vol.2 (2), ISSN: 2617-1260 (print), 2617-8141(online)
www.kjps.isnra.org

$$I_{oc} = K P_t \rho_{BS} \int_0^{2\pi} \int_{2R_c}^{R} z^{1-\lambda} \, dz \, d\theta$$

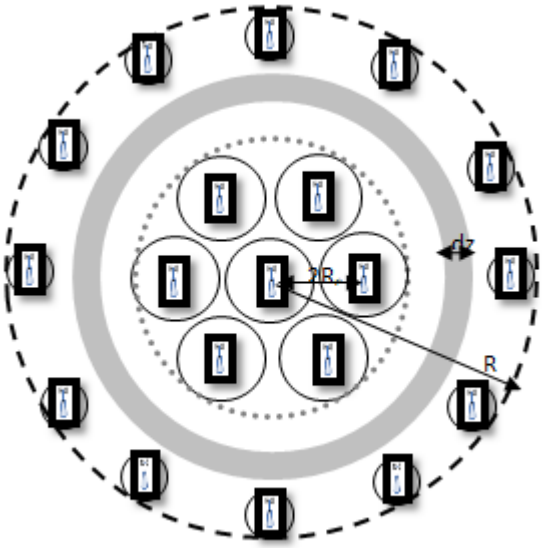

Figure 4: frequency reuse

4. Conclusions

For wireless communications, a smart antenna system offers several advantages over conventional antennas. These include range extension, capacity increasing lower power consumption. The impact on power reduction at mobile base station has been presented. It has been noticed that gain obtained by using smart antenna leads to reduce the cellular phone transmitted power and its effect on the human brain, which means the reduction of Pollution caused by RF radiation. The power reduction will contribute to cellular base-station network reduction.

References

[1]Adheed H. Sallomi, Ahmed, Sulaiman, ***"Elman Recurrent Neural Network Application in Adaptive Beamforming of Smart Antenna System"***, International Journal of Computer Applications, Vol. 129, No.11, 2015, pp38-43.

[2]Durrani, Salman, ***"Investigations into Smart Antennas for CDMA Wireless Systems"***, A Ph.D. thesis submitted to the School of Information Technology at the University of Queensland, Australia, 2004.

[3]EL Zooghby, A. H., ***"Potentials of Smart Antennas in CDMA Systems and Uplink Improvements,"*** IEEE Antennas and Propagation Magazine, Vol. 43, No. 5, October 2001, pp. 172-177.

[4] Sallomi, Adhered Hasan, Hussein Ali Hussein, ***"Adaptive Antenna Capabilities in GSM Systems Performance Improvement"***, Eng &Tech Journal, Vol. 33, Part A, No. 3, 2015, pp. 548-559.

[5] Ch. Santhi Rani, P. V. Subbaiah, K. Chennakesava Reddy, S. Sudha Rani, ***"LMS and RLS Algorithms for Smart Antennas in A W-CDMA Mobile Communication Environment"***, ARPN Journal of Engineering and Applied Sciences, Vol. 4, No. 6, 2009, pp. 78-88.

[6]*Why Have Smart Antennas Not Yet Gained Traction with Wireless Network Operators"*, IEEE Antennas and Propagation Magazine, Vol. 47, No. 6, December 2005, pp. 124–126.

KJPS Al-Kitab Journal for Pure Science
Vol.2 (2), ISSN: 2617-1260 (print), 2617-8141(online)
www.kjps.isnra.org

DOI: http://10.32441/kjps.02.02.p7

Effect of Addition Of Zirconium Oxide Nanoparticles on Flexural Strength and Porosity of Heat Cure Acrylic Resin

Ranj A. Omer (*); Fahd S. Ikram(**)

(*) B.D.S., Master student at Hawler College of dentistry department of Prosthodontics. Email: omerranj@gmail.com

(**) B.D.S., M.Sc., Ph.D., Lecturer at the college of Dentistry- Hawler Medical University. Email: Fahd77f@yahoo.com

Abstract

Heat cure denture base is the most commonly used material for fabrication of removable prosthesis to the present day. However difficulties persist in fabrication of satisfactory prosthesis due to poor mechanical properties which have resulted in frequent repairs in dental practice. The present study is aimed to investigate the effect of Zirconium oxide nanoparticles (ZrO_2NPs) on flexural strength and porosity of denture base and its correlation. X-ray diffraction (XRD) was used to check the purity of NPs. NPs was dispersed at 1%, 3% and 5% by weight to the monomer of methyl methacrylate with aid of probe sonicator. In addition, Scanning Electron Microscope (SEM) was used to observe agglomeration of particles within the acrylic. The results revealed significant flexural strength difference ($p<0.05$) between each concentration of ZrO_2NPs. The analysis showed 17% and 11% reduction for 1% and 3% ZrO_2NPs respectively while 5% caused a drastic reduction by 32% in reference to control. In regards to porosity, the results present no statistically significant difference among the concentrations in contrast to control. Pearson correlation showed strong and a negative relation (-0.83) between flexural strength and porosity. However, the results was not statistically significant ($p=0.369$). Within the limitations of this study, it can be concluded that the addition of ZrO_2 caused reduction in flexural strength for all

KJPS Al-Kitab Journal for Pure Science
Vol.2 (2), ISSN: 2617-1260 (print), 2617-8141(online)
www.kjps.isnra.org

concentrations added. While it caused non-significant effect on porosity of acrylic. Considering the negative effect it had on mechanical strength it won't be considered a suitable additive to enhance the properties of PMMA.

Keywords: Zirconium oxide nanoparticle, flexural strength, porosity, planimeter.

تأثير إضافة جزيئات أكسيد الزركونيوم النانوية على قوة الانضغاط ومسامية المعالجة الحرارية للأكريليك

الخلاصة

تعتبر مادة الأكريليك هي المادة الأكثر استخدامًا لتصنيع الأسنان حتى يومنا هذا٠ تهدف هذه الدراسة إلى تأثير جزيئات أكسيد الزركونيوم على قوة الانثناء ومسامية٠ تم استخدام XRD للتحقق من نقاء جسيمات أكسيد الزركونيوم النانوية قبل استخدامها في الدراسة٠ تم اضافه الجسيمات النانوية ب ١٪ ، ٣٪ و ٥٪ بالوزن إلى مونومر الميثيل ميثاكريلات مع مساعدة Sonicator ٠ اتم إعداد أربعين عينة٠ بالإضافة إلى ذلك ، تم إجرا فحص SEM لمراقبة تكتل الجزيئات داخل الأكريليك٠أظهرت النتائج اختلاف كبير في قوة الانثناء بين كل تركيز من جسيمات أكسيد الزركونيوم النانوية٠ بحيث اضهرت انخفاضاً بنسبة ١٧٪ و ١١٪ لـ ١٪ و ٣٪ من أكسيد الزركونيوم على التوالي في حين أن ٥٪ تسبب في انخفاض حاد بنسبة ٣٢٪٠ في فيما يتعلق بالمسامية ، يضهر النتائج فروق ذات دلالة إحصائية٠ أظهرت Person correlation علاقة سلبية بين قوة الانثناء والمسامية ومع ذلك ، لم تكن النتائج ذات دلالة إحصائية٠ ضمن حدود هذه الدراسة ، يمكن الاستنتاج أن إضافة أكسيد الزركونيوم تسبب في انخفاض في قوة الانثناء لجميع التركيزات المضافة في حين أنه يؤدي إلى تأثير غير معنوي على مسامية الأكريليك وبالنظر إلى التأثير السلبي الذي لديه على القوة الميكانيكية ، فإنه لن يعتبر مادة مضافة مناسبة لتعزيز خصائصPMMA ٠

1. Introduction

Throughout the years, researchers are trying to improve the quality of biomaterials for fabrication of denture base because of increase in life expectancy of human beings and increasing demand of patients for better aesthetics, function and comfort. [1] Complete and partial dentures that are made from acrylic considered the most popular method because it provides a much affordable option for reconstruction than other available prosthesis. [2] Numerous materials with their modifications have been put to the market with enhanced mechanical and biological properties; despite this, there is still no single material that can fulfil the ideal requirements for denture base material. [3]

Polymethyl methacrylate (PMMA) is a derivative of acrylic acid, which related to as acrylic resin [4] that was introduced in 1937, by Walter Bauer, which gradually took the place of the traditional metal base and became most widely used material in clinical practice [5,6] because of its good biocompatibility, dimensional stability, the absence of taste and odour, good tissue response and outstanding toxicity profile.[7] Despite those excellent properties, PMMA demonstrates high porosity [8] and frequent fracture under load due to fatigue and chemical degradation.[9,10] Fracture resistance of PMMA does not show satisfactory results.[11] According to a survey, 68% of dentures had broken within 3 years of their construction. [12]

Due to their unsatisfactory properties, PMMA remain as an active material for research.[7] Generally speaking, there are three methods manufacture uses to enhance mechanical properties of denture base: discovery or development of new material to PMMA; chemical alteration of PMMA to fabricate high impact resin; and reinforcement of PMMA by other materials (e.g. nanoparticles). [13–15] Addition of nanoparticles (NPs) to the polymer matrix will result in alteration of mechanical properties by providing resistance against stress causing cracking. [14, 16, 17] Depending on the way the material will be enhanced it would be based on the size, shape, type and concentration of the added material. [17]

Alveolar ridge resorption is a continuous and irregular operation that causes uneven prosthesis support [18] with perpetual chewing cycles will result in generation of micro-

cracks in the material and continual application of force will cause propagation of cracks and flexural fatigue that commonly manifest itself as midline fracture. [15, 19] Studies had tried to improve the flexural properties of the material to overcome the consequence of fracturing and enhancing patient's satisfaction. [20] Study by Xin-jing et al. [21] that added nano Zirconium oxide (ZrO_2) NPs to acrylic at seven different concentrations (0.5%, 1%, 1.5%, 2%, 2.5%, 3% and 3.5%). Out off all the proportions 1.5% showed the highest mean value. On the same year, Al_2O_3 and ZrO_2 particles were incorporated to PMMA at 5% that improved flexural property. [22] Also, elevation of flexural value was demonstrated in another study that used 1.5%, 3%, 5% and 7% ZrO_2 in PMMA; the results revealed a direct relation between concentrations and strength value.[23] Furthermore, 10% and 20% ZrO_2 showed a statistically significant effect on increase of flexural mean of high impact acrylic by 32% and 23% respectively when compared to control.[24] Gad and his colleagues in 2016 [17] showed a raise in flexural strength at 2% only, while opposite effect was seen for 5%. Recently, Ergun et al.[25] added ZrO_2 NPs to heat cure PMMA at 5%, 10% and 20%. Results showed inverse relation with statistically significant effect for all concentrations.

Porosity considered as a quality of solid that is related to their structure and is expressed in the presence of voids between separate grains, layers, crystals, and other elements of a coarse structure of solid. [26] Porosity of PMMA is one of the most unfavourable characteristics because it causes high internal stress and increase susceptibility to distortion and warpage. [27] It has been attributed to variety of factors that include: monomer contraction during polymerization; air entrapment during mixing; monomer vaporization associated with exothermic reaction; presence of residual monomer; inadequate pressure on the flask and processing temperature higher than 74 °C. [28,29] It has been declared that 11% porosity in acrylic resin is linked to poor esthetic and reduction in mechanical properties. [30] The main concerns with the spongy areas is the harbour microorganisms and retain fluids which cause calculus deposition and staining that does not follow the definition of hygienically acceptable prosthesis.[9, 14]

Several methods have been utilized to calculate porosity of acrylic samples which are the classical, [31] photographical method that uses microscope [27] and mercury

porosimetry.[32] In this study, photographical method with aid of planimeter was used. To this date the influence of NPs on porosity of acrylic resin is very much restrained by the limitation of literatures available. A research by Acosta- Torres and his colleagues[33] that used classical method to measure the effect of TiO_2 and iron oxide (Fe_2O_3) NPs at 0.0150g and 0.009g respectively on porosity of PMMA. The result showed reduction in porosity of acrylic by 5.9% in contrast to unmodified. The findings suggested that metal oxide NPs can be a suitable additive for improvement of PMMA since high porosity considered as a critical drawback in Prosthodontic applications. [34] Furthermore, impregnated ZrO_2 NPs at 3%, 5% and 7% to heat cure PMMA revealed decrease in porosity by 18%, 38% and 55% for 3%, 5% and 7% ZrO_2 respectively. [35]

This study is attempted to investigate the effect of ZrO_2 NPs on flexural strength and porosity as well as it is correlation on conventional heat cure acrylic.

2. Materials and Methods

The ZrO_2 NPs were characterized using X-ray diffraction (PANalytical X'pert powder) with Cu-Kα X-ray source at a wavelength of λ= 1.54060$\dot{A}$. Diffraction data was recorded at 2θ range from 10° to 79.9950° with step size 0.0100° per 0.5s. Low scan speed was elected to provide higher sensitivity for detection of impurities. [36] The PANalytical software was then used to compare X-ray patterns to identify the nanoparticle.

In addition, SEM was used to check for agglomeration of ZrO_2 NPs within acrylic. The samples had dimensions of 30x10x2.5 mm (Length x width x thickness) and were cut in the middle, width wise. The specimens were cleaned for 10 minutes using ultra-sound cleaning device and then dried.[37] Looking at nonconductive material such as acrylic causes negative charge accumulation. [38] To overcome this, gold was sputter coated at a thickness of 300 $\dot{A}$ for 300s. Planetary rotation was used during coating process to provide a more uniform thickness. [39] Scanning was done using Quanta 450 SEM. Photographs were taken at 15,000x at accelerated voltage 15.00kV [40] using high vacuum mode.

The NPs was bought from Richest Group Company in China with 50nm in size and surface treated with saline coupling agent. The saline agent will provide a better bond between particles and acrylic [41] and minimizes agglomeration. [17,30] In order to reduce agglomeration of NPs, they were added to acrylic monomer first and then mixed with powder [23,25,29] with aid of probe sonicator (Biosafer 900-02) using the settings provided below:

a. Power Rate: 80%
b. Power: 900w
c. Probe size: 12 Φ
d. Processing time: 1-minute
e. Pulse on: 8s
f. Pulse off: 2s
g. Temperature warning: 37 °C.

Sonication was started with 8s on and 3s off to keep the temperature within the set range. After the sonication time was over, polymer powder was added immediately to the suspension (within 10s) to prevent re-agglomeration of NPs. [16] The mix was polymerized using conventional flasking and pressure packing technique. After polymerization was over, de-flasking was done and samples with gross porosity were divorced according to revised ADA specification number 12 for denture base polymer.[42]

3. Flexural strength test

For flexure strength test, 5 samples were prepared for each concentration of ZrO_2 making a total of 20 samples including the unmodified group. Each sample had a dimension of 65 mm length x 10mm width x 3mm thickness and were stored in distilled water at 37 ± 1 °C for 50 ± 2 hours, in compliance with International Standard Organization (ISO) 1567:1999 Denture Base Polymers. [43] The flexural value was obtained by doing a three-point bending test using universal testing machine. The samples were placed on circular supports (3.2mm in diameter and 10.5mm in length) that are 50 mm apart (Figure 1). Then force was applied perpendicular to the centre of the specimen using the loading nose at a crosshead speed of

5.00 ± 1 mm/ min until it breaks.[43] The maximum load required to fracture the specimen was recorded.

Then flexural strength was calculated using the formula: $\delta = \frac{3Fl}{2bh^2}$

Where: F: is the maximum load, in Newton, exerted on the specimen; l: is the distance, in millimetre, between the supports, accurate to ±0.01; b: is the width, in millimetre, of the specimen measured immediately prior to water storage and h: is the height, in millimetre, of the specimen measured immediately prior to water storage.

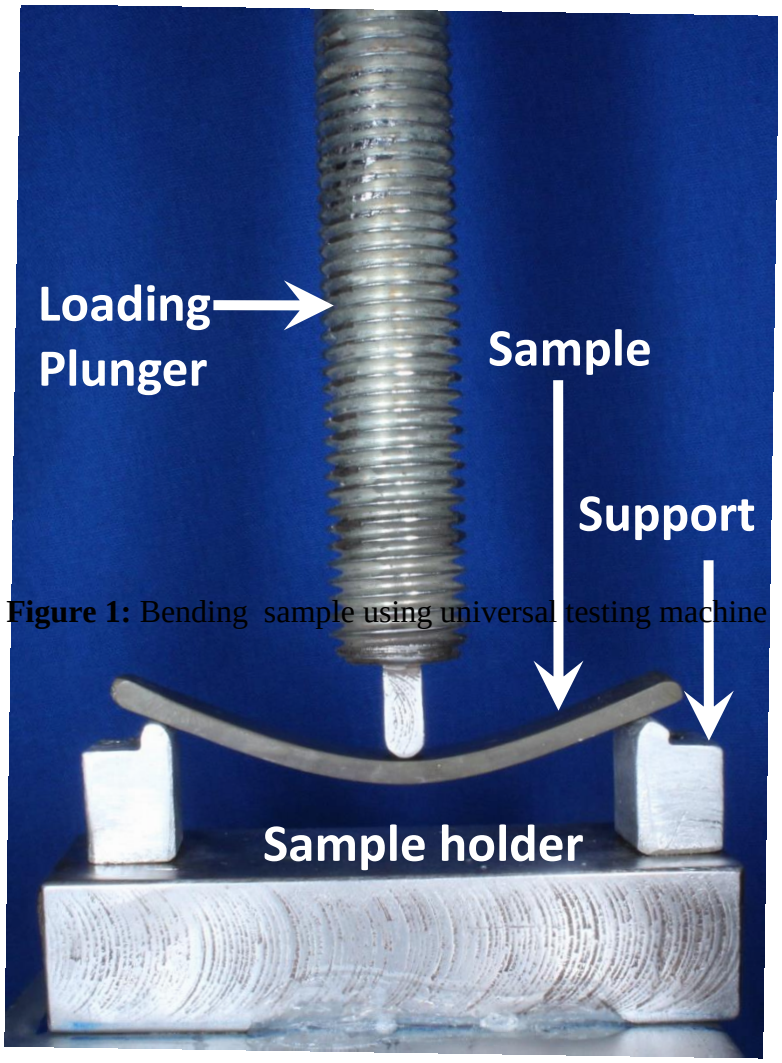

Figure 1: Bending sample using universal testing machine

KJPS Al-Kitab Journal for Pure Science
Vol.2 (2), ISSN: 2617-1260 (print), 2617-8141(online)
www.kjps.isnra.org

4. Porosity test

For this test, five samples were prepared for each concentration in addition to five samples for control group. Each sample had dimensions of 40 x 10 x 3mm [44] (Figure 2a). Each specimen was cut in three parts to produce three cross-sectional areas (Figure 2b). First cut was 1mm from the start of the sample; second and third cuts were 13mm apart. The surfaces were polished and observed under Maozua Digital Microscope under 8x magnifications and an image of the sample was captured and printed. Area of each pore evident on the photographs was outlined using a fine pen then perimeter of each pore was measured using a planimeter (Figure 3). Then total areas of pores on each surface were calculated using the formula:

$$\frac{Total\ porous\ area\ of\ specimen\ (mm^2)}{Cross\ sectional\ area\ of\ specimen\ (mm^2)}\ X\ 100 = \text{Area (\%)}$$

After that, the average of the three cross sectional areas was taken to be considered as a total porous area for a single sample.

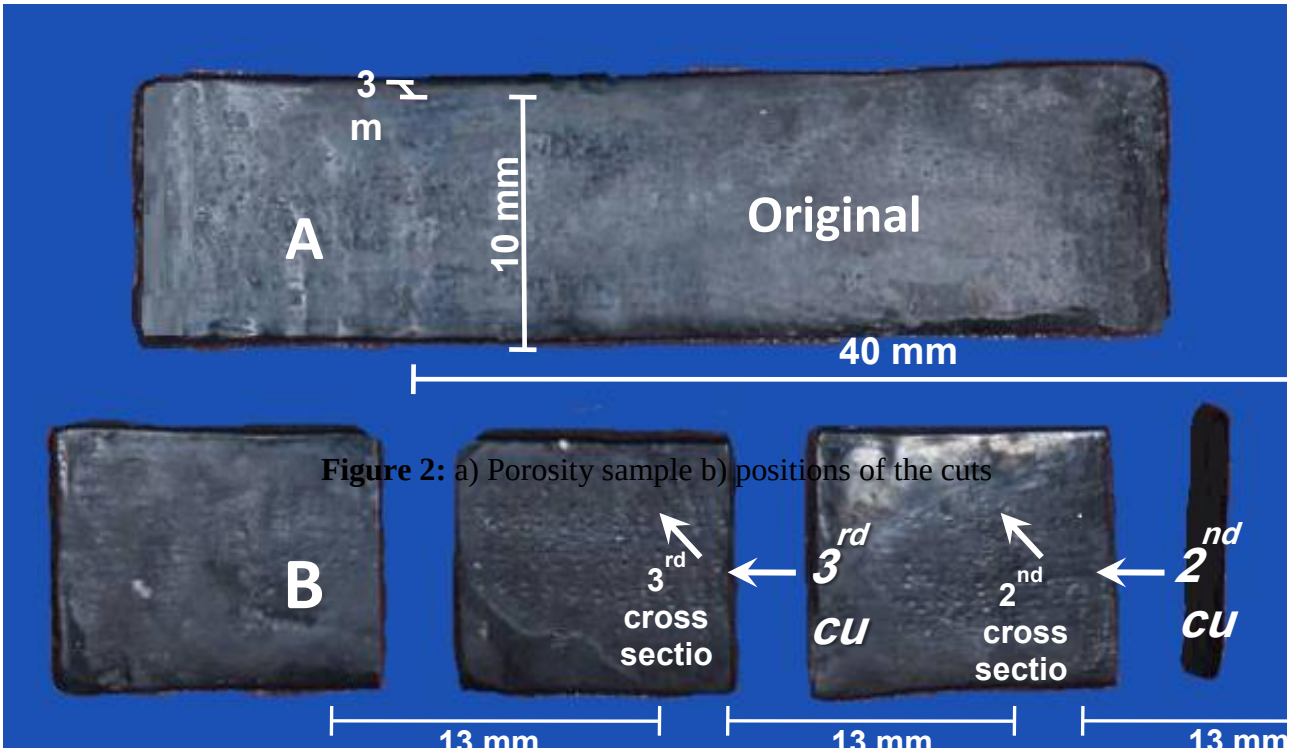

Figure 2: a) Porosity sample b) positions of the cuts

KJPS Al-Kitab Journal for Pure Science
Vol.2 (2), ISSN: 2617-1260 (print), 2617-8141(online)
www.kjps.isnra.org

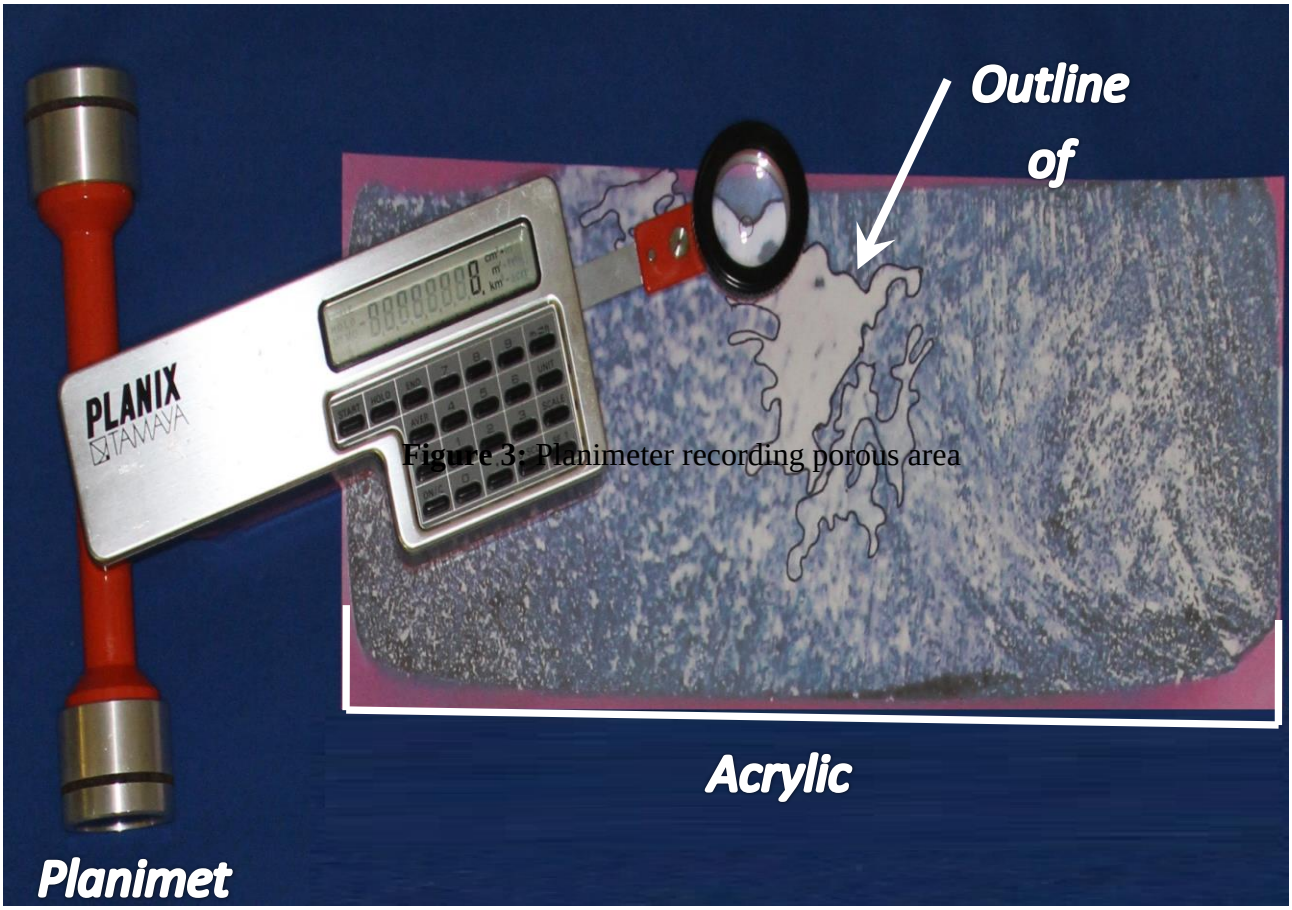

Figure 3: Planimeter recording porous area

The results were analyzed using Statistical Package for Social Sciences (SPSS, version 23). One-way ANOVA with Tukey's Honest Significant Difference (HSD) was performed to determine if there is a statistically significant difference between each concentration of ZrO_2 when compared to control. In addition, Pearson correlation coefficient (PCC) was used to measure and describe the relation between flexural strength and porosity. For statistical analysis, significant level $\alpha = 0.05$ was considered.

KJPS Al-Kitab Journal for Pure Science
Vol.2 (2), ISSN: 2617-1260 (print), 2617-8141(online)
www.kjps.isnra.org

5. Results

ZrO_2 NPs was analyzed using XRD. The PANalytical software was used to compare the XRD pattern. The Sample was identified as ZrO_2 NPs and it is diffraction pattern is shown in Figure 4.

The data that was obtained from flexural strength and porosity test were analysed using one way ANOVA with HSD to find out the effect of addition of NPs at the three concentrations (1, 3, and 5%). The flexural strength results, revealed statistically significant differences ($p< 0.05$) between each concentration of ZrO_2 in reference to control. The results for 1% and 3%, revealed 17% and 11% reduction in flexural mean respectively, while 5% showed a drastic reduction by 32%. Is worth mentioning that the flexural mean for 1% and 3% ZrO_2 NPs did not jeopardize the strength beyond the standard requirement (65 MPa) that has been set for Type 1 denture base polymer [43] except for 5% (59.43 MPa) that did not exceed the minimal limit. The highest value is registered for control group (87.205 MPa) that presented in Table 1.

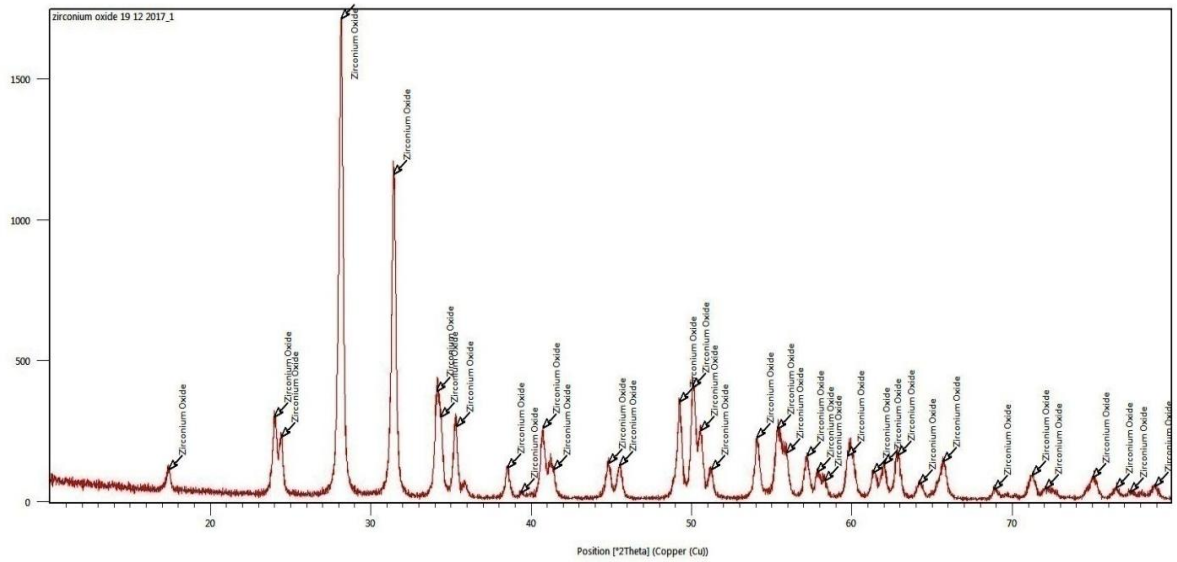

Figure 4: XRD pattern for Zirconium oxide nanoparticle

KJPS Al-Kitab Journal for Pure Science
Vol.2 (2), ISSN: 2617-1260 (print), 2617-8141(online)
www.kjps.isnra.org

Table 1: Descriptive statistics and comparisons of each concentration of ZrO_2 NPs with control group for flexural strength

Nanoparticle	Concentration %	Mean (MPa)	SD	ANOVA P value of concentration with control
Zirconium oxide	1	72.278	1.492	0.00
	3	77.281	0.874	0.00
	5	59.425	1.943	0.00
Control		87.205	2.499	

In regards to porosity test, all the concentrations did not show statistically significant difference when compared to control because their p values were greater than 0.05. 1% and 3% addition of ZrO_2 showed 11% and 6% reduction respectively however 5% caused a 4% increase in porosity in regard to control. The summary for porosity values is illustrated in Table 2. As the table shows the highest porosity mean was for 5% (13.30%) while 1% (11.34%) showed the lowest value among the group.

Table 2: Descriptive statistics and comparisons of each concentration of $ZrO_2$with control group for porosity test.

Nanoparticle	Concentration (%)	Porosity mean (%)	SD	ANOVA P value of concentration with control
Zirconium oxide	1	11.338	2.688	0.450
	3	11.942	0.598	0.817
	5	13.300	0.982	0.940
Control		12.766	0.550	

With regards to correlation, PCC test showed strong and a negative relation (-0.83) between flexural and porosity for ZrO_2. However, the results did not show statistically significant because their p values were greater than 0.05 (p=0.369).

Based upon the data obtained from flexural strength test, ZrO_2 3% and 5% was sent for scanning to check for dispersion and agglomeration of NPs within the matrix of heat cure PMMA. SEM images were taken at 15,000x magnification for all samples. SEM image of 3% (Figure 5) and 5% (Figure 6) of ZrO_2 showed drastically different agglomeration state. The 5% revealed a very high agglomeration within the acrylic in contrast to 3%.

KJPS Al-Kitab Journal for Pure Science
Vol.2 (2), ISSN: 2617-1260 (print), 2617-8141(online)
www.kjps.isnra.org

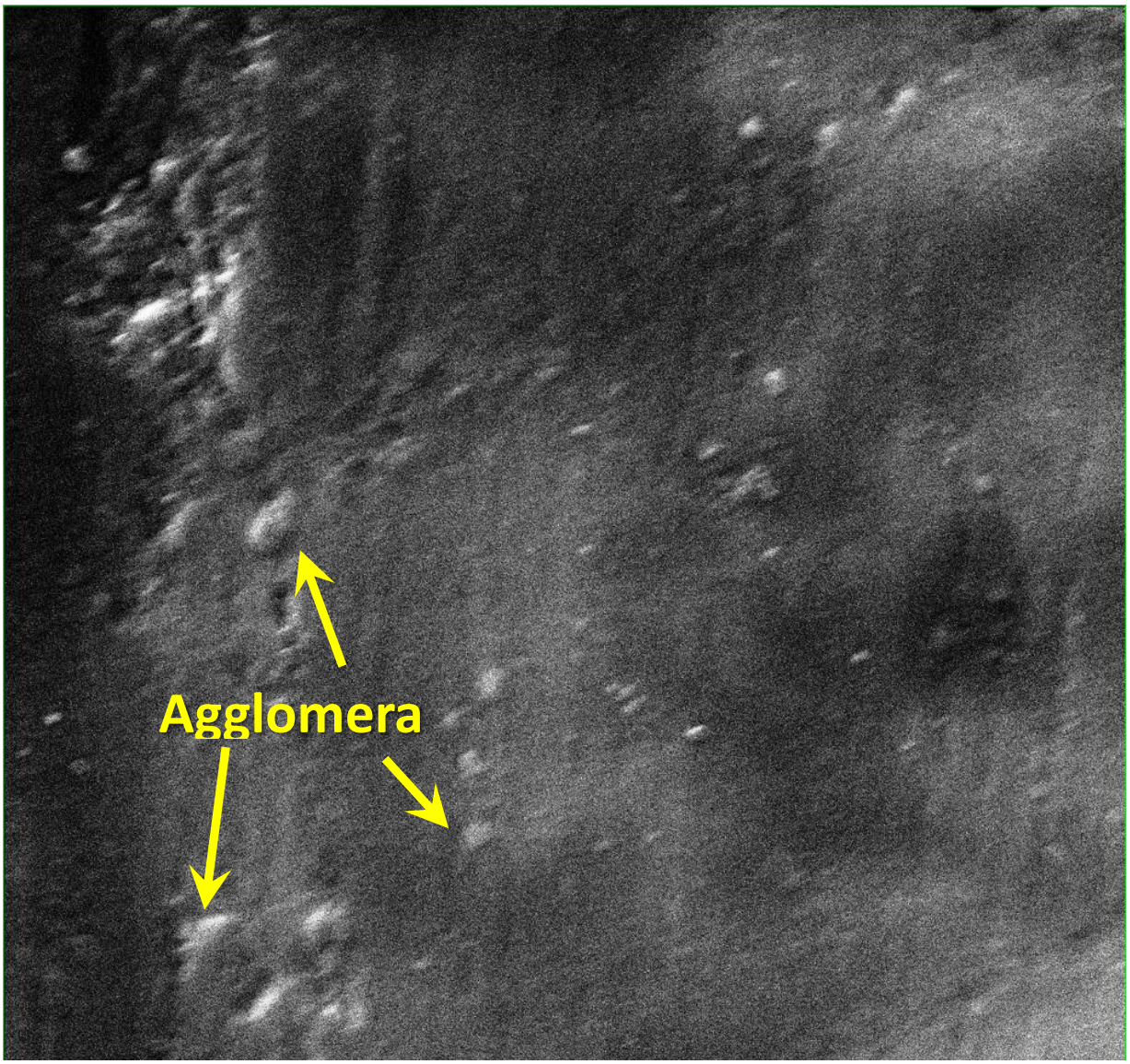

Figure 5: SEM image represents agglomeration of ZrO_2 NPs at 3%.

KJPS Al-Kitab Journal for Pure Science
Vol.2 (2), ISSN: 2617-1260 (print), 2617-8141(online)
www.kjps.isnra.org

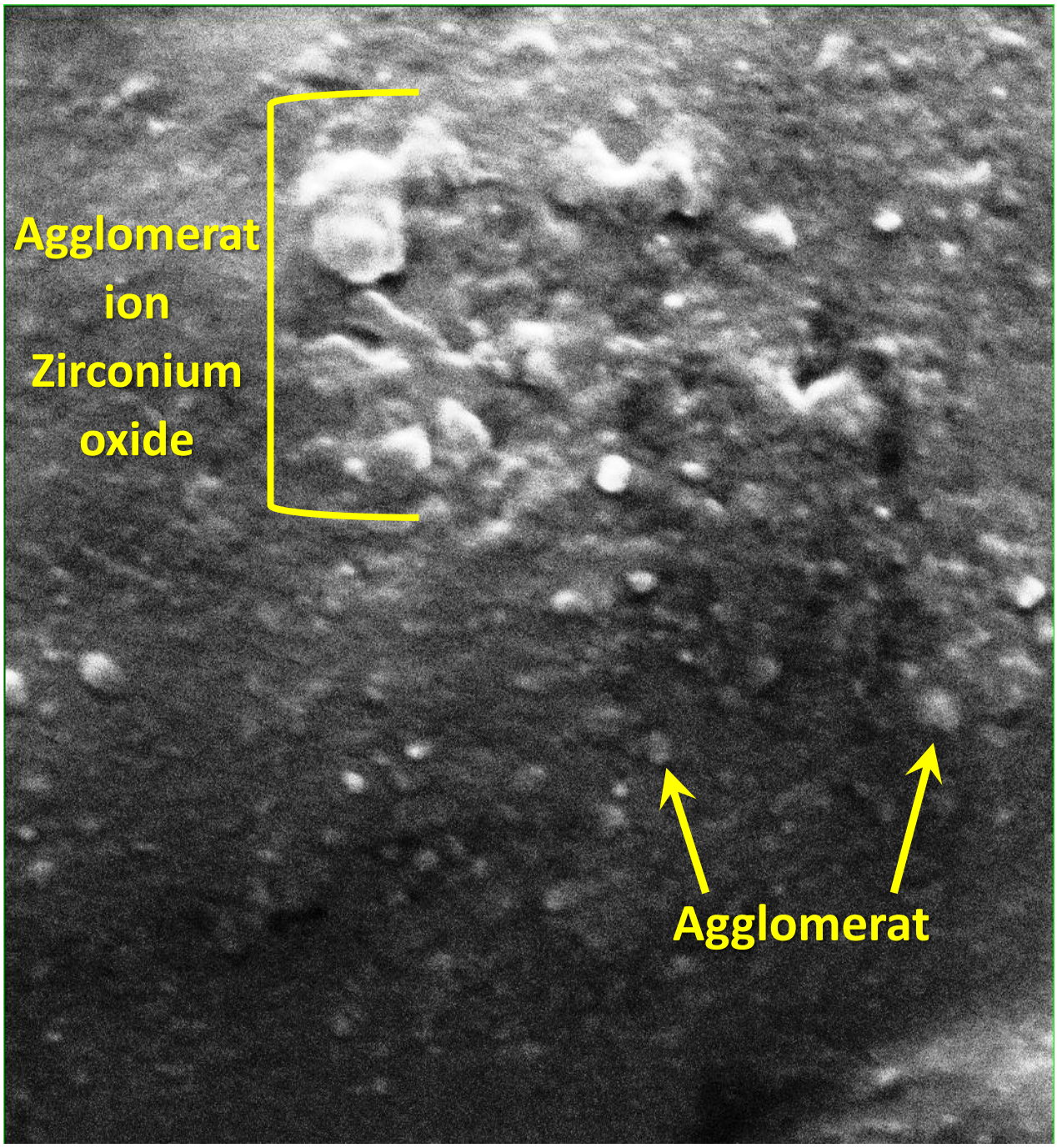

Figure 6: SEM image represents agglomeration of ZrO_2 NPs at 5%.

6. Discussion

Acrylic resin is the most commonly used material in fabrication of dental prosthesis [45] due to its aesthetics, good tissue response and ease of manipulation [9] but its mechanical properties is not satisfactory. [46] The occurrence of denture fracture has been reported in the literature with high rate which compromises the longevity of the prosthesis. [23] Movement and distortion of the denture during mastication with gradual bone resorption will result in unsupported prosthesis which in turn cause stress formation. [47] This commonly termed as flexural fatigue that manifest itself as midline fracture. [48] To mimic the clinical condition the material faces during their use, flexural strength was conducted.

The results of this study showed when ZrO_2 NPs were dispersed in acrylic at 1%, 3% and 5% caused a drastic reduction in flexural strength by 17%, 13%, and 32% respectively. The findings are in disagreement with Xin-jing et al. [21], Alhareb [22] and Ahmed et al.'s[23] research that revealed enhancement in flexural value. As it can be seen from the bending test, the values decreases progressively with increase in NPs concentration which is in agreement with Gad et al.'s [17] and Ergun et al.'s [25] findings. This effect can be linked to many factors. One of the causes is dispersion of NPs which had shown to play an important role in reinforcing material; increasing the filler content in addition to poor dispersion will results in suspending resin matrix continuity and creating defect in the material which weakens it in the outcome. [24] It will also interfere with the reaction of methylmethacrylate which causes an increase in uncreative monomer that behaves as a plasticizer.[34,49] The plasticizer capable in getting between polymer chains which induces the separate chains to become more tenuous and reduce the attraction force between molecules as a consequence the acrylic will be more flexible but brittle. [50]

Another consequence of improper dispersion is agglomeration which causes reduction in strength [51] since too many fillers will act as a stress concentrating point [12,51–53] that will alter the modulus of elasticity of the resin and mode of crack propagation through the polymerized specimen as well as hindering integrity of polymer matrix. [17,54] This concurs with our flexural strength data that showed 5% ZrO_2 had the lowest value (59.43 MPa) in

contrast to 3% (77.28 MPa) which revealed a superior effect that can be linked to a better dispersion with less agglomeration. This can clearly be seen in SEM findings (Figure 5 and 6). Furthermore, agglomeration will brings about micro-cracks and micro-pores as a structural defect which endangers mechanical properties of the polymer.[34] Another reason, is the polymer has reached to a saturation point and the resin cannot incorporate further more filler particles any effort after reaching this point will cause suspending in matrix continuity and compromising the flexural strength of reinforced material in the outcome. [24] In addition to this, NPs might have acted as impurities within the PMMA which led to unfavourable decrease in mechanical strength [55, 56] due to lack of chemical bond will result in poor adhesion between particles and acrylic resin. [51, 57]

Porosity is complex phenomena of multifactorial origin.[32] Several factors have contributed to porosity that includes; polymerization method, thickness and the material of chose, air entrapment during mixing; monomer vaporization associated with exothermic reaction and presence of residual monomer. [28,29] Porosity in a material considered unfavourable condition that can weaken the denture and cause high internal stress which result in a greater vulnerability to distortion.[31]

Based on the results of this study, ZrO_2 NPs at 1% and 3% caused no significant reduction in porosity by 11% and 6% respectively. The obtained results are in consistence with Acosta-Torres et al.'s [33] and Hameed and Rahman's [35] that showed reduction in porosity when NPs were added to acrylic. This is due to well dispersion nano-sized particles that is capable of entering between linear macromolecular chains of the polymer and occupy the spaces between them in the result will decrease the porosity by increasing the density of acrylic without changing the basic structure of PMMA chains. [35,53] Another reason is the fillers will occupy the space inside material leading to a decrease in the number of pores that open up to the external surface. [35] While, 5% caused a 4% increase with the same statistical effect as the other concentrations in reference to control. It has been stated that the concentration of benzoyl peroxide is linked to porosity in an inverse manner.[30,58] Since, 5% ZrO_2 were added to acrylic without reduction in monomer this might increased in the amount of unreacted monomer that will raise the chance for porosity. In addition, NPs in

high concentration will also act as impurity that will interfere with the polymerization reaction thus acting as a plasticizer leading to increase in amount of residual unreacted monomer. [52, 54] This explains the direct proportional relation of NPs concentrations with porosity.

In regards to the relation between flexural strength and porosity, 5% ZrO_2 showed highest porosity as well as lowest flexural value because excessive addition of NPs will affect the polymerization of PMMA resulting in an increase in porosity as well as making the polymer more brittle as a result it will be more prone to breakage during bending test. [50, 59] It is noticeable that all concentrations of NPs had caused porosity of heat cure acrylic to be more than 11%; this would cause unsatisfactory aesthetic and inferior mechanical properties according to the literature. [30]

7. Conclusions

Within the limitations of this study, it can be concluded that the addition of Zirconium oxide caused a reduction in flexural strength for all concentrations added. While it result in a non-significant effect on porosity of acrylic. Considering the negative effect it had on mechanical strength it won't be considered a suitable additive to enhance the properties of PMMA.

References

1. Alla R.K., Swamy R., Vyas R. and Konakanchi A., ***"Conventional and Contemporary Polymers for the Fabrication of Denture Prosthesis: Part I–Overview, Composition and Properties",*** Int J Appl Dent Sci.,1(4),82–89(2015).

2. Campbell S.D., Cooper L., Craddock H., Hyde T.P., Nattress B., Pavitt S.H., et al., **"Removable Partial Dentures: the Clinical Need for Innovation",** The Journal of Prosthetic Dentistry,118(3),273-80(2017).

3. Arora S., Khindaria S.K., Garg S. and Mittal S., **"Comparative Evaluation of Linear Dimensional Changes of Four Commercially Available Heat Cure Acrylic Resins",** Contemporary Clinical Dentistry,2(3),182 (2011).

4. Raghdaa K.J. and Ali A.M., **"Evaluation and Comparison of the Effect of Repeated Microwave Irradiations on Some Mechanical and Physical Properties of Heat Cure Acrylic Resin and Valplast (Nylon) Denture Base Materials",** Journal of Baghdad, College of Dentistry,23(3),6–10(2011).

5. Yli-Urpo A., Lappalainen R. and Huuskonen O., **"Frequency of Damage to and Need for Repairs of Removable Dentures",** Proceedings of the Finnish Dental Society Suomen Hammaslaakariseuran Toimituksia, 81(3),151(1985).

6. Kim Y.K., Grandini S., Ames J.M., Gu L., Kim S.K., Pashley D.H., et al., **"Critical Review on Methacrylate Resin–Based Root Canal Sealers",** Journal of Endodontics, 36(3),383–399 (2010).

7. Spasojevic P., Zrilic M., Panic V., Stamenkovic D., Seslija S. and Velickovic S., **"The Mechanical Properties of a Poly (Methyl Methacrylate) Denture Base Material Modified with Dimethyl Itaconate and Di-N-Butyl Itaconate",** International Journal of Polymer Science, 2015,1-9(2015).

8. Price C.A.,**"A History of Dental Polymers",** Aust Prosthodont J, 8,47-54(1994).

9. Jagger D.C., Harrison A. and Jandt K.D., **"The Reinforcement of Dentures",** Journal of Oral Rehabilitation, 26(3),185–194 (1999).

10. Vivek R. and Soni R. **"Denture Base Materials: Some Relevant Properties and their Determination",** Int J Dent Oral Health, 1(4) (2015).

11. Nejatian T., Sefat F. and Johnson T., **"Impact of Packing and Processing Technique on Mechanical Properties of Acrylic Denture Base Materials",** Materials, 8(5),2093–2109 (2015).

12. Nejatian T., Johnson A. and Van Noort R., **"Reinforcement of Denture Base Resin. In: Advances in Science and Technology",** Trans Tech Publ., 49,124-129 (2006).

13. Hamedi-Rad F., Ghaffari T., Rezaii F. and Ramazani A., **"Effect of Nanosilver on Thermal and Mechanical Properties of Acrylic Base Complete Dentures",** Journal of Dentistry (Tehran University of Medical Sciences), 11(5),495–505 (2014).

14. Alla R.K., Sajjan S., Alluri V.R., Ginjupalli K. and Upadhya N., **"Influence of Fiber Reinforcement on the Properties of Denture Base Resins",** Journal of Biomaterials and Nanobiotechnology,4(1),91–7 (2013).

15. Arıkan A., Ozkan Y.K., Arda T. and Akalın B., **"Effect of 180 Days of Water Storage on the Transverse Strength of Acetal Resin Denture Base Material",** Journal of Prosthodontics: Implant, Esthetic and Reconstructive Dentistry, 19(1),47–51(2010).

16. Alnamel H.A. and Mudhaffer M., **"The Effect of Silicon Di Oxide Nano-Fillers Reinforcement on Some Properties of Heat Cure Polymethyl Methacrylate Denture Base Material",** Journal of Baghdad College of Dentistry, 26(1),32–36(2014).

17. Gad M., ArRejaie A.S., Abdel-Halim M.S. and Rahoma A., **"The Reinforcement Effect of Nano-Zirconia on the Transverse Strength of Repaired Acrylic Denture Base",** International Journal of Dentistry, 2016,1–6(2016).

18. Ajaj-ALKordy N.M. and Alsaadi M.H., **"Elastic Modulus and Flexural Strength Comparisons of High-Impact and Traditional Denture Base Acrylic Resins",** The Saudi Dental Journal, 26(1),15–18(2014).

19. Venkat R., Gopichander N. and Vasantakumar M., **"Comprehensive Analysis of Repair/Reinforcement Materials for Polymethyl Methacrylate Denture Bases: Mechanical and Dimensional Stability Characteristics",** The Journal of Indian Prosthodontic Society, 13(4),439–449(2013).

20. Kanie T., Arikawa H., Fujii K. and Ban S., **"Impact Strength of Acrylic Denture Base Resin Reinforced with Woven Glass Fiber",** Dental Materials Journal, 22(1),30–38(2003).

21. Xin-jing Z., Xiu-yin Z., Bang-shang Z.H., Lu Z. and Chen Q., **"Effect of Nano ZrO_2 on Flexural Strength and Surface Hardness of Polymethylmethacrylate",** Shanghai Journal of Stomatology, 20(4)(2011).

22. Alhareb A. and Ahmad Z., **"Effect of Al_2O_3/ZrO_2 Reinforcement on the Mechanical Properties of PMMA Denture Base",** Journal of Reinforced Plastics and Composites, 30(1),86–93 (2011).

23. Ahmed M.A. and Ebrahim M.I., **"Effect of Zirconium Oxide Nano-Fillers Addition on the Flexural Strength, Fracture Toughness, and Hardness of Heat-Polymerized Acrylic Resin",** World Journal of Nano Science and Engineering, 4(2),50–7(2014).

24. Asopa V., Suresh S., Khandelwal M., Sharma V., Asopa S.S. and Kaira L.S., **"A Comparative Evaluation of Properties of Zirconia Reinforced High Impact Acrylic Resin with that of High Impact Acrylic Resin",** The Saudi Journal for Dental Research, 6(2),146–51(2015).

25. Ergun G., Sahin Z. and Ataol A.S., **"The Effects of Adding Various Ratios of Zirconium Oxide Nanoparticles to Poly (Methyl Methacrylate) on Physical and Mechanical Properties",** Journal of Oral Science, 60(2), 304–315(2018).

26. Pero A.C., Barbosa D.B., Marra J., Ruvolo-Filho A.C. and Compagnoni M.A., **"Influence of Microwave Polymerization Method and Thickness on Porosity of Acrylic Resin",** Journal of Prosthodontics, 17(2),125–129(2008).

27. Wolfaardt J.F., Cleaton-Jones P. and Fatti P., **"The Occurrence of Porosity in a Heat-Cured Poly (Methyl Methacrylate) Denture Base Resin",** Journal of Prosthetic Dentistry, 55(3),393–400(1986).

28. Abood L.N., **"Porosity of Different Thickness of Acrylic Polymerized by Different Methods",** Al-Rafidain Dental Journal, 7(2),173–179(2007).

29. Kasina S.P., Ajaz T., Attili S., Surapaneni H., Cherukuri M. and Srinath H.P., **"To Evaluate and Compare the Porosities in the Acrylic Mandibular Denture Bases Processed by Two Different Polymerization Techniques, Using Two Different Brands of Commercially Available Denture Base Resins-an in Vitro Study",** Journal of International Oral Health, 6(1),72(2014).

30. Keller J.C. and Lautenschalger E.P., **"Porosity Reduction and its Associated Effect on the Diametral Tensile Strength of Activated Acrylic Resins",** Journal of Prosthetic Dentistry,53(3),374–379(1985).

31. Figuerôa R.M., Conterno B., Arrais C.A., Sugio C.Y., Urban V.M. and Neppelenbroek K.H., **"Porosity, Water Sorption and Solubility of Denture Base Acrylic Resins Polymerized Conventionally or in Microwave",** Journal of Applied Oral Science, 26,1-7(2018).

32. Pero A.C., Marra J., Paleari A.G., Pereira W.R., Barbosa D.B. and Compagnoni M.A., **"Measurement of Interfacial Porosity at the Acrylic Resin/Denture Tooth Interface",** Journal of Prosthodontics: Implant, Esthetic and Reconstructive Dentistry, 19(1),42–46 (2010).

33. Acosta-Torres L.S., López-Marín L.M., Núñez-Anita R.E., Hernández-Padrón G. and Castaño V.M., **"Biocompatible Metal-Oxide Nanoparticles: Nanotechnology Improvement of Conventional Prosthetic Acrylic Resins",** Journal of Nanomaterials, 2011,1–8 (2011).

34. Shirkavand S. and Moslehifard E., **"Effect of TiO_2 Nanoparticles on Tensile Strength of Dental Acrylic Resins",** Journal Of Dental Research, Dental Clinics, Dental Prospects,8(4),197(2014).

35. Hameed H.K. and Rahman H.A., ***"The Effect of Addition Nano Particle ZrO_2 on Some Properties of Autoclave Processed Heat Cure Acrylic Denture Base Material",*** Journal of Baghdad College of Dentistry, 27(1),32–39(2015).

36. Ruparelia J.P., Chatterjee A.K., Duttagupta S.P. and Mukherji S. ***"Strain Specificity in Antimicrobial Activity of Silver and Copper Nanoparticles",*** Acta Biomaterialia,4(3),707–716(2008).

37. Vuorinen A.M., Dyer S.R., Lassila L.V. and Vallittu P., ***"Effect of Rigid Rod Polymer Filler on Mechanical Properties of Poly-Methyl Methacrylate Denture Base Material",*** Dental Materials, 24(5),708–713 (2008).

38. Sawyer L., Grubb D.T. and Meyers G.F., "***Polymer microscopy",*** Third Edition, Springer Science & Business Media, New York (2008).

39. Kashin A.S. and Ananikov V.P., ***"A SEM Study of Nanosized Metal Films and Metal Nanoparticles Obtained by Magnetron Sputtering",*** Russian Chemical Bulletin, 60(12), 2602–2607 (2011).

40. Rahamneh A., Abdellateef A. and Mneizel T., ***"Scanning Electron Microscopy of Some Acrylic Resin Specimens After the Addition of Different Types of Fibres",*** JRMS, 14(3),41–45 (2007).

41. Salahuddin N., El-Kemary M. and Ibrahim E., ***"Reinforcement of Polymethyl Methacrylate Denture Base Resin with ZnO Nanostructures"***, International Journal of Applied Ceramic Technology, 15(2),448–459 (2018).

42. Revised American Dental Association specification No. 12 for denture base polymers. The Journal of the American Dental Association, 90(2), 451–458(1975).

43. ISO 1567:1999 Denture Base Polymers.

44. Yannikakis S., Zissis A., Polyzois G. and Andreopoulos A., ***"Evaluation of Porosity in Microwave-Processed Acrylic Resin Using a Photographic Method",*** The Journal of Prosthetic Dentistry, 87(6),613–619 (2002).

45. Özdemir D.H. and Aladag L.İ., ***"The Effect of Different Polymerization Periods on Water Sorption of Acrylic Resins",*** Atatürk Üniversitesi Diş Hekimliği Fakültesi Dergisi, 23(2) (2013).

46. Kawaguchi T., Lassila L.V., Sasaki H., Takahashi Y. and Vallittu P.K., ***"Effect of Heat Treatment of Polymethyl Methacrylate Powder on Mechanical Properties of Denture Base Resin",*** Journal of the Mechanical Behavior of Biomedical Materials, 39,73–78(2014).

47. Beyli M.S. and Von Fraunhofer J.A., ***"An Analysis of Causes of Fracture of Acrylic Resin Dentures",*** Journal of Prosthetic Dentistry, 46(3), 238–241 (1981).

48. Hashem M., Alsaleem S.O., Assery M.K., Abdeslam E.B., Vellappally S. and Anil S.A., ***"Comparative Study of the Mechanical Properties of the Light-Cure and Conventional Denture Base Resins",*** Oral Health Dent Manag., 13(2),311–5(2014).

49. Nazirkar G., Bhanushali S., Singh S., Pattanaik B. and Raj N., ***"Effect of Anatase Titanium Dioxide Nanoparticles on the Flexural Strength of Heat Cured Poly Methyl Methacrylate Resins: an in-vitro Study",*** The Journal of Indian Prosthodontic Society, 14(S1),144–9(2014).

50. Tandra E., Wahyuningtyas E. and Sugiatno E., ***"The Effect of Nanoparticles TiO_2 on the Flexural Strength of Acrylic Resin Denture Plate",*** Padjadjaran Journal of Dentistry, 30(1)(2018).

51. Sodagar A., Bahador A., Khalil S., Saffar Shahroudi A. and Zaman Kassaee M., ***"The Effect of TiO_2 and SiO_2 Nanoparticles on Flexural Strength of Poly (Methyl Methacrylate) Acrylic Resins",*** Journal of Prosthodontic Research, 57(1),15–9 (2013).

52. Kul E., Aladağ L.İ. and Yesildal R., ***"Evaluation of Thermal Conductivity and Flexural Strength Properties of Poly (Methyl Methacrylate) Denture Base Material Reinforced With Different Fillers",*** The Journal of Prosthetic Dentistry,116(5),803–810 (2016).

53. Chladek G., Basa K., Mertas A., Pakiela W., Żmudzki J., Bobela E., et al., ***"Effect of Storage in Distilled Water for Three Months on the Antimicrobial Properties of Poly (Methyl Methacrylate) Denture Base Material Doped with Inorganic Filler",*** Materials, 9(5),328 (2016).

54. Vojdani M., Bagheri R. and Khaledi A.R., ***"Effects of Aluminum Oxide Addition on the Flexural Strength, Surface Hardness, and Roughness of Heat-Polymerized Acrylic Resin",*** Journal of Dental Sciences, 7(3),238–244 (2012).

55. Köroğlu A., ŞAHİN O., KÜRKÇÜOĞLU I., DEDE DÖ., ÖZDEMİR T. and Hazer B., ***"Silver Nanoparticle Incorporation Effect on Mechanical and Thermal Properties of Denture Base Acrylic Resins",*** Journal of Applied Oral Science, 24(6),590–596(2016).

56. Ghaffari T., Hamedirad F. and Ezzati B., ***"In vitro Comparison of Compressive and Tensile Strengths of Acrylic Resins Reinforced by Silver Nanoparticles at 2% and 0. 2% Concentrations",*** Journal of Dental Research, Dental Clinics, Dental Prospects, 8(4),204(2014).

57. Oyar P., Asghari Sana F. and Durkan R., ***"Comparison of Mechanical Properties of Heat-Polymerized Acrylic Resin with Silver Nanoparticles Added at Different Concentrations and Sizes",*** Journal of Applied Polymer Science, 135(6), 1-6(2018).

58. Jerolimov V., Brooks S.C., Huggett R. and Bates J.F., ***"Rapid Curing of Acrylic Denture-Base Materials",*** Dental Materials, 5(1),18–22(1989).

59. Cevik P. and Yildirim-Bicer A.Z., ***"The Effect of Silica and Prepolymer Nanoparticles on the Mechanical Properties of Denture Base Acrylic Resin",*** Journal of Prosthodontics, 1–8 (2016).

KJPS Al-Kitab Journal for Pure Science
Vol.2 (2), ISSN: 2617-1260 (print), 2617-8141(online)
www.kjps.isnra.org

DOI: http://10.32441/kjps.02.02.p8

The Effect of Coca Cola Drink on the Impact Strength and Surface Roughness of Acrylic Denture Base

Fahd S. Ikram
B.D.S., M.Sc., Ph.D., Lecturer at the college of Dentistry- Hawler Medical University. Email: Fahd77f@yahoo.com

Abstract

Background: Despite the development of many denture base material like chrome-cobalt, fluid and plastic material but the heat cure polymethylmethacrylate considered as the most widely used denture base material. The aims of this study to evaluate and compare the impact strength and surface roughness of heat cured denture base resin after immersing in coca-cola drink for two and four weeks. **Methods**: A total number of 40 samples were prepared, 30 samples for impact strength test and 10 samples for surface roughness test. The samples were divided into three group; A (control), B (2 weeks immersed in coca cola drink), and C (4 weeks immersed in coca cola drink). **Result**: Data analyzed by using SPSS software with ANOVA test indicated a non significant differences between the different tested groups, however the samples that were immersed in coca cola drink for 4 weeks revealed non dramatic increase in surface roughness, while the samples that were immersed for 2 weeks showed a non dramatic decrease in the impact strength. **Conclusions**: The coca cola drink non significantly caused dropping in the tested properties in comparison to the control group.

Key Words: Impact strength, surface roughness, heat cured resins, coca-cola.

KJPS Al-Kitab Journal for Pure Science
Vol.2 (2), ISSN: 2617-1260 (print), 2617-8141(online)
www.kjps.isnra.org

تأثير مشروب الكوكا كولا على قوة الصلابة و خشونة سطح قاعدة الاكريليك

الخلاصة:

الخلفية: على الرغم من تطوير العديد من المواد الأساسية مثل مادة الكروم-كوبالت ، والمواد السائلة والبلاستيكية ، إلا أن مادة polymethylmethacrylate المعالجة الحرارياً تعتبر الأكثر استخداما على نطاق واسع لصنع قاعدة الطقم. وتهدف هذه الدراسة إلى تقييم ومقارنة القوة التصادمية و خشونة السطح لراتنج قاعدة أسنان المعالجة حرارياً بعد غمسها في شراب الكولا كولا لمدة أسبوعين وأربعة أسابيع. الطريقة: تم تحضير عدد إجمالي من 40 عينة ، 30 عينة لاختبار قوة التصادمية و 10 عينات لاختبار خشونة السطح. تم تقسيم العينات إلى ثلاث مجموعات. ا (السيطرة) ، ب (مغمورة لأسبوعين في مشروب الكولا كولا) ، و ج (مغمورة لاربعة أسابيع في شراب الكولا كولا). النتيجة: أظهرت البيانات التي تم تحليلها باستخدام برنامج SPSS مع اختبار ANOVA إلى وجود اختلافات غير مهمة بين المجموعات المختلفة التي تم اختبارها ، إلا أن العينات التي تم غمرها في مشروب الكوكا كولا لمدة 4 أسابيع كشفت عن زيادة غير مهمة في خشونة السطح ، في حين أن العينات التي تم غمرها لمدة أسبوعين أظهر انخفاض غير مهم في قوة التصادم.الخلاصة: إن مشروب الكوكا يشرب الكولا تؤثربشكل ملحوض في الخصائص المختبرة مقارنة بالمجموعة الضابطة.

الكلمات المفتاحية: قوة التصادمية ، خشونة السطح ، راتنج المعالجة الحرارياً ، مشروب الكوكا كولا.

1. INTRODUCTION

In 1937 polymethyl methacrylate was introduced by Dr. Walter, Wright1 and the Vernon brothers. but the material at that time was lacking to good esthetic, mechanical strength and other physical properties, thanks to the chemical properties of the PMMA and its ease of processing that allows huge modifications to take place and changes several properties of this material to reach acceptable esthetics, mechanical and physical properties. [8, 11] Since that time polymethyl methacrylate resin polymers undergo several modifications to improve the construction of denture bases, now a day 95% of all dentures are made from polymethyl methacrylate polymers. [8, 9] The presence of Saliva and Oral fluids and the oral consumption of the individuals have their effect on the denture base and teeth. Variations of PH and temperature of fluids and foods have been considered to change some properties of

KJPS Al-Kitab Journal for Pure Science
Vol.2 (2), ISSN: 2617-1260 (print), 2617-8141(online)
www.kjps.isnra.org

the denture base materials . These fluids have a tendency to interfere or weakened the chains which are already formed by means of polymerization. [8]

The phenomena that responsible for the soluble substances leached out during storage in water and in the oral fluids termed solubility. This phenomena cause deleterious changes in the denture base material. These changes may include mechanical and physical changes such as swelling and plasticization consequently and softening, and chemical changes such as oxidation and hydrolysis. [7, 8, 13] The carbonated drinks like Pepsi and coca cola are the most newly produces popular drinks with consumers drinking more than 1.8 billion beverage servings each day . [2] The effect of these various beverages has not been studied in detail in the past. Keeping this as a background this in vitro study is proposed

2. MATERIALS AMD METHODS

2.1. PREPARATION OF TEST SAMPLES

For impact strength test thirty samples were prepared, each sample had dimensions of 80 ± 2 x 10 ± 0.2 x 4 ± 0.2 mm (Figure 2.6) according to ISO 179-1: 2010. The specimens were conditioned at least 16 hours at 23 ± 2 °C and 50 ± 5 % relative humidity according to ISO 291:2008 Plastics - Standard atmospheres for conditioning and testing. Figure 1

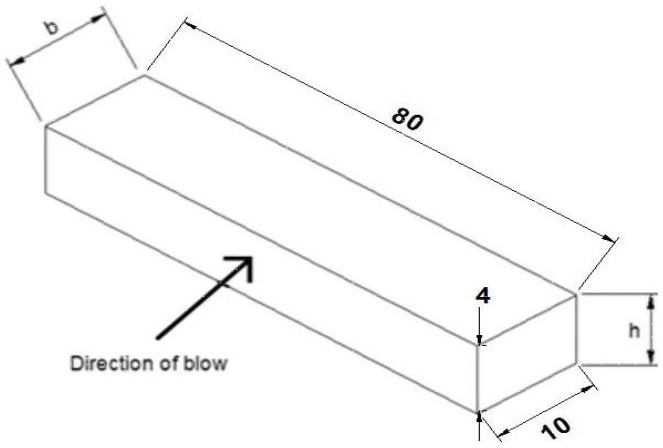

Figure 1: Specimen dimensions for impact strength test

For surface roughness test, ten samples were prepared in total. Each square sample had dimensions of 50 x 50 x 3 mm. The excessive flash was cut using a cutting disk then

tungsten carbide bur was used to bring the samples to the required dimensions. The samples then finished with stone bur until no sharp edges nor irregularities were detected, after that they were polished with 900 grade sand paper for 15 minutes then with 1200 grade sand paper for the same time to get a well polished surface.

After that the samples were polished and placed for 300s in an ultrasonic cleaner that is filled with distilled water to allow removal of impurities that was created during finish and polishing before starting the test.

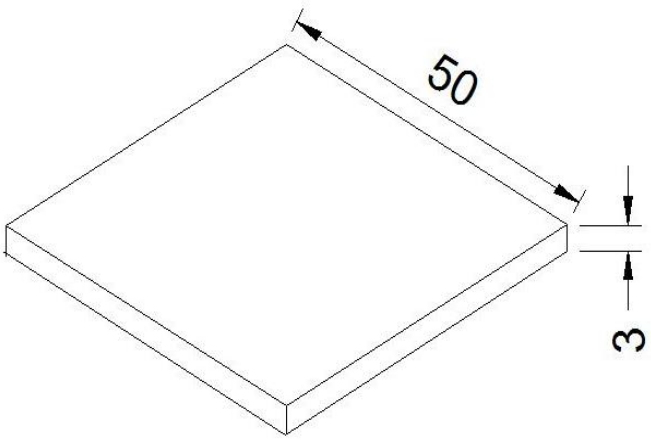

Figure 2: Surface roughness sample

Metal mold with former dimensions were used to make impact strength and surface roughness samples. These molds were flasked in a bronze mold, after that the powder and liquid of acrylic resin were mixed in a ratio of 3:1 by volume according to manufacturer's instructions. Then the mixed PMMA was packed into the molds by compression molding technique with 2 bar/pressure. Samples of resin inside the flasks were placed in a water bath, the temperature of the water was 25 C, the automatic water bath heater turned on until it reached 70 degree centigrade, the flasks remain immersed at that temperature for 45 minutes, after that the heater turned off. Once the water cooled and it's temperature reached 25C the flasks removed and opened and the samples were removed from the flasks.

2.2 Testing procedure

A total number of 30 samples were prepared from heat cured PMMA for impact strength test. And 10 sample from same material for surface roughness test. These impact strength samples were subgrouped in to three groups; group A the control group (10 samples), group B the number of samples were same as group A and were immersed in coca cola drink for two weeks, and the last one group C with same sample quantity as former groups but were immersed in coca cola drink for one month. Regarding surface roughness samples they were first place in distilled water for 24 hours, after that they were tested for surface roughness then the same samples immersed in coca cola drink for two weeks and tested again and replaced in the drink for another two weeks, finally the same samples were removed from the drink and tested lastly for the surface roughness

The samples were immersed in coca-cola drink for the mentioned times and kept in a tight seal plastic jar, the drink was daily replaced to keep it's freshness.

For impact strength test a Charpy type digital impact tester was used to determine the impact strength figure 3. For testing the acrylic samples, a pendulum of one joule was installed on impact tester. Before starting the procedure, a test was performed without the sample to check for air frication. The air friction value was reduced from impact strength value for each sample. The procedure was followed according to ISO 179-1:2010 for the un notched specimen. After that, the sample was fractured and reading was recorded.

KJPS Al-Kitab Journal for Pure Science
Vol.2 (2), ISSN: 2617-1260 (print), 2617-8141(online)
www.kjps.isnra.org

Figure 3: Charpy type digital impact tester

The Charpy impact strength of un notched specimens was calculated in KJ/m^2 using the below formula:

$$a_{cU} = \frac{E_C}{h.b} x\ 10^3$$ (ISO 179-1:2010)

Where:

Ec is the corrected energy, in joules, absorbed by breaking the test specimen;
h is the thickness, in millimeters, of the test specimen;
b is the width, in millimeters, of the test specimen.

For surface roughness test a portable contact profilometer (Qualitest TR-200) (Figure 4) was used to measure arithmetical average (Ra) of the samples, measured in µm. Surface roughness was measured in three different areas in the same direction for each sample then the average was taken to be used for statistical analysis.

The samples for group B and C before testing were conditioned in distilled water for 24 hours to remove any residue of the drink

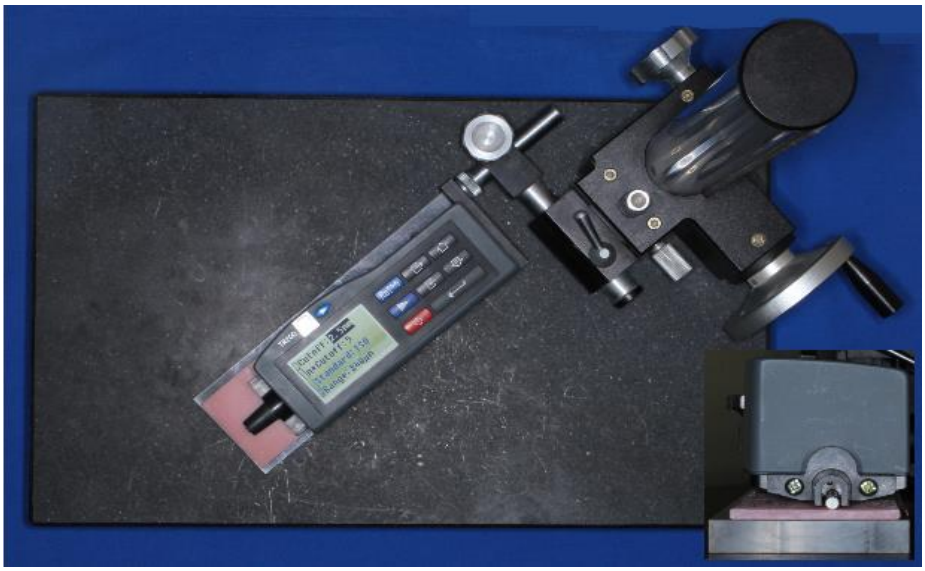

Figure 4: Portable surface roughness tester

3. RESULTS

The results were analyzed using Statistical Package for Social Sciences (SPSS, version 23). One-way ANOVA with Tukey's Honest Significant Difference (HSD) was performed to determine if there is a statistically significant difference between the two groups when compared to control. . For statistical analysis, significant level $\alpha = 0.05$ was considered.

The results for surface roughness test showed that the specimens immersed in coca-cola drink for different periods did not revealed a statistically significant difference as illustrated in Table 1, however the samples that were immersed in coca cola drink for 4 weeks showed increase in the surface roughness by about 5% as shown in Figure 5.

KJPS Al-Kitab Journal for Pure Science
Vol.2 (2), ISSN: 2617-1260 (print), 2617-8141(online)
www.kjps.isnra.org

Table 1: Descriptive statistics and comparisons of each group with control group for surface roughness.

	Mean (Ra)	SD	ANOVA P value
2 weeks 4 weeks	9.963	0.982	0.395
Control			0.848
4 weeks 2 weeks	10.412	0.861	0.395
Control			0.300
Control 2 weeks	9.863	1.533	0.848
4 weeks			0.300

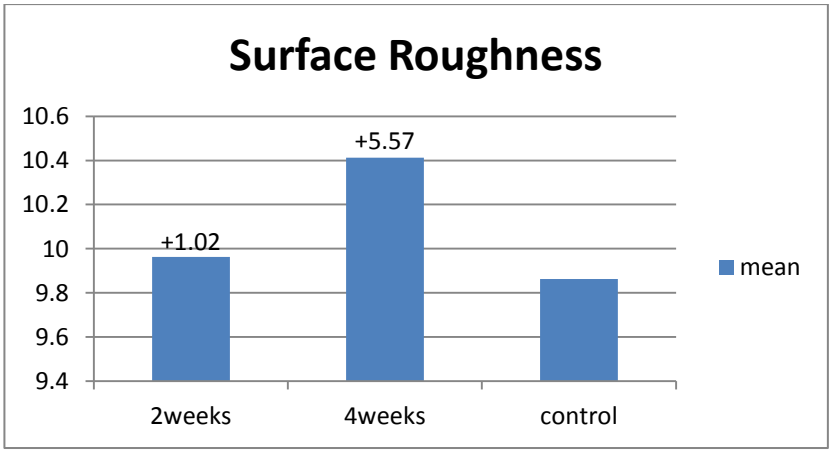

Figure 5: Mean values for Surface roughness

Regarding impact strength test similar to the former test also did not reveal statistically significant difference among the tested groups, however the samples that immersed in the coca cola drink for 4 weeks showed higher value in contra verse to those which immersed for 2 weeks showed the lowest Impact strength Figure 6.

KJPS Al-Kitab Journal for Pure Science
Vol.2 (2), ISSN: 2617-1260 (print), 2617-8141(online)
www.kjps.isnra.org

Table 2: Descriptive statistics and comparisons of each group with control group for impact strength

	Mean	SD	ANOVA P value
2 weeks 4 weeks	20.703	5.746	0.574
control			0.873
4 weeks 2 weeks	21.995	6.338	0.574
control			0.688
Control 2 weeks	21.071	3.504	0.873
4 weeks			0.688

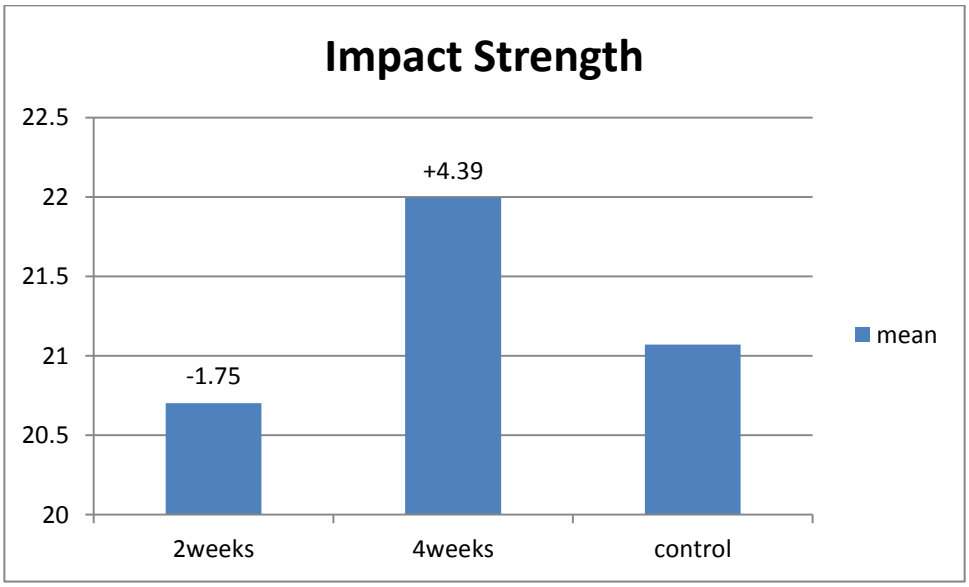

Figure 5: Mean values for Impact strength

4. CONCLUSIONS

When artificial acrylic teeth and denture base are exposed to the oral cavity, they will be in contact with saliva, beverages, and cleaning agents, and such materials are prone to the absorption and adsorption processes to denture base resins. [5, 10,12,15]

It has been shown that certain kinds of foods that are routinely ingested in a human diet can promote surface degradation and changes in other properties of the polymers.[4, 6] However the result showed a nonsignificant difference in the statistical analysis for the tested groups, but there was a slight drop in the impact strength and surface roughness parameters recorded that indicates the influence of carbonated beverage solutions on the denture base resin. The most probably factors is the PH of coca cola which is 2.74 because this drink contains phosphoric acid. [16] The presence of phosphoric acid in the coca cola drink may have to be considered as a causative factor which acts as a plasticizer and causes the changes in the impact strength and surface roughness. [1, 14]

Another possible reason for this drop in the mentioned mechanical properties was may be to the hydrolysis of the bond between molecules by the beverage. The development of stress concentration and entrap of air at the bond interface area weaken the impact strength. This result may be attributed to the acidic nature and basic composition of beverage which cause the hydrolysis of polymethyl methacrylate. [7] The PMMA contain ester group which easily hydrolyze in acidic pH which converts methacrylate to carboxylate and alcohol. The first step in the reaction involves the attachment of oxygen atom of carbonyl group with the proton (acidic hydrogen), in this step, there will be an increase in the electrophilicity of the carbon of the carbonyl group then the attachment of nucleophile (HO) group form carboxylic acid and alcohol. This could be attributed to the decrease in the impact strength.

While the data for the tested properties for group C showed a nonsignificant difference with compare to the group B that immersed in coca-cola for two weeks, this is probably due to that the dissolved surface particles precipitated on the underlying layer and provided more resistance against the acid.

It is known that the composition pH, and polarity of the liquid medium to which the polymers are subjected, as well as the immersion time, are factors that can change its solubility and cause polymer degradation. [4, 6]

REFERENCES

[1] Aydin AK, Terzioglu H, Akinay AE, Ulubayram K, and Hasirci N, **"Bond strength and failure analysis of lining materials to denture resin",** J Dent Mater, 15 (3), 211-8 (1999).

[2] Bartow J. Elmore**," Citizen Coke: An Environmental and Political History of the Coca-Cola Company"**, Cambridge University, UK, 717-31 (2013).

[3] De Clerck JP, **"Microwave polymerization of acrylic resins used in dental prostheses"**. Journal. of Prosth. Dentistry,57 (5), 650-8 (1987).

[4] Ghahramanloo A, Madani AS, Sohrabi K, and Sabzevari S, **"An evaluation of color stability of reinforced composite resin compared with dental porcelain in commonly consumed beverages "**, J Calif Dent Assoc, 36 (9), 673-80 (2008).

[5] Hersek N, Canay S, Uzun G and Yildiz F, **"Color stability of denture base acrylic resins in three food colorants"**. J Prosthet Dent, 81 (4), 375-9 (1999).

[6] Horsted-Bindslev P and Mjor IA, **"Dentística Operatória Moderna",** 3rd ed, São Paulo: Santos, (1999).

[7] Leite VM, Pisani MX, Paranhos HF, Souza RF and Silva-Lovato CH, **"Effect of aging and immersion in different beverages on properties of denture lining materials"**, J. Appl. Oral Sci, 18 (4), 372-8 (2010).

[8] Meng and Latta et al, **"Physical properties of four acrylic denture"**. J Contemp Dent Pract.,15, 6(4), 93-100 (2005).

[9] Phoenix et al R. D, **"Denture base materials"**. Dent Clin North Am.,40 (1),113-20, (1996).

[10] Polyzois GL, Yannikakis SA, Zissis AJ and Demetriou PP. **"Color changes of denture base materials after disinfection and sterilization immersion"**. Int J Prosthodont, 10 (1), 83-9 (1997).

[11] Renu Tandon, Saurabh Gupta, Samarth Kumar Agarwal, **"Denture base materials: From past to future"**. Indian Journal of Dental Sciences, 2 (2), 33-39 (2010).

[12] Satoh Y, Nagai E, Azaki M, Morikawa M, Ohyama T and Toyoma H, et al, **"Study on high-strength plastic teeth. Tooth discoloration"**, J Nihon Univ Sch Dent, 35 (3), 192-9 (1993).

[13] Singh, et al, **"Effect of Tea, Coffee and Turmeric Solutions on the Colour of Denture Base Acrylic Resin: An In Vitro Study"**, The Journal of Indian Prosthodontic Society, 12 (3), 149-153 (2012).

[14] Takahashi Y, Chai J, Takahashi T and Habu T. **"Bond strength of denture teeth to denture base resins".** Int J Prosthodont, 13 (1), 59-65 (2000).

[15] Wong DM, Cheng LY, Chow TW and Clark RK, **"Effect of processing method on the dimensional accuracy and water sorption of acrylic resin dentures",** J Prosthet Dent, 81 (3), 300-4 (1999).

[16] Wongkhantee S, Patanapiradej V, Maneenut C and Tantbirojn D, **"Effect of acidic food and drinks on surface hardness of enamel, dentine, and tooth-coloured filling materials"** J Dent., 34(3), 214-20 (2006)**.**

KJPS Al-Kitab Journal for Pure Science
Vol.2 (2), ISSN: 2617-1260 (print), 2617-8141(online)
www.kjps.isnra.org

DOI: http://10.32441/kjps.02.02.p9

A Proposed Design of Campus IP Network for Duhok University Using OPNET

Asst. Prof. Dr. Raghad Zuhair Yousif [1], Prof.Dr.Ayad Ghay Ismaeel[2]

[1,] Department of Applied Physics- Communication, Salahaddin University, Erbil, Iraq.

[2] President of Al-Kitab University-Altun Kupri-Kirkuk.

[1]Raghad.yousif@su.edu.krd, [2] dr.ayad.ghany.ismaeel@gmail.com

ABSTRACT

Duhok University has two main campuses. The first is the Malta campus located at the western part of the city and consists of seven colleges. The second one is the Duhok center which is located in the city center, it comprises six colleges in addition to the university chancellor office. This research paper proposes a network design for Duhok University to enable student and academic staff exchanges their academic and administrative information efficiently. The proposed IP Network design is made of three layers of which the core layer consists of two Cisco SONET 12012 which is connected by dual links. One of the SONETs is assigned to the Malta Campus and the other to Duhok center campus. The minimum spanning tree is calculated for the proposed IP network by using real distances between university colleges. At the distribution layer, a hierarchical topology is used to connect the college campus to its nearest main campus. The network is attached to the two main FTP and HTTP servers. The data stream of each college is forwarded to Cisco router 4700. The user layer in each department is implemented using star topology through a Cisco switch 2924. Mobility access is added to the proposed design to support wireless devices. The design is implemented using OPNET 14.5 modular. Network performance and server's quality are tested by calculating (packet/second), delays, traffic send, traffic receives utility, and throughput in case of heavy load the network performance and server's quality. The results show that the proposed Duhok University IP network fulfills the network requirements and future expansion.

Keywords: IP-Networks, Cisco, Minimum Spanning tree, OPNET

KJPS Al-Kitab Journal for Pure Science
Vol.2 (2), ISSN: 2617-1260 (print), 2617-8141(online)
www.kjps.isnra.org

تصمصم مقترح لشبكة IP لجامعة دهوك باستخدام OPNET

أ.م.د ، رغد زهير يوسف أ.د.أياد غني اسماعيل

[1] قسم الفيزياء التطبيقية– الاتصالات ، جامعة صلاح الدين ، أربيل ، العراق.

[2] رئيس جامعة الكتاب – ألتون كوبري – كركوك.العراق.

[1]alitaqi@uokirkuk.edu.iq, [2]abdalla22sd@gmail.com

الملخص

جامعة دهوك لديها حرمين جامعيين. الأول هو حرم مالطا الواقع في الجزء الغربي من المدينة ويتكون من سبع كليات. والثاني هو مركز دهوك الموجود في المدينة. وهي تضم ست كليات بالإضافة إلى مكتب الجامعة. تقترح ورقة البحث هذه تصميم شبكة جامعة دهوك لتمكين الطلاب والأكاديميين من تبادل المعلومات الأكاديمية والإدارية بكفاءة. يتكون تصميم شبكة IP المقترحة من ثلاث طبقات تتكون الطبقة الأساسية منها من اثنين من Cisco SONET 12012 متصل بواسطة روابط ثنائية. تم تعيين واحد من SONETs إلى الحرم الاول في مالطة والآخر إلى الحرم الجامعي الرئيسي في دهوك. تم حساب الحد الأدنى لشجرة التوزيع لشبكة IP المقترحة من خلال استخدام المسافات الحقيقية بين كليات الجامعة. في طبقة التوزيع ، تم استخدام طوبولوجيا هرمية لتوصيل حرم الكلية إلى أقرب حرمها الرئيسي. تم إرفاق الشبكة بخادمي FTP و HTTP الرئيسيين. تم توجيه دفق البيانات لكل كلية إلى موجه Cisco 4700. تم تنفيذ طبقة المستخدم في كل قسم باستخدام طبولوجيا النجوم من خلال مفتاح Cisco 2924. إضافة للتصميم المقترح دعم الأجهزة اللاسلكية. نفذ التصميم المقدم باستخدام برنامج OPNET 14.5. اختبر أداء الشبكة وجودة الخادم من خلال حساب (الحزمة / الثانية) ، والتأخير ، وإرسال حركة المرور ، واستلام حركة المرور ، والإنتاجية في حالة التحميل الثقيل لأداء الشبكة وجودة الخادم. وأظهرت النتائج أن شبكة IP في جامعة دهوك المقترحة تلبي متطلبات الشبكة والتوسع المستقبلي.

الكلمات الدالة: الحد انى للشجرة الممتدة, Cisco, P–Network, OPNET

KJPS Al-Kitab Journal for Pure Science
Vol.2 (2), ISSN: 2617-1260 (print), 2617-8141(online)
www.kjps.isnra.org

1. Introduction

Information technology is important to sustain the progress and facilitate task implementation in business and academic enterprises. Universities encounter increasing challenges to provide faster communication services and enhance the individual's capabilities and skills. University IP-Network helps universities to be more collaborative centers. It helps them achieve and implement efficient academic programs. There are four important components in the proposed architecture, which are: Services like HTTP protocol, Network Control, Core Switching and Edge Access [1]. The present research proposes an easily upgraded, reliable and robust design for Duhok University campus Duhok University. It is also possible for the model to be expanded in case of an increase in the number of colleges which eventually leads to an increase in the number of students and staff. The Minimum Spanning Tree (MST) is calculated for the proposed network based on real distances between colleges and university to minimize the costs of additional links. Duhok university campus is divided into three layers: the access, distribution and core layers respectively with the core network layer providing the backbone for the network while the distribution layer aggregates multiple technologies from the access layer. Many kinds of research and projects have been conducted to network modeling, simulation, and verification: Junaid Ahmed Zubairi et al [2]. Their proposed campus design has recently shifted to switched Ethernet subnets and Gigabit Ethernet backbone and has studied the performance of the time-sensitive applications on campus network under varying load conditions using OPNET. A model of SUNY Fredonia university campus network was developed in OPNET. The Ethernet delay, traffic statistics, and other interesting data were calculated and a new innovative algorithm for handling real-time speech traffic over the existing IPv4 network was tested via OPNET simulation. Theunis et al [3] came up with an OPNET based design for the educational network which led to an improvement in the practical skills of future network engineers. V. Hnatyshin et al [4], examined the student and faculty usage of network applications and their impact on the Rowan university network design model. D. Akbas [5], on the other hand, studied the influence of Firewall and VPN (Virtual Private Network) on typical enterprise network performance. Thus both the real

enterprise network prototype and virtual OPNET simulation models were constructed and compared. Ibikunle Frank et al[6]proposed a means of improving campus network performance by presenting a network model based on Multiprotocol Label Switching-Virtual Private Networks (MPLS-VPNS), a technique basically used by network service providers. Tush et al, [7] used many routing and switching protocols like OSPF, BGP, EIGRP, STP, HSRP, VTP, to design industry standard hierarchical layout of a campus network. Malek N. Algabri et al [8] presented two scenarios for designing a campus network for Sanaa University which was in lack for efficient campus network which would connect its remote campuses such as Arhab, Mahaweet, Khawlan, Medicine colleges, and the Old University campus. The first scenario is based on IPV6 protocol over MPLS and the second one is based on IPV6. protocol over MPLS -VPN techniques. Dhirendra Sharma et al, [9] presented a campus network design for six universities in the Western Himalayan region of India with three phases. In the first, the efficiency of different campus networks was calculated. In the second phase is data handling capacity per user in the networks was calculated in terms of network throughput of core-switch. then the segment/ component- wise efficiency for the real network system was found. Agueda Sofia Tavares, [10] studied reference model architecture of the university campus network in China that could be followed or adapted to build a robust yet flexible network. Bagus Mulyawan et al, [11] presented an IP-network design for the campus of Tarumanagara University based on the hierarchical structure at the core layer with redundant devices at both the distribution and access layers. Baek-Young Choi et al. [12] Made failure analysis of a university campus network using a huge set of both node outage and link failure data. Modhar A. Hammoudi [13] also built a model for Mosul University campus made up of two routers cisco 2600, core switch, Cisco 6509, two servers with IP32 cloud, and 37 VLANs. He discussed the application of VoIP on the proposed design. Meanwhile, Potemans et al, [14] proposed a student network design project for the Katholieke Universiteit Leuven with the VoIP services. B. Rodgers, [15], on their part, built a model with ring-like SONET backbone at the K.U. Leuven University in Belgium.

KJPS Al-Kitab Journal for Pure Science
Vol.2 (2), ISSN: 2617-1260 (print), 2617-8141(online)
www.kjps.isnra.org

2. Theory

The suggested model for Duhok University IP-network is initiated by selecting a suitable network layout which is a very important factor to be considered in endpoints (nodes) connection via communication lines

The objective is to find the least network connection cost. Such problems can be handled by constructing the minimum spanning tree throughout the network. The prim algorithm [16]: can be used to solve this problem. The Prims Algorithm is described by the pseudo code below:

Algorithm 1 Prime's Algorithm

Input:A weighted connected graph G with n vertices and m edges
G with n vertices and m edges
Output: A minimum spanning tree T for G
Q = new heap-based priority queue
s = a vertex of G pick up any vertex s of G
Initialize T to null
$\forall$[v]$\in G.vertices()$
if $(v = s)$ **then**
  setDistance(v, 0) set the key to zero
else
  setDistance(v, ∞)
  setParent(v, ϕ)parent edge of each vertex is null
end if
Initialize the Q with an item (u,null), $D[u]$ for each vertex u where (u,null) is the element and $D[u]$ is the key.
D[u] is the distance of u
while $\neg Q.isEmpty()$ **do**
  $(u, e) \leftarrow [Q.removeMin()]$
  Add vertex u and edge e to T
  $\forall$[e]$\in G.incidentEdges(u)$
  $z \leftarrow$G.opposite(u,e)
  for each vertex z adjacent to u such that z is in Q
  $r \leftarrow weight(e)$ $[= w(u, z)]$
  if $r < getDistance(z)$ **then**
    setDistance(z,r)update the$D[z]$ in Q
    setParent(z,e)update the parent of z in Q
  end if
end while
return the tree T

KJPS Al-Kitab Journal for Pure Science
Vol.2 (2), ISSN: 2617-1260 (print), 2617-8141(online)
www.kjps.isnra.org

The resultant minimum spanning tree of the proposed IP-is depicted network is illustrated in the (see figure1), where the distances marked between colleges are real. Java applet is used to construct the minimum spanning tree in which the blue and red lines indicate the shortest paths with each link marking the distance. The gray lines indicate the canceled links while the red lines indicate that the college is connected via a single path, as is the case with the colleges of science, medicine, and dentistry. In proposed design required the technical institutes are also included. The design should be expanded so as to include all academic institutions in Duhok city. (Fig2) shows the distribution of Duhok university colleges in both campuses (Malta and Duhok-center) based on the real map. In the design, a SONET for each campus is dedicated.

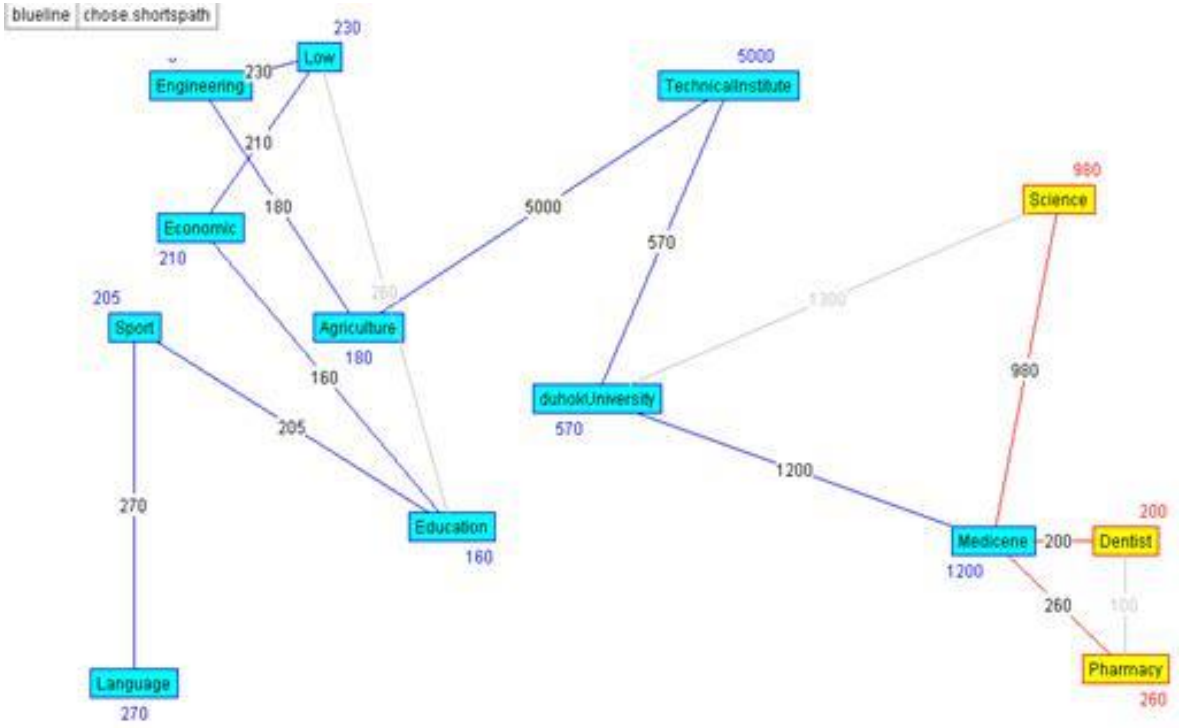

Fig. 1. The prim algorithm on the backbone.

KJPS Al-Kitab Journal for Pure Science
Vol.2 (2), ISSN: 2617-1260 (print), 2617-8141(online)
www.kjps.isnra.org

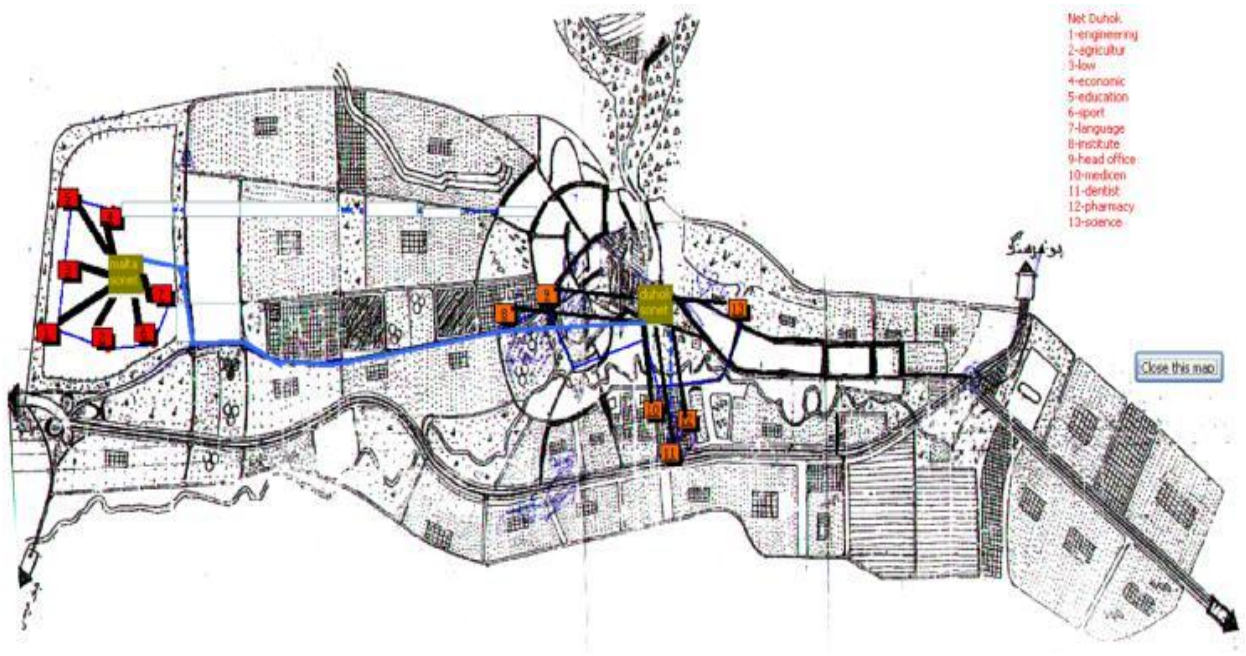

Fig. 2. Marking colleges and campuses on a real map of Duhok city.

The proposed design at the core layer is illustrated in fig 3. The university two sub-campuses are connected to Cisco SONET of type 12012 individually, then both of the SONETs are mounted in a ring-like topology to the PopSONET7650 this device can be used in case of network future extension or expansion of the proposed design. Dual Ring topology based DWDM (Dense Wavelength division multiplexing) is used in this layer to interconnect devices using the optical cable of type OC-48 with transmission speed up to 2488.32 Mbit/s (payload: 2405.376 Mbit/s (2.405376 Gbit/s); overhead: 82.944 Mbit/s) [17].

KJPS Al-Kitab Journal for Pure Science
Vol.2 (2), ISSN: 2617-1260 (print), 2617-8141(online)
www.kjps.isnra.org

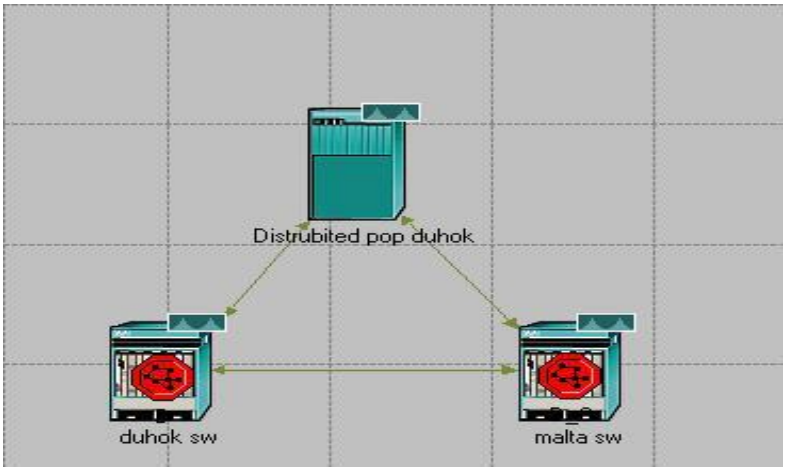

Fig. 3. Core layer for Duhok University IP-Network.

Figure 4 shows the Distribution layers for Duhok University IP-Network. A group of Cisco access points of type 4700 is used to connect each college access point to the nearest SONET. The network topology at this level is hybrid topology between (bus and star) typologies each college access point is connected through dedicated optical link of type OC-12 to the nearest campus center, which ensure a transmission speeds of up to 622.08 Mbit/s (payload: 601.344 Mbit/s; overhead: 20.736 Mbit/s)[17]. The bus topology can be seen between colleges access points this type of connection increases the cost with the benefit of increasing network reliability and availability. Hence any failure may happen at any direct link of the SONET the auxiliary line with the nearest college can replace it such that the data stream can be directed to the SONET through this auxiliary link then after through college dedicated link. Two data servers were attached to the proposed network the FTP-server and HTTP server.

KJPS Al-Kitab Journal for Pure Science
Vol.2 (2), ISSN: 2617-1260 (print), 2617-8141(online)
www.kjps.isnra.org

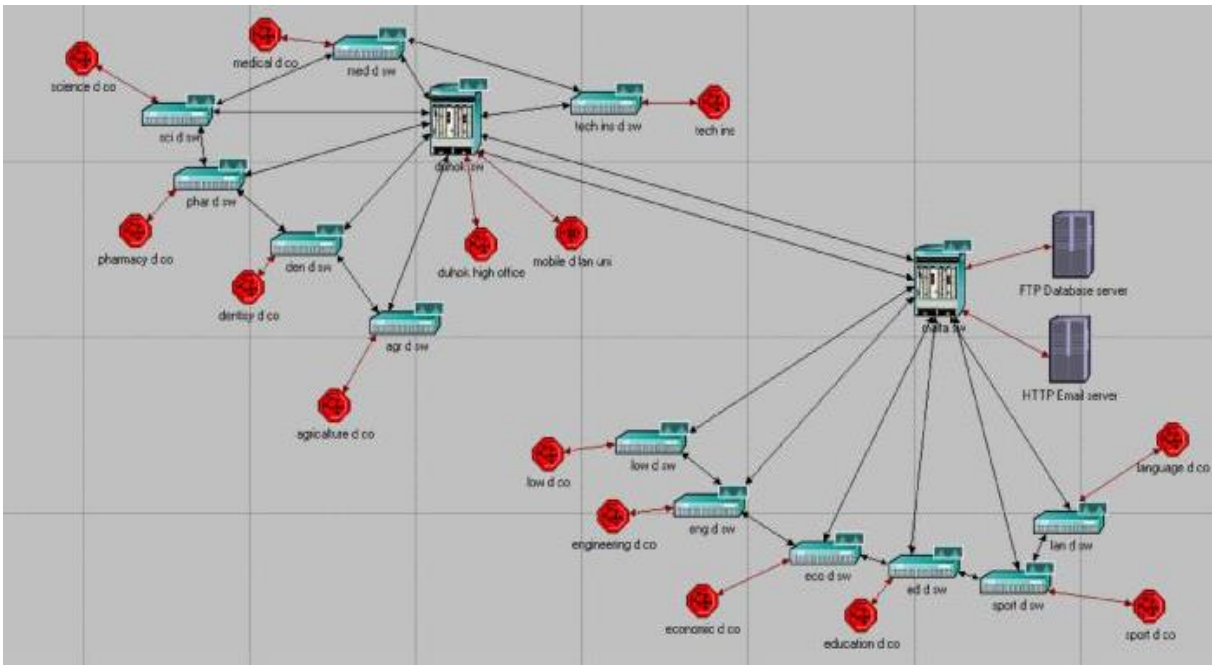

Fig. 4. Core and Distribution layers for Duhok University IP-Network

For the campus of Duhok center, two additional networks were added the mobile network and the chancellor and university administrative network, to facilitate the job of university admiration. The mobile network is depicted in fig5 below:

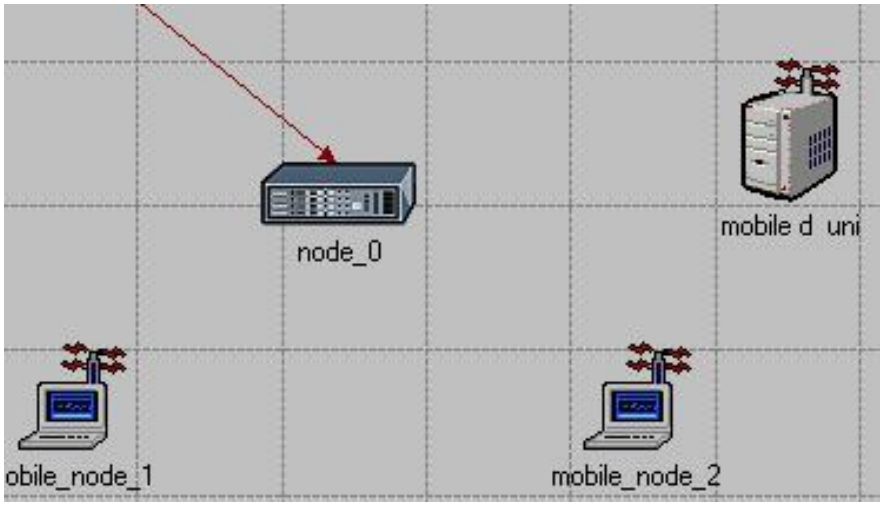

Fig. 5. Mobility server of Duhok University IP-Network

KJPS Al-Kitab Journal for Pure Science
Vol.2 (2), ISSN: 2617-1260 (print), 2617-8141(online)
www.kjps.isnra.org

fig 4 shows the Distribution layers for Duhok University IP-Network. A group of Cisco access points of type 4700 is used to connect each college access point to the nearest SONET. The network topology at this level is hybrid topology between (bus and star) typologies each college access point is connected through dedicated optical link of type OC-12 to the nearest campus center, which ensure a transmission speeds of up to 622.08 Mbit/s (payload: 601.344 Mbit/s; overhead: 20.736 Mbit/s)[17]. The bus topology can be seen between access layer the network is divided into two sublayers, each sublayer is based on a star topology. The switch used at this level is the cisco 2924 and the links are all UTP of type 100baseT. A local server is added here to give each college an additional opportunity to add new servers to its clients. The number of computers which can access the network at a time is limited to 14 computers. Fig.6 shows the design at the access layer.

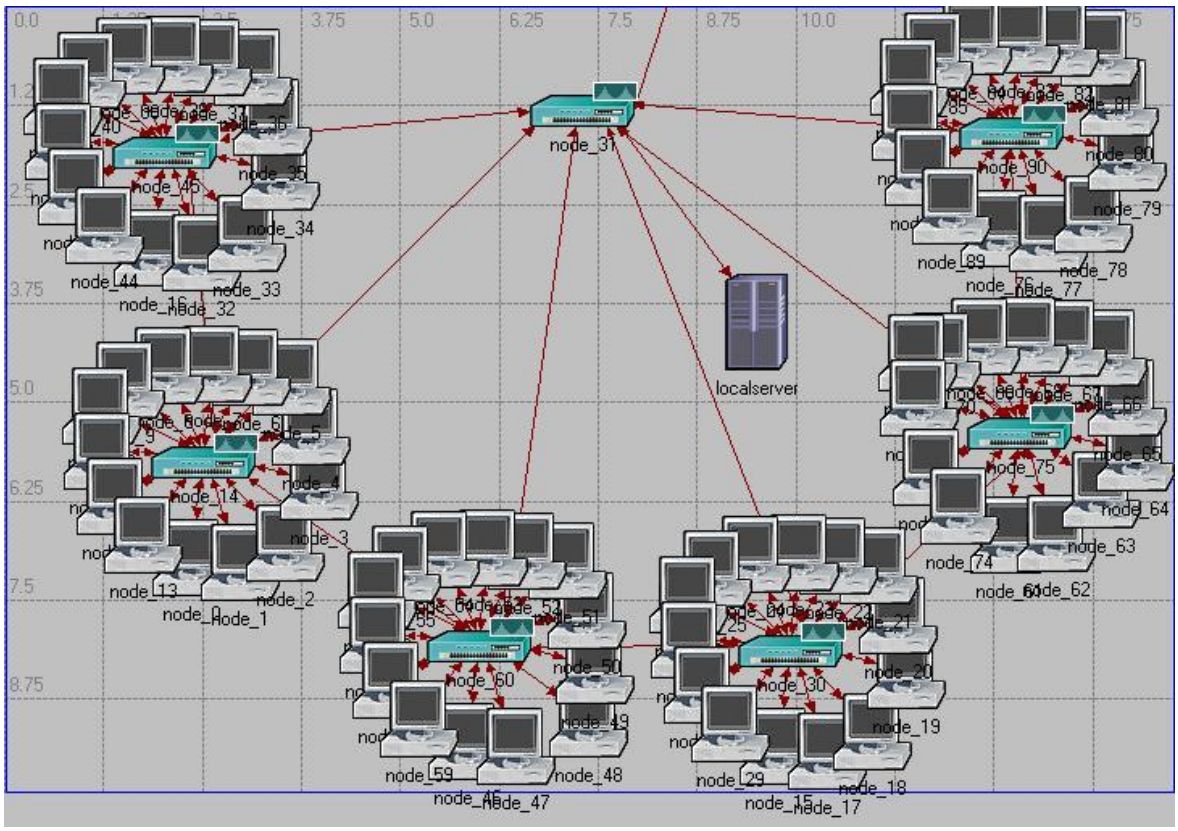

Fig. 6. One college LAN Heretical design for Duhok University IP-Network.

KJPS Al-Kitab Journal for Pure Science
Vol.2 (2), ISSN: 2617-1260 (print), 2617-8141(online)
www.kjps.isnra.org

3. Results and Calculations

This section presents the performance of the proposed model by calculating the standard statistics monitoring characteristics such as bit error rate or delay and throughput.

A. Mobility server client simulation

The mobility server load, server traffic sends, server traffic received, and task processing time for HTTP protocol are illustrated in fig7. The first three quantities were measured in Byte/seconds, while the last quantity is measured in second. It is clear that the maximum task processing time is about 0.006 sec.

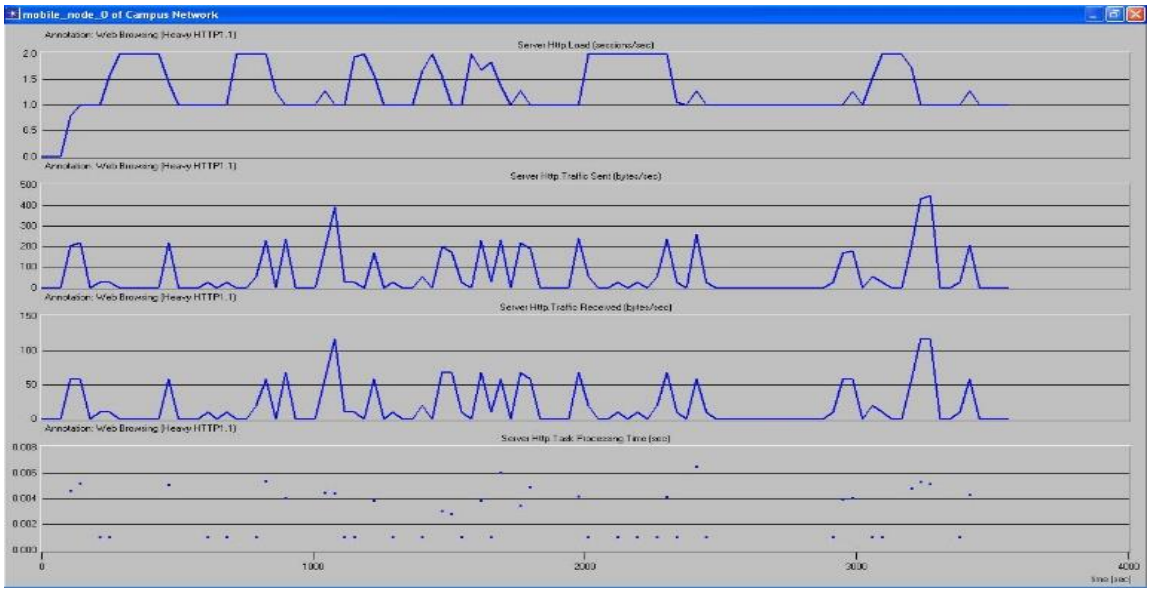

Fig. 7. Mobility server statistical results.

In another place, the average server task processing time is about 2825 sec. The TCP connection aborts, TCP delay, and TCP retransmission for mobility are illustrated in fig8. The maximum TCP delay is 0.045 msec whereas the maximum re-transmission during the simulation time is 7msec.

KJPS Al-Kitab Journal for Pure Science
Vol.2 (2), ISSN: 2617-1260 (print), 2617-8141(online)
www.kjps.isnra.org

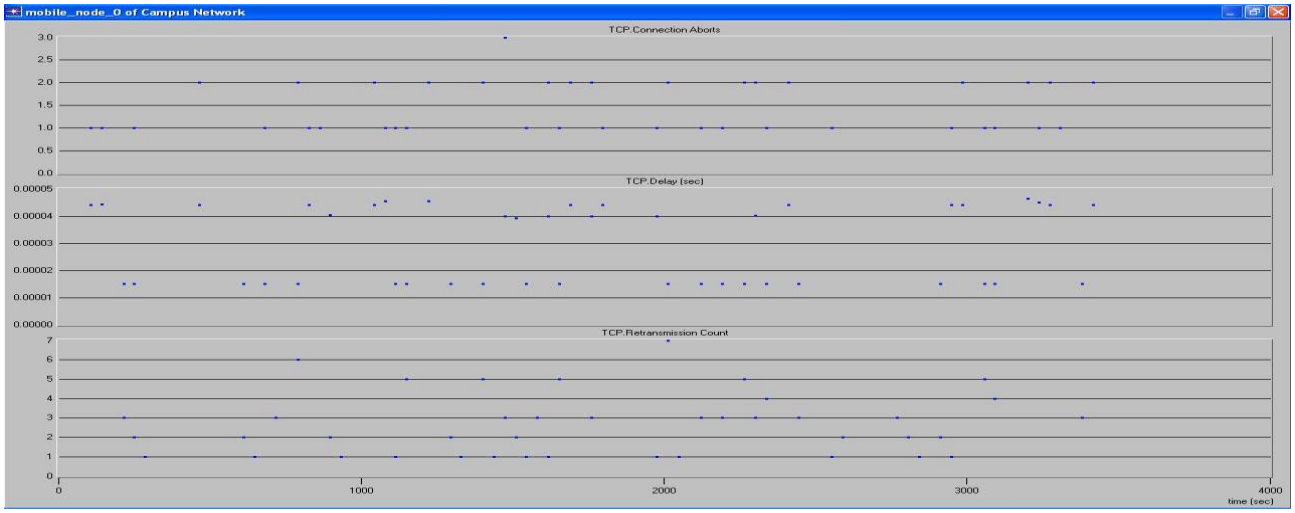

Fig. 8. Mobility TCP Task Network.

B. Ethernet Network Statistical Measurements

The simulation results for the local Ethernet server contains the point-to-point queuing delay, server task, and server HTTP application loading and task processing. All these measurements were computed during a 4000sec network operating time. fig.9 describes server HTTP task in this figure the server HTTP load is given in session/second while the server HTTP task processing time with TCP delay is in second. There is the time of halting starts after the sec 900 until approximately 2500th sec in which the server received no load. It is clear that the maximum TCP delay is about 0.0004sec.

KJPS Al-Kitab Journal for Pure Science
Vol.2 (2), ISSN: 2617-1260 (print), 2617-8141(online)
www.kjps.isnra.org

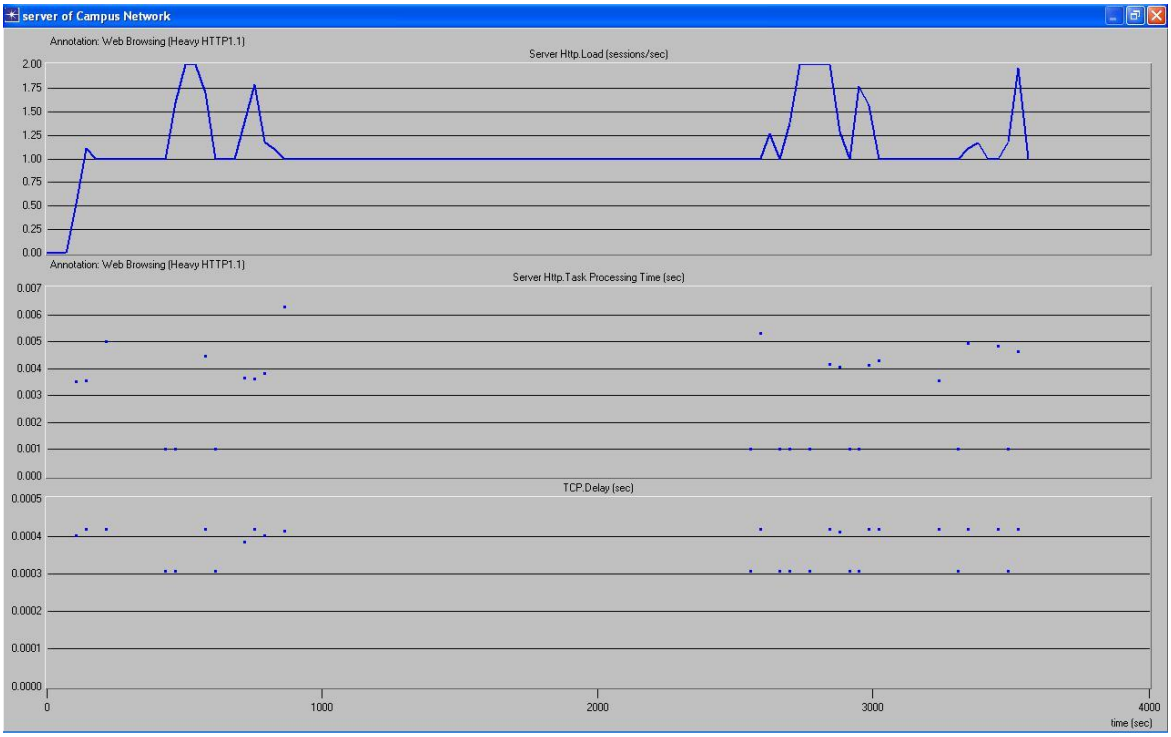

Fig. 9. HTTP server tasks

In fig.10 the point-to-point task analysis provides the queuing delay received and transmitted with received and transmitted throughput: also, a very short queuing delay between transmitted and received was detected (about 3.93 sec queuing delay difference is detected between sender and receiver points). There are two scenarios in designing campus level network. The first scenario is to connect different LANs with hubs and connect these child hubs to the parent access point. The other one depends on the child switches connected to the parent access point.

KJPS Al-Kitab Journal for Pure Science
Vol.2 (2), ISSN: 2617-1260 (print), 2617-8141(online)
www.kjps.isnra.org

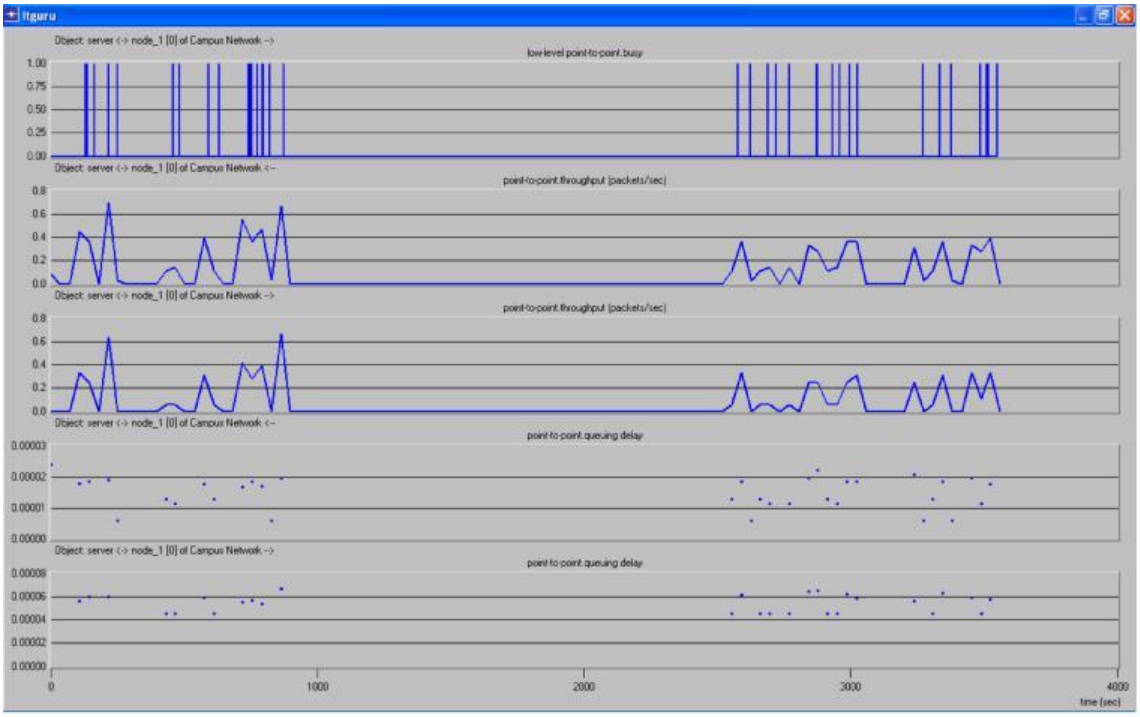

Fig. 10 Point-to-point task analyses.

To investigate the advantages of each of the proposed scenarios using OPNET package network performance is calculated in term of point to point throughput between two extreme points in campus network as illustrated in fig.11, in this figure it is clear that the throughput of hub-based design is higher than switch-based design and that led to reduce network performance and increase network utilization. The switch-based network has an average throughput of 0.031945 packet/sec with a max of 0.111 packet/sec, while in the hub-based network the average throughput is 1.6833 packet/sec with a max of 3.8889 packet/sec. Hence, the throughput increases in the hub-based network as compared to a switch-based network in spite of the fact that the delay in the first scenario is reduced. The Ethernet load (bit/sec) on campus network based on switch and hub is plotted in fig.12 for 4000 sec of network operation.

KJPS Al-Kitab Journal for Pure Science
Vol.2 (2), ISSN: 2617-1260 (print), 2617-8141(online)
www.kjps.isnra.org

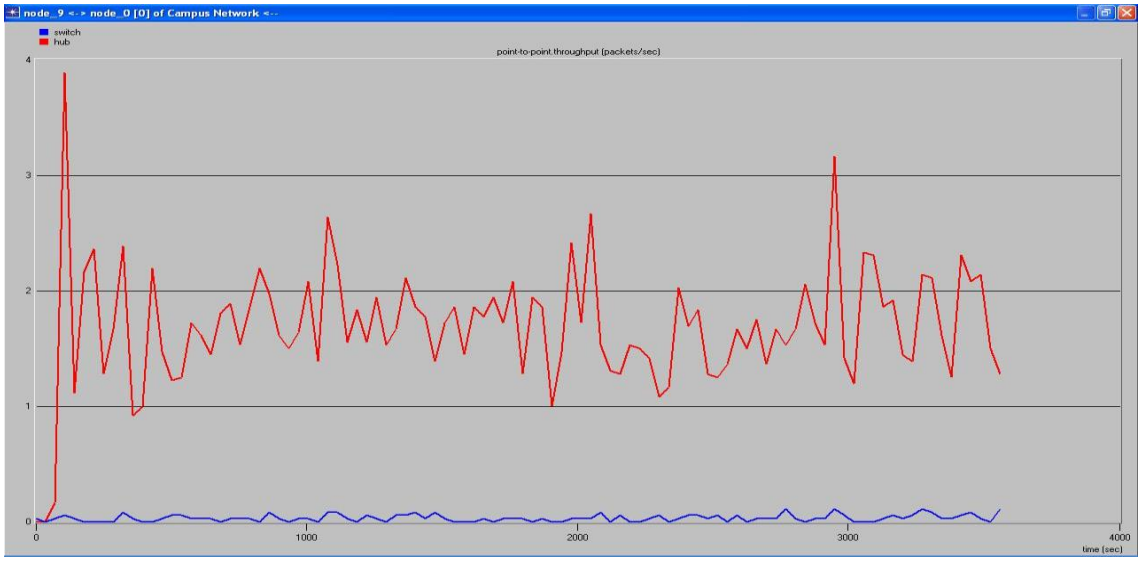

Fig. 11. Point to point throughput plotting.

Ethernet load for the switch-based network is averaged on 97.89 bit/sec with a peak of 394bit/sec. While in hub-based a campus, the average is 104.507 bit/sec with a peak of 657.778 bit/sec which means employing hub reduces the network performance approximatel to half.

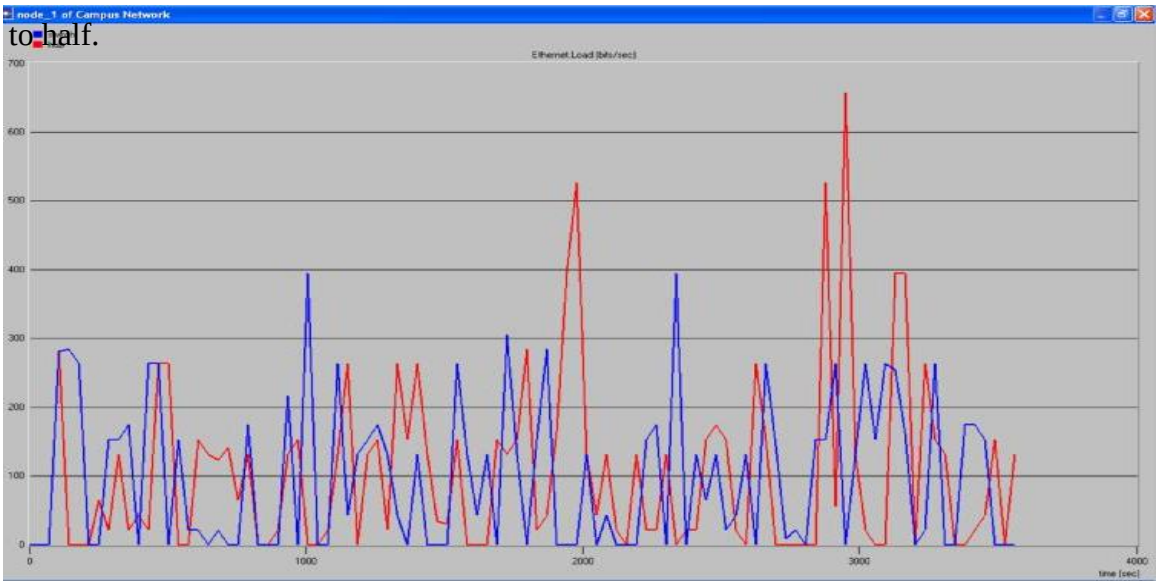

Fig. 12. Point to point throughput plotting

For comparison, the proposed Network utilizes network presented in [15] for K.U.L in Queuing delay by about (246 sec) due to employing optical technology (SONET).

4. CONCLUSIONS

The performance results for the proposed Duhok University IP-network using OPNET package showed that the proposed design can fit multimedia transmission and (voice over IP) because of its high reliability and its low delay due to its dependency on the optical communication technology and proposed hybrid and hierarchical typologies The proposed design takes into consideration the future expansion in the university atmosphere when the scientific establishment and institution numbers I expands both horizontally and vertically As depicted in simulation results, the switch utilized hub and improved the network performance by reducing delay, load, and throughput. Employing hub reduces the network performance approximately to half. The increment in Ethernet delay using switch can tolerate in term of increasing reliability.

References

[1] Ammar. O. Hasan, Raghad Z.Yousif **"An optimized Salahaddin University new campus IP-Network design using OPNET "**International Journal of Advanced Computer Science and Applications(IJACSA), vol. 8,Issue 12, pp. 463468, December 2017.

[2] Junaid Ahmed Zubairi, Mike Zuber, "**Suny Fredonia campus network simulation and performance analysis using OPNET**" Department of Mathematics and Computer Science State University of New York College at Fredonia, Fredonia, NY 14063,2000.

[3] J. Theunis, B. Van den Broeck, P. Leys, J. Potemans, E. Van Lil, A. Van de Capelle, **"OPNET in Advanced Networking Education",** OPNETWORK 2002, Washington D.C., USA.

[4] V. Hnatyshin, A. F. Lobo, P. Bashkirtsev, R. Domenico, A. Fabian, G. Gramatges, J. Metting, M. Simmons, M. Stiefel, **"Modeling a University Computer Laboratory using OPNET Software",** Computer Science Department, Rowan University, New Jersey, USA, 2006.

[5] D. Akbas, H. Gmkaya **"Real and OPNET modeling and analysis of an enterprise network and its security structures",** Elsevier Procedia Computer

Science 3. Istanbul, vol 3. pp. 10381024, 2011 [Digests World Conference on Information Technology, 6-10 October 2010 Istanbul, Turkey, p.1,1608].

[6] I. Frank, O. Segun, E. Phillips, **"Campus network visualization using Multiprotocol Label Switching Virtual Private Networks (MPLS-VPNs)",** International Journal of Applied Information Science, USA, Vol.5, No.8, pp.1-9, June 2013 (ISSN: 2249-0868).

[7] T. Krishna, A.Banerjee, **"Automation and analysis of enterprise campus network design, PARipex"**, Indian Journal of researches, Vol 5,issue5,pp.101-104, May 2016.

[8] M. N. Algabri, S. A. Alhomdy, G. Alselwi, Ameen A. M. Alawite, N.Al-Sharaby **"Performance analysis Of IPV6 Over MPLls MPLS-VPN For Sana University"**, JISET Vol 3, Issue 5, Pages 165-169, May 2016.

[9] D. Sharma, V. Kumar, M. Zennaro, V.Singh **"A Study of Efficiency- campus networks in Western Himalayan Universities of India"** ,IEEE Xplore: Workshops of International Conference on Advanced Information Networking and Applications,pp.751-756, [Digests 2011 IEEE Workshops of International Conference on Advanced Information Networking and Applications ,22-25 March 2011 Singapore, Singapore].

[10] A.Sofia, "**Network architecture for university campus network",** Master thesis, in Communication Engineering of Chongqing University, Chongqing, China, May2011.

[11] B. Mulyawan, **"Campus network design and implementation using a top-down approach",** Proceedings of the 1st International Conference on Information Systems for Business Competitiveness (ICISBC)2011, pp.1-6. [ICISBC, 8th to 9th December 2011, Semarang, Central Java, Indonesia].

[12] B. Choi, S. Song, G. Koffler, D. Medhi**," Outage analysis of a university campus network,"** IEEE 16th International Conference on Computer Communications and Networks (ICCCN), Honolulu, Hawaii, August 2007.

[13] Modhar A. Hammoudi, "**building model for the University of Mosul computer network using OPNET simulator"**, Tikrit Journal of Eng.Sciences, Vol.18, No.2, pp.34-44, June 2011.

[14] J. Potemans, J. Theunis, M. Teughels, E. Van Lil, A. Van de Capelle**," Student network design projects using OPNET"**, OPNETWORK2001,2001.

[15] B.Rodiers, "**Analysis and Simulation of The K.U.Leuven- network**", Master Thesis in Electronics Engineering, K.U.Leuven, Belgium, June2002.

[16] Algos, **"prims algorithm",** INRIA, USA copyright 2004.

[17] B.Forouzan, **"Data communications and networking"** (5th ed.). New York: McGraw-Hill, Higher Education (2015).

Asst. Prof. Dr. Raghad Z. Yousif was born in Baghdad in 1975. He Received a B.S. in Electronic and Communication Engineering from College of Engineering Baghdad University Department of Electronic and Communication Eng. in 1998, M.S. in Electronic and Communication Engineering form department of Electrical Engineering Al-Mustansriyha university –Baghdad in 2001, then he received a Ph.D. degree in communication Engineering from Baghdad University of Technology Department of Electronics and Electrical Engineering in 2005 . He is currently an Assistance Professor in the Department of Applied Physics –Communication at Salahaddin University also he is the lecturer at Department Information technology at CUE(Catholic university in Erbil). His Fields of interest are Network Coding, Medical Imaging, Swarms, Wireless Communication system, and optical communication system and data security. He is a supervisor of many MSc thesis and Ph.D. thesis he was also a member of examination committee of many MSc and Ph.D. theses. He was Awarded the prize of third best Arabic research in data security in the age of Information technology in 2003 awarded by the Association of Arab Universities.

KJPS Al-Kitab Journal for Pure Science
Vol.2 (2), ISSN: 2617-1260 (print), 2617-8141(online)
www.kjps.isnra.org

DOI: http://10.32441/kjps.02.02.p10

The Comparison of Retention between Hot Curing and Fluid Denture Base Acrylic Resin (In Vivo)

Bestun Luqman Akram **Rizgar Mohammed ameen Hasan**
Bestun.luqman@den.hmu.edu.krd Rizgar.hasan@den.hmu.edu.krd
Department of Prosthodontic College of Dentistry
Hawler Medical University
Erbil, Iraq

Abstract

Background and objectives: Adequate retention is a basic requirement for the acceptance of complete denture. The aim of this study was to evaluate the retention quality of fluid denture base materials and compare it with conventional acrylic denture base materials

Method: Sixteen edentulous male patients with an age 45-60 years participated in the study. For each patient two denture bases were constructed, one of them made from fluid denture base materials and the other made from hot acrylic denture base materials. A specially designed strain gauge measuring device was used to measure the force required to dislodge the two dentures from basal seats. Six measurements of retention of newly inserted denture base were recorded for each patient (three for maxillary acrylic denture base and three for maxillary fluid denture base).

Results: The results of the retention test showed that the fluid denture base materials required more force in order to dislodge denture than the heat cure denture base materials, which means a significant improvement in retention quality obtained by fluid denture base materials.

Conclusions: It has appeared that the fluid acrylic denture base materials produce denture base material with excellent retentive efficiency to the underlying tissue when compared to conventional denture base materials.

Keywords: Fluid acrylic, Heat cures acrylic, Retention test.

KJPS Al-Kitab Journal for Pure Science
Vol.2 (2), ISSN: 2617-1260 (print), 2617-8141(online)
www.kjps.isnra.org

الاحتفاظ الكافي هو مطلب أساسي لقبول طقم الأسنان الكامل. كان الهدف من هذه الدراسة هو تقييم جودة الاحتفاظ بمواد قاعدة أسنان السوائل ومقارنتها بمواد أسنان تقليدية من الأكريليك.

شارك في الدراسة ستة عشر من المرضى الذكور الذين يعانون من العمر مع 45-60 سنة. لكل مريض تم بناء قاعدتي أسنان, أحدهما مصنوع من مواد قاعدة أسنان السائل والآخر مصنوع من مواد قاعدة أسنان أكريليكية ساخنة. تم استخدام جهاز قياس قياس سلالة مصمم خصيصا لقياس القوة المطلوبة لإزالة الطقمين من المقاعد القاعدية. تم تسجيل ست قياسات للاحتفاظ بقاعدة أسنان تم إدخالها حديثًا لكل مريض (ثلاثة لقاعدة أسنان أكريليكية للفك العلوي وثلاثة لقاعدة أسنان الفك العلوي).

النتائج: أظهرت نتائج اختبار الاحتفاظ أن مواد قاعدة أسنان السوائل تتطلب المزيد من القوة من أجل طرد الطقم من مواد قاعدة أسنان المعالجة الحرارية ، مما يعني تحسنًا كبيرًا في جودة الاحتفاظ التي يتم الحصول عليها عن طريق مواد قاعدة أسنان سائلة.

لقد ظهر أن مواد قاعدة أسنان الأكريليك السائلة تنتج مواد قاعدة أسنان ذات كفاءة فائقة في الاحتفاظ بها للأنسجة الكامنة عند مقارنتها بالمواد الأساسية للأجهزة الصناعية.

1. Introduction

Polymethyl methacrylate (PMMA) is the most commonly used denture base resin, and its polymerization process may take place by different mechanisms[(1)]. PMMA was introduced in the 1930s, these resins are easy to handle, have reduced cost, and allow satisfactory clinical outcomes[(2)]. Several alternative methods to conventional compression-molding processing for denture base have been developed to increase the adaptation of the denture base, such as injection molding[(3)], and fluid resin[(4)] techniques. Later on, many manufacturers have introduced newer denture processing systems using light-curable and microwave-curing resins[(5)]. Therefore, the adaptation accuracy or dimensional changes in the denture bases has become a focus of many studies in removal prosthodontics.

Fluid resin technique employs a pourable, chemically activated resin for the fabrication of denture bases. The resin is supplied in the form of powder and liquid components. When

mixed in the proper proportions, these components yield a low viscosity resin. This resin is poured into a mold cavity, subjected to increase atmospheric pressure, and allowed to polymerize[6].

The pouring method of denture base resin was developed in the 1960s using agar hydrocolloids as investment material[7], and has been one of the most popular polymerization techniques because of three merits: It is simple to use, less time consuming, and it offers better adaptation accuracy than the heat polymerization method[5, 8].

The chemical composition of the pour type of denture resin is similar to the polymethyl methacrylate materials. The principal difference is that pour type of denture resins have higher molecular weight powder particles that are much smaller and when they are mixed with the monomer, the resulting mix is very fluid. Therefore, they are referred to as fluid resins. They are used with a significantly lower powder-liquid ratio[9].

The accurate fit of the denture base is a principal criterion in the physical mechanisms of complete denture retention [10, 11]. It is widely accepted that the successful function of a complete denture is dependent upon its accuracy of fit[12]. Denture base adaptation depends upon a number of factors, both clinical and laboratory in nature, as well as the dimensional accuracy of the material from which it is constructed[13].

The aim of this study is to the evaluation of the retention, denture adaptation and dimensional changes of maxillary denture base made from fluid denture base materials and compare it with maxillary denture base made from conventional heat-cure acrylic denture base materials.

2.

3. Method

This study was designed to compare the amount of retention provided by two types of acrylic resin denture bases materials, the first group was 16 conventional heat cure acrylic denture base resin and the second group was 16 fluid acrylic denture base resins. The first group of dentures constructed using conventional heat cure technique and the second group of denture bases was processed using the fluid resin technique (Castlevania, Netherland).

4. Fluid acrylic resin system:

These systems of acrylic resin are generally composed of fluid acrylic resin, specially designed flask, agar-agar duplicating material and curing chamber machine. Fluid resin poured in to a mold prepared by wax elimination of a wax pattern invested by a gel material in to a special flask that possesses 3 openings, from one opening the fluid resin is poured and the air exuded through the other openings and when the fluid resin exude through these opening means that the mold has been filled. For curing, the flask will be placed in a chamber containing warm water and the pressure applies into the chamber.

2.3.1. Fluid acrylic resin (Castavaria):

This type of acrylic resin is composed of powder and liquid, the main components are methyl methacrylate, crosslinker accelerator one, accelerator two and an ultraviolet absorber. It is chemical composition monomer based on methyl methacrylate (CH2= (CH3) COOH3). Fluid acrylic resin is mixed according to manufacturer instruction in a mixing ratio by volume/parts by weight are 1 ml / 0.95 g liquid (monomer) 1.7 g powder (polymer), It needs up to 4.5 minutes till reach to the working time, Itis working time is still 13 minutes and the curing time 30 minutes at 55 °C under a pressure of 2.5 bar.

5. Retention test

Patient selection criteria

Sixteen edentulous male patients aged from 45-60 years old participated for treatment with new dentures from the clinical Prosthodontics Department, College of Dentistry, Hawler Medical University.

6. Measuring of dislodging force

For the purpose of this study, retention has been expressed in terms of the force required to vertically dislodge a maxillary denture using a specially designed strain gauge force transducer in order to measure the force values required to dislodge the maxillary denture[(14)]. The constructed experimental apparatus was consisting of the parts as shown in (Fig.1.1):

KJPS Al-Kitab Journal for Pure Science
Vol.2 (2), ISSN: 2617-1260 (print), 2617-8141(online)
www.kjps.isnra.org

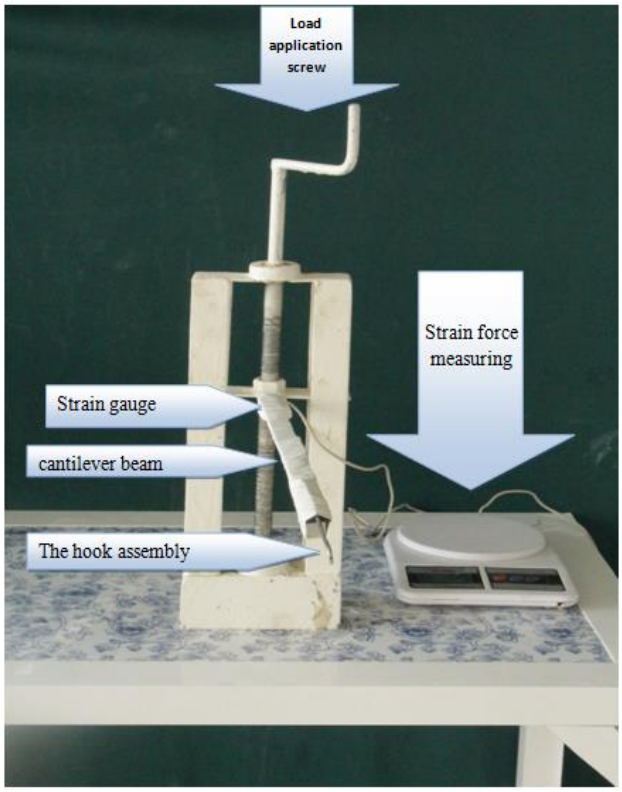

Figure (1.1): Force measuring device

7. Clinical testing

After completing the setting and calibration for the retention force measuring device, the measurement of retention force was followed by clinical testing regimen according to the following steps:

1.A string of about 1 inch length made from stainless steel was secured on the polished palatal surface of the maxillary denture in the region relating to the second premolar and first molar[12], with auto-polymerize acrylic resin so as to serve as a mean of connection for the hook assembly, as shown in Fig.(1.2).

KJPS Al-Kitab Journal for Pure Science
Vol.2 (2), ISSN: 2617-1260 (print), 2617-8141(online)
www.kjps.isnra.org

Figure (1.2): String attached to denture bases

2.Each patient asked to sit on the dental chair and to rinse his mouth by water, the denture was inserted into the mouth and held in position on the ridge by hand.

3. The patient's head was held firmly on the headrest by using two adjoining tornica and additional commercial headrest. The dental chair and headrest adjusted in such away occlusal plane of the maxillary teeth parallel to the floor, as shown in Figs. (1.3and 1.4).

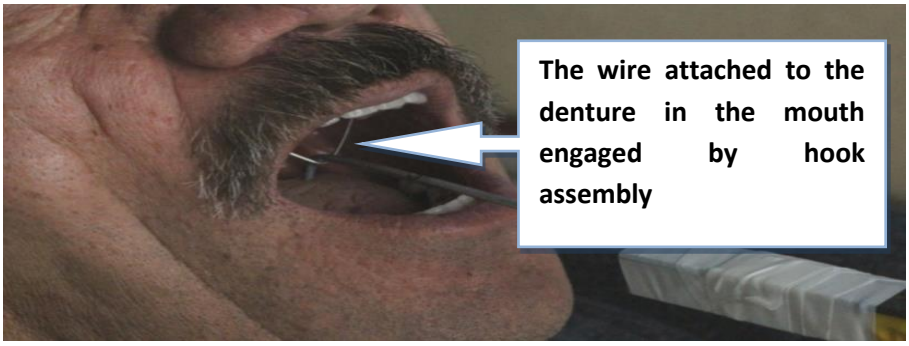

Figure (1.3): Hook assembly engages strings in his patient's mouth.

Figure (1.4): Patients head was held firmly on the headrest with occlusal the plane of maxillary teeth parallel to the floor.

KJPS Al-Kitab Journal for Pure Science
Vol.2 (2), ISSN: 2617-1260 (print), 2617-8141(online)
www.kjps.isnra.org

4. The device was then carried anteriorly till the hook assembly engages the string and properly centered in position in the patient's mouth in such a way it could travel freely to dislodge the denture from the palate, as shown in Fig. (1.5).

Figure (1.5): Position of the cantilever beam in relation to the patient's mouth.

5. In the same visit, the retention of the two dentures was evaluated for the patient. The conventional denture withdraws vertically at steadily increasing force until it was completely dislodged from the palate. Immediately following completion of registering the force values for the conventional maxillary complete denture, the retention of fluid denture base was recorded by using strain gauge measuring force device.

8. Method of calculation

Two measurements were made for all the patients who received new dentures. The first one was for the conventional maxillary complete dentures. The force values that required to dislodging the conventional maxillary complete denture calculated during the clinical testing and the reading were obtained by the strain-measuring device. The mean values of three readings at five-minute intervals were made for every patient, these reading served as

baseline data. The same procedure was followed for the same patients with fluid denture base materials.

9. Statistical analysis

The data were recorded into specially designed forms containing the following information: Code name, age, gender, type of denture base, and retention forces in. To facilitate the analysis and presentation of data in tables, numerical codes were assigned for each variable. Data were analyzed using Statistical Package for Social Sciences SPSS (SPSS Inc., Chicago, USA) version 23.0. Using descriptive statistics and independent-test was used for two independent samples and paired t-test (comparing one sample but in two occasions) using statistical analysis at a significance level of $P<0.05$ to compare variables between groups. All data regarding patient identification and medical history were kept confidential.

10. Results

Retention test

The retention forces for 32 maxillary denture bases (heat curing and fluid acrylic resin) s were studied on 16 patients. For each patient two dentures constructed, one fluid acrylic maxillary denture and one hot cure acrylic maxillary denture, 16 of them made from hot curing acrylic resins while the other 16 made from fluid acrylic resins.

The means of retention forces that were recorded for conventional maxillary complete denture and fluid denture base for individual patients are shown in Table (1.1). In this repeated measures study and with the purpose of eliminating possible differences in

KJPS Al-Kitab Journal for Pure Science
Vol.2 (2), ISSN: 2617-1260 (print), 2617-8141(online)
www.kjps.isnra.org

retention capacity attributable to the sequence in which the force was applied, calculations were made of the arithmetic means of the three retention force measurements.

There were substantial variations in the forces, both between patients and within patients for all measurements. The higher value among patients in conventional maxillary complete denture was 240.8 gm, while the lowest value was 155.8 gm.

The maximum reading among patients in conventional complete denture obtained for the patient among the three reading was 258.4 gm while the lowest reading recorded for the patient was 142.7 gm.

Regarding the fluid denture base, the highest value among patients was 268.9 gm, while the lower value was 170 gm.

The maximum reading of retention force among patients in fluid denture bases was 288.8 gm, while the lowest reading was 160 gm.

Table (1.1): The mean retention forces in (gm) for the conventional maxillary complete dentures and fluid maxillary denture base.

No	Mean of retention test of fluid maxillary denture base in (gm)	Mean of retention test of conventional maxillary denture base in (gm)
1	210	200.5
2	200	180
3	221.5	240.8
4	185	155.8
5	219	190.3
6	180.43	158.5
7	215.5	200.2
8	200.6	156.7
9	170	160.9
10	239.8	200.3
11	175.6	160

KJPS Al-Kitab Journal for Pure Science
Vol.2 (2), ISSN: 2617-1260 (print), 2617-8141(online)
www.kjps.isnra.org

12	240.5	178.4
13	250.8	210.9
14	268.9	230.3
15	214	210.8
16	198.8	200
Total mean	211.9	189.65

Note: 1gm =0.0098newton

The variables in this study were dependent to each other so paired samples t-test was used to indicate the difference between retention forces of the two groups of denture bases (fluid and hot), the results showed a significant difference in the mean retention when (p=0.001) as shown in Table(1.2). The mean retention forces for conventional heat cured and fluid acrylic maxillary denture base were based on 3 measurements at 3 times intervals for 16 patients. For fluid denture bases, the mean retention forces for the whole group was 211.902 gm, while for conventional acrylic maxillary complete dentures the mean retention force was 189.650 gm, retention means of fluid denture base for the whole patients were higher than retention mean of acrylic denture base made from hot curing acrylic resin.

Table (1.2): Paired t-test samples statistics comparing the mean of the retention forces exerted by two types of denture bases (fluid and heat cure).

Material	Mean (gm)	N	Minimum	Maximum	SD	SE	p	Significant
Fluid group	211.9	16	170.00	268.90	27.98	6.997	0.001	HS
Heat cure group	189.6	16	155.80	240.80	26.76	6.691		

KJPS Al-Kitab Journal for Pure Science
Vol.2 (2), ISSN: 2617-1260 (print), 2617-8141(online)
www.kjps.isnra.org

11. Discussion

In the present study two types of denture bases were constructed for each patient (heat curing and fluid acrylic denture base), the fluid denture bases had shown more resistance to the displaced forces and an increase in the mean of the retention forces in comparison with conventional heat curing acrylic denture base, this increase in retention mean was statistically significant (Table 1.2).

One of the causes may be due to the fluid acrylic resins did not require the application of thermal energy to initiate material polymerization. Instead of heat, chemical activators are added to the material and polymerization can be completed at room temperature, the processing is similar to that for heat cured resins, except that the flask is left at room temperature[(11)].

On the other hand, another factor which makes the fluid acrylic to show higher retention force may be due to the type of the investment material that had been used in this study; the agar-agar investment material used for the fluid denture bases and dental stone investment material used for the heat cured denture bases. Denture produced by agar-agar investment material may produce a surface with less porosity, more accurate and, more adaptable.

Another causative factor that made fluid acrylic denture bases provide more retention quality may be due to the simplicity in the procedure of finishing and polishing, which was only needed ground away the pouring channel with a metal bur and less finishing time and no warpage formed when compared to the heat cured denture bases, that means less heat generation produced during finished time, less dimensional change occurred and more adaptable denture base produced.

On the other hand, another factor may be due to the internal strain during produced packing procedure, when the acrylic resin flashing procedure is performed under routine laboratory conditions, the flask is placed in traditional clamps after final pressing in a hydraulic press. This condition may lead to a release of residual internal stresses from the acrylic resin dough before polymerization. The release of residual internal stress along with polymerization shrinkage, thermal contraction during flask cooling and strain accompanying stress release during deflasking may cause diminished adaptation of the denture to the tissues[(15)], the

amount of strain in a denture will depend upon the shape and size of the samples, the types of separating medium used, the rate of heat application, the temperature range attained during polymerization, the rate of cooling after processing and the type of treatment during finishing and polishing[16], while the fluid denture base poured in to the sprue holes directly without any press, therefore there was not produce internal strain, less polymerization shrinkage, during cooling there was no produce strain, and finally produce denture with more adaptable and retentive quality when compared to the conventional heat curing denture base.

12. Conclusions

Fluid denture base has more retention than heat-cure denture base in the static state.

References

1. Powers. RG, Craig. Restorative dental materials. 11th ed. ed.; London: St. Louis: Mosby. 2002;347.
2. Craig RG. Restorative Dental Materials. St. Louis: Mosby,1993 Sep. 478.
3. Pryor WJ. Injection molding of plastics for dentures. The Journal of the American Dental Association. 1942;29(11):1400-8.
4. Fairchild J. The fluid resin technique of denture base formation. Journal-California Dental Association. 1967;43(2):127.
5. Takamata T, Setcos JC, Phillips RW, Boone ME. Adaptation of acrylic resin dentures as influenced by the activation mode of polymerization. The Journal of the American Dental Association. 1989;119(2):271-6.
6. Maryanchik I, Brendlinger EJ, Fallis DW, Vandewalle KS. Shear bond strength of orthodontic brackets bonded to various esthetic pontic materials. American Journal of Orthodontics and Dentofacial Orthopedics. 2010;137(5):684-9.
7. Shepard WL. Denture bases processed from a fluid resin. The Journal of prosthetic dentistry. 1968;19(6):561-72.
8. Goodkind RJ, Schulte RC. Dimensional accuracy of pour acrylic resin and conventional processing of cold-curing acrylic resin bases. The Journal of prosthetic dentistry. 1970; 24(6):662-8.
9. Manappallil JJ. basic dental materials. 2nd ed. ed. New Delhi: Jaypee medical publisher. 2003;153.
10. Anthony D, Peyton F. Dimensional accuracy of various denture-base materials. The Journal of Prosthetic Dentistry. 1962;12(1):67-81.
11. Darvell BW. Acrylics. In: Darvell. B, editor. Materials Science for Dentistry. 9th edition ed. United Kingdom.: Wood head publishing.; 2009. 108-27.
12. Green AJ, Harman L. Influence of diuretics on complete denture retention: a preliminary report. The Journal of prosthetic dentistry. 1980;43(5):506.

13. Zissis A, Huggett R, Harrison A. Measurement methods used for the determination of dimensional accuracy and stability of denture base materials. Journal of dentistry. 1991;19(4):199-206.
14. Abdulkareem HS. Comparison between Retention of Maxillary Acrylic and Nylon Denture base Materials. College of dentistry, Hawler Medical University. ; 2010;40-4.
15. Lechner S, Thomas G. Changes caused by processing complete denture. J Prosthet Dent. 1951;1:551-9.
16. Woelfel J, Paffenbarger G, Sweeney W. Dimensional changes occurring in artificial dentures. Int Dent J. 1959;9(4):451-60.

KJPS Al-Kitab Journal for Pure Science
Vol.2 (2), ISSN: 2617-1260 (print), 2617-8141(online)
www.kjps.isnra.org

DOI: http://10.32441/kjps.02.02.p11

The Effect of Denture Cleansers on Color Stability, Water Sorption and Solubility of Stained Denture Base Materials

Mahabad Mahmud Saleh **Salem Abdul-Latif Salem**
Mahabad.saleh@den.hmu.edu.krd
College of Dentistry, Hawler Medical University

Abstract

Background and Objectives: Denture cleanser is the most widely used method by the patients to maintain clean and healthy dentures but the prolonged use of such cleansers may affect the properties of the denture. The present study was carried out to evaluate the effect of three prepared denture cleansers which were the 4% citric acid, 4% tartaric acid, and 4% oxalic acid in addition to the Protefix a commercially available denture cleansers, on some mechanical and physical properties (color stability, water sorption, and solubility) of acrylic resin (Stellon QC-20) and flexible nylon (Vaplast) denture base materials after immersion in tea solution. **Methods:** One hundred specimens (100) were prepared in two equal major groups: acrylic resin and Valplast. For each test of the physical and mechanical properties, 50 specimens were prepared, 25 from acrylic resin and 25 from Valplast. Later on, divided into five groups, one group used as a control and immersed in distilled water, and remaining 4 groups used as test groups; by immersing in one of the denture cleansers after staining in tea solutions for 10 days. The effect of denture cleansers on the properties was studied and compared with the control group. **Results:** Visual examination method showed no color changes for acrylic and slight color change for valplast specimens. Valplast specimens showed higher water sorption and solubility than acrylic. **Conclusions:** The findings showed that the 4 denture cleansers were equally effective, and did not cause significant alteration in the tested properties. Except acrylic specimens immersed in oxalic acid showed less color stability.

Key words: Denture cleansers, Acrylic resin, Valplast, Color stability, Water sorption and Solubility.

KJPS Al-Kitab Journal for Pure Science
Vol.2 (2), ISSN: 2617-1260 (print), 2617-8141(online)
www.kjps.isnra.org

تأثير منظفات الأطقم على بعض خواص مواد قاعدة أطقم الاسنان المصبغة

الخلاصة

الابقاء على نظافة، جمالية و منع الروائح الغير المرغوب بها فى أطقم الأسنان هو مهم لصحة المريض؛ و هذا يمكن الحصول عليه من خلال استعمال منظفات الاطقم. يعتبر منظف الأطقم الكيميائيه هى الطريقة الأكثر شيوعا لهذا الغرض ولكن الاستعمال الطويل لهذه المنظفات ربما يؤدى إلى تأثيرمضر على مكونات الأطقم. هذه الدراسة الحالية أجريت لتقييم تأثير ثلاث منظفات أطقم محضرة و أللتى كانت (4% حامض ألستريك، 4% حامض التارتاريك، و 4% حامض الاوكزاليك) إضافة إلى استعمال منظف الأطقم بروتفكس المتوفر تجاريا على بعض الخواص الميكانيكية و الفيزيائية (ثباتية اللون، إمتصاص الماء و الإذابة فى الماء) لقاعدة طقم الأسنان الاكريلى الرا تنجي (QC-20) والنايلون المرن (فالبلاست) بعد الغمر فى محلول الشاي. تمَ تحضير مئتا عينة في مجموعتين رئيسيتين: الاكريليك و الفالبلاست. تمّ تحضير خمسون عينة لكل اختبار الخواص الفيزيائية والميكانيكية ، 25 منها من الاكريليك 25 من الفالبلاست. ثم قسّمت فيما بعد الى خمسة مجموعات، استعملت مجموعة كمجموعة القياسية (كونترول) و تم غمرها فى الماء المقطر، اما المجموعات الاربع المتبقية استعملت لمجموعات اختبارية؛ بغمرهن فى منظفات أطقم الأسنان بعد أن تم غمرهن فى محلول الشاي لمدة عشرة ايام لغرض التصبيغ. بعد ذلك تمت دراسة تأثير منظفات الأطقم على الخواص الفيزيائية والميكانيكية وتم مقارنتها مع المجموعة القياسية (كونترول). اظهرت النتائج ان منظفات أطقم الأسنان الأربع لم تسبب فى أي تغيير فى ثباتية اللون، إمتصاص الماء والإذابة فى الماء لكل من الاكريليك والفالبلاست. كلتا المادتين اظهرتا قابلية كافية من ثبات اللون بعد غمرهما فى منظفات الأطقم و الماء المقطر بعد فحصهم بواسطة طريقة سبكتروسكوب، ما عدا عينة الاكريليك التى غمرت فى حامض الاوكزاليك والتى أظهرت فرقاً معنوياً عالياً بالمقارنه مع المجموعة القياسية.

KJPS Al-Kitab Journal for Pure Science
Vol.2 (2), ISSN: 2617-1260 (print), 2617-8141(online)
www.kjps.isnra.org

1. Introduction

Various materials have been used to construct dentures. Acrylic resin is now the material of choice: this material has a required aesthetic quality and is cheap and easy to process using inexpensive techniques [1]. Thermoplastic materials for dental prostheses, Valplast and Flexiplast, were introduced in the 1950s. Both materials were similar grades of polyamides [2]. The chief advantage of nylon lies in its resistance to shock and repeated stressing [3]. It could be extremely useful in the treatment of patients who demonstrate repeated fracture of dentures and those that show tissue reactions of a proven allergic nature [4].

The maintenance of clean denture prostheses is important for the health of a patient, to maintain an aesthetic, odor free prosthesis, and to reduce the number of the microorganisms on the dentures [5]. Dentures can be cleaned mechanically (brushing), chemically (immersion), or through a combination of both [6]. The immersion cleansers are preferred by patients because they are easy to prepare and effective in removing deposits if used regularly [7].

Most immersion cleansers can be divided into three classes; alkaline peroxide, alkaline hypochlorite, and dilute mineral acid. Protefix Active cleanser is a peroxide type of denture cleanser. It has sufficient oxygen to clean the denture independently, thoroughly and quickly without attacking the denture material. It removes food remains, coffee, tea, and nicotine thoroughly.

2. Materials & Methods

Experimental design: One hundred specimens (100) were prepared in two equal major groups: acrylic resin and Valplast. They were evaluated for changes in color stability, sorption and solubility after immersion in four denture cleansers (4% Oxalic acid, 4% Tartaric acid & 4% Citric acid and Prefix tablets) in addition to distilled water. For each test of the physical and mechanical properties, 50 specimens were prepared, 25 from acrylic resin and 25 from Valplast. Later on, divided into five groups, one group used as a control and remaining 4 groups used as test groups as follow:

Group 1: specimens were immersed in 4% citric acid denture cleanser solution.

Group 2: specimens were immersed in 4% tartaric acid denture cleanser solution.

Group 3: specimens were immersed in 4% oxalic acid denture cleanser solution.

Group 4: specimens were immersed in Protefix denture cleanser solution.

Group 5: specimens were immersed in distilled water (control group).

All groups except group 5 were immersed in tea solution for 10 days for staining before they were immersed in denture cleansers.

Metal pattern preparation: Metal disk specimens of (50 ± 1 mm in diameter and 0.5 ± 0.1 mm in thickness) were constructed for sorption and solubility tests. Concerning the color stability test rectangular metal specimens were constructed with the dimension of (25 × 4 × 0.5) mm length, width and thickness respectively to fit into the cuvette of the spectrophotometer.

Preparation of the specimens: The specimens were constructed by preparing molds by investing the metal patterns prepared with mentioned dimensions. The acrylic resin specimens were prepared by conventional compression mold technique, while the nylon specimens were prepared by injection mold technique.

After finishing and polishing, all the specimens were conditioned in distilled water at 37ºC ± 2ºC for 50 ± 2 hours before they were tested according to ADA specification No. 12 (1999) [8].

3. Preparation of the solutions

1. Tea solution: A standard solution of tea was prepared from 4 grams of dry tea which boiled in 500 ml of distilled water for 4 minutes and allowed to cool at room temperature, and then the solution was decanted from tea leaves [9]. This solution was used for staining the test specimens. (A fresh tea solution was prepared prior to use).

2. Protefix solution: The Protefix solution was prepared according to the manufactures instructions (1 tablet of Protefix added to 150 ml of lukewarm water).

3. The experimental denture cleanser solutions: A fresh denture cleanser solutions prepared by dissolving each of the citric acid, tartaric acid and oxalic acid in the isopropyl alcohol (the isopropyl alcohol was chosen as a solvent for the acid powder due to the antiseptic effect) [9] as follow:

4 gm of each acid powder + 100 ml. of isopropyl alcohol → 4% w/v of acid denture cleanser solution

Then, prior to the use, each prepared denture cleanser solutions was diluted with an equivalent volume of distilled water, as follow:

50 ml. of distilled water + 50 ml. of prepared denture cleanser solutions → 100 ml. of fresh diluted denture cleanser solution

The prepared denture cleanser solutions were stored in a closed container and inside the refrigerator to prevent evaporation, changes in concentration or any deterioration.

Mechanical and physical tests which were used in this study:

1. Water sorption and solubility test: The specimens' preparation and testing procedure were done according to the ADA specification No. 12 for denture base resin (1999) [8]. The specimens were dried in a desiccator containing freshly dried silica gel arranged according to their specific group separated by filter paper. The desiccator was stored in an incubator at a 37ºC ± 2ºC for 24 hours. After 24 hours, the specimens were removed to a similar desiccator at room temperature for one hour then weighed with a digital balance on the precision of 0.0001 mg. This cycle was repeated until a constant mass (M_1) "conditioned mass" was reached. (Weight loss for each disk should not more than 0.5 mg in 24 hours period). Then the discs of a group (1, 2, 3, and 4) were immersed in fresh tea solution for 10 days, followed by 24 hours in denture cleanser solutions, while group 5 were immersed in distilled water at 37ºC ± 2ºC for 11 days. After that the discs in all groups were removed from the solutions with tweezers, they were wiped by a clean dry hand towel until they became free from moisture. The discs were then waved in the air for 15 seconds and weighed one minute after removal from the solutions. This mass was recorded as (M_2). After that to obtain the value of solubility test, the discs were reconditioned to a constant mass in the desiccator at 37ºC ± 2ºC as done previously for sorption test and the constant reconditioned mass was recorded as (M_3).

The values for sorption and solubility were calculated for each disc from the following equations. (The final value for sorption should be rounded to the nearest 0.1 mg/cm^2, and for the solubility was determined to the nearest 0.01 mg/cm^2).

$WSP = M_2 - M_1 / S$ $WSL = M_1 - M_3 / S$

KJPS Al-Kitab Journal for Pure Science
Vol.2 (2), ISSN: 2617-1260 (print), 2617-8141(online)
www.kjps.isnra.org

Where:

WSP = Sorption mg/cm^{2,} WSL = Solubility (mg/cm^2)

M_1 = the mass of the disc before immersion (conditioned mass, Constant mass) (mg).

M_2 = the mass of the disc after immersion (mg), M3 = the reconditioned mass (mg)

S = Surface areas of the disc (cm^2).

2. Color stability test: The color stability test was measured by two methods:

Objective method (spectroscopic study) and Subjective method (visual examination).

A spectrophotometer device was used to measure the light absorption of each specimen at 500 nm (nanometer). For all groups, the light absorption for each specimen was measured before immersion of the specimens in the solutions.

Following immersion of tested groups in tea solution for 10 days, they were immersed in the denture cleansing solution for 24 hours. While the control group immersed only in the distilled water for 11 days. Light absorption of the specimens was measured before and after the immersion procedure by using a spectrophotometer at 500 nm and the difference between the two readings was measured.

The visual examination of staining removal was assessed by 10 independent observers (dentist). Each observer read the samples after their removal from the solutions. The samples were evaluated visually for stain removal by comparing the tested samples with the control group by placing the specimens on a white background and they were graded for the amount of staining on a scale of (No = 0, Slight = 1, Mild = 2, Moderate = 3, Severe = 4) [9]. The reading of the samples should not be delayed more than 3 days because with time the color of the samples will be affected.

The Statistical Package for Social Sciences (SPSS, version 15) was used for data entry and analysis, using ANOVA test, Dunnett test for multiple comparisons within the groups, and t-test for comparison between the groups.

If P-value ≤ 0.01 statistically was regarded as highly significant (HS).

If $0.01 <$ P-value ≤ 0.05 statistically was regarded as significant (S).

If P-value > 0.05 statistically was regarded as nonsignificant (NS).

KJPS Al-Kitab Journal for Pure Science
Vol.2 (2), ISSN: 2617-1260 (print), 2617-8141(online)
www.kjps.isnra.org

4.Results

Color stability: by visual examination, one way ANOVA for both acrylic resin and Valplast statistically revealed a significant difference between the groups. (P=0.024 for acrylic, and P=0.031 for Valplast). The Dunnett test for acrylic reveals no significant difference between oxalic acid and Protefix, and significant difference between citric and tartaric acid compared with the control group. For Valplast it reveals a significant difference between citric acid, tartaric acid, and oxalic acid as compared with the control group, while Protefix showed no significant difference with a control group. The independent t-test statistically revealed no significant difference between citric acid and oxalic acid and significant difference between tartaric acid and Protefix solution, Fig (1).

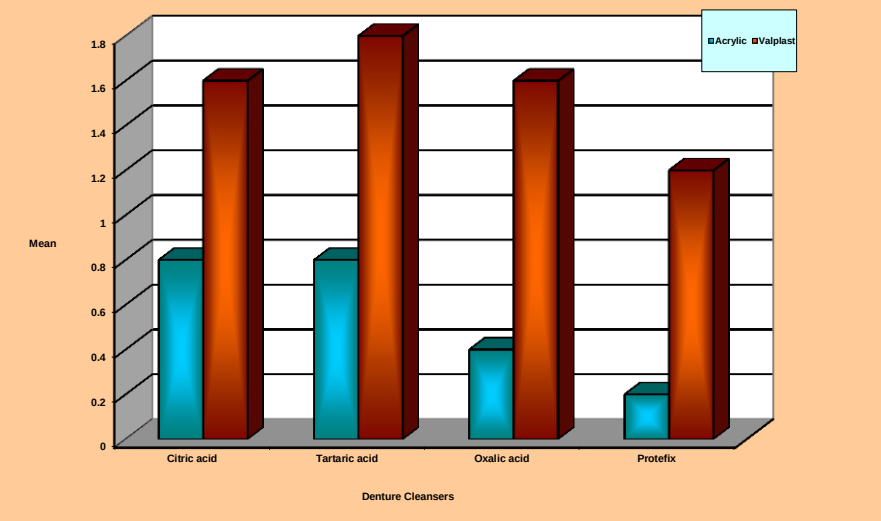

Fig (1): Bar chart of color stability test; visual examination method.

By the use of spectrophotometer device, the result of ANOVA test revealed a highly significant difference between the groups of the acrylic resin (P = 0.001) and no significant difference between the groups of Valplast (P = 0.057). The Dunnett test for the acrylic reveals that statistically citric acid, tartaric acid, and Protefix showed no significant difference, while, oxalic acid shows high significant difference comparing with control group. While for Valplast it reveals no significant difference. Finally, the independent t-test

revealed no significant difference between citric acid, tartaric acid, Protefix, and distilled water, while oxalic acid shows a significant difference, Fig (2).

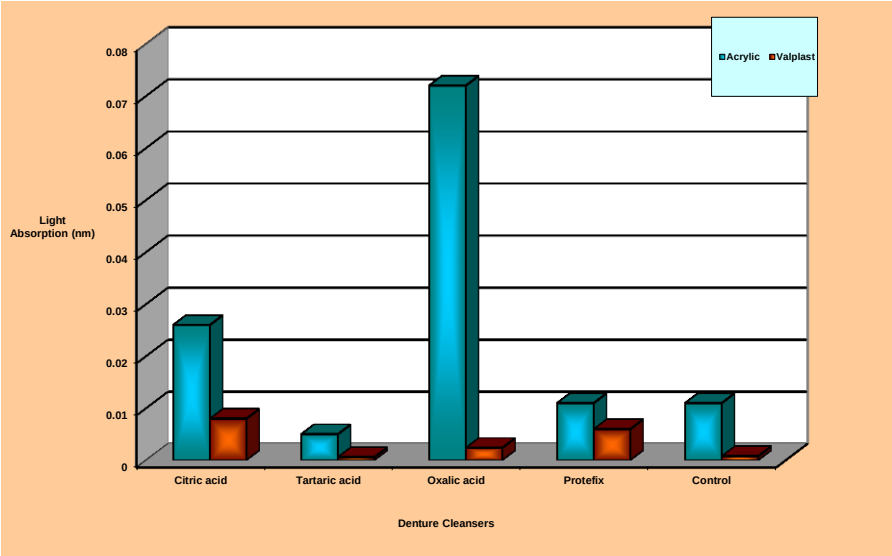

Fig (2): Bar chart of color stability test; objective method.

Water sorption: The sorption values for all groups of both denture base materials are within the ADA specification limit No. 12 for denture base polymers (the uptake should not be more than 0.8 mg/ cm^2). ANOVA test revealed that statistically there was a highly significant difference between the five groups for both types of denture base materials. (P = 0.000 for acrylic) and (P = 0.000 for Valplast). The result of the Dunnett test for both acrylic resin and valplast statistically revealed a highly significant difference between citric acid, tartaric acid, and oxalic acid with the control group and no significant difference between Protefix and distilled water. Finally, the result of t-test revealed that statistically there was a highly significant difference between two denture bases materials immersed in three prepared denture cleanser solutions, and no significant difference between two types of materials immersed in Protefix and distilled water, Fig (3).

KJPS Al-Kitab Journal for Pure Science
Vol.2 (2), ISSN: 2617-1260 (print), 2617-8141(online)
www.kjps.isnra.org

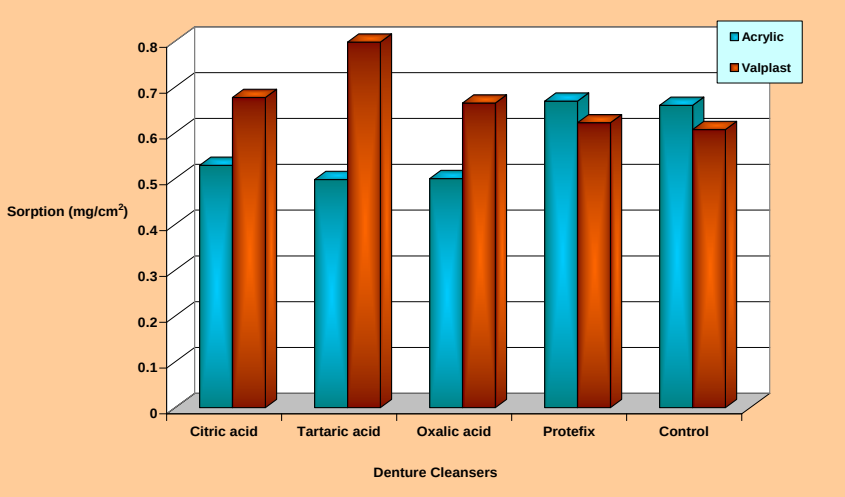

Fig (3): Bar chart of sorption test

Water solubility: The solubility values for both denture base materials have complied with the ADA specification limit No. 12 for denture base polymers (the loss in weight should not be more than 0.04 mg/ cm^2). ANOVA test for acrylic resin and Valplast materials statistically revealed no significant difference between the groups (P = 0.634 for acrylic, and P = 0.237 for Valplast). The result of the Dunnett test statistically revealed no significant difference for both acrylic resin and Valplast. Finally, the independent t-test showed a highly significant difference between two denture base materials, and acrylic specimens showed a lower value than Valplast, Fig (4).

KJPS Al-Kitab Journal for Pure Science
Vol.2 (2), ISSN: 2617-1260 (print), 2617-8141(online)
www.kjps.isnra.org

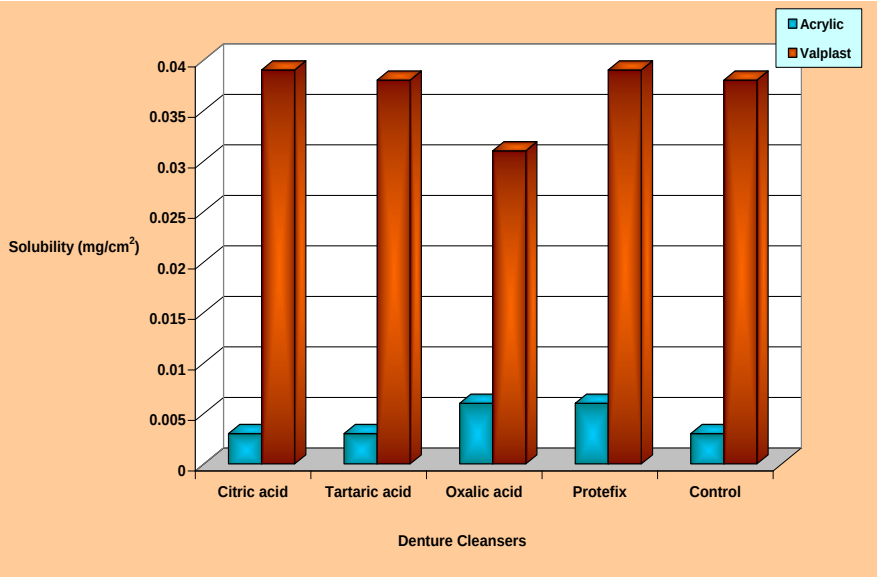

Fig (4): Bar chart of solubility test

5. Discussion

Color stability: In this study, color stability was measured by using two methods, visual examination, and spectrophotometer study.

In visual examination, there was no significant difference in color change of both acrylic resin and Valplast materials after immersion in citric and oxalic acids and significant color change after immersion in tartaric acid and Protefix. The mean values for acrylic specimens showed no color change (mean value < 1) among the tested groups. For Valplast it reveals a slight color change in all tested groups (mean value >1) comparing with control. These findings are in agreement with Goiato et al [10] when they found that Valplast presented the greatest chromatic alteration after accelerated aging, which was significantly different from Triplex (heat-cure acrylic). Also, Al-khafaji [9], [11] used the same denture cleansers and found no color change by visual examination in acrylic samples after immersion in the denture cleanser solutions and in the distilled water. However, Visual shade matching and color perception is a psychophysical phenomenon with variations, both between individuals and within an individual at different times so it is not more dependable and instrumental measurement has the advantage of obviating the subjective errors of color assessment [12].

The use of spectrophotometer method is an objective study, the result of this study revealed no significant color change at 500 nm levels between the acrylic resin and Valplast materials after immersion in distilled water and denture cleansers. Except for specimens immersed in oxalic acid which show a significant difference. These results are in agreement with Sato et al [13], Al-khafaji [9], [11], and Kortrakulkij [14]. The oxalic acid has a greater effect on the color of acrylic resin specimens; this may be due to that the oxalic acid absorbs at the same wavelength (500 nm), or it may react with our material (QC-20) and give a product which absorbs at the same wavelength and increasing the color intensity. Although no significant difference was observed concerning the same materials when the visual examination method was used.

Water sorption: The results of sorption test show that statistically there is a highly significant difference between acrylic and Valplast immersed in prepared denture cleanser solutions, Valplast specimens exhibited higher values of water sorption. This finding is in agreement with Lai et al [15], and Takabayashi [16]. This phenomenon is explained by the water absorption occurring among the molecular chains due to the high hydrophilicity of the numerous amide bonds forming the main chains of the polyamide resin. It is also thought that the higher the amide group concentration, the greater the water absorption. For both materials regarding the sorption test statistically, there is a highly significant difference among the tested samples that were immersed in prepared denture cleansers compared to that immersed in distilled water. This is disagreeing with Al-khafaji [9], [11], used the same prepared denture cleansers. She found that the denture cleanser solution caused no effect on the sorption of light-cured acrylic resin and those cured by water bath and microwave.

Water solubility: The results of the solubility test shows that statistically there is a highly significant difference between acrylic and Valplast immersed in denture cleanser solutions and distilled water.Valplast specimens exhibited higher values of solubility, but, all have complied with ADA specification limit which stated that the loss of weight should not be more than 0.04 mg/cm^2. Regarding the effect of denture cleanser, the result reveals no significant difference between tested groups with a control group; this is in agreement with Al-khafaji [9], [11].

References

[1] Noort RV. ***Introduction to dental materials***. 3rd edition Edinburgh: Mosby; 2007.

[2] Negrutiu M, Sinescu C, Romanu M, Pop D, Lakatos S. ***Thermoplastic resins for flexible framework removable partial dentures.*** Timisoara Med J. 2005; 56 (3): 295- 299.

[3] John J, Gangadhar SA, Shah I. ***Flexural strength of heat-polymerized polymethyl methacrylate denture resin reinforced with glass, aramid or nylon fibers.*** J Prosthet Dent. 2001; 86(4): 424-7.

[4] Stafford GD, Hugget R, McGregor AR, Graham J. ***The use of nylon as a denture base material.*** J Dent. 1986; 14: 18-22.

[5] Gornitsky M, Paradis I, Landaverde G, Malo AM, Velly AM. ***A clinical and microbiological evaluation of denture cleansers for geriatric patients in long term care institutions.*** J Canada Dent Assoc. 2002; 68(1): 39-45.

[6] Nikawa H, Hamada T, Yamashiro H, Kumaga H. ***A review of in vitro and in vivo methods to evaluate the efficacy of denture cleansers.*** Int J Prosthodont. 1999; 12: 153-9.

[7] Salem ALS; Al-Khafaji AMH; Al-Khafaji MT. ***The effect of denture cleansers on surface roughness and microhardness of stained light cured denture base material.*** Mustansiria Dent J. 2007; 4(2): 182-187.

[8] ADA. ***American national standards institute/ American dental association specification No. 12 for denture base polymer.*** Chicago: Council on dental material and devices; 1999.

[9] Al-Khafaji AMH. ***The effect of prepared denture cleansers on some properties of stained acrylic resin denture base material cured by two different techniques*** M.Sc. Thesis University of Baghdad, College of dentistry; 2004.

[10] Goiato MC, Santos DM, Haddad MF, Pesqueira AA. ***Effect of accelerated aging on the microhardness and color stability of flexible resins for dentures.*** Braz Oral Res. 2010; 24 (1): 114-9.

[11] Al-Khafaji AMH. ***The effect of denture cleansers on the color stability, water sorption and water solubility of stained light cured acrylic denture base material.*** Mustansiria Dent J. 2007; 4(2): 174-181.

[12] Gupta R, Parkash H, Shah N, Jain V. ***A spectroscopic evaluation of color changes of various tooth colored veneering materials after exposure to commonly consumed beverages.*** J Indian Prosthodont Soc. 2005; 5(2): 72-8.

[13] Sato S, Cavalcante MRS, Orsi IA, Paranhos HFO, Zaniquelli O. ***Assessment of flexural strength and color alteration of heat-polymerized acrylic resins after simulated use of denture cleansers.*** Braz. Dent. J. 2005; 16(2).

[14] Kortrakulkij K. ***Effect of denture cleanser on color stability and flexural strength of denture base materials.*** M.Sc. Thesis, Mahidol University; 2008.

[15] Lai Y, Lui H, Lee S. ***In vitro color stability, stain resistance, and water sorption of four removable gingival flange materials.*** J Prosthet Dent. 2003; 89: 293-300.

[16] Takabayashi Y. ***Characteristics of denture thermoplastic resins for non- metal clasp dentures.*** Dent Material J. 2010; 29(4): 353- 361.

KJPS Al-Kitab Journal for Pure Science
Vol.2 (2), ISSN: 2617-1260 (print), 2617-8141(online)
www.kjps.isnra.org

DOI: http://10.32441/kjps.02.02.p12

Robust Digital Image Encryption Approach Based on Extended Large-Scale Randomization Key-Stream Generator

Raghad Zuhair Yousif [1],.Ayad Ghay Ismaeel[2]

[1,] Department of Applied Physics- Communication, Salahaddin University, Erbil, Iraq.

[2] President of Al-Kitab University-Altun Kupri-Kirkuk.

[1]Raghad.yousif@su.edu.krd, [2] dr.ayad.ghany.ismaeel@gmail.com

ABSTRACT

This paper presents a novel image encryption scheme based on extended large-scale randomization key-stream generator. The basic form of the key-stream generator is presented, and employed in digital image ciphering. The modification of the basic form also, presented, and gives encouraging results in image encryption as compared with classical non-linear stream cipher generators and the basic form. Pixel shuffling is performed via vertical and horizontal permutation. Shuffling is used to expand diffusion in the image and dissipate high correlation among image pixels the sequences generated from all presented generators are introduced to five well-known statistical tests of randomness to judge their randomness characteristic. The ciphered images are tested for their residual intelligibility subjectively. The measures applied to images ciphered by one of the classical key-stream cipher generators (Threshold generator) for the purpose of comparison with the presented key-stream algorithms. Experiments results show that the proposed algorithm achieves the image security. In order to evaluate performance, the proposed algorithm was measured through a series of tests. Experimental results illustrate that the proposed scheme shows a good resistance against brute-force and statistical attacks.

Keywords: image encryption, stream cipher, data security

KJPS Al-Kitab Journal for Pure Science
Vol.2 (2), ISSN: 2617-1260 (print), 2617-8141(online)
www.kjps.isnra.org

نظام محكم لتشفير الصور الرقمية يعتمد على موسع مفتاح التوزيع العشوائي واسع النطاق

رغد زهير يوسف[1] .أياد غني اسماعيل[2]

[1] قسم الفيزياء التطبيقية– الاتصالات ، جامعة صلاح الدين ، أربيل ، العراق.

[2] رئيس جامعة الكتاب – ألتون كوبري – كركوك.العراق.

[1]Raghad.yousif@su.edu.krd, [2] dr.ayad.ghany.ismaeel@gmail.com

الملخص

تقدم هذه الورقة مخططا جديدا لتشفير الصور يقوم على تمديد المولد واسع النطاق العشوائي. لقد قدم الشكل الأساسي لمولد تيار المفتاح، واستخدم في التشفير الصورة الرقمية. تعديل الشكل الأساسي أيضا، قدم، واعطى نتائج مشجعة في تشفير الصور بالمقارنة مع مولدات الشفرات غير الخطية الكلاسيكية والشكل الأساسي. حيث تم تنفيذ خلط عناصر الصورة عن طريق التقليب الرأسي والأفقي. يتم استخدام المراوغة لتوسيع الانتشار في الصورة وتبديد الارتباط البيني بين عناصر الصور ت ايضا عرض المفتاح العشوائي من جميع المولدات المقدمة إلى خمسة اختبارات إحصائية معروفة من العشوائية للحكم على الخصائص العشوائية الخاصة بهم. وتوضح النتائج التجريبية أن الطريقة المقدمة، اظهرت مقاومة جيدة ضد القوة الغاشمة والهجمات الإحصائية.

الكلمات الدالة: تشفير الصور ، دفق التشفير ، أمن البيانات

INTRODUCTION

As computer –networks widely adapted by societies, network security issue becomes essential in this century. Many people need data privacy and feeling it is necessary when they sending or receiving information against unauthorized people [2]. Consequently, digital images represent one of the important information, transmitted through communication networks; hence there must be some techniques to conceal them. The most reliable way is by

KJPS Al-Kitab Journal for Pure Science
Vol.2 (2), ISSN: 2617-1260 (print), 2617-8141(online)
www.kjps.isnra.org

employing ciphering algorithm to convert the digital image to unintelligible information. Image coding such as (Huffman code), can be also considered as one of the ways of image data concealment, but coding gives constant (codebook)[3], to each image to be ciphered. On other hand ciphering provides many cipher text to each image, through different transformation keys employing. Fortunately, security algorithms do not have to be expensive or complicated. Such as, stream cipher algorithms that will be focused during the work of this paper and will be applied for image ciphering because of such generators simplicity and perfection (close to one-time-pad) [2],[3],[4]and fast implementation of ciphering process .

2. Image Encryption Using Large–Scale Randomization Stream Cipher Scheme

The Large –Scale Randomization algorithm is composed of mainly two parts as shown in figure (1).

The driving sub-system. The non-linear combining subsystem.

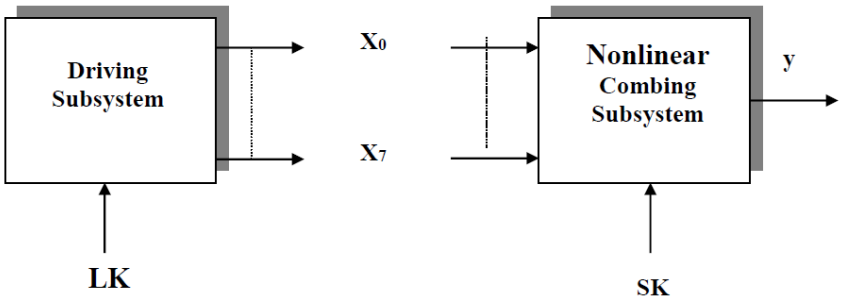

Figure (1) Block diagram of proposed stream cipher generator.

According to deriving sub-system design there are two forms for the presented key-stream generator that will be introduced in the next stage.

Basic Form of the Presented Algorithm

The deriving sub-system for the basic form of the presented algorithm consist of also Two parts as illustrated in figure (2). the first part is the deriving sub-system that involves single group of (LFSRs), this group is called choosing group that illustrated in figure (3).

KJPS Al-Kitab Journal for Pure Science
Vol.2 (2), ISSN: 2617-1260 (print), 2617-8141(online)
www.kjps.isnra.org

These five bits generate an address to any cell in the g^ container that consist of 32 locations (Session-key). These contents should be selected randomly in other word the container should include random combination of ones and zeros. Ruppel key-stream generator can be used to generate this key.

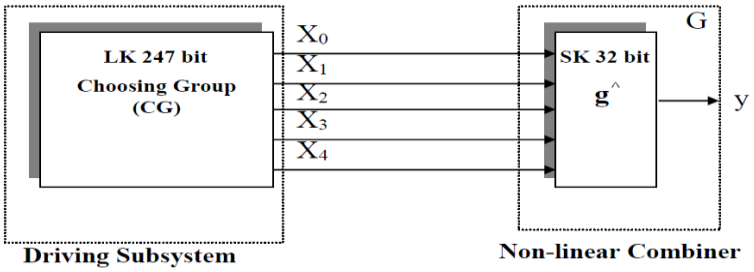

Figure (2) proposed system components

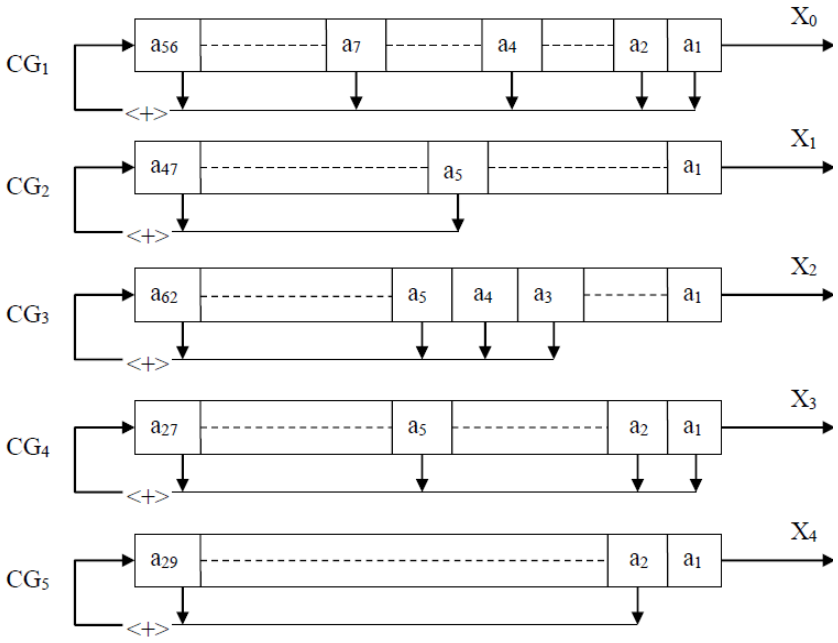

Figure (3) Driving subsystem (Basic form)

Developed Form of the Presented Algorithm

The developed form of the presented algorithm can be considered as an extended form of that presented previously. The extension here applied for driving sub-system and non-linear sub-system. The driving subsystem consists of three groups LFSRs:

KJPS Al-Kitab Journal for Pure Science
Vol.2 (2), ISSN: 2617-1260 (print), 2617-8141(online)
www.kjps.isnra.org

1-Choosing group (CG): consists of five LFSRs (CG1 – CG5).

2-Rotation group (RG): consists of two LFSRs (RG1, RG2).

3- Directives registers (DR). The deriving sub-system is illustrated in figure (2).

Where, registers of each group have relatively different prime lengths. The content of each LFSR is filled with the sequence of bits derived from the secret key (LK) that will be discussed later. In the design of the non-linear combining sub-system (G) the following requirements have been considered [10],

(1) (G) must transfer the statistical properties of the periodic driving sequences to the generated running key in the sense that, when the input sequences have good properties, so is the output sequence.

(2) (G) must be maximizing the complexity of the running key relative to the complexities of the driving system generators. Linear methods to reliably predict future key stream digits

$$G: \text{Binary}^8 \rightarrow \text{Binary}$$

from any observed part of the key stream is made unfeasible. In the suggested stream cipher generator, the non-linear part assumed is a Boolean function (G) of type:

Which is given in the form:

$$y_j = (g^{\wedge}_j (X_{0}j, X_{1}j, X_{2j}, X_{3j}, X_{4j}, S^{\wedge}_j (X_{5j}, X_{6j}), P^{\wedge}_j (X_{7j})) <+> X_{4j} <+> X_{6j} <+> X_{7j}) \quad (1)$$

Where:

$$S^{\wedge}_j (X_{5j}, X_{6j}) = (X_{5j} + X_{6j}) << 1 \quad (2)$$

And:

$$P^{\wedge}_j (X_{7j}) = \begin{cases} \text{ROTR } (g^{\wedge}, S^{\wedge}) \text{ if } X_{7j} \neq 0 \\ \text{ROTL } (g^{\wedge}, S^{\wedge}) \text{ if } X_{7j} \equiv 0 \end{cases} \quad (3)$$

Where, yj is the output of the function at time j, (X_{0j}, …X_{7j}) are the output bits of the driving stage at time(j) g^j is a 5-bit combining function, it works as a 32-bit container whose contents are initialized by the secret session key (S_k).

KJPS Al-Kitab Journal for Pure Science
Vol.2 (2), ISSN: 2617-1260 (print), 2617-8141(online)
www.kjps.isnra.org

The input to the function is three groups, where the first group (i.e. X_{0j}, X_{1j}, …X_{4j}) is considered as address, to a certain location (cell) in the container. The second group (X_{5j}, X_{6j}) pass through the operator (Ŝ), whose output will specify the amount of rotation (i.e. the bits length of the rotation). Finally, (X_{7j}) bit which is pushed to the operator (P^) whose output bit will specify the direction of the rotation. The importance of the (Ŝ) and (P^) functions is to increase the immunity that will be illustrated. Figure (4) shows the complete structure of previously presented scheme.

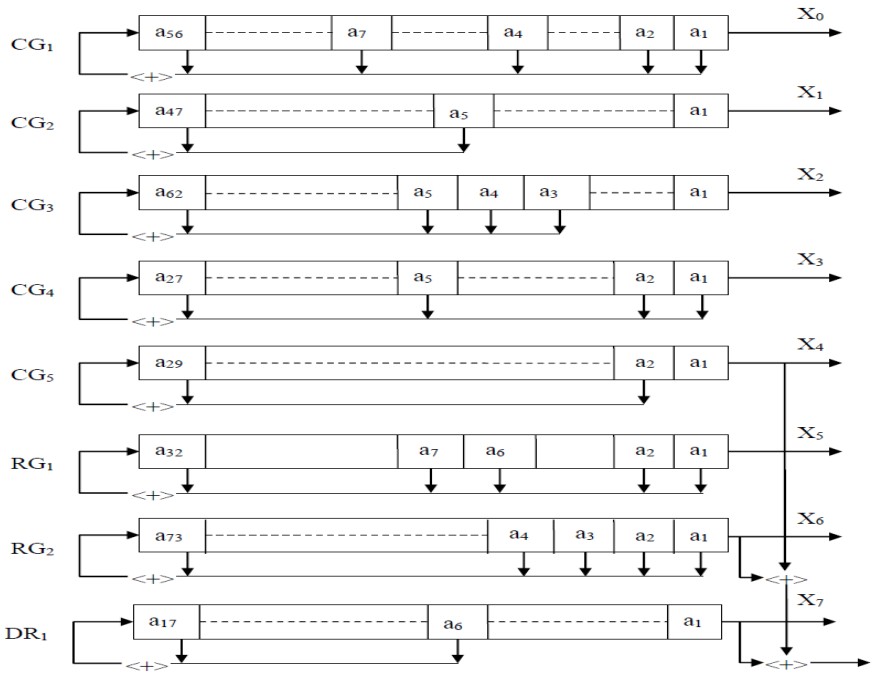

Figure (4) proposed system internal structure

Key Structure

Two different secret keys are involved with the suggested generator these keys are: Session key (SK): 32 bits that should be generated randomly (by the user) with correlation rate equal (0.5). The random generator selected to construct this key is the Reuppel-generator. The value of this generator initial key is: (1011,0101,1100,0100,0110,1101,0111,1010) b (0Xb5C46d7A) H. Linear key (LK): (343) bits are used to initialize the contents of LFSRs with the driving subsystem. Three keys are used; thus, the adopted three keys contain different levels of redundancies, and randomness

KJPS Al-Kitab Journal for Pure Science
Vol.2 (2), ISSN: 2617-1260 (print), 2617-8141(online)
www.kjps.isnra.org

which will be considered as a weak randomness (key 1) to the good randomness (key 3). Figure (5) below shows Complete system components

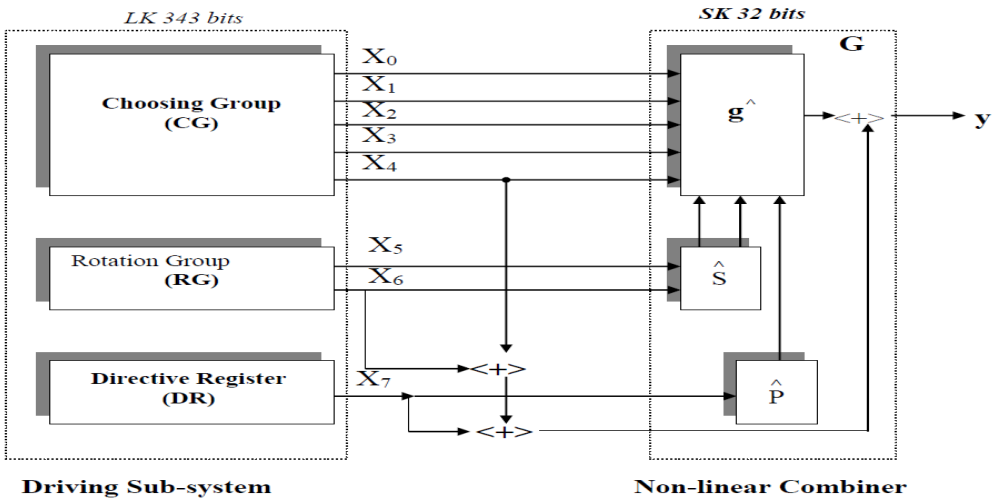

Figure (5) Complete system components

Initialization and Operation

The initialization operation is done by first loading the (LK) (343) bit, to initialize the registers starting from (CG1…CG5) then RG1, RG2, and finally DR receptively. The operation of bits stream generation is started by producing five bits from CG as an address to the session key that is resident in the (g^) container, and then the content of (g^) will be rotated before producing its value. The rotation operation depends on the output of the function (Ŝ) which decide how many positions can be rotated, but the direction of rotation decided by direction operation (P^) (when(X_{j7}=0) to be rotated container content (g^) right and when (X_{7j} =1) the content is rotated to the left). The output bit of generator produced by XORing of the output of (g^) function and output of three registers (CG5, RG2, and DR). XORed together. This operation can be repeated to generate a key sequence [7]. The outline of generator operations can be shown in the following pseudo code, which written in C++ notation:

Step1: Input = SK, LK, no. of cycles.

Step2: Initial LFSRs with LK.

Initial ($g^{\wedge}$) with SK.

Step3: I=1

Step4: If I>no. of cycles then go to step 12.

Step5: Shifting of LFSRs, and producing $X_0, X_1, \ldots, X_7$.

Step6: Address = 0.

Step7: For j=0; j <5 ; j ++

Address = Address $\oplus$ X_j << j

End for.

Step8: No. of rotations = X_5+X_6 << 1;

Step9: For K = 0; K < no. of rotations; K ++

IF X_7 = = 0 the rotate ($g^{\wedge}$) to the left

Else

Rotate ($g^{\wedge}$) to the right

End for

Step10: Output = ($g^{\wedge}$[Address] + X_4 +X_6 +X_7) mod (2);

Step11: I = I+1, Goto step 4.

Step12: Stop

Expected Sequence Period

The architecture of this algorithm is chosen so that the size of period (L) is such that the system is computationally secure against linearization attacking i.e. $L \cong 2^{343}$. This value is derived by the fact that the period (Li) of the sub-generators (i) is given by:

$$\mathbf{L = \prod_{i=1}^{N} L} \qquad \ldots(4)$$

KJPS Al-Kitab Journal for Pure Science
Vol.2 (2), ISSN: 2617-1260 (print), 2617-8141(online)
www.kjps.isnra.org

Where N = number of sub-generators. Then it can be show that, the period of sub-generators: $L_1 = \prod_{i=1}^{8} (2^{Li} - 1) \approx 2^{343}$ **bits**

On the other hand, the period of the non-linear part is the period of three functions (g^), (S^), (P^) which can be computed as:

$$L_2 = \prod_{i=1}^{3} 2^{Li} = 2^1 * 2^2 * 2^{32} = 2^{35} \quad \textbf{bits}$$

Therefore, the overall period (L) of the system becomes :

$$L_T = (L_1) * (L_2) \approx 2^{378} \quad \textbf{bits.}$$

The size of period makes attack becomes unfeasible and suitable for huge data (such as image information) ciphering the different (LFSRs)[5].One of the classical Non-linear stream cipher generators is threshold generator in which the combination function checks the majority of ones ,thus if more than half the output bits from each sub-generator(X1,X2,X3…).Includes '1'more than '0' then the output of generator is '0'.The output of generator can be written as[1]:

$$y=(X_1<*>X_2)<+>(X_1<*>X_3)<+>(X_2<*>X_3) \quad \ldots(5)$$

Where y is the output of generator and <*>denotes logical AND.

3. Image Ciphering by Presented Algorithm

To cipher digital images by the proposed algorithm .The following procedure must be followed .If M represents whole image pixel values M is divided in to successive parts mij ,i.e.,m11 ,m12 ,…..mn1 n2 where 1<i , j < n1 , n2 ,then if m11 ,m12 ,…..mn1 n2 ∈M ,and mij stands for one image data pixel (8-bit for gray-scale images) with in a set of whole images pixels M .The encryption engine enciphers mij (8-bit) at a time with the Key-stream element kl (where kl ∈K) , kl is the entire Key-Stream and 1< l < n1n2 . The process of encryption is as follows [2]:

Equation (a):

$T_k(M) : M \rightarrow C = t_{k1}(m_{11})\ t_{k2}(m_{12}) \ldots\ldots t_{kl}(m_{n1\ n2})$.

KJPS Al-Kitab Journal for Pure Science
Vol.2 (2), ISSN: 2617-1260 (print), 2617-8141(online)
www.kjps.isnra.org

Where $T_k(M)$ and $t_{kl}(m_{n1n2})$ are the encryption of whole message and a single pixel in image respectively .

Equation (b):

$$T_k^{-1}(C) : C \rightarrow M : t_k^{-1}(c_{11})t_k^{-1}(c_{12}).....t_k^{-1}(c_{n1n2}) .$$

Where and $T_k^{-1}(C)$ and $t_k^{-1}(c_{n1n2})$ are the encryption of whole message and a single pixel in image respectively. Equation (a) is applied to each pixel in image frame in row-wise manner, until the final row in image. Then the same key-stream is applied to the previously resulted image frame in column- wise to deals with image data as a two-dimensional message. The same procedure is applied by equation (b) to decipher the images and reconstruct the original image without loss in image quality (recovered image). Image encryption scheme illustrated in figure (5).

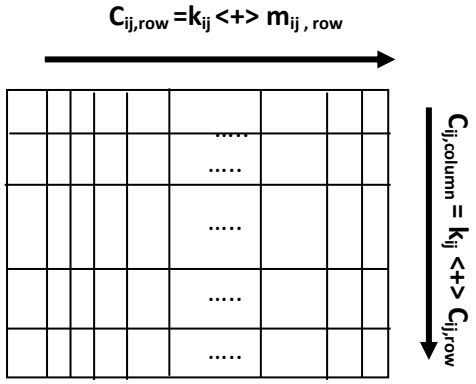

Figure (5) Image ciphering scheme

4. Residual Intelligibility and Regularity of Digital image

When ciphering systems are constructed, there must be some techniques to show the amount of residual intelligibility in ciphered images, and the quality of the reconstructed images. The ciphered image must be considered nearly as a white noise (chaotic) with low residual intelligibility and low quality, on other side the reconstructed (deciphered) image, must give high intelligibility and high quality with high level of regularity.

KJPS Al-Kitab Journal for Pure Science
Vol.2 (2), ISSN: 2617-1260 (print), 2617-8141(online)
www.kjps.isnra.org

Subjective Fidelity Criteria

Human are good at identifying geometric objects (such as circles, rectangles, triangles, and lines) and shapes in general. Images, which contain-mostly recognizable shapes, are called regular images. If an image is not regular, i.e. does not contain identifiable objects or patterns, or its too chaotic (such as white noise), it is difficult for humans to compare or recall it [9]. Thus, for image ciphering systems it is suitable that the ciphered image To have bad subjective quality, (low visual quality), and the deciphered image to have high visual quality. The histogram of an image is a plot of gray-level values, versus the number of pixels at that value. The shape of histogram provides information about the nature of image. The histogram measures are statistically based features, where the histogram is used as model of the probability distribution of gray levels. The first order histogram probability P(g) can be defined as:

$$\mathbf{P(g) = \frac{N(g)}{Mp}} \qquad \ldots(6)$$

(Mp) is the number of pixels in the image or sub-image, and N(g) is the number of pixels at gray level g. The statistical measure based on histogram probability used to measure image regularity is the entropy which is a measure of randomness achieving is highest value when all gray levels of image are equal so, it is given by [10]:

$$\mathbf{H = -\sum_{g=0}^{N_L-1} P(g)\log_2[P(g)]} \qquad \ldots(7)$$

As, the pixel values in the image are distributed among more gray levels, the entropy increase [5]. Hence, the ciphered image must have maximum entropy, but the deciphered image must have less amount of entropy (flat histogram distribution).

Objective Fidelity Criteria

The objective fidelity criteria provide equations that can be used to measure the amount of error in the reconstructed (deciphered) images or to measure the amount of error between pure image and ciphered image. Commonly used objective measures are the root-mean-square error (erms), and the peak signal-to-noise ratio (PSNR) [10]. The root-mean-square

KJPS Al-Kitab Journal for Pure Science
Vol.2 (2), ISSN: 2617-1260 (print), 2617-8141(online)
www.kjps.isnra.org

error is found by taking the square root of the total error divided by the total number of pixels in the image of size (N×N):

$$e_{rms} = \sqrt{\frac{1}{N^2}\sum_{x=0}^{N-1}\sum_{y=0}^{N-1}[I\hat{}(x,y) - I(x,y)]^2} \quad \ldots(8)$$

Hence, the smaller the value of erms metrics, the better the deciphered image represents the original image and the larger the value of error metrics. The better the ciphered image conceal pure image information. Alternatively, with (PSNR) metrics, a larger number implies a better deciphered image, and smaller number implies better image concealment of original image is obtained. the peak signal–to–noise ratio, is defined as:

$$PSNR = 10\log_{10}\frac{(N_L - 1)^2}{\frac{1}{N^2}\sum_{x=o}^{N-1}\sum_{y=0}^{N-1}[I\hat{}(x,y) - I(x,y)]^2} \quad \ldots(9)$$

Where NL = number of gray levels (for 8-bits NL = 256) . Also, as a useful indicator for intelligibility losses in deciphered or residual intelligibility in ciphered image, because all pixel in spectral domain represents a contribution of all image pixels in spatial domain [10]. The spectral signal–to–noise ratio for the digital image can be defined as:

$$SSNR = 10\log_{10}\frac{\sum_{u=0}^{N-1}\sum_{v=0}^{N-1}|If(u,v)|^2}{\sum_{u=0}^{N-1}\sum_{v=0}^{N-1}|If(u,v) - I\hat{}f(u,v)|^2} \quad \ldots(10)$$

Where If(u,v) is the two-dimensional Discrete Fourier Transform (2DDFT) of original image and I^f (u,v) is the (2DDFT) for ciphered image equation (19) is defined in [8] for one-dimensional discrete signal as a scrambled signal quality measure as:

$$SNR = 10\log_{10}\frac{\sum_{u=1}^{N}|If(u)|^2}{\sum_{u=1}^{N}|If(u) - If\hat{}(u)|^2} \quad \ldots(11)$$

KJPS Al-Kitab Journal for Pure Science
Vol.2 (2), ISSN: 2617-1260 (print), 2617-8141(online)
www.kjps.isnra.org

Similarity Measure

The most common form of the similarity measure can be interpreted in two given matrices A_{ij} and B_{ij} .The inner product can be defined as $\sum_{i=1}^{N}\sum_{j=1}^{N} a_{ij}b_{ij}$ Alternatively; each element in the matrix is subtracted from the image mean value as illustrated below:

$$\left(a_{ij} = a_{ij} - \sum_{g=0}^{N_L} g \times p(g)\right)_{i=0,j=0}^{i=N,j=N} \quad \text{...(12)}$$

$$\left(b_{ij} = b_{ij} - \sum_{g=0}^{N_L} g \times p(g)\right)_{i=0,j=0}^{i=N,j=N}$$

Then, the similarity test finally is given by (after normalization) [5]:

$$\text{CORR2}\ (A_{ij}, B_{ij}) = \frac{\sum_{i=1}^{N}\sum_{j=1}^{N} a_{ij}b_{ij}}{\sqrt{\sum_{i=1}^{N}\sum_{j=1}^{N} a_{ij}^2}\sqrt{\sum_{i=1}^{N}\sum_{j=1}^{N} b_{ij}^2}} \quad \ldots(14)$$

By considering Aij and Bij as two image matrices. The similarity measure shows the amount of correlation between Aij and Bij. Therefore, when the similarity between the ciphered image and the original image, is small, then good concealment to the original image is obtained. The similarity between any two-image matrices gives its maximum value of (1) if the two images are perfectly similar.

Statistical Tests of Randomness

Numerous statistical tests can be applied to a sequence. In the current work, five particular tests will be described and some remarks about their usefulness will be presented to give an indication of their usefulness. The five tests are:

KJPS Al-Kitab Journal for Pure Science
Vol.2 (2), ISSN: 2617-1260 (print), 2617-8141(online)
www.kjps.isnra.org

Frequency Test

This is perhaps the most obvious test in comparison with other tests, occurred in the sequence and it is applied to ensure that there is roughly the same number of '0s' and '1s'. Let n0 zeros and n1 ones be in a sample of (nt = n0 + n1) bits. Then[6] :

$$\chi^2 = (n_0 - n_1)^2/n_t \quad \ldots(15)$$

Clearly if n0 = n1 then χ^2 = 0. To decide if the value obtained is good enough for the sequence to pass, the value of test can be compared with a table of χ^2 distribution (Appendix (B)), for one degree of freedom (DOF). It is obvious that the value of χ^2 for 5% significant level is (3.84). So, simply, if the test value is no greater than (3.84) the sequence passes, otherwise it is rejected.

Serial Test

The serial test is used to check that the number of bit transitions of the binary sections (01,10,00,11) in the stream of length nt are occurred roughly (the same number of times). If a sample passes this test it suggests that each bit is independent of its predecessors. If n00 represents the frequency of the section 00, n_{01} the frequency of the section 01, n10 is the frequency of the section 10, and n11 is the frequency of the section 11, then the following equations will always hold

n00 + n01 = n1 or n1-1 …(16)

n10 + n11 = n1 or n1-1 …(17)

n10 - n01 = 0 or 1 …(18)

n00 + n01 + n10 + n11 = nt-1 …(19)

(Note the (–1) occur because for a section of length L there are only L-1 transitions).

Ideally:

$$n01 = n10 = n00 = n11 \approx \frac{n_t - 1}{4}$$

as showed by [12], and,[30],[31] ,hence the serial test ST is given by:

KJPS Al-Kitab Journal for Pure Science
Vol.2 (2), ISSN: 2617-1260 (print), 2617-8141(online)
www.kjps.isnra.org

$$S_T = \frac{4}{n_t - 1} \sum_{i=0}^{1} \sum_{j=0}^{1} (n_{ij})^2 - \frac{2}{n_t} \sum_{i=0}^{1} (n_i)^2 + 1 \qquad \ldots(20)$$

Is approximately, distributed with two degrees of freedom. From χ^2 distribution table. Thus, the value of χ^2 corresponding to a 5% significant level is 5.99. It is becoming clear that for this test any sequence for which the value is greater than 5.99 must be rejected.

Auto-correlation Test

If the binary stream to be tested is $x_1, x_2, x_3, \ldots x_{n_t}$ then:

$$A_C(d) = \sum_{i=1}^{n_t - d} x_i * x_{i+d} \qquad 0 \le d < n_t\text{-}1 \qquad \ldots \quad (25)$$

$$A_C(0) = \sum_{i=1}^{n_t} (x_i)^2 = \sum_{i=1}^{n_t} x_i^2 = n_1$$

If the stream contains n0 of '0s' n1 of '1s', then the expected value for A (d) where d ≠ 0 is:

$$\mu = \frac{n_1^2 (n_t - d)}{n_t^2} \qquad \ldots(26)$$

The test will be successful if χ^2 ≤ 3.841 for all d, where χ^2 can be calculated as follows:

$$\chi^2 = \frac{(A_c(d) - \mu)^2}{\mu} \qquad \ldots(27)$$

This test enables to decide whether the sequence under test is believed to have 'random' distribution or not [8] [9]

KJPS Al-Kitab Journal for Pure Science
Vol.2 (2), ISSN: 2617-1260 (print), 2617-8141(online)
www.kjps.isnra.org

The Run Test

For this test, the sequence is divided into runs of zeros and ones, a run of zeros is defined as a consecutive string of zeros preceded and followed by ones a run of ones is defined similarly.

The (i) successive 0-bits preceded and followed by a '1' are called a 0-run of length (i): $\underbrace{10000001}_{\text{Length -i}}$

The successive 1-bits preceded and followed by a '0' are called a 1-run of length i:

$$\underbrace{01111110}_{\text{Length -i}}$$

For example, the sequence 011000101101 contains:

3 of 0-runs of length 1

1 of 0-runs of length 3

2 of 1-runs of length 1

2 of 1-runs of length 2

n0i = number of 0-runs of length i.

n1i = number of 1-runs of length i.

The expected number of runs of length i (both 0-runs and 1-runs T0, T1) is :

$$T_0 = \sum_{i=1}^{k_f} \frac{\left(n_{0i} - \frac{n_t}{2^i}\right)^2}{\frac{n_t}{2^i}} \quad \ldots(28)$$

$$T_1 = \sum_{i=1}^{k_f} \frac{\left(n_{1i} - \frac{n_t}{2^i}\right)^2}{\frac{n_t}{2^i}} \quad \ldots(29)$$

Which is approximately χ^2 distribution with (kf -1) degree of freedom.

KJPS Al-Kitab Journal for Pure Science
Vol.2 (2), ISSN: 2617-1260 (print), 2617-8141(online)
www.kjps.isnra.org

Results and conclusions

The results for Image regularity and residual intelligibility are all illustrated in Table (1) for the image beach. The ciphered images are all shown in figure (6)

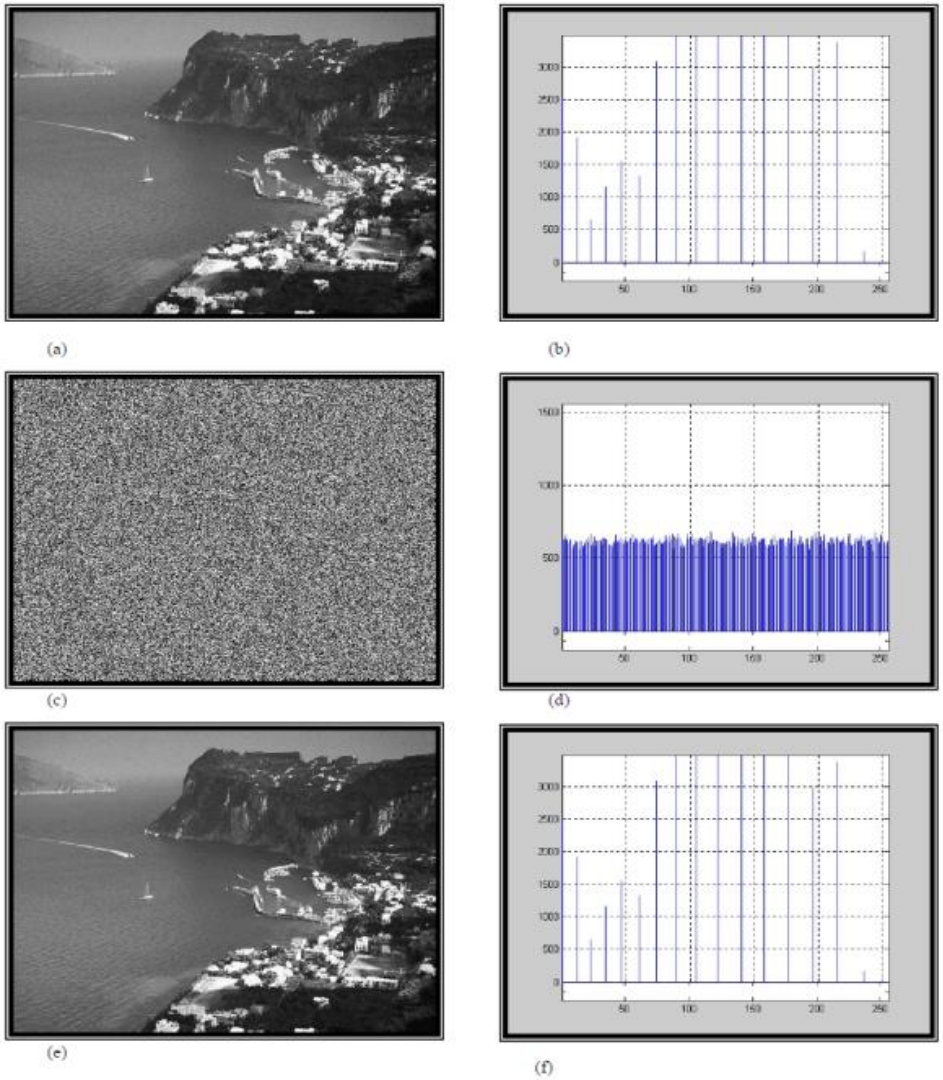

Figure:(6) Image called beach ciphered using presented algorithm
(a)&(b): original image with histogram
(c)&(d): ciphered image from preseuted Algorithm with histogram.
(e)&(f): deciphered image with histogram.

for the proposed non-linear key-stream generator and traditional Non-linear key-stream generator which is called Threshold generator for sake of comparison. The results of testing randomness of LFSRs are shown by tables (2) and table (3) below

Table (1) Regularity and Residual Ineligibility Measures for ciphered images

Image name	Entropy of pure image	Entropy	Similarity	SSNR (dB)	PSNR (dB)	e_{RMS}
The results of residual intelligibility for presented stream cipher generator						
Beach	7.4504	7.9023	-0.0431	0.6225	1.9258	204.367
The results of residual intelligibility for Threshold stream cipher generator						
Beach	7.0144	7.4289	0.4843	5.3219	7.1756	118.017

The requirements of the proposed algorithm are:

Both the sender and receivers need to have the identical functioning programs for enciphering and deciphering.

(2) The receivers must have obtained the randomization key string K(l) and the scheme description before the receipt of ciphertext from the senders. Therefore, a good key exchange protocol, like Diffie-Hellman scheme, must be performed. This may have employed in future as further development for the presented algorithm.

(3) The results of residual intelligibility that have been applied for image called Bridge and image called Fighter shows that the residual intelligibility for images ciphered by the presented algorithm is lower than the values obtained from the same images encrypted by Threshold non-linear stream cipher generator (see table (1)). Furthermore, the subjective quality for ciphered images by the presented algorithm is very close to the white noise (chaotic with flat histogram) as compared by the same results obtained from Threshold non-linear stream cipher generator.

(4) The correlation immunity of the presented generator with high period could be considered as the most important advantages of the presented algorithm. Finally, the simulation results show that the proposed algorithm achieves the image secrecy.

KJPS Al-Kitab Journal for Pure Science
Vol.2 (2), ISSN: 2617-1260 (print), 2617-8141(online)
www.kjps.isnra.org

Table (2) Statistical Tests of Randomness Results from classical method

Test		Key 1	Key 2	Key 3	Pass value
Frequency test		0.0269	0.3618	2.3687	must be ≤ 3.84
Run test	T_0	18.972	13.103	17.67	must be ≤ 22.362
	T_1	20.540	17.4062	15.8021	
Poker test $\beta = 5$		5.6026	5.1986	5.4849	must be ≤ 11.1
Serial test		0.84118	1.4497	3.6787	must be ≤ 5.99
Auto – Correlation test, for first ten bits	Shift 1	0.20334	0.2739	0.32610	must be ≤ 3.48
	Shift 2	0.69133	0.12747	0.08966	
	Shift 3	0.13613	0.06818	0.01968	
	Shift 4	0.04478	0.11389	1.21773	
	Shift 5	0.05576	0.60407	0.02818	
	Shift 6	0.45618	0.24653	0.2070	
	Shift 7	0.86701	0.54944	0.2762	
	Shift 8	0.7377	0.20560	0.38185	
	Shift 9	0.04525	0.33720	0.9558	
	Shift10	0.13753	2.27516	0.36748	
Maximum Auto – Corr. value		1.735	0.5251	0.8235	≤ 3.48

Table (3) Statistical Tests of Randomness Results from Large-Scale Randomization stream cipher scheme without ($\hat{S}, \hat{P}$)

Test		Key 1	Key 2	Key 3	Pass value
Frequency test		0.52711	0.05034	0.2586	must be ≤ 3.84
Run test	T0	*23.9218*	13.5559	15.8021	must be ≤ 22.362
	T1	20.8031	*38.9101*	7.27472	
Poker test $\beta = 5$		4.0218	3.627	7.747	must be ≤ 11.1
Serial test		0.3399	0.2567	0.50396	must be ≤ 5.99
Auto – Correlation test, for first ten bits	Shift 1	0.01522	0.4374	0.3217	must be ≤ 3.48
	Shift 2	0.8057	0.7043	1.23908	
	Shift 3	*3.8671*	3.5211	0.2597	
	Shift 4	0.2973	0.10312	*3.952*	
	Shift 5	0.01610	0.0064	4.1525	
	Shift 6	*4.47603*	3.215	0.8121	
	Shift 7	0.2735	*4.872*	0.33413	
	Shift 8	0.0058	0.0281	1.19559	
	Shift 9	*3.6902*	3.216	0.3979	
	Shift10	0.10022	0.04618	0.03205	
Maximum Auto – Corr .value		*4.482*	*8.2863*	2.61902	≤ 3.48

REFRENCES:

[1] B. Schneier, " Applied Cryptography ", NewYork, Wiley 1996.

[2] Tak-Ming Law,"Encryption Algorithm for Chinese Text Messages by Internal Code Structure", International Conference in Theory and Applications of Cryptography, Hong Kong University, 1999.pp246-250.

[3] W. Diffe, and M. E. Hellman, " Privacy and Authentication: An Introduction to Cryptography ", Proceeding of the IEEE, Vol.67. No.3, March 1979.pp 379-423

[4]Vera.S.Pless,"Encryption Schemes for Computer Confidentiality", IEEE Trans. On Computer, Vol. C-26, No.11, November 1977. pp. 1133-1136.

[5] J. C. A. Van Der Lubbe, " Basic Methods of Cryptography ", Cambridge University Press, 1998.

[6] T. Sigenthaler, " Correlation Immunity of Non-Linear Combining Function for Cryptographic Applications ", IEEE Trans. Info. Theory, Vol. IT-30, Sep. 1984, pp. 776-780.

[7] J. K. Ruben, "Analysis And Design of Large Scale Randomization Key-Stream Generator ", Springer-Verlage Proce. Eurocypt'97 ICTACT, May 11-15, 1998. pp 1229-1234.

[8] S. Sridhan, and E. Dawson, " Fast Fourier Transform Based Speech Encryption System ", IEE Proceeding, Vol. 138, No. 3, June 1991. pp 215-223.

[9] A. Perring, and D. Song, " Hash Visualization: A New Technique to Improve Real-World Security ", International Conference in Theory and Applications of Cryptography, Hong Kong University, 1999.pp131-138.

[10] E. U. Scotte, " Computer Vision and Image Processing: Practical Approach Using CVIP Tools ", Prentice-Hall, 1998.

KJPS Al-Kitab Journal for Pure Science
Vol.2 (2), ISSN: 2617-1260 (print), 2617-8141(online)
www.kjps.isnra.org

DOI: http://10.32441/kjps.02.02.p13

Out-Lab Therapy Approach Based on Elected A Restriction Enzyme to Transfer Target Gene

Ayad Ghany Ismaeel
Department of Computer Technical Engineering, Al-Kitab University College, Kirkuk-IRAQ.
dr_a_gh_i@yahoo.com, dr.ayad.ghany.ismaeel@gmail.com

Abstract

An important approach of therapy the target gene sequence causes diseases via repair/recombine the mutated gene (gene transfer) using a restriction enzymes in the laboratory. This approach will cause multiple problems happening accompany to biological laboratory if ruled out problems outside of it like the digested DNA ran as a smear on an agarose gel, incomplete restriction enzyme digestion, extra bands in the gel, etc. The paper suggested new approach of therapy via repair/replacement mutated gene caused disease by detecting primers and finding restriction enzymes using bioinformatics tools, software, packages etc. then achieving the repair/ recombine of mutations before going to the biologic lab (out-lab) to avoid the problems associated these laboratories. Implement and apply this a proposed therapy approach on TP53 gene (which caused more than 50% of human cancers) and after confirming there is mutations on P53 tumor protein shows an effective cost, friendly therapy methodology and comprehensive.

Keywords — Therapy, Gene Transfer, Target Sequence, Polymerase Chain Reaction, Primers, Restriction Enzymes, P53 Tumor Protein.

KJPS Al-Kitab Journal for Pure Science
Vol.2 (2), ISSN: 2617-1260 (print), 2617-8141(online)
www.kjps.isnra.org

1. INTRODUCTION

THERAPY of mutated gene caused diseases may be done by replacing the damaged gene with another non-damaged using restriction enzymes and that needed to scan along a DNA looking for a particular sequence of bases in general from 4-6 base pairs in length within laboratory that will take approximately 3 days. The restriction digestion in the lab takes place overnight and can be kept in the freezer until the next class period when it will be used for gel electrophoresis, the gels may be stained overnight prior to
photographing or recording results.

n this pargraph will explain briefly some terminologies like DNA template is sample DNA contains the target sequence (means the gene sequence which needed therapy). DNA polymerase a type of enzyme, which is synthesizes new strands of DNA complementary to the target sequence. PCR is based on using the ability of DNA polymerase to synthesize new strand of DNA complementary to the offered template strand. Primers - short pieces of single-stranded DNA that are complementary to the target sequence [1].

Process of gene transfer explained in following steps:

- Isolation of gene and vector (by PCR): Fig. 1 shows this task.

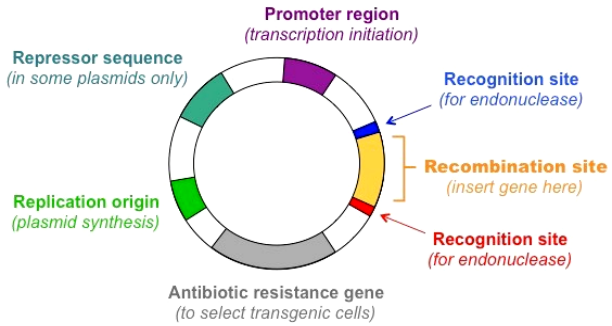

Fig. 1. Reveals Isolation of gene and vector.

Digestion of gene and vector (by restriction endonuclease): Both must be cut with restriction enzymes at specific recognition sites as show in Fig. 2

KJPS Al-Kitab Journal for Pure Science
Vol.2 (2), ISSN: 2617-1260 (print), 2617-8141(online)
www.kjps.isnra.org

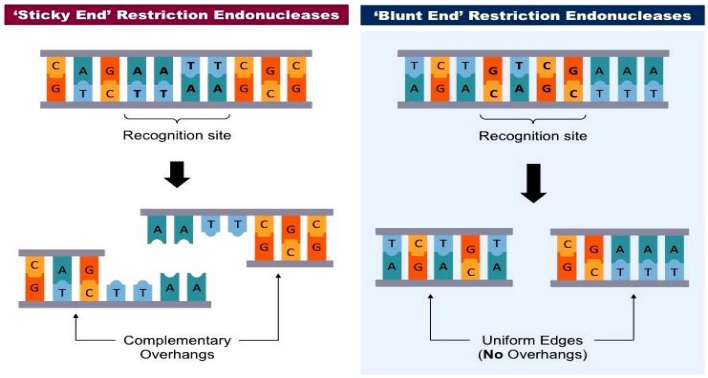

Fig. 2. Shows Digestion of gene and vector.

- Ligation of Vector and Insert (by DNA ligase): Fig. 3 shows a format of a recombinant construct.

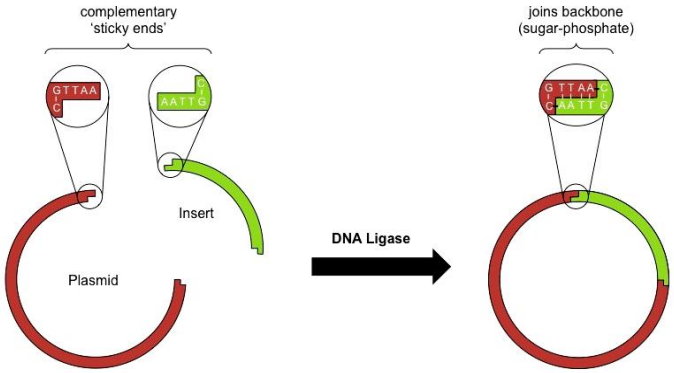

Fig. 3. Reveals Ligation of Vector and Insert.

Many of problems happening accompany to biological laboratory if ruled out problems outside of it like finding genes, primers, diagnosis and classify mutations, etc. Some of important problems are [2]:

1) Extra bands in the gel that may cause if larger bands than expected are seen in the gel, this may indicate binding of the enzyme(s) to the substrate and partial restriction enzyme digest.
2) No transforming that causes restriction enzyme(s) didn't cleave completely.
3) Partial restriction enzyme digestion will cause cleavage is blocked by methylation, Inhibition by PCR components, too few units of enzyme used, addition may lead to presence of slow sites, DNA is contaminated with an inhibitor, etc.

4) Digested DNA ran as a smear on an agarose gel this causes the restriction enzyme(s) is bound to the substrate DNA.

So needed to integrate new approach for replacement a mutated gene (which caused diseases) via candidate restriction enzymes that done by employing programs, online took and software (supported bioinformatics tools) can produce integrated therapy approach outside the laboratory to avoid the problems related.

2. RELATED WORK

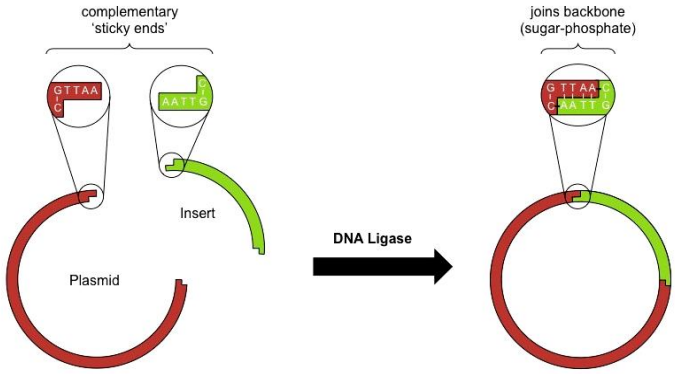

Fig. 3. Reveals ligation of Vector and Insert.

Colosimo A, Guida V, Antonucci, and others [2007], reveals gene therapy has been proposed as a definitive cure for □-thalassemia applied a gene targeting approach, based on the introduction of small DNA fragments (SDF) into erythroid progenitor cells, to specifically modify the □-globin gene sequence at codon 39. The strategy was first tested in normal individuals by delivering mutant SDF that were able to produce the □39 (C=>T) mutation. Secondly, wild-type SDF were electroporated into target cells of □39/□39. □-thalassemic patients to correct the endogenous mutation in both cases, gene modification was assayed by allele-specific polymerase chain reaction of DNA and mRNA, by restriction fragment length polymorphism analysis and by direct sequencing. Unfortunately, the number of corrected cells remaining from each experiment was insufficient to carry out protein studies by MALDI-TOF analysis. More importantly, improvements in delivery approaches

and/or design of SDF are clearly required to yield sufficient quantities of corrected cells for a significant therapeutic benefit. [3].

Owen T. M. Chan, MD, PhD, Kenneth D. Westover, and others [2010], suggested methods that assay hemoglobin β-globin chain variants can have limited clinical sensitivity when applied techniques identify only a predefined panel of mutations. Even sequence-based assays may be limited depending on which gene regions are investigated. They sought to develop a clinically practical yet inclusive molecular assay to identify β-globin mutations in multicultural populations. The paper highlights the β-globin mutation detection assay (β-GMDA), an extensive gene sequencing assay. The polymerase chain reaction (PCR) primers are located to encompass virtually all hemoglobin β locus (HBB) mutations. In addition, this assay is able to detect, by gap PCR, a common large deletion (Δ619 base pair), which would be missed by sequencing alone. We describe our 5-year experience with the β-GMDA and indicate its capability for detecting homozygous, heterozygous, and compound heterozygous sequence changes, including previously unknown HBB variants. The β-GMDA offers superior sensitivity and ease of use with comprehensive detection of HBB mutations that result in β-globin chain variants. [4].

The drawbacks of these methods (If you do not take into account the determinants of their own), implementing the therapy of mutation gene caused diseases done within laboratory and as referring to in section (1) there are multiple problems associated to the lab. The motivation overcome those drawbacks in previous techniques to reach a new therapy methodology, can replacement a mutated gene by predict the restriction enzymes based on bioinformatics tools and software then later can go to biological laboratory to implement the plan of replacement mutated gene via CAT methodology after classifying mutations at protein (not only in its gene) too because "two sequences may have big differences in DNA sequence but have similar protein" [5, 6].

3. PROPOSED THERAPY APPROACH

The proposed therapy approach started with find the gene (Homology normal gene) using NCBI (DNA template). after that diagnoses and classify there is mutation, If GC% content excepted then continue, else return from start to find another DNA Diagnosis and

KJPS Al-Kitab Journal for Pure Science
Vol.2 (2), ISSN: 2617-1260 (print), 2617-8141(online)
www.kjps.isnra.org

Classifying is there mutations at Person's gene and at protein too using ClustalW within BioEdit. The algorithm for therapy approach as PCR application shows as follow:

4. EXPERIMENTAL RESULTS

The implement and applied of proposed therapy approach (shown in subsection 3) on mutated TP53 gene and confirm stile there is mutation on the tumor protein P53 (which caused more than 50% types of human cancers) explained as follow:

Algorithm of Proposed Therapy Approach

Input: DNA template includes sequence of gene target, and sequence of mutated gene for the Person holds disease.
Output: Recombine gene of the patient holds disease via predicting of restriction enzymes.

BEGIN
Step 1: Determine the primers of normal gene via package, program, etc to avoid them when used the restriction enzymes.

Step 2: Predicting restriction enzymes using program of Analyze Sequence.

Step 3: While (there is mutation) do:

i. Selecting the adjacent enzymes (around the mutilation which needed replacement).
ii. Obtaining the foreign (Homology Normal) gene sequence to replace a mutated gene for Person.
iii. Expected replacement mutated gene using restriction enzymes which predicted in (a) above.

End While-do
END

Sequence.

A. Tools and Software are Required

The tools and software needed to implement and applied the proposed therapy approach for replacement/ recombine is summarised in:

1) Searching a NCBI for nucleotide (DNA sequence) via the gene name to obtain the DNA template (TP53 gene) then saved as FASTA format.
2) Determine unmuted TP53 Gene (Homology Normal Gene) using COSMIC/GENSCAN Web Server at MIT within the gene sequence which obtained at (1) above, will paste as shown in Fig. 4, A; this package can be extracted the normal TP53 gene (target sequence) and save it (in FASTA file) as shown in Fig. 4, B [8].

KJPS Al-Kitab Journal for Pure Science
Vol.2 (2), ISSN: 2617-1260 (print), 2617-8141(online)
www.kjps.isnra.org

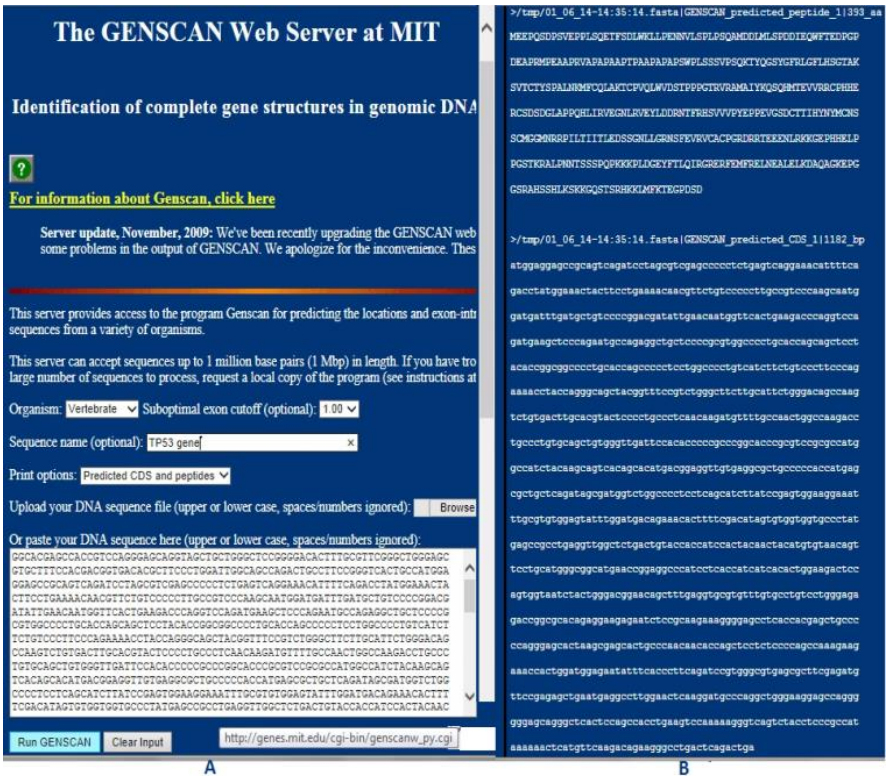

Fig.4. Shows extract target TP53 sequence via GENSCAN

3) The FASTA file which obtained in steps (1 and 2) will use in ClustalW to display result of alignment, i.e. diagnosis there is malignant mutations by comparing the normal TP53 gene sequence with one sequence (or more than one) TP53 gene sequences for persons at the same time. That is done using BioEdit by selecting Accessory Application→ ClustalW Multiple Alignment→ Run ClustalW, then obtained the result whether there is malignant mutation or not, and as example will suppose mutation at codon 349 in TP53 gene for certain Person comparing with normal TP53 gene shown mutation on that codon.

This classification on (3) above not enough as referring to in section (2) [5, 6], so needed to transform the normal homology TP53 gene to tumor protein P53 as well as TP53 gene for the Person transform to the tumor protein P53 then using the same tool ClustalW via BioEdit package for diagnosis still there is mutation (in level of proteins) or not. In this experiment shows the mutation at codon 349 (GAA→ TAA) when transform to tumor P53 will transformation from (E) to (stop) at Person's P53 gene. This confirm will classify

KJPS Al-Kitab Journal for Pure Science
Vol.2 (2), ISSN: 2617-1260 (print), 2617-8141(online)
www.kjps.isnra.org

in protein level in this mutation (position, which discovered) may cause lung cancer, head or neck cancers based on the database (UMD_Cell_line_2010) of TP53 website as modern and comprehensive database (URL: http://p53.free.fr/Database/p53_MUT_MAT.html [9]).

B. Applied the Algorithm of Therapy Approach

This subsection applies the algorithm of therapy approach as following using the mutated TP53 gene (of Person) and the normal TP53 gene as referring to them in (A) above:

1) Step 1: determine the primers at normal TP53 gene (target sequence) that is done using BioEdit by selecting normal TP53 gene→ BLAST NCBI→ then select Primer-BLAST→ paste the FASTA sequence of normal TP53 gene, finally will obtain the primers determines in (10), some of them shown in Fig. 5.

2) Step 2: Predict restriction enzymes via program of Analyze Sequence to select adjacent enzymes (around each mutation of mutations at TP53 gene), can obtain by open Analyze Sequence → paste the FASTA sequence.

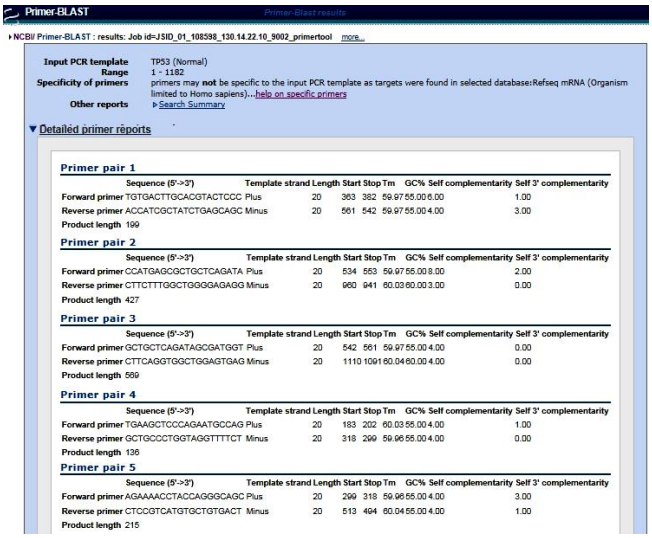

Fig. 5. Reveals part of extract primers using NCBI-BLAST

KJPS Al-Kitab Journal for Pure Science
Vol.2 (2), ISSN: 2617-1260 (print), 2617-8141(online)
www.kjps.isnra.org

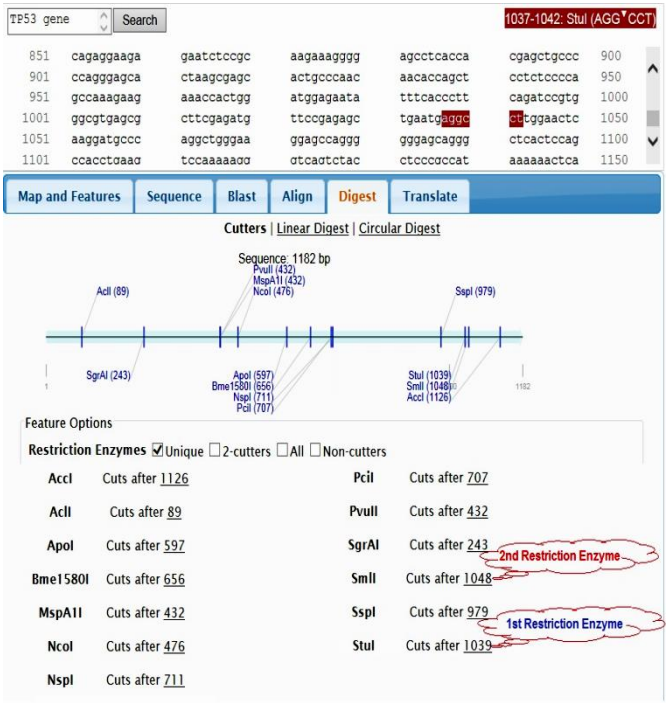

Fig. 6. Shows part of restriction enzymes at normal TP53 sequence

2) Step 3: Multiple steps required to implement continuity while there is mutation in TP53 gene as follow:

i. Selected the restriction enzymes (using program of analyze sequence), which are around (adjacent) the mutation at codon 349 in TP53 gene are the Eco147I (StuI) restriction enzyme recognizes AGG^CCT sites (Blund end) and cuts best at 37°C in B buffer (Isoschizomers: AatI, PceI, SseBI, StuI). While the second restriction enzyme recognizes is SmoI (SmlI), where C^TYRAG sites (overhang) and cuts best at 55°C in Tango buffer (Isoschizomers: SmlI) [10, 11].

ii. Obtained the foreign TP53 sequence (without mutation and not primer) (AGGCCTTGGAACTCAAG) will use for replacement the mutated TP53 sequence of Person (AGGCCTTGTAACTCAAG) as shown the mutation at codon 349 (in red), while restriction enzymes (in blue).

iii. Fig. 7 reveals an expected procedure in biologic lab (before going to the laboratory) to replace PT53 gene of Person which has mutation at codon 349 with foreign TP53 sequence (Normal gene).

KJPS Al-Kitab Journal for Pure Science
Vol.2 (2), ISSN: 2617-1260 (print), 2617-8141(online)
www.kjps.isnra.org

C. Discussion the Results

3) Table 1 shows comparing the results of proposed therapy approach of replacement mutated gene with other methods.

5. CONCLUSIONS

The proposed therapy approach of replacement mutated genes via predicting the restriction enzymes out-lab shows the following conclusions:

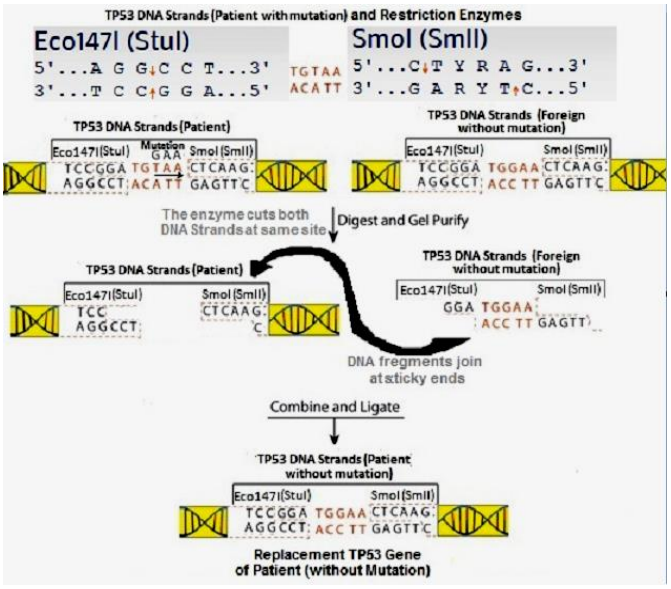

Fig. 7. Reveals an expected procedure of replacement TP53 gene by foreign sequence in biologic laboratory.

KJPS Al-Kitab Journal for Pure Science
Vol.2 (2), ISSN: 2617-1260 (print), 2617-8141(online)
www.kjps.isnra.org

TABLE I
SHOWS THE COMPARISON OF PROPOSED THERAPY APPROACH WITH OTHER TECHNIQUES/METHODS

Proposed Therapy Approach	Method of Colosimo A, and et al. **[3]**	Method of Owen T. M. Chan, and et al. **[4]**
Integrity the proposed therapy approach out the lab starting with finding DNA template, target gene, mutations in gene and its protein, primers; finally replacement mutated Person's gene causes disease.	**Focus on doing these operations within lab**	**Focus on doing these operations within lab**
Predict the restriction enzymes via bioinformatics tools, software, programs, etc.	Not applicable	Not applicable
Effective cost for analysis, predict mutating gene and restriction enzymes, etc may reach about $3000 [6].	**Doesn't has this effective-cost**	**Doesn't has this effective-cost**

The following conclusions:

a) Proposed therapy approach will classify the mutations at Person's TP53 gene and confirm with its P53 tumor protein, and then start the process of replacement/correction the mutated gene.

b) The proposed therapy approach offers friendly diagnosis for mutations at gene causes disease and predicting restriction enzymes, and finally replacement mutated gene for Person has diseases (e.g. cancer) as referring to in Table 1 Can use this therapy approach by researcher or any other person interested, who needed to therapy malignant mutations gene and its' protein caused diseases.

c) That therapy approach reveals the finding of target gene from DNA template, detecting primers, predict restriction enzymes, etc. before going to biologic lab make reduce to the problems associative to laboratory which referring to them in section 1.

d) As future works:

- Using the Cas-Analyzer as tool in CRISPR RGEN [12] to simulate the implementation of the replacement/recombine of mutated gene (as referring to it in subsection 4; B; 3; iii and shown in Fig. 7) instead of keeping it manually.
- Create database based on the proposed therapy approach for all mutations (in codons) of TP53 gene and their TP53 tumor protein caused diseases (50% of human cancers) addition to any other important genes like breast cancer (BRCA1 and BRCA2 genes). This database will allow mining technique and flexible retrieving the results related in replacement a mutated gene using predicting restriction enzymes.

REFERENCES

[1] NCBI, " PCR", URL: http://www.ncbi.nlm.nih.gov/genome/probe/doc/TechPCR.shtml.

[2] New England Biolabs (2014), "Restriction Enzyme Troubleshooting Guide", © Copyright. https://www.neb.com/tools-and-resources/troubleshooting-guides/restriction-enzyme-troubleshooting-guide. Recombinant DNA and Gene Cloning http://www.biology-pages.info/R/RecombinantDNA.html

[3] Colosimo A, Guida V, Antonucci, and others (2007), "Sequence-specific modification of a □-thalassemia locus by small DNA fragments in human erythroid progenitor cells", the hematology journal, Haematologica; 92:129-130.

[4] Owen T. M. Chan, MD, PhD, Kenneth D. Westover, and others (2010), " Comprehensive and Efficient HBB Mutation Analysis for Detection of -Hemoglobinopathies in a Pan-Ethnic Population ", © American Society for Clinical Pathology, DOI: 10.1309/AJCP7HQ2KWGHECIO. Pages 700-707.

[5] Ayad Ghany Ismaeel, Anar Auda Ablahad (2013), "Novel Method for Mutational Disease Prediction using Bioinformatics Techniques and Backpropopagation Algorithm", IRACST- Engineering Science and Technology: An International Journal Vol. 3, No. 1, (ESTIJ), pages 150-156.

[6] Ayad Ghany Ismaeel, Anar Auda Ablahad (2013), "Enhancement of a Novel Method for Mutational Disease Prediction using Bioinformatics Techniques and Backpropagation

Algorithm", INTERNATIONAL JOURNAL OF SCIENTIFIC & ENGINEERING RESEARCH, VOLUME 4, ISSUE 6, JUNE. Pages 1169-1173.

[7] Ayad Ghany Ismaeel (2013), "New Approach for Prediction Pre-cancer via Detecting Mutated in Tumor Protein P53", INTERNATIONAL JOURNAL OF SCIENTIFIC & ENGINEERING RESEARCH, VOLUME 4, ISSUE 10, OCT. Pages 463-468.

[8] GENSCAN Web Server at MIT to find gene under URL: http://genes.mit.edu/GENSCAN.html

[9] France database of TP53 gene (2010), can accessed at URL:http://p53.free.fr/Database/p53_MUT_MAT.html

[10] Analyze Sequence under addgene web server, the URL: http://www.addgene.org/tools/analyze/bd572822b12fc8847c35e013a0f4989d9e9997d3/default/

[11] Thermo Fisher Scientific Inc, © Copyright 2013 URL: http://www.thermoscientificbio.com/.

[12] "CRISPR RGEN Tools/Cas-Analyzer", Website is maintained by Center for Genome Engineering, Institute for Basic Science, Korea. DNA repair systems of several groups at January 2013, and updated at 2015/02/23. See URL: http://www.rgenome.net/cas-analyzer/#!

KJPS Al-Kitab Journal for Pure Science
Vol.2 (2), ISSN: 2617-1260 (print), 2617-8141(online)
www.kjps.isnra.org

DOI: http://10.32441/kjps.02.02.p14

A Comparison of Mammography and Ultrasonography in the Evaluation of Breast Masses in Early Stage

Salwa Sadoon Mustafa Muhammed Naseer Samirah Saadoon Mustafa Warqaa Naseer
salwa_sadoon484@yahoo.com jubory11@yahoo.com samiramustafa77@yahoo.com
dr_warqaa1122@yahoo.com

Abstract

Breasts are one of the secondary sexual characteristics in females. They are the rout for of nutrition & growing of infant till 4-6 months of age.

Breast diseases are one of the most common diseases in the females of any society. Multiple types of benign breast lesions like fibroadenomas, simple cyst, breast abscess, lymph nodes enlargement and different malignancies are common pathologies of the breast.

Up to 30% of women suffer from benign breast disease at any time of their life and this compels them to take the treatment.

The prospective clinical study was achieved for 283 women (age was ranged between 20–60 years) had palpable breast lesion referred by their managing surgeons to the radiological department at Azadi Teaching Hospital, for a period of 8 months (from January 2018 to August of the same year). The study depended firstly in all women on clinical examination/self-breast examination.

Results:- 283 patients were included in this study with age between 20 _ 60 ys, most of the patients were diagnosed as fibroadenoma which is most common around 54.9% of the total cases studied, Fibrocystic diseases (Duct ectasia, cysts, and galactocele) 19.3 %.Followed by infection as mastitis 15.4%, and phyllodes tumor less than 1% approximately and finally carcinoma 9.5%.

KJPS Al-Kitab Journal for Pure Science
Vol.2 (2), ISSN: 2617-1260 (print), 2617-8141(online)
www.kjps.isnra.org

In conclusions, the results of our study are encouraging to applying the US for masses for differentiating if it pointing to benignant or malignancy status and sonography shouldn't be generally applied to defer the biopsy of a solid mass.

Keywords— Ultrasonography, Mammography, Breast Masses.

مقارنة بين التصوير الشعاعي للثدي و الفحص بالموجات فوق الصوتية في الكشف عن كتلة الثدي في مرحلة مبكرة

الخلاصة

الثدي هو احد المميزات او الصفات الجنسية الثانوية للاناث. وهو الوسية لتغذية الطفل الرضيع خلال 4- 6 أشهر الاولى من العمر. امراض الثدي هي احد اكثر الامراض انتشارا لدى الاناث في جميع المجتمعات. هناك انواع متعددة من امراض الثدي منها الحميدة مثل الورم الغدي الليفي, كيس بسيط, خراج الثدي والتهاب العقد اللمفاوية و منها الخبيثة كسرطان الثدي.

30% من النساء تعاني من امراض الثدي الحميدة في اي وقت من حياة المرأة و يجبرها على اخذ العلاج.

يتضمن الفحص السريري , الصور الشعاعية (الفحص بالموجات فوق الصوتية و التصوير الشعاعي للثدي) و الفحص النسيجي الذي يمتاز الآن بدوره الاساسي في تشخيص كتلة (ورم) الثدي.

تم انجاز دراسة استطلاعية ل 283 انثى (بعمر بين 20 الى 60 سنة) لديها كتلة في الثدي وثم احالتها من خلال الجراح المعالج لقسم الاشعة والسونار في مستشفى آزادي التعليمي في مدينة كركوك ولمدة 8 اشهر (من شهر كانون الثاني 2018 الى شهر اب للسنة نفسها) , الدراسة اعتمدت مبدئيا على الفحص الذاتي و الفحص السريري للثدي.

KJPS Al-Kitab Journal for Pure Science
Vol.2 (2), ISSN: 2617-1260 (print), 2617-8141(online)
www.kjps.isnra.org

شملت الدراسة 283 مريضة من عمر 20 الى 60 سنة معظمهم كانو يعانون من ورم غدي ليفي بنسبة 54.9 % من الحالات و مرض الثدي الكيسي الليفي (توسع القنوات الثديية , كيس بسيط و قيلة لبنية) بنسبة 19.3% يتبعها التهاب الثدي 15.4% ثم ورم فايلود (ورم ورقي الشكل) بنسبة اقل من 1% تقريبا وأخيرا سرطان الثدي بنسبة 9.5 %..

خلصت هذه الدراسة الى التشجيع على استخدام الفحص بالموجات فوق الصوتية لتشخيص كتل الثدي و تمييزها ان كانت حميدة أم خبيثة وان الفحص بالموجات فوق الصوتية غير قادر على تشخيص الكتل الصلبة.

1. INTRODUCTION

Breasts are one of the secondary sexual characteristics in females. They are the rout for of nutrition & growing of infant till 4-6 months of age. This tender, sensitive and delicate complex structure is constantly under the influence of hormones.[1]

Multiple types of benign breast lesions like fibroadenomas, simple cyst, breast abscess, lymph nodes enlargement and different malignancies are common pathologies of the breast. [2]

Breast cancer is the commonest cause of malignant mortality in women, while this cancer in males presented only 0.7% of all breast cancer. [3]

Up to 30% of women suffer from benign breast disease at any time of their life and this compels them to take the treatment. Even though the majority of the breast complaints are benign breast disease, compared to malignancy it is a neglected entity. So, an in-depth understanding of its significance and right treatment can be instituted so that long term follow up can be avoided.

The percentage of occurring of benign breast lesions begins to increase during the second decades of life and reached the top between 40 – 60 yrs of age, whereas, in malignant type, the incidence continues to increase after menopause also. [4]

Screening and diagnostic effort:- Triple assessment, includes clinical examination, imaging, and histopathology examination is now presented as a gold standard role in the diagnosis of the breast lump. Early diagnosis and treatment will avoid unnecessary surgery and patient's anxiety of having breast lump as carcinoma will be relieved.

Diagnosis of breast carcinoma in the earliest possible stage is the ultimate goal in imaging the breast, and the role of the radiologist is therefore vital. Radiology mainly includes MG (mammography) and USG (ultrasonography) then the biopsy. The percentage of carcinoma occulting which leading to deaths can be decreased by 30 % by the routine screening of healthy women with mammography. Asymmetry, no density, distortion of fibroglandular content & micro_calcifications are detected earlier than those become clinically palpable, or which are detected by self-examination. [4,5]

Ultrasonography plays an excellent role in differentiating cystic and solid lumps. It is useful in the evaluation of palpable masses not visible radiologically in dense breasts, abscesses, masses that are not completely evaluable with and in a young female who has susception of radiation damage.[6]

Both mammography and ultrasonography methods have been used in attempts to reduce the negative to positive biopsy ratio.[7]

Normal breast parenchymal patterns:-

In the young non-lactating one, the parenchyma primarily consists of fibroglandular tissue, few or no subcutaneous fat. With increasing age and parity, a lot of fat will be deposited in both the subcutaneous and retromammary tissue.

Common abnormal appearances and lesions of the breast: -

Breast cysts: It is the commonest cause of breast masses in women between thirty-five and fifty yrs. this lump occurs when fluid accumulated due to obstruction of the extralobular terminal ducts. It is seen on USG as a well-defined, round or oval, anechoic structure with a thin wall. It may be solitary or multiple [8]

Duct ectasia: This lesion has a variable appearance. Typically, duct ectasia may appear as a single tubular structure filled with fluid or sometimes may show multiple such structures as well. Old cellular debris may appear as echogenic content. If the debris fills the lumen, it can be sometimes mistaken for a solid mass, unless the tubular shape is picked up[5][6]

Chronic abscess of the breast: Patients may present with fever, pain, tenderness to touch and increased white cell count, most commonly located in the central or subareolar area. An abscess may show an ill-defined or a well-defined outline. It may be anechoic or may reveal low-level internal echoes and posterior enhancement.

A variety of inflammatory and reactive changes can be seen in the breast. While some of these changes are a result of infectious agents, others do not have a well-understood etiology and may represent the local reaction to a systemic disease, or a localized antigen-antibody reaction, and are classified as idiopathic.

Fibroadenoma: It is an estrogen-induced tumor that forms in adolescence. It is the third most common breast lesion. It usually presents as a firm, smooth, oval-shaped, freely movable mass It is rarely tender or painful. The size is usually under 5 cm. Calcifications may occur. On USG, it appears as a well-defined lesion. The echotexture is usually homogenous and hypoechoic as compared to the breast parenchyma.[9]

Cystosarcoma phyllodes: It is a big mass or lump which is occurring usually with increasing females 'age. Some consider it as a giant fibroadenoma. It may involve the whole of the breast. Usually appear as well marginated area & an inhomogeneous echostructure, may present with variable cystic lesions. The chance of malignant changing is low.

Malignant lesion: It presents clinically with lesion or mass, retracted nipple, pain & discharge of blood, ulceration over breast skin. these lesions on MG appear irregular lump, speculated or lobulated margins, focal, asymmetry, the lesion appears longer than wider, the nipple is retracted, calcification may be linear, granular, clustered with surrounding architectural distortion.[3]

Various limitations of mammography (MG) and ultrasonography (USG):- In mammography, Solid & cystic lesions can't be differentiated, intracystic lesions cannot be detected in young one has dense fibroglandular tissue with obscure masses, mastitis may mask the margins of a lump benign lump appears malignant & overlapping structures some time limit complete visualization of a mass abscess and tuberculosis may mimic carcinoma.

In ultrasonography, Operator dependent, isoechoic masses may be missed mostly when are small, circumscribed carcinoma may be labeled as benign masses, lesions within large fatty breasts are difficult to diagnosis.[5]

2. AIM OF WORK

1. To study the accuracy of ultrasonography & mammography separately and in combination for diagnosis of breast lesions (correlation between them) and association of the age with the suitable device.

2. To confirm the combining ultrasound with the mammogram to increase the cancer detection rate in early stages.

3. Patients and methods

The prospective study was achieved for 283 women (age range was 20–60 years) had palpable breast lesion referred by their managing surgeons to the radiological department at Azadi Teaching Hospital, for the period of 8 months (from January 2018 to August of the same year). Study depended firstly in all women on clinical examination/self-breast examination. All US examinations were performed with the type of ultrasonography, siemens versa with a 7-MHz linear-array transducer& mammography type BP34 78533 BUC CEDEX-FRANCE.

If we had adopted about any cases, referred to fine needle aspiration and biopsy and wait for the result to confirm the diagnosis.

Inclusion criteria *:*

All patients with clinically palpable lump; no obvious mass on palpation but prominent axillary nodes and those have signs of redness over the breast, dryness, nipple retraction, discharge or shape changing.

Exclusion criteria

Cases with any obvious cancer or previous biopsy has proven malignant diseases which had b treated for malignancy earlier or operated were excluded.

4.RESULTS & DISCUSSION:

A total of 283 patients were included in this study with age between 20 _ 60 ys, most of the patients were diagnosed a fibroadenoma which is most common around 54.9%of the total cases studied, Fibrocystic diseases (Duct ectasia, cysts, and galactocele) 19.3 %. Our study was consistent with the study done by Shilpa N et al[11]and Mallikarjuna et al[12] ;Shilpa N et al[11] reported 55.68% fibroadenoma followed by fibroadenosis 20.45% cases and Mallikarjuna et al. [12] reported 72% cases of fibroadenoma with about 13% in Malik MAN et al.[13] Followed by infection as mastitis15.4%, and phyllodes tumor less than 1% approximately similar to Malik MAN et al.[13]which was 0.4% and dislike with Dr. GolamSarwar's study[14] which was 8%; finally carcinoma 9.5%.

KJPS Al-Kitab Journal for Pure Science
Vol.2 (2), ISSN: 2617-1260 (print), 2617-8141(online)
www.kjps.isnra.org

Table 1 was represented 107 patients between 20 _30 ys were most of them had Fibroadenoma then Infection; Mastitis, a fibrocystic disease similar to *Selvakumaran S et al.* [4] study and two cases had carcinoma.

Table 1:- The relation between patients 'age and types of lesion.

Type of lesion	Age Group (years)	Infection ; Mastitis 44	Fibrocystic disease 53	Fibroadeno -ma 158	Phylloids tumour 2	Carcinoma 26	Total 283
No. of patients	20 - 30	24	6	75	-	2	107
	30 - 40	16	23	60	1	6	106
	40 - 50	4	20	18	1	10	53
	50 - 60	-	4	5	-	8	17

While between 30_40 is mainly also had Fibroadenoma but the fibrocystic disease was more than the first category and less had Infection, our results similar proximity to similar to *Selvakumaran S et al.* [4] and Dr. GolamSarwar's study[14]; with 2& 6 cases of carcinoma respectively in both age. By age of 30_40, 40 _50 & 50_60 ys, this table is shown decrease incidence of benign masses but unfortunately, the bad news is increasing the incidence of malignant lesion out of 6, 10 & 8 cases respectively; this gone with Chlebowski et al & ABMZ Sadik et al[16]studies.

Table 2: USG & MG finding in diagnosis various types of breast lesion with comparative analysis

Types of lesion	No. Of Cases	USG Alone	Mammography Alone	Combined
infection;mastitis	44	42 (95%)	36 (82%)	44 (100%)
Fibrocystic disease	53	53(100%)	28(52%)	53(100%)
Fibroadenoma	158	91(58%)	128(81%)	150(96%)
Phyllodes a tumor	2	1 (50%)	2 (100)	2 (100%)
Carcinoma	26	16 (70%)	24 (89%)	25 (96%)
Total	283	247	194	281

In table 2 this study revealed 26 patients diagnosed as carcinoma where the MG detected 24 (89%) like K. TAORI *ET AL.*[3]studies who said(Mammography is nearly 87% accurate in detecting cancer)& USG alone detected only 16(70%), as same as Stavros *et al.*[17] who found overall accuracy of 72.9% but dislike with P.K. Tiwari et al· [7]study in which (22.22%) only diagnosed cancer in USG it may be because ultrasounds are unable to detect microcalcifications (small mineral deposits in the breast that indicate the possibility of malignancy)[18], while combined of them missed only one case which confirmed by fine needle aspiration..Out of 44 cases of fibrocystic mastitis, MG alone picked 36 whereas the USG missed only 2 and combined way detected 100% of cases. There were 55 cases of the cyst, which was clearly 100% detected byUSG, but the MG picked up only 28. Of 156 cases of fibroadenoma, the MG detected 128 and the USG detected 91 with combined test missed only 6 cases. Finally, 2 cases of phyllodes tumor diagnosed, 1 by USG while both cases detected by MG successfully

In the general US can diagnose approximately two-thirds of a benign solid breast mass and distinguish from malignant one, the result goes with dr. Osamah Ayad study. [19]

All these results make understanding that the value of combined mammographic and sonographic imaging in symptomatic patients very high which reached 100% in some types of lesion, but is not 100 % sensitive and specific that similar to P.K. Tiwari et al study. [7]

5. Conclusions and Recommendations

In conclusions, the results of our study are encouraging to applying the US for masses for differentiating if it pointing to benign or malignancy status and sonography should not be generally applied to defer the biopsy of a solid mass.

We suggest further studies that include a larger number of cases, a longer period of study.

We recommend making use of biopsies (Fine Needle Aspiration and True-cut) in adopt breast mass

Breast imaging inves should be encouraged and make it a routine screen, available countrywide in order to reduce cancer mortality especially in older women

References

[1] Clarke D, Sudhakaran N. Replace fine needle aspiration cytology with automated core biopsy in the triple assessment of breast cancer. Ann R Coll Surg Engl 2001; 83:110–2.

[2] Schoonjans JM, Brem RF. Fourteen-gauge ultrasonographically guided large-core needle biopsy of breast masses. J Ultrasound Med 2001; 20:967.

[3] Kishor Taori, Suresh Dhakate, Jawahar Rathod, Anand Hatgaonkar, Amit Disawal, Prasad Wavare, Vishal Bakare, Rakhi P. Puria. "Evaluation of Breast Masses Using Mammography and Sonography as First Line Investigations," Open Journal of Medical Imaging, Vol. 3 No. 1, 2013, pp. 40-49.

[4] Selvakumaran S, Sangma MB. “Study of various benign breast diseases”. Int Surg J 2017;4:339-43.

[5] Sachin Prasad N, Dana Houserkova. Comparison of mammography and ultrasonography in the evaluation of breast masses. 2007, 151(2):315–322

[6] Wendie A. Berg, Lorena Gutierrez, Moriel S. Ness River, W. Bradford Carter, Mythreyi Bhargavan, Rebecca S. Lewis, and Olga B. Ioff. Diagnostic Accuracy of mammography,

Clinical Examination, US, and MR Imaging in Preoperative Assessment of Breast Cancer; Radiology. 2004;233:830- 49.

[7] P.K. Tiwari, Suvendu Ghosh, V K Agrawal. Diagnostic accuracy of mammography and ultrasonography in the assessment of breast cancer. International Journal of Contemporary Medical Research 2017;4(1):81-83.

[8] Howlett DC, Marchbank NDP. Sonographic assessment of symptomatic breast.J Diagnostic Radiography & Imaging. 2003;5:3–12

[9] Zhi H, Ou B, Luo BM, Feng X, Wen YL, Yang HY. Comparison of Ultrasound Elastography, Mammography, and Sonography in the Diagnosis of Solid Breast Lesions. J Ultrasound Med. 2007;26:807–15.

[10] Donegan WL. Common benign conditions of the breast. In: Donegan WL, Spratt JS, eds. Cancer of the Breast, Fifth Edition. St. Louis, MO: Saunders,2002:67–110.

[11] N Shilpa and SH Shridevi. Cytological Correlation of Benign Breast Diseases with Histopathology. jmscr, 2016;04:13256-13259.

[12] Mallikarjuna and Maralihalli S. Clinicopathological study of benign breast disease" Indian Journal of Basic and Applied Medical Research 2015;4:39-46.

[13] Malik MAN, Salahuddin O, Azhar M, Dilwar O, Irshad H, et al. Breast disease; spectrum in Wah Cantt; POF hospital experience. Professional Med J 2010;17:366-72.

[14] Dr. GolamSarwar, Dr. SnehansuPan, "Benign Breast Lump-Value of Age and FNAC. "IOSR Journal of Dental and Medical Sciences (IOSR-JDMS), vol. 17, no. 5, 2018, pp 14-17

[15] Rowan T. Chlebowski and Garnet L. Anderson. Menopausal hormone therapy and breast cancer mortality: clinical implications. Ther Adv Drug Saf. 2015 Apr; 6(2): 45–56.

[16] ABM Sadik, MM Hasan, HEZA Haque, FU Ahmed, MZ Kabir. Different Types of Breast Lump in Relation to Different Age Groups. Faridpur Med. Coll. J. 2013;8(2):56-58

[17] A. T. Stavros, D. Thickman, C. L. Rapp, M. A. Dennis, S. H. Parker, and G. A. Sisney, “Solid Breast Nodules: Use of Ultrasonography to Distinguish between Benign and Malignant Lesions,” Radio123_134.

[18] Elmore JG, Armstrong K, Lehman CD, Fletcher SW. Screening for breast cancer. JAMA. 2005 Mar 9;293(10):1245-56.

[19] Osamah Ayad Abdulsattar. The validity of Sonography in distinguishing benign solid breast mass from malignant. AL-Qadisiya Medical Journal 2015, Vol.11 No.19.Howlett DC, Marchbank NDP. Sonographic assessment of symptomatic breast.J Diagnostic Radiography & Imaging. 2003;5:3–12

KJPS Al-Kitab Journal for Pure Science
Vol.2 (2), ISSN: 2617-1260 (print), 2617-8141(online)
www.kjps.isnra.org

DOI: http://10.32441/kjps.02.02.p15

Seroprevalence of Human Papilloma Virus in Aborted Women in Kirkuk City

[1*] Jacklen Zaea khoshaba, [2] Salwa Sadoon Mustafa, [3] Muhannad Abdulla Alazzawy,
[1,2,3] Kirkuk Health Directorate, Kirkuk, Iraq
[1]Jaklen_khoshaba@yahoo.com, [2]salwa_sadoon484@yahoo.com

ABSTRACT

The aimed of the study was to evaluate the Seroprevalence of human papilloma virus (HPV) in aborted women. A cross-sectional study was carried out in Kirkuk city from 10th of March 2017 to 10th of July 2017 . The number of aborted women understudy were 65 women who attended for curettage in Kirkuk general hospital. The control group who were matched to the patients studied included 30 normal pregnant women at the full term of pregnancy, women with *Toxoplasma gondii*, rubella and cytomegalovirus infections were excluded from the study. Five ml of blood was collected by vein puncture from each woman in the study, the obtained sera then organized to determine of HPV 16 E7 protein in patients and control using ELISA technique.

The study showed that the highest rate of HPV infection (35.38%) was recorded among women with abortion comparing with the control group, with a highly significant relation. The study showed that 75.38% of women had aborted in the 1st trimester of pregnancy and the lowest rate of abortion 9.24% was in the 3rd trimester. The study showed that the highest rate of HPV infection was found in women with 1st trimester of abortion (38.78%) and the lowest rate was in the 3rd trimester of abortion. The study showed that the highest rate of HPV infection was recorded among aborted women who have suffered from one abortion during their marriage life.

It was concluded that there was a significant relation of HPV with abortion spatially in women who were aborted in the first trimester of pregnancy.

Keywords: HPV; Seroprevalence; abortion; Kirkuk.

KJPS Al-Kitab Journal for Pure Science
Vol.2 (2), ISSN: 2617-1260 (print), 2617-8141(online)
www.kjps.isnra.org

الانتشار المصلي لفيروس الورم الحليمي البشري في النساء المجهضات في مدينة كركوك

جاكلين زيا خوشابا سلوى سعدون مصطفى مهند عبدالله العزاوي

دائرة صحة محافظة كركوك

الخلاصة

الهدف من هذه الدراسة هو تقييم الانتشار المصلي لفيروس الورم الحليمي البشري (HPV) في النساء المجهضات. أجريت دراسة مقطعية مستعرضة في مدينة كركوك من 10 مارس 2017 إلى 10 يوليو 2017. وكان عدد النساء اللاتي تم إجهاضهن من النساء 65 امرأة اللواتي شاركن في التجريف في مستشفى كركوك العام. شملت المجموعة الضابطة التي تمت مقارنتها مع المرضى ، 30 امرأة حوامل عاديات في فترة الحمل الكاملة ، وتم استبعاد النساء المصابات بمرض داء القطط Toxoplasma gondii ، والحصبة الألمانية ، والعدوى بفيروس المضخم للخلايا من الدراسة. تم جمع خمسة مل من الدم عن طريق ثقب في الوريد من كل امرأة في الدراسة ، تم الحصول على الأمصال التي تم الحصول عليها بعد ذلك لتحديد البروتين HPV 16 E7 في المرضى والتحكم باستخدام تقنية ELISA.

وأظهرت الدراسة أن أعلى معدل للإصابة بفيروس الورم الحليمي البشري (35.38 ٪) تم تسجيله بين النساء اللواتي يعانين من الإجهاض مقارنة بالمجموعة الضابطة ، مع وجود علاقة ذات أهمية كبيرة. أظهرت الدراسة أن 75.38٪ من النساء تم إجهاضهن في الثلث الأول من الحمل وأن أقل معدل للإجهاض كان 9.24٪ في الربع الثالث من الحمل. وأظهرت الدراسة أن أعلى معدل للإصابة بفيروس الورم الحليمي البشري تم العثور عليه في النساء ذوات الثلث الأول من الإجهاض (38.78٪) وأدنى معدل في الثلث الثالث من الإجهاض. وأظهرت الدراسة أن أعلى معدل من عدوى فيروس

KJPS Al-Kitab Journal for Pure Science
Vol.2 (2), ISSN: 2617-1260 (print), 2617-8141(online)
www.kjps.isnra.org

الورم الحليمي البشري تم تسجيله بين النساء اللاتي تعرضن للإجهاض اللائي عانين من إجهاض واحد خلال فترة زواجهن.

وخلص إلى أن هناك علاقة كبيرة بين فيروس الورم الحليمي البشري والإجهاض مكانيا في النساء اللواتي اجهضن في الأشهر الثلاثة الأولى من الحمل.

الكلمات الرئيسية: فيروس الورم الحليمي البشري ؛ الانتشار المصلي. الإجهاض؛ كركوك.

1. Introduction

Recurrent miscarriage, habitual abortion, or recurrent pregnancy loss (RPL) is three or more consecutive pregnancy losses [1]. Infertility differs because it is the inability to conceive. In many cases the cause of RPL is unknown. Recurrent miscarriage (RM) is defined as the occurrence of three or more consecutive losses of pregnancy. According to this definition, it affects about 1% of couples trying to have a baby [2]. However, many clinicians define RM as two or more losses; this increases the percentage of RM from 1% to 5% of all couples trying to conceive [3]. Mammalian pregnancy is thought to be a state of immunological tolerance. The mechanisms underlying this phenomenon are still poorly understood, successful mammalian pregnancy depends upon the tolerance of a genetically incompatible fetus by the maternal immune system. When tolerance is not achieved pregnancies fail [1].

Human papillomavirus (HPV) is a viral infection that is passed between people through skin-to-skin contact. There are more than 100 varieties of HPV, 40 of which are passed through sexual contact and can affect your genitals, mouth, or throat [4]. Human Papillomavirus (HPV), which is known as a well-established cause for cervical cancer, does though constitute a candidate. The over 180 known HPV-types are small, double-stranded DNA viruses with a circular genome of nearly 8,000 base pairs [5]. HPV infections are common, but about 90% of all infections can be cleared within less than 2 years by unknown

mechanisms [6]. HPV-6 and HPV-11 are the most common low-risk types and are found to be causative for genital warts [4]. Cancer associated high-risk types include HPV-16 and HPV-18 [5] and there is growing evidence of HPV infections playing a relevant role in other anogenital and head and neck cancers [7]. Worth to mention is also the morbidity of cutaneous HPV lesions, particularly in immunosuppressed people [8]. There is some evidence that elevated steroid hormone levels during pregnancy influence the increase of HPV virus replication by interacting with hormone response elements in the viral genome, thereby giving another possible explanation for the higher incidence of HPV infection during pregnancy [9, 10].

2. Material and methods

A cross-sectional study was carried out in Kirkuk city from 10th of March 2017 to 10th of July 2017 . The number of aborted women understudy were 65 women who attended for curettage in Kirkuk general hospital). Included 30 normal pregnant women at the full term of pregnancy, women with *Toxoplasma gondii*, rubella and cytomegalovirus infections were excluded from the study.

2.1. Methods

Five ml of blood was collected by vein puncture from each woman in the study, the obtained sera then organized to determine of HPV 16 E7 protein in patients and control using ELISA technique.

2.2. Statistical analysis:

Computerized statistically analysis was performed using IBM SPSS ver 23.1 statistic program. A comparison was carried out using Chi-square (X^2). The *P*. value <0.05 was considered statistically significant, and for the result which its *P*. value *was* less than 0.01 was considered highly significant, while for those which its *P*. value was greater than 0.05 considered non-significant statistically.

KJPS Al-Kitab Journal for Pure Science
Vol.2 (2), ISSN: 2617-1260 (print), 2617-8141(online)
www.kjps.isnra.org

3. Results

Table 1 show that the highest rate of HPV infection (35.38%) was recorded among women with abortion comparing with the control group, with a highly significant relation.

Table 1: Seroprevalence of HPV in aborted and pregnant women.

HPV 16 E7 -ELISA	Aborted women		The control group (pregnant women)		P. value
	No.	%	No.	%	
Positive	23	35.38	3	10	0.0091
Negative	42	64.61	27	90	
Total	65	100	30	100	

Table 2 shows that 75.38% of women had aborted in the 1st trimester of pregnancy and the lowest rate of abortion 9.24% was in the 3rd trimester.

Table 2: Distribution of aborted women according to trimester of pregnancy

Trimester of abortion	HPV positive result	
	No.	%
1st trimester	49	75.38
2nd trimester	10	15.38
3rd trimester	6	9.24
Total	65	100

The study showed that the highest rate of HPV infection was found in women with 1st trimester of abortion (38.78%) and the lowest rate was in the 3rd trimester of abortion, Table 3.

Table 3: Distribution of HPV positive result according to trimester of abortion.

Trimester of abortion	Total No.	HPV positive result	
		No.	%
1st trimester	49	19	38.78
2nd trimester	10	3	30
3rd trimester	6	1	16.67

KJPS Al-Kitab Journal for Pure Science
Vol.2 (2), ISSN: 2617-1260 (print), 2617-8141(online)
www.kjps.isnra.org

Figure 1 shows that the highest rate of HPV infection was recorded among aborted women who have suffered from one abortion during their marriage life.

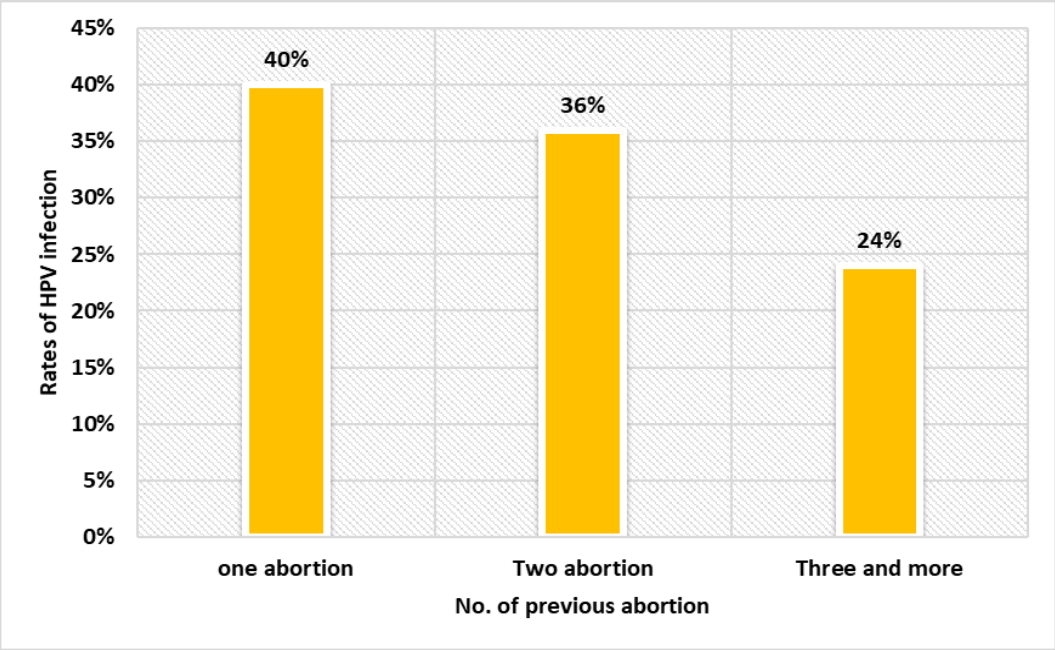

Figure 1: Distribution of aborted women according to number of abortions.

4. Discussion:

In comparison to HPV prevalence found in normal pregnancies and spontaneous abortions and were found to have higher HPV positive detection rates ($P < 0.01$). Pregnancy has previously proven to be a state of mild immunosuppression due to the decrease in the number of natural killer cells [11], possibly making pregnant women more prone to infections with, for example, HPV. Various immunological theories have been discussed to explain the possibility for pregnancy and the survival of the "semiallogeneic" fetus. Theories include immunological privilege in the uterus, antigenic immaturity of the fetus, and maternal Also there is some evidence that elevated steroid hormone levels during pregnancy influence the increase of HPV virus replication by interacting with hormone response elements in the viral genome, thereby giving another possible explanation for the higher incidence of HPV infection during pregnancy [12]. In 2014, Liu *et al.* [13]

conducted a systematic review on HPV prevalence in pregnant and nonpregnant women and reported an increased risk of HPV infection in pregnant women, thereby supporting the debate of how far HPV may be involved in adverse pregnancy outcomes. Various authors report infection with HPV during pregnancy to be associated with the risk of spontaneous abortion, spontaneous preterm delivery, and placental abnormalities [14-16]. However, it can be stated that studies from the USA consistently report a significantly higher HPV prevalence in spontaneous abortions and spontaneous preterm deliveries compared to normal pregnancies, in both cervical and placental tissue [15, 17, 18]. The result of the current study was supported by several studies done earlier. Carlson *et al* [19] and Yong *et al* [20] presented that women who suffer from spontaneous abortion are in 1st trimester and 2nd trimester while some of the women were multigravida had a previous stillbirth, preterm birth, multiple birth, and previous miscarriage. Chetty *et al* [21] demonstrated a significant relation of abortion number with women investigated with a previous miscarriage. Strobino *et al* [22] found that 38% of women with abortion were aborted two times due to infections. In theory, either fetal or maternal pathology could lead to recurrent spontaneous abortions [23]. Several studies demonstrated that women with repeated abortion were more likely to have chromosomally normal rather than chromosomally abnormal losses and the usual causes were maternal infection [24-26].

5. Conclusions:

It was concluded that there was a significant relation of HPV with abortion spatially in women who were aborted in the first trimester of pregnancy.

6. References.

[1] Y. H. Li and A. Marren, ***"Recurrent pregnancy loss"***, Australian J General Pract, 47(7), 43 (2018).

[2] A. M. Quaas, ***"Infertility and Recurrent Pregnancy Loss"***, Glass' Office Gynecology, 2014:12(1),205(2014).

[3] A. Bashiri, A. Harlev and A. Agarwal, ***"Recurrent pregnancy loss. Evidence-based evaluation, diagnosis and treatment",*** Switzerland: Springer International Publishing (2016).

[4] R. Wang-Shick, ***"Molecular Virology of Human Pathogenic Viruses",*** 1st ed, London Wall, London EC2Y 5AS, UK Academic Press is an imprint of Elsevier, 221 (2017).

[5] J. Louten, ***"Essential Human Virology"*** 2nd ed, London Wall, Elsevier Inc, (2016).

[6] M. W. Taylor, ***"Viruses and Man: A History of Interactions"***, 1st ed, Springer International Publishing. New York, 90 (2016).

[7] J. E. cLudert H. A. Flor, F. A. Pujol and J. M. Arbiza, ***"Human Virology in Latin America From Biology to control",*** 1st ed, Springer International Publishing, Switzerland, 10 (2017).

[8] H. U. Bernard, R. D. Burk, Z. Chen, K. van Doorslaer, H. Z. Hausen, and E. M. de Villiers, ***"Classification of papillomaviruses (PVs) based on 189 PV types and proposal of taxonomic amendments",*** Virology, 401(1), 70 (2010).

[9] J. Doorbar, ***"The papillomavirus life cycle",*** Journal of Clinical Virology, 32, 7 (2005).

[10] P. Aggarwal, ***"Cervical cancer: can it be prevented?"*** World Journal of Clinical Oncology,5(4), 775(2014).

[11] E. D.Weinberg, **"Pregnancy-associated depression of cell-mediated immunity",** Reviews of Infectious Diseases, 6 (6), 814(1984).

[12] C. Worda, A. Huber and G. Hudelist, ***"Prevalence of cervical and intrauterine human papillomavirus infected in the third trimester in asymptomatic women",*** Journal of the Society for Gynecologic Investigation, 12 (6), 440 (2005).

[13] P. Liu, L. Xu, Y. Sun, and Z. Wang, "***The prevalence and risk of human papillomavirus infection in pregnant women",*** Epidemiology & Infection, 142(8), 1567 (2014).

[14] L. M. Gomez, Y.Ma, C. Ho, C. M. McGrath, D. B.Nelson, and S. Parry, ***"Placental infection with human papillomavirus is associated with spontaneous preterm delivery",*** Human Reproduction, 23(3), 709(2008).

[15] Z. Zuo, S. Goel, and J. E. Carter, ***"Association of cervical cytology and HPV DNA status during pregnancy with placental abnormalities and preterm birth"***, American Journal of Clinical Pathology, 136 (2), 206 (2011).

[16] M. Rabreau and J. Saurel, ***"Presence of human papilloma viruses in the deciduous membranes of early abortion products"***, La Presse medicale, 26, 1724 (1997).

[17] Y. H. Kim, J. S. Park and E. R. Norwitz, ***"Genotypic prevalence of human papillomavirus infection during normal pregnancy: a cross-sectional study"***, Journal of Obstetrics and Gynaecology Research, 40(1), 200 (2014).

[18] B. Xiong and A. Yi-Quan, ***"The Risk of Human Papillomavirus Infection for Spontaneous Abortion, Spontaneous Preterm Birth, and Pregnancy Rate of Assisted Reproductive***

Technologies: A Systematic Review and Meta-Analysis", Gynecologic and obstetric investigation, 136 (2), (2018).

[19] E. Carlson and M. Mourgova, ***"Demographic consequences of social inequality in pregnancy outcomes",*** Genus, 20(3), 11(2003).

[20] C. Yong, F. Wang and F. Famine, ***"Social Disruption, and Miscarriage: Evidence from Chinese Survey Dat, Center for Studies in Demography and Ecology***", (CSDE) Working Paper (2006).

[21] M. Chetty and W. Duncan, ***"A clinical approach to recurrent pregnancy loss"*** Obstetrics, Gynaecol Reprod Med,12(5),113 (2018).

[22] G. A. Abdullah and N. K. Mahdi, ***"The Role of Cytokines among Women with Spontaneous Miscarriage***", Med J Islamic World Acad of Sc, 21(3), 119(2015).

[23] C. Garrido-Gimenez and J. Alijotas-Reig, ***"Recurrent miscarriage: causes, evaluation and management",*** Post Med J, 91(1073), 151(2015).

[24] J. A. Keelan and m. S. Payne, ***"Vaginal microbiota during pregnancy: Pathways of risk of preterm delivery in the absence of intrauterine infection?",*** Proceed Nat Acad Sc 2015;112(47): 6414-.6421.

[25] F. R. Helmo, E. A. Alves and R. A. Moreira RA***, "Intrauterine infection, immune system and premature birth***', J Maternal-Fet Neonat Med , 31(9),1227(2018).

[26] R. Catalano, T. Bruckner, D. Karasek, N. Adler and L Mortensen, "***Shared risk aversion in spontaneous and induced abortion"***, Human Rep, 31(5),1113 (2016).

KJPS Al-Kitab Journal for Pure Science
Vol.2 (2), ISSN: 2617-1260 (print), 2617-8141(online)
www.kjps.isnra.org

DOI: http://10.32441/kjps.02.02.p16

بناء نظام خبير للتحويل التلقائي لمرحلة تطوير البرمجيات

د.صفوان عمر حسون[1] ، فاطمة محمدرافع يونس

[1] قسم هندسة البرمجيات، كلية علوم الحاسوب والرياضيات، جامعة الموصل، موصل، العراق.

[1] Dr.safwan1971@yahoo.com

الملخص

نتيجة للتطور الحاصل في مجالات الحاسوب ولاسيما في مجال هندسة البرمجيات، ظهرت الحاجة إلى بناء أداة ذكية لتحويل التلقائية من مرحلة التصميم إلى مرحلة البرمجة، لانتاج الشفرة المصدرية من نموذج الخوارزمية المتمثلة بالرمز الزائف، وتنفيذها بالاعتماد على بناء نظام خبير مما يقلل من الكلفة والوقت المستغرق والأخطاء التي قد تحصل أثناء عملية التحويل، حيث تمت بناء قاعدة المعرفة، ومحرك الاستدلال، وواجهة المستخدم، وتتكون قاعدة المعرفة من الحقائق والقواعد لعملية التحويل التلقائي، وقورنت النتائج مع مجموعة من الشبكات العصبية وهي الشبكة العصبية ذات التغذية الأمامية، والشبكة العصبية المتتالية، و شبكة دالة القاعدة الشعاعية، وظهرت النتائج تفوق النظام الخبير من ناحية سرعة عملية التحويل التلقائي، وكذلك سهولة عملية اضافة، حذف، او تعديل القواعد او البيانات للرمز الزائف مقارنتا مع الشبكات العصبية المذكورة سابقا.

الكلمات الدالة: الشبكات العصبية, الانظمة الخبيرة, الانظمة الذكية.

KJPS Al-Kitab Journal for Pure Science
Vol.2 (2), ISSN: 2617-1260 (print), 2617-8141(online)
www.kjps.isnra.org

Constructing Expert System to Automatic Translation for Software development

Dr. Safwan Omar Hasoon[1] Fatima Mohammed Rafie Younis

[1]Department of Software Engineering, College of Computer Sciences and Mathematics, Mosul University, Mosul, Iraq.

[1]Dr.safwan1971@yahoo.com

ABSTRACT

the development in computer fields, especially in the software engineering, emerged the need to construct intelligence tool for automatic translation from design phase to coding phase, for producing the source code from the algorithm model represented in pseudo code, and execute it depending on the constructing expert system which reduces the cost, time and errors that may occur during the translation process, which has been built the knowledge base, inference engine, and the user interface. The knowledge bases consist of the facts and the rules for the automatic transition. The results are compared with a set of neural networks, which are Back propagation neural network, Cascade-Forward network, and Radial Basis Function network. The results showed the superiority of the expert system in automatic transition process speed, as well as easy to add, delete or modify process for rules or data of the pseudo code compared with previously mentioned neural networks.

1. المقدمة

هندسة البرمجيات هو انضباط يهدف إلى إنتاج برنامج خالٍ من الأخطاء، يسلم البرنامج في الوقت المناسب وضمن الميزانية المحددة، الذي ترضي احتياجات الزبون. فضلاً عن ذلك، فإن البرنامج يجب أن يكون سهل التغير على وفق تغير احتياجات الزبون [1].

دورة حياة تطوير البرمجيات هي عملية تطوير البرمجيات، وهذه العملية تنقسم إلى عدة مراحل ومنها مرحلة التصميم ومرحلة الترميز[2].

KJPS Al-Kitab Journal for Pure Science
Vol.2 (2), ISSN: 2617-1260 (print), 2617-8141(online)
www.kjps.isnra.org

في هذا البحث تم استخدام تقنية ذكائية من خلال بناء نظام خبير يحوي على قاعدة معرفة مؤلفة من مجموعه من القواعد والقوانين التي تصف عملية تطوير البرمجيات وتحويل الخوارزمية المتمثلة بالرمز الزائف الى شفرة مصدرية بشكل تلقائي.

2.الجزء النظري

1. مرحلة التصميم

تقع مرحلة التصميم في قلب تقانة عملية هندسة البرمجيات [3]. وهي المرحلة الاكثر ابداعا في دورة حياة هندسة البرمجيات [2]. الهدف من مرحلة التصميم هو تصميم الحل استنادا الى متطلبات المحددة والقرارات المتخذة في مرحلة التحليل. يقسم التصميم الى تصميم المستوى العالي: وهو تكوين الهيكلية المعمارية لأجزاء مكونات البرنامج وقاعدة البيانات وواجهة المستخدم وبيئة التشغيل للبرنامج. والتصميم المستوى المنخفض: يتم توضيح تفاصيل الخوارزميات وهياكل البيانات المطلوبة لتطوير البرنامج [4].

بدون تصميم، فإننا نخاطر في بناء نظام غير مستقر– ومن هذه المخاطر قد يفشل النظام عند إجراء تغييرات صغيرة عليه؛ وقد يكون من الصعب الاختبار؛ والنوعية لا يمكن تقييمها حتى وقت متأخر في عملية هندسة البرمجيات [3]. وتشير مرحلة التصميم إلى مجموعة من النشاطات التي تتضمن تحديد الخوارزمية لكل مكون يتكون منه البرنامج [5]. ويجب تعريف تفاصيل الخوارزمية لكل مكون، وغالباً ما يتم ذلك عن طريق الرمز الزائف [6].

في قلب تصميم برنامج الحاسوب هناك هدفان [7]:

1. تصميم خوارزمية تكون سهلة الفهم، والترميز، والاختبار.
2. تصميم الخوارزمية التي تحسن من استخدام مصادر الحاسوب.

توجد مجموعه من الطرائق لتصميم الخوارزمية ومنها المخطط الانسيابي والرمز الزائف، في هذا البحث تم استخدام طريقة الرمز الزائف لتمثيل مرحلة تصميم البرامج.

KJPS Al-Kitab Journal for Pure Science
Vol.2 (2), ISSN: 2617-1260 (print), 2617-8141(online)
www.kjps.isnra.org

2-1 الرمز الزائف

الرمز الزائف هو أحد طرائق تصميم البرامج [8]. ويعد طريقة واضحة لتمثيل الخوارزمية [9]. لأنه يعد سهل القراءة والكتابة ويسمح للمبرمج التركيز على منطق المشكلة [10]. وهي لغة شكلية (غير رسمية) [11]، ويستعمل بشكل واسع جدا وفي بعض الأحيان يظهر تحت عناوين أخرى [12] مثلاً يدعى بلغة تصميم برنامج (PDL) Program Design Language أو هيكلية الإنجليزية Structured English [3]، ولكن يعرف بسهولة، حتى عندما يختفي وراء مثل هذه العناوين [12]. ويشبه لغات البرمجة العالية المستوى كالجافا (Java) أو سي (C) والخ [9]. إذ يدمج الهيكل المنطقي (السلسلة، والاختيار، والحلقة) للغة البرمجة مع القدرة على التعبير بشكل حر للغة الطبيعية (على سبيل المثال، اللغة الإنجليزية). يكون جزء منها لغة انكليزية والجزء الاخر الهيكل المنطقي [13]، ويعتبر الرمز الزائف "الام" لكل لغات البرمجة [9]. لم يتفق علماء الحاسوب أبداً على نموذج واحد للرمز الزائف، ويترك المؤلفون تصاميم خاصة بهم "اللهجات". لحسن الحظ هذه اللهجات قريبة جداً من بعضها البعض، وأي شخص مطلع على لغات البرمجية الحديثة يجب أن يكون قادراً على فهمها جميعاً [14]. الرمز الزائف يستخدم على نطاق واسع جداً، كالمستوى المنخفض من التجريد، فإن توفير مستوى التجريد مهم؛ لأنه يسمح للمصمم التفكير في تسلسل مفصل للحل، في حين ما زالت بعيدة عن أشكال تفصيلية من الحل. ومع ذلك، من أجل القيام بذلك على نحو فعال، فإنه من الضروري ضمان أن لا يصبح الرمز الزائف كثيراً مثل لغة البرمجة [12].

2-2-1 فوائد الرمز الزائف ومساوئه

إن فوائد الرمز الزائف ومساوئه يمكن تلخيصها على النحو الآتي [15]:

الفوائد:

1. تحويل الرمز الزائف إلى لغة البرنامج أسهل بكثير مقارنة مع تحويل المخطط الانسيابي.
2. مقارنة مع المخطط الانسيابي، فمن الأسهل تعديل الرمز الزائف لمنطق البرنامج حينما تبرمج التعديلات الضرورية.
3. كتابة الرمز الزائف يتضمن وقتاً وجهداً أقل بكثير من المخطط الانسيابي المكافئ.

KJPS Al-Kitab Journal for Pure Science
Vol.2 (2), ISSN: 2617-1260 (print), 2617-8141(online)
www.kjps.isnra.org

4. الرمز الزائف هو أسهل في الكتابة من كتابة برنامج بلغة البرمجة؛ لأن الرمز الزائف كطريقة لديه عدد قليل من القواعد الواجب اتباعها.

المساوئ:

1. في حالة الرمز الزائف، صورة تخطيطية لمنطق البرنامج ليست متوافرة كما هو الحال مع مخططات انسيابية.
2. ليس هناك معيار للإتباع في استعمال الرمز الزائف، إذ يستعمل المصممون أسلوبهم الخاص لكتابة الرمز الزائف, وبالتالي تحدث مشاكل الاتصال بسبب قلة توحيد المقياس.
3. بالنسبة للمبتدئ، فان استعمال الرمز الزائف يعد أكثر صعوبة لاتباعه المنطق بالمقارنة مع المخطط الانسابي.

3. مرحلة التنفيذ

يطلق على مرحلة التنفيذ أيضا الترميز (coding) [12]. يتم كتابة التعليمات البرمجية الحقيقية في هذه المرحلة. أي كتابة الشفرة المصدرية (source code) بلغة برمجية معينة. والغرض من البرمجة هو إنشاء الشفرة المصدرية يؤدي السلوك المطلوب الذي انشئ البرنامج من أجله [16]. تشير مرحلة التنفيذ إلى طلب مجموعة من النشاطات لإكمال البرنامج وينفذ بشكل صحيح على الحاسوب، يستطيع أي شخص أن يستعمله ومن هذه النشاطات هو تحويل الخوارزمية لحل مشكلة معينة إلى برنامج بلغة برمجية وتنفيذه [5]. إن القفز مباشرة إلى مرحلة التنفيذ بدون تصميم الحل الصحيح ينتج عادة برنامجاً يحتوي على العديد من الأخطاء، ويقضي المبرمج وقتاً مهماً لإيجاد تلك الأخطاء وتصحيحها [10]. ان اتفاقيات الرمز هي مجموعة من المبادئ التوجيهية للغة برمجية معينة التي توصي باتباع أسلوب وممارسات وأساليب البرمجة لكل سمة لكتابة برنامج بهذه اللغة. وينصح مبرمجو البرمجيات دائماً لاتباع هذه المبادئ التوجيهية للمساعدة في تحسين سهولة قراءة الشفرة المصدرية ولجعل عملية صيانة البرامج سهلة [16].

استخدم النظام الخبير للتقليل من الاخطاء التي قد تحصل اثناء عملية التصميم مع الاخذ بنظر الاعتبار الوقت المستغرق لتصحيح هذه الاخطاء للتحويل من مرحلة التصميم الى مرحلة التنفيذ من ناحية سهولة التعامل والتقليل من الوقت المستغرق لهذه العملية.

KJPS Al-Kitab Journal for Pure Science
Vol.2 (2), ISSN: 2617-1260 (print), 2617-8141(online)
www.kjps.isnra.org

4.النظام الخبير

النظام الخبير هو برنامج حاسوبي أو نظام ينظم المعرفة ضمن قواعد أو إجراءات لحل مشكلة أو مهمة معينة. ويمكن أن ينجز المهمة بمستوى قريب من الخبير البشري إذا كانت مصممة بشكل صحيح [17]. والأنظمة الخبيرة هي جزء من تطبيقات الذكاء الاصطناعي. إن الهدف الرئيس للنظام الخبير هو توفير نصيحة الخبراء في الحالات المتخصصة [18].

4-1 هيكلية النظام الخبير

يتكون النظام الخبير عادة من قاعدة المعرفة ومحرك الاستدلال وواجهة المستخدم كما مبين بالشكل (1) [19].

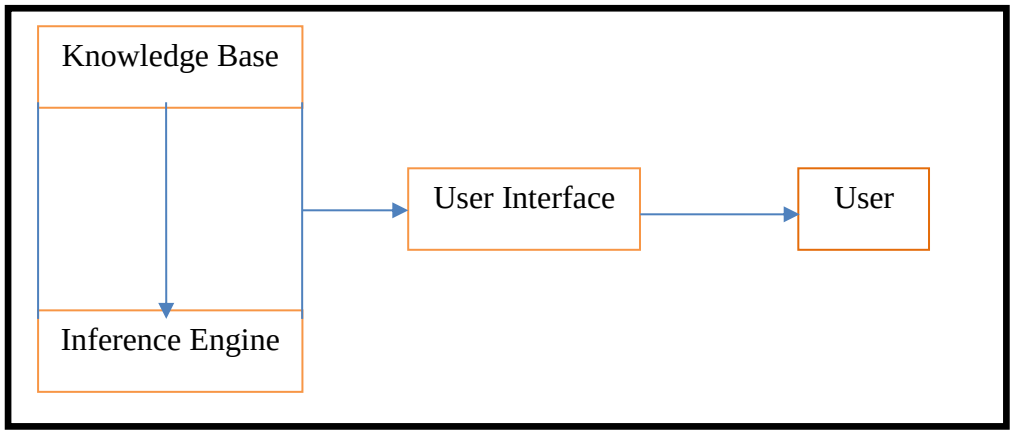

شكل1 هيكلية النظام الخبير

- **قاعدة المعرفة**

قاعدة المعرفة تعد قلب النظام الخبير [20]. تحتوي على قواعد لحل المشكلة، وبيانات جوهرية ذات العلاقة بمجال المشكلة [21]. وتتكون من قبل مهندسي المعرفة، الذي يحول خبرة البشر الحقيقية إلى معرفة أو بيانات في صيغة يفهمها الحاسوب [18]. يتم التعبير عن قاعدة المعرفة بقواعد اللغة الطبيعية If…Then [22].

- **محرك الاستدلال**

محرك الاستدلال هو البرنامج الذي يتحكم في عمل النظام بأكمله [23]. ويعد هو الدماغ في النظام الخبير. ويعمل كمترجماً يحلل ويعالج القواعد [24]. ويحتوي على طرائق السيطرة التي تشير إلى كيف ستعالج المعرفة

KJPS Al-Kitab Journal for Pure Science
Vol.2 (2), ISSN: 2617-1260 (print), 2617-8141(online)
www.kjps.isnra.org

الحالية، لكي تحصل على الحلول والاستنتاجات للمشكلة [25]. والنظام الخبير يستخدم طريقتين للاستدلال هما التسلسل الأمامي والتسلسل الخلفي [24].

1. **التسلسل الأمامي**

يتضمن فحص جزء الشرط للقاعدة لتحديد هل صحيحه أم خاطئه، إذا كان الشرط صحيحاً، إذن جزء فعّال (Action) للقاعدة صحيح أيضاً، واذا خاطئ ينتقل الى فحص القاعدة التي تليها. يستمر هذا الإجراء للوصول إلى الحل أو نهاية مسدودة [18].

2. **التسلسل الخلفي**

التسلسل الخلفي هو عكس التسلسل الأمامي. يستعمل للتراجع من الهدف إلى الطرائق التي تؤدي إلى الهدف. والتسلسل الخلفي جيد جداً عندما تكون كل النتائج معروفه وعدد من النتائج المحتملة ليس كبيراً، في هذه الحالة، الهدف محدد والنظام الخبير يحاول أن يحدد ما هو الشرط الذي يحتاجه للوصول إلى الهدف المحدد [18].

- **واجهة المستخدم**

يتفاعل المستخدم مع النظام الخبير عبر واجهة المستخدم التي تجعل الوصول أكثر راحة للإنسان ويخفي الكثير من تعقيد النظام [20]. وهو جزء من النظام الذي يأخذ في الاستعلام المستخدم في شكل مقروء ويمررها إلى محرك الاستدلال. ثم يعرض النتائج للمستخدم [19]. والنظام الخبير الجيد ليس مفيداً جداً مالم يحتوي على واجهة فعّالة [23].

5.النظام المقترح لتحويل التلقائي من الرمز الزائف الى الشفرة المصدرية

تم بناء النظام الخبير الذي يعمل على التحويل التلقائي من مرحلة التصميم الى مرحلة التنفيذ باستخدام لغة (Matlab R2013a). يبدا المصمم بكتابة اولا الهيكلية العامة للبرنامج ومن ثم يبدا بكتابة تفاصيل البرنامج عن طريق

KJPS Al-Kitab Journal for Pure Science
Vol.2 (2), ISSN: 2617-1260 (print), 2617-8141(online)
www.kjps.isnra.org

الخوارزمية المتمثلة بالرمز الزائف لحل مشكلة معينة في ملف نصي ذات امتداد txt. في برنامج ال Notpad على وفق الاتفاقيات التي وضعت في مشروع البحث، وبعدها يقوم بفحص التصميم لمراجعة متطلبات الزبون هل تم تصميمها بشكل صحيح، وقد تم وضع اتفاقيات لكتابة الرمز الزائف تشمل اغلب الاتفاقات التي يتم استخدامها من قبل المصممين وذلك لعدم وجود صيغة ثابتة لكتابة الرمز الزائف، والاتفاقيات التي وضعها في البحث هي على النحو الآتي:-

1. كتابة الكلمات المفتاحية للرمز الزائف بحروف صغيرة أو بحروف كبيرة.
2. الجمل تكون مكتوبة بالانكليزية البسيطة.
3. كل سطر في الرمز الزائف يجب أن يعبر عن نشاط واحد فقط (أي كل إيعاز يكتب بسطر واحد).
4. المتغيرات والثوابت وأسماء البرامج الفرعية ربما تكون أكثر من كلمة واحدة وذلك يجب ربطها برمز (_).
5. الجمع والعدادات يجب أن يوضع لها قيماً ابتدائية تساوي صفراً، وباقي المتغيرات التي يجب أن تحتوي قيما ابتدائية يجب أن يوضع لها قيماً ابتدائية.
6. مجموعة من الجمل تشكل على شكل برنامج فرعي، يكتب البرنامج الفرعي في نص آخر ليس النص نفسه الذي يستدعى ويخزن البرنامج الفرعي بالاسم نفسه عند تحويله إلى شفرة مصدرية.

5-1 اجزاء النظام الخبير المقترح

هو التقانة المستخدمة في البحث، إذ يعد النظام الخبير برنامجاً حاسوبياً ينظم المعرفة مبنياً على القواعد لعملية تحويل الرمز الزائف في مرحلة التصميم إلى شفرة مصدرية في مرحلة التنفيذ لإنتاج البرنامج.

يتألف النظام الخبير من :-

1. واجهة المستخدم: تتألف الواجهة لإدخال الرمز الزائف وعرض الشفرة المصدرية وسرعة التحويل التلقائي. عند تشغيل النظام المقترح تظهر لنا الواجهة الرسومية الرئيسية للمستخدم وكما موضح بالشكل(2).

KJPS Al-Kitab Journal for Pure Science
Vol.2 (2), ISSN: 2617-1260 (print), 2617-8141(online)
www.kjps.isnra.org

شكل2 الواجهة الرئيسية

وعند الضغط على اختيار ادخال ملف الرمز الزائف تظهر الواجهة الخاصة بإدخال اسم ملف الرمز الزائف كما في الشكل(3)، الذي كتبه عن طريق استخدام Notepad حيث يتم اختيار اسم الملف المراد تحويلة من الرموز الزائفة الى شفرة مصدرية مكتوبة بلغة MATLAB.

شكل3 واجهه ادخال رمز الزائف

KJPS Al-Kitab Journal for Pure Science
Vol.2 (2), ISSN: 2617-1260 (print), 2617-8141(online)
www.kjps.isnra.org

ومن ثم الرجوع الى الواجهة الرسومية الرئيسية لتطبيق النظام الخبير المقترح من خلال اختيار تطبيق النظام الخبير كما موضح بالشكل(4) حيث يظهر الوقت المستغرق لعملية التحويل التلقائي من ملف الرمز الزائف الى ملف برمجي مكتوب بلغة MATLAB بشكل تلقائي بالاعتماد على قاعدة المعرفة التي ستذكر لاحقا.

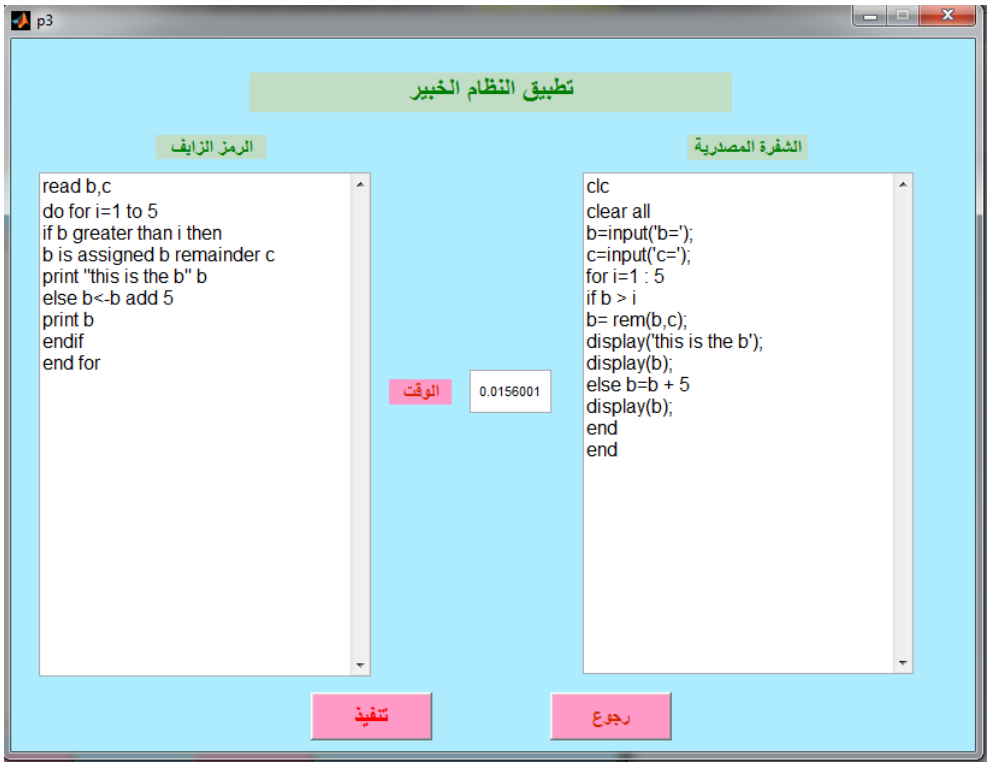

شكل4 تطبيق النظام الخبير

2. محرك الاستدلال: ماكنة الاستنتاج المستخدمة من نوع التسلسل الأمامي للبحث إذ يتوصل إلى الهدف المطلوب عبر تدقيق جزء الشرط للقاعدة.

3. قاعدة المعرفة: تتألف قاعدة المعرفة من مجموعة قوانين وكما في الجدول(1) :-

جدول 1 قوانين قاعة المعرفة

sequence	Condition	Action
Rule1	**If** "read" or "enter" or "get"	**Then** input
Rule2	**If** "write" or "output" or "print" or "show"	**Then** display

KJPS Al-Kitab Journal for Pure Science
Vol.2 (2), ISSN: 2617-1260 (print), 2617-8141(online)
www.kjps.isnra.org

Rule3	**If** "select case" or "case where" or "select" or "case of"	**Then** switch
Rule4	**If** "case else" or "others" or "default"	**Then** otherwise
Rule5	**If** "do while"	**Then** while
Rule6	**If** "do for" or "loop" or "loop for" or "do forever"	**Then** for
Rule7	**If** "to" or "down to" or "step" or "down to" or ";"	**Then** :
Rule8	**If** "procedure" or "method" or "subprogram" or "subroutine"	**Then** function
Rule9	**If** "<-" or ":=" or "set" or "initialize" or "is assigned"	**Then** =
Rule10	**If** "comment" or "//"	**Then** %
Rule11	**If** "<>" or "not equal to"	**Then** ~=
Rule12	**If** "add" or "addition"	**Then** +
Rule13	**If** "sub" or "subtraction"	**Then** –
Rule14	**If** "div" or "division" or "divide"	**Then** /
Rule15	**If** "multiplication" or "multiply"	**Then** *
Rule16	**If** "**" or "exponential"	**Then** ^
Rule17	**If** "not"	**Then** ~
Rule18	**If** "less than or equal to"	**Then** <=
Rule19	**If** "greater than or equal to"	**Then** >=
Rule20	**If** "greater than"	**Then** >
Rule21	**If** "less than"	**Then** <
Rule22	**If** "and"	**Then** &&
Rule23	**If** "or"	**Then** ||
Rule24	**If** "equal to"	**Then** ==

KJPS Al-Kitab Journal for Pure Science
Vol.2 (2), ISSN: 2617-1260 (print), 2617-8141(online)
www.kjps.isnra.org

Rule25	**If** "exclusive-or"	**Then** xor
Rule26	**If** "exit"	**Then** break
Rule27	**If** "remainder" or "integer modulo" or "integer remainder" or "modulus"	**Then** rem
Rule28	**If** "case close" or "end switch" or "end select" or "end case" or "end if" or "end while" or "end loop" or "next" or "end do"	**Then** end

5-1-1 الية عمل النظام الخبير

الشكل (5) يوضح خطوات تحويل الرمز الزائف الى برنامج باستخدام النظام الخبير. من خلال استخدام محرك الاستدلال ذات التسلسل الامامي.

KJPS Al-Kitab Journal for Pure Science
Vol.2 (2), ISSN: 2617-1260 (print), 2617-8141(online)
www.kjps.isnra.org

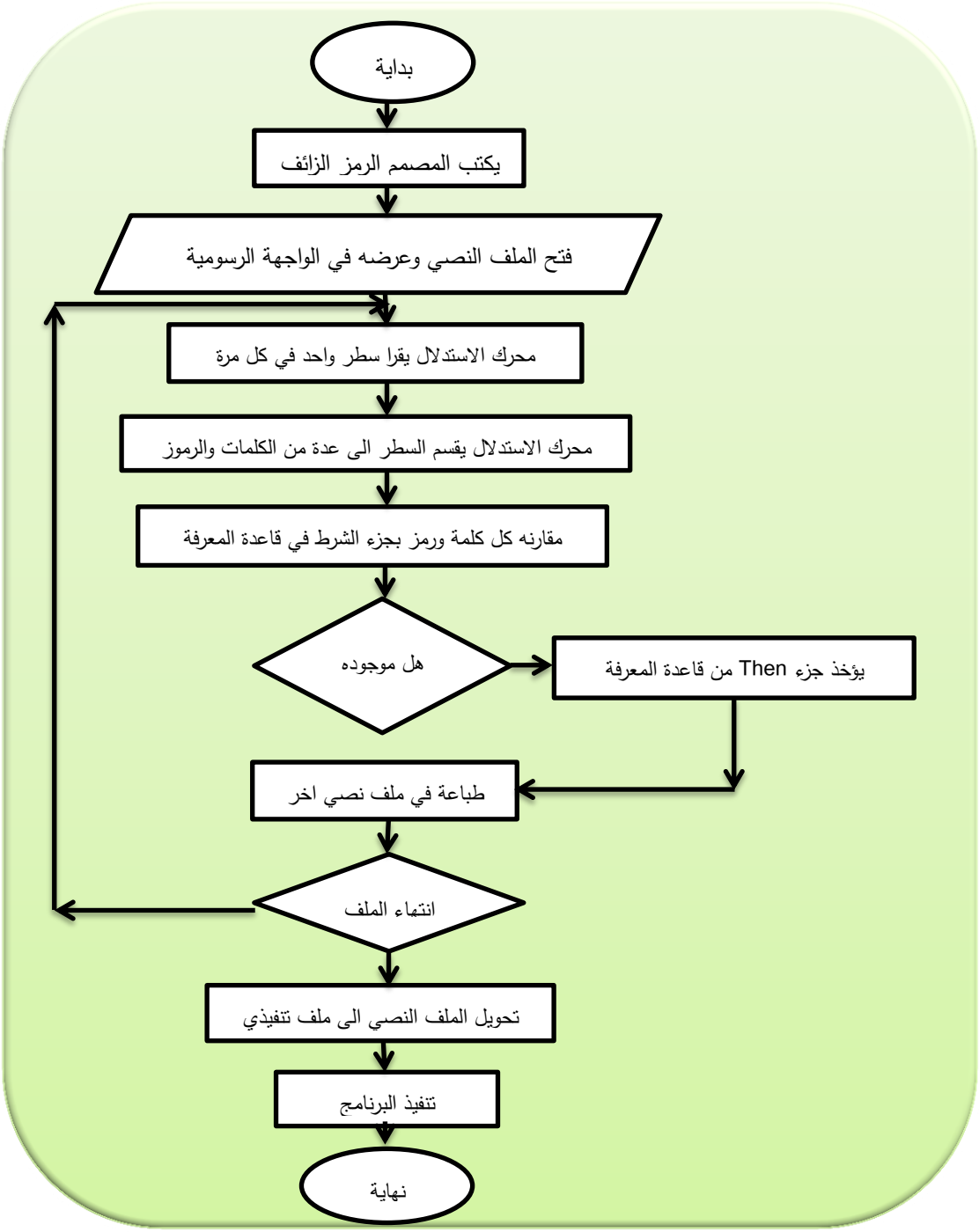

شكل5 المخطط الانسيابي لعملية التحويل التلقائي للنظام المقترح

KJPS Al-Kitab Journal for Pure Science
Vol.2 (2), ISSN: 2617-1260 (print), 2617-8141(online)
www.kjps.isnra.org

6. النتائج والمنافشة

اجريت عملية مقارنه من خلال استخدام عدد من الشبكات العصبية وهي(شبكة الانتشار العكسي، شبكة المتتالية الامامية و شبكة دالة القاعدة الشعاعية) للتحويل التلقائي [26]. ومقارنتها مع النظام الخبير المقترح حيث اظهرت النتائج سرعة نظام الخبير المقترح في عملية التحويل التلقائي وحسب الجدول (2).

جدول 2 يوضح عملية التحويل التلقائي للتقانات المستخدمة

نوع التقانة الذكائية	وقت التحويل التلقائي
شبكة الانتشار العكسي	**1.40401**
شبكة المتتالية الامامية	**1.37281**
شبكة دالة القاعدة الشعاعية	**1.79401**
النظام الخبير	**0.0156001**

7. الاستنتاجات

إمكانية الأداة على التحويل التلقائي من مرحلة التصميم إلى مرحلة التنفيذ (أي تحويل الرمز الزائف إلى شفرة مصدرية). لأي عملية تصميم حتى بعد إجراء أي تعديل أو إضافة أو حذف على الرمز الكاذب.

1. قورنت الشبكات العصبية (شبكة الانتشار العكسي، شبكة المتتالية الامامية، شبكة دالة القاعدة الشعاعية) مع النظام الخبير إذ استنتج بإن أسرع طريقة ذكائية في عملية التحويل التلقائي هي النظام الخبير وأبطأ طريقة في عملية التحويل التلقائي هي شبكة دالة القاعدة الشعاعية.
2. إن استخدام الأداة المقترحة سوف يقلل من الوقت والكلفة والأخطاء التي قد تحدث أثناء عملية التحويل.
3. ان النظام الخبير اسهل واسرع في عملية اضافة، او حذف، او تعديل قواعد او بيانات للرمز الكاذب من الشبكات العصبية حيث يحتاج الى تدريب الشبكة العصبية من جديد.
4. ان الاداة المقترحة لعملية التحويل التلقائي يكون اسرع من التحويل اليدوي (المبرمج) وبدون الوقوع باخطاء.

5. استخدام الذكاء الاصطناعي من خلال الانظمة الخبيرة مع عملية التحويل من الرمز الكاذب إلى شفرة مصدرية تم بصورة تلقائية مما سهل على المتدربين التعلم في هذا المجال.
6. يساعد الطلاب والمبتدئين في التفكير العميق لحل أي مشكلة معينة بمهارة وكيفية التعبير عنها بكتابة الرمز الكاذب قبل البدء بعملية البرمجة.

المصادر

1) Stephen R. Schach, "***Object-Oriented and Classical Software Engineering***", Eighth Edition, McGraw-Hill, (2010), pp. (2).
2) Naresh Kumar, Zadgaonkar A. S., Abhinav Shukla," ***Evolving a New Software Development Life Cycle Model SDLC-2013 with Client Satisfaction***", International Journal of Soft Computing and Engineering (IJSCE), Volume-3, Issue-1, March (2013), pp.(216).
3) Roger S. Pressman., "***Software Engineering: A Practitioner's Approach***", 7th Edition, McGraw-Hill, New York, USA, (2010), pp.(218,301).
4) John W. Satzinger, Robert B. Jackson, Stephen D. Burd, ***" Systems Analysis and Design in a Changing World***", Fifth Edition, Cengage Learning , (2010), pp(46).
5) Rick Mercer, " ***Introduction to Computer Science***", Citeseer, pp.(4,7).
6) Hassan Gomaa, " ***Software modeling and design***", Cambridge University Press, 2011,pp(41).
7) Clifford A. Shaffer, " ***A Practical Introduction to Data Structures and Algorithm Analysis***" Third Edition (Java), April 16, 2009, pp(3,4).
8) Kenneth Leroy Busbee, " ***Programming Fundamentals - A Modular Structured Approach using C++*** ", Rice University, Houston, Texas, 2008, pp.(26).
9) Andreas de Vries, "***Algorithmics and Optimization***", Lecture Notes in Business Information Systems (2nd Semester), February 3, 2014, pp.(15,10).
10) Lesley Anne Robertson, "***Simple Program Design A Step-by-Step Approach***", Fifth Edition, Thomson Learning, Inc., 2007, pp.(7,2).
11) Ivan Marsic, " ***software engineering*** ", Rutgers University, New Brunswick, New Jersey, 2012, pp.(24).

12) David Budgen, "***Software Design***", second edition, Addison Wesley, 2003, pp.(166,167,48).

13) Richard F. Gilberg, Behrouz A. Forouzan, " ***Data Structures: A Pseudocode Approach with C***", Second Edition, Printed in the United States of America, 2005, pp.(5).

14) Anany Levitin,"***Introduction to the design & analysis of algorithms***", 3rd ed., Addison Wesley, 2012, pp(3,13).

15) Kenneth Leroy Busbee, " ***Programming Fundamentals - A Modular Structured Approach using C++*** ", Rice University, Houston, Texas, 2008, pp.(26).

16) en.wikibooks.org, " ***Introduction to Software Engineering***", https://upload.wikimedia.org/wikipedia/commons/5/55/Introduction_to_Software_Engineering.pdf, December 29, 2013, pp.(137,147).

17) Thomas B. Cross, "***Knowledge Engineering: The Uses of Artificial Intelligence in Business*** ", TECHtionary Corporation, 2014.

18) Ranjit Ravi Iyer, " ***EXPERT SYSTEM FOR TREE SELECTION IN URBAN HORTICULTURE*** ", A THESIS PRESENTED TO THE GRADUATE SCHOOL OF THE UNIVERSITY OF FLORIDA IN PARTIAL FULFILLMENT OF THE EQUIREMENTS FOR THE DEGREE OF MASTER OF SCIENCE UNIVERSITY OF FLORIDA, 2005,pp(5,8,9).

19) Ms. Supriya Mahajan, Mr. Vansh Raheja, " ***A STUDY ON EXPERT SYSTEM, ITS TYPES AND THEIR ROLE IN MANAGEMENT*** ", Research journali's Journal of Management Vol. 1 | No. 1, November 2013, pp.(3).

20) أعداد: م. إسراء عبد الأمير عبد الجبار, تعديل والإضافة: م. علي حسن حمادي، "***Expert Systems (Artificial Intelligence) class***" 3rd ، الجامعة التكنولوجية، قسم علوم الحاسوب، 2011-2012.

21) ADEDEJI B. BADIRU, JOHN Y. CHEUNG, " ***FUZZY ENGINEERING EXPERT SYSTEMS WITH NEURAL NETWORK APPLICATIONS***", John Wiley & Sons, 2002.

22) Dr. Mohsen Kahani, " ***Expert System & Knowledge Engineering in Wikipedia***", PDF generated using the open source mwlib toolkit. See http://code.pediapress.com/ for more information. Fri, 14 Sep 2012 17:46:15 UTC. pp.(2).

23) Nikola K. Kasabov , " ***Foundations of neural networks, fuzzy systems, and knowledge engineering*** ",2nd, A Bradford Book, The MIT press, Cambridge, Massachusetts, Landon, England, 1998, pp.(129).

24) K P Tripathi, "***A Review on Knowledge-based Expert System: Concept and Architecture***", IJCA Special Issue on "Artificial Intelligence Techniques - Novel Approaches & Practical pplications", AIT, 2011, pp(20).

25) Soteris A. Kalogirou, " ***ARTIFICIAL INTELLIGENCE IN RENEWABLE ENERGY SYSTEMS MODELLING AND PREDICTION***", World Renewable Energy Congress VII , Elsevier Science Ltd, 2002, pp(2).

26) Dr. safwan Omer Hasson and Fatima Mohammed Rafie Younis "***Automatic Pseudocode to Source Code Translation Using Neural Network Technique***", International Journal of Engineering and Innovative Technology (IJEIT) Volume 3, Issue 11, May 2014, pp.(84,85).

KJPS Al-Kitab Journal for Pure Science
Vol.2 (2), ISSN: 2617-1260 (print), 2617-8141(online)
www.kjps.isnra.org

DOI: http://10.32441/kjps.02.02.p17

مساهمة الغلاف المزدوج في زيادة كفاءة الطاقة للمباني السكنية بمدينة كركوك

د. سعاد حسن دانوك*, كمال جلال توفيق, أشرف نجم الدين حسين

[1]talebshebab@yahoo.com

الخلاصة

يعتبر استخدام الغلاف المزدوج احدى معالجات التصاميم السلبية والذي يساهم في زيادة كفاءة الطاقة للوصول الى نفس مستويات الراحة البشرية باقل صرف للطاقة, في هذا البحث تم محاكاة تأثير استخدام الاغلفة المزدوجة على طاقة المباني السكنية في مدينة كركوك بأخذ نموذج بناية ذي الشكل المربع والاستعانة ببرنامج محاكاة طاقة المباني Ecotect بالاستناد على معلومات المناخ الساعية السنوية لمدينة كركوك, وبعد اجراء الاختبارات تم التوصل الى اعظم ادخار في حمل التكييف السنوي بنسبة (9.764)% عند استخدام الغلاف المزدوج لمجموع قيم الادخار للحالات المثلى التي تم التوصل اليها من خلال استخدام الجدران المزدوجة والتي حققت نسبة ادخار (6.822)% وكانت الواجهة الغربية افضل الواجهات حققت ادخار بنسبة (2.822)% وساهمت استخدام الارضية الميته ذي توجيه الفتحات الشرقية/الغربية واستخدام السقف الكاذب اسفل السقف الرئيسي بنسب ادخار (1.444 و 1.44)% على التوالي من احمال التكييف السنوية.

KJPS Al-Kitab Journal for Pure Science
Vol.2 (2), ISSN: 2617-1260 (print), 2617-8141(online)
www.kjps.isnra.org

The Contribution of Double Envelopment to Increase Energy Efficiency In Residential Building In Kirkuk City

Suad Hassan Danook, Kamal Jalal Tofeeq, Ashraf Najmadeen Hussein

Abstract

Using of double envelopment is one of the passive designs processor's, Which contributed to increase energy efficiency by get same human comfort with less energy consumption in for air conditioning in building, In this investigate Was simulation the effect the effect of using double envelopment by select Existing building at same dimensions of all façade by building energy simulation program (Ecotect) based on hourly weather data of Kirkuk city, after conducting the tests was to reach the greatest savings of HVAC annual loat at rate (9.764%) when using the double envelopment of total savings optimal for situations that have been reached through the use of double walls which has achieved a rate of savings values (6.822%) were the western facade best interfaces achieved savings rate (2.822%) and contributed to the use of ground dead with a ventilated gap East / Western and when using the false ceiling below the main ceiling rates savings (1.444 and 1.44)%, respectively for the annual loads of air-conditioning.

1.المقدمة:

يشهد العصر الذي نمر به طلبا كبيرا على الطاقة, حيث اصبحت الحاجة اليها في جميع قطاعات المجتمع في تسير الحياة اليومية وان للتطورات التقنية والعمرانية تأثير في زيادة الطلب على الطاقة مما ادى الى زيادة التوجهات اللازمة الى ترشيد استهلاك الطاقة والاعتماد على العوامل المساهمة في تقليل صرف الطاقة في البنايات للحصول على نفس مستويات الراحة البشرية وباقل استهلاك للطاقة.

ويمثل قطاع المباني السكنية من اهم القطاعات المستهلكة للطاقة وان مقدار الطاقة الكهربائية المطلوبة للمباني السكنية يقدر بـ(41.6)% لعام 2016[1], ومعظم هذه الطاقة تكون لأغراض تكييف الهواء, ويعد غلاف البناية العامل

KJPS Al-Kitab Journal for Pure Science
Vol.2 (2), ISSN: 2617-1260 (print), 2617-8141(online)
www.kjps.isnra.org

الرئيسي لتحديد سعة التكييف اللازمة نتيجة انتقال الحرارة بين الحيز الداخلي والبيئة الخارجية حيث يقدر مابين(50-70)% [2], من طاقة احمال التبريد والتدفئة للبناية.

هناك عدة معالجات تصميمة من وسائل التصاميم السلبية يتم استخدامها لتقليل مقدار السريان الحراري من خلال غلاف المبنى كاستخدام الاغلفة المزدوجة المتمثلة بـ(الجدران المزدوجة, السقف المزدوج الخارجي والسقف الكاذب, الارضية الميتة) وتعزيز استخدام الاعشاب المتسلقة او زيادة انعكاسية الجدران باستخدام الاصباغ او استخدام مواد متغيرة الطور (PCM) علاوة عن استخدام طبقات مواد العزل الحراري لتقليل مقادير الانتقال الحراري المتبادل بين البيئة الداخلية والمحيط الخارجي من خلال مكونات غلاف البناية.

ومن خلال تطبيق الية الغلاف المزدوج يمكن مراعاة تقليل التبادل الحراري باستثمار الطبقة الهوائية بين المتكونة بين الغلافين لخزن الحرارة المكتسبة من الشمس في فصل الشتاء واستثمارها كمجرى في تدوير الهواء لتهوية الغلاف الرئيسي بطريقة طبيعية او ميكانيكية.

2.الغلاف المزدوج:

يتكون غلاف البناية من الاجزاء المعتمة والاجزاء النافذة وان معظم غلاف البناية يتألف من الاجزاء المعتمة التي يمكن استخدام الية الغلاف المزدوج فيها ويصنف الغلاف المزدوج الى:-

2-1. الجدران المزدوجة:

وهو عبارة عن قشرتين من مواد المكون للجدران او القطع الكونكريتية يكون بينهما فجوة هوائية[3], استخدمت الجدران المزدوجة في بادئ الامر كممرات في الواجهات التي يصعب السيطرة على الاشعاع الشمسي الساقط نتيجة منع دخول الاشعاع المباشر الى داخل حجرات البناية في المناطق الحارة وتعزيز دوران الهواء لزيادة مقادير التهوية وزيادة التبريد الطبيعي نتيجة زيادة التبادل الحراري بالحمل او التبخير في المساكن القديمة كما مبين في الشكل (1) [4] من ثم تم تصميم الجدران المزدوجة من خلال اضافة قشرة ثانوية امام الجدران الرئيسية يطلق عليها احيانا بالستارة لمنع الاشعاع الشمسي

KJPS Al-Kitab Journal for Pure Science
Vol.2 (2), ISSN: 2617-1260 (print), 2617-8141(online)
www.kjps.isnra.org

الساقط على الجدران بالشكل المباشر او المنتشر في فصل الصيف وتزويد الجدران الثانوية بفتحات لضمان تدوير الهواء لتبريد الجدران الرئيسية لغلاف البناية من اجل تقليل انتقال الحرارة من الخارج الى الداخل في فصل الصيف والاستفادة من الهواء المحصور بين الجدارين كمصدر للخزن الحراري في فصل الشتاء لتقليل التسريب والانتقال الحراري من الحيز الدافئ الداخلي الى البيئة الخارجية الباردة.

وهناك عدة تصاميم للجدران المزدوجة بحسب الية التهوية لها اما بالشكل الطبيعي او الميكانيكي, ووجود الفتحات او عدم وجودها وطبيعة حركة الهواء ببين الجدارين بشكل متعاكس او دوران الهواء باتجاه واحد من طرف الحيز المكيف او المحيط الخارجي للجدران[5] كما مبين في الشكل (2), وان سمك الجدران التي يتم اضافة عليها الغلاف المزدوج يجب ان لا يقل عن 90ملم ويحدد سمك الطبقة الهوائية بين الجدارين مابين (50–100)ملم من اجل تحقيق زيادة المقاومة الحرارية للجدران[3] .

2–2. السقف المزدوج:

ان للسقف اهمية من ناحية انتقال الحرارة في فصل الصيف اكثر من ما هو عليه في الشتاء بسبب الارتفاع الشمسي العالي لفصل الصيف حيث ان هناك اختلاف في زاوية الارتفاع الشمسي يقدر بـ(47°) [6], بين فصلي الصيف والشتاء, ولزيادة مقدار العزل للسقوف يتم استخدام نوعيين من السقف المزدوج لتكوين حاجز هوائي بين حيز الهوائي الداخلي والبيئة الخارجية وهي :-

2–2–1. السقف المزدوج الخارجي:-

وهي عبارة عن قشرة خارجية يتم اضافتها من الخارج فوق السقف الرئيسي ويتم تزويدها بالفتحات لتهوية السقف في فصل الصيف وهذه الطريقة يكون فعالا عن استخدامها مع السقوف المائلة للاستفادة في زيادة دوران الهواء بطريقة السيفون الحراري(thermo–siphon) في مواسم الحر والمساهمة في ازالة الصقيع والثلوج المتراكم على سقف المبنى في فصل الشتاء[6].

KJPS Al-Kitab Journal for Pure Science
Vol.2 (2), ISSN: 2617-1260 (print), 2617-8141(online)
www.kjps.isnra.org

2-2-2. السقف الكاذب:-

وهي سقف مزدوج داخلي يتم تثبيتها اسفل السقف الرئيسي من الداخل مكونا حيز هوائي بين السقفين يتم استخدامها غالبا لإمرار الاسلاك الكهربائية ومجاري التكييف لتوزيع الهواء في البناية علاوة عن مساهمتها في تقليل السريان الحراري ما بين البيئة المكيفة الداخلية والمحيط الخارجي.

2-3. الارضية الميته:

يتم استخدام الحيز الهوائي السفلي او الحجرات تحت سطح الارض (السرداب) لتقليل مقدار الانتقال الحراري بالتوصيل من خلال الارضية وذلك نتيجة فراغ هوائي بين ارضية البناية والقشرة الارضية ويمكن استثمار هذه الطبقة بتزويدها بفتحة هوائية من الجانبين المقابلين لزيادة مدار التهوية للأرضية في فصل الشتاء ,والشكل (3) يبين طريقتين لاستخدام الارضية السفلية المزدوجة في فصلي لصيف والشتاء[6].

3. طرق انتقال الحرارة:

يتم تحديد مقدار الحرارة المنتقلة خلال غلاف البناية بالاعتماد على معامل اجمالي انتقال الحرارة (U) وهو يمثل مقلوب مجموع المقاومات الحرارية لمكونات الانشائية لغلاف البناية, ويتم الاعتماد على المعادلات التالية لحساب الانتقال الحراري خلال المواد الانشائية للغلاف[7].

$$U=.\frac{1}{Rth..} \quad \text{... .....(1)}$$

$$Rth.=\frac{1}{hi}+\frac{X1}{K1}+\frac{X2}{K2}+\cdots\cdots+\frac{Xn}{Kn}+\frac{1}{C1}+\frac{1}{C2}+\cdots\cdots+\frac{1}{Cn}+\frac{1}{ho}\ldots(2)$$

$$Q_{trassfer}=U \times A \times (T_o - T_i) \quad \ldots\ldots\ldots\ldots\ldots\ldots\ldots\ldots\ldots\ldots(3)$$

ويصنف طرق انتقال الحرارة الى ثلاثة اصناف وهي:-

3−1. انتقال الحرارة بالتوصيل

يتم الانتقال الحراري بالتوصيل من خلال المواد الانشائية المعتمة في البناية المتمثلة بالجدران والسقوف والارضيات ومن خلال اطار النوافذ والابواب وتعتمد على معامل التوصيل الحراري(K) لكل مادة وتستخدم معادلة فورير لحساب الانتقال الحراري بالتوصيل التي تنص الاتي[8]:−

$$Q_{cond.} = -K \times A \times \frac{dT}{dX} \quad \text{...(4)}$$

3−2. الانتقال الحراري بالحمل:

يعتمد الانتقال الحراري بالحمل على طبيعة الوسط الناقل لها, حيث ان الهواء او اي مائع يقوم بنقل الحرارة بين منطقتين مختلفتين في درجة حرارتهما بالاعتماد على سرعة حركتها التي تحدد مقدار معامل الانتقال الحراري بالحمل (h), ويتم حساب مقدار الانتقال الحراري باستخدام المعادلة التالية[8].

$$Q_{conv.} = h \times A \times (T_2 - T_1) \quad \text{.. (5)}$$

وان الحرارة المنتقلة بالحمل يكون من خلال غلاف البناية نتيجة التسريب($\mathbf{V}_{inf}$) التي تحدث من خلال السقوف والفتحات وحافات الابواب والنوافذ بالاضافة الى التهوية اللازمة لزيادة نقاوة الهواء, ومقدار الحرارة المنتقلة بشكل كامن او محسوس ويحسب بالاعتماد على المعادلتين التاليتين[9]

$$Q_{Sinsible} = 1.22 \times \mathbf{V}_{inf} \times (T_{out} - T_{in}) \quad \text{.......................................(6)}$$

$$Q_{Latent} = 3000 \times \mathbf{V}_{inf} \times (W_{out} - W_{in}) \quad \text{.................................(7)}$$

ويقدر مقدار التسريب والتهوية التي تحدث بالبناية بحساب عدد مرات تغيير الهواء خلال الساعة (ACH) حسب نوعية الغلاف ودرجة التهوية التي تنص الاتي[10]

$$ACH = a + b \times V_{air} \times c\,(T_o - T_i) \quad \text{...(8)}$$

KJPS Al-Kitab Journal for Pure Science
Vol.2 (2), ISSN: 2617-1260 (print), 2617-8141(online)
www.kjps.isnra.org

a,b,c= ثوابت يأخذ من جداول خاصة بالاعتماد على درجة احكام غلاف البناية (جيد, متوسط, ردئ)

3-3. انتقال الحرارة بالإشعاع:

يتأثر البناية بمقدار الاشعاع الشمسي الساقط عليها, ويحدث الانتقال الحراري بالإشعاع خلال الاجزاء النافذة والفتحات الموجودة خلال غلاف البناية, ويتحدد مقدار النفاذية للنوافذ من خلال معامل الكسب الحراري المباشر (SHGC) ومعامل مقدار التظليل للنوافذ (SC) ويستخدم المعادلاتين التاليتين لحسابهما[9].

$$SHGC=\frac{q\ sol.gain}{q\ sol.anciden} \quad \text{.....(9)}$$

$$Q=SHGC\times A_{glaz.}\times q_{sol.ancident} \quad \text{.....(10)}$$

اما تأثير الاشعاع الشمسي على الاسطح المعتمة فيتم تمثيلها على شكل درجة حرارة خارجية على سطح الجدران والسقوف يطلق عليها درجة حرارة الهواء الشمسيةالذي يحسب بالاعتماد على المعادلة (11) ومن ثم يحسب مقدار الاشعاع المتأثر مع مقدار الحرارة المنتقلة بالحمل وتعويض درجة حرارة الهواء الشمسية بدرجة الحرارة لسطح الغلاف الخارجي.

$$T_{sol.\ air}=T_{am}+\frac{\propto\times q\cdot sol}{ho}-\frac{\varepsilon\times\ell\times(Tamb-Tsur)}{ho}\ldots\ldots \quad \text{.....(11)}$$

4. الجانب العملي:

1. تم اخذ بناية سكنية في مدينة كركوك ذي الشكل المربع لكون مساحات الجدران للواجهات الاربعة متساوية بأبعاد (11.6 × 3)م^2 وبالتوجيه الجنوبي لواجهة الرئيسة للبناية كما مبين في الشكل (4):-
2. تهيئة برنامج محاكاة طاقة المباني Ecotectلأجراء الاختباراتبالاعتماد على معلومات الطقس الساعية لمناخ مدينة كركوك كما مبين في الشكل (5)ومعايرة مسار الاشعاع الشمسي بإدخال خطوط الطول (44.45°) والعرض (35.47°) لمدينة كركوك كما مبين في الشكل (6), وادخال معلومات الخصائص الحرارية الداخلية اللازمة لمواصفات البنايات كما مبين في الجدول (1)[3,9,10,11].

KJPS Al-Kitab Journal for Pure Science
Vol.2 (2), ISSN: 2617-1260 (print), 2617-8141(online)
www.kjps.isnra.org

3. اضافة الجدران المزدوجة من الخارج للواجهات الاربعة بسمك 100ملم بالتصميم الذي يحتوي على اطول فتحات ممكنة من الجزء الاعلى والاسفل للجدران من الخارج لضمان التهوية باستثمار حركة الهواء الطبيعية في اطراف البناية من خلال وضع الفتحات بالشكل المفتوح عند محاكاة حمل التبريد السنوي واعتبار الفتحات بالشكل المغلق عند محاكاة حمل التدفئة السنوي للاستفادة من الفراغ الهوائي لخزن الحرارة المكتسبة نتيجة سقوط الاشعاع الشمسي كمامبين في الشكل (7), وتم تحديد الجدران الثانوية الخارجية ضمن حيز خارجي un-thermal zone في برنامج Ecotectلضمان عدم دخول مساحة الجدران الخارجية عند حسابات الاحمال الحرارية المطلوبة خلال الحيز الداخلي للبناية.
4. تم رفع ارضية البناية 200 ملم للأعلى لتكوين الحيز الهوائي بين ارضية البناية والقشرة الخارجية لتكوين الارضية الميته عند فصل الشتاء واجراء الاختبارات لطريقة استخدام الفتحات المتقابلة لعملية التهوية في الارضية المزدوجة بأتجاه الشمال/الجنوب للحالة الاولى وبأتجاه الشرق/الغرب للحالة الثانية للوصول الى اعظم كفاءة للطاقة كما مبين في الشكل(8).
5. تم اختبار السقف الثانوي من خلال السقف الكاذب الداخلي المتكون من مادة الجبس بسمك 10 ملم وبفراغ هوائي 20سم بين السطح الداخلي للسقف الرئيسي وسطح طبقة الجبس واجراء المحاكاة مع افضل نموذج لتسطيح السقف المتكون من (قطع كونكريت40ملم+ رمل نظيف 40ملم + تراب نظيف 100ملم+ الواح زجاجية الخلوية 80ملم+صبة كونكريتية150ملم+ثلاث طبقات قير ولباد 30ملم+ بياض بالجص 20ملم) لحساب اعظم ادخار في حمل التكييف السنوي التي يمكن الحصول عليها من خلال استخدام السقف الكاذب.

5.النتائج والمناقشة:-

بعد عملية المحاكاة للجدران المزدوجة في الواجهات الاربعة تم التوصل الى النتائج التالية المبينة في الجدول (2), والشكل(9) يبين العلاقة بين نسب الادخار لحمل التكييف السنوي لاستخدام الجدران المزدوجة في التوجيهات الاربعة ومن خلال الجدول (2)يبين بأنه تم التوصل الى ادخار بنسبة (6.487%) عند استخدام الجدران المزدوجة في جميع واجهات البناية حيث كانت اعظم ادخار في الجدران المزدوجة في

KJPS Al-Kitab Journal for Pure Science
Vol.2 (2), ISSN: 2617-1260 (print), 2617-8141(online)
www.kjps.isnra.org

الواجهات الغربية بنسبة (2.8222%) من حمل التكييف السنوي للبناية ومن ثم يليها الجدران الشرقية وبنسبة ادخار مقاربة مما هو عليه في الجدران الغربية حيثكانت الادخار بنسبة (2.622%)اما بالنسبة للواجهات الجنوبية فقد تبين عدم وجود فائدة كبيرة عند استخدام الجدران المزدوجة فيها حيث لم يتعدى نسبة الادخار فيها (0.058%) من حمل التكييف السنوي وتم ملاحظ ان الادخار في حمل التبريد للجدران المزدوجة الغربية كانت بنسبة(3.4457%) اكثر من الادخار لحمل التبريد في الجهة الشرقية التي كانت بنسبة (2.668%) مما يدل على ان حركة الرياح في الجهة الغربية اسرع او اكثر مماهو عليه في الجهة الشرقية وان نسبة الادخار لحمل التدفئة في الجدران المزدوجة الشرقية اكثر من الجدران المزدوجة الغربية وذلك لان الخزن الحراري التي يحدث في الفجوة التي بين الجداران المزدوجة في فترات الشروق يقوم بفقدها بوقت اطول نتيجة استمرار البناية باستلام الاشعاع الشمسي بعد فترة الصباح من طرف الواجهة الجنوبية بعكس الخزن الحراري التي تحدث بين الجدران المزدوجة الغربيين التي تتأثر بفترة الليل التي يقوم بها الارض بإرجاع الموجات الحرارية الطويلة الى السماء التي قام بخزنها في ساعات النهار.

يبين الجدول (3) والشكل(10) أن استخدام الارضية المزدوجة ذي الفتحة باتجاه الشرق/الغرب افضل من الفتحة باتجاه الشمال/الجنوب ولذلك لمساهمتها بنسبة ادخار (1.444%) من حمل التكييف السنوي اما عند استخدام الفتحات بالتوجيه الشمال/الجنوب كانت هناك فارق في بنسبة الادخار (0.2361)% بالنسبة لافضل حالة التي تم التوصل اليها. ويتبين لنا من الجدول(4) والشكل(11)بأنه عند استخدام السقف الكاذب فأنهيساهم في ادخار حمل التكييف السنوي بنسبة (1.44%)نتيجة عملها كمنطقة هوائية عازلة بين الحيز الداخلي وبين السقف الرئيسي للبناية.

6.الاستنتاجات:

1- اعلى كفاءة طاقة يمكن الحصول عليه عند استخدام الية الجدران المزدوج في البناية يقدر بنسبة(6.487%) من حمل التكييف السنوي لمجموع نسب الادخار في الواجهات الاربعة.

KJPS Al-Kitab Journal for Pure Science
Vol.2 (2), ISSN: 2617-1260 (print), 2617-8141(online)
www.kjps.isnra.org

2- ان افضل حالة لاستخدام الجدران المزدوجة هي الجدران المزدوجة في الواجهة الغربية حيث يساهم بأعظم ادخار في حمل التكييف السنوي بنسبة(2.822)% يليها استخدام الجدران المزدوجة في الواجهة الشرقية حيث يساهم في بنسبة ادخار (2.622)% من حمل التكييف السنوي.

3- تم التوصل الى اعظم ادخار في حمل التكييف السنوي بنسبة (1.444)% عند استخدام تقنية الارضية الميته ذي الفتحات المفتوحة باتجاه الشرق/الغرب عند محاكاة حمل التبريد السنوي.

4- عند اضافة السقف المزدوج الكاذب يمكن المساهمة في ادخار حمل التكييف السنوي بنسبة (1.44%)

5- اعلى كفاءة طاقة يمكن الحصول عليه عند استخدام الية الغلاف المزدوج في جميع اجزاء البناية يقدر ب(9.371%) من حمل التكييف السنوي للبناية.

6- من خلال محاكاة توجيه الجدران المزدوجة واتجاه الفتحات للأرضية المزدوجة نستنتج بأن اكبر كمية هبوب الرياح في مدينة كركوك هي الرياح الغربي

المصادر:

1- ورقة جمهورية العراق لمؤتمر الطاقة العربي العاشر(2014), الطاقة والتعاون العربي, ابوظبي دولة الامارات العربية المتحدة 21-23 كانون الاول/ديسمبر

2- وائل عواد العقيلي, م د ابراهيم جواد ال يوسف(2007) "تقليل حمل التبريد بتطبيق منظومة الغلاف المبنى الذكي" الجامعة التكنلوجية , بغداد.

3- وائل عواد العقيلي, م د ابراهيم جواد ال يوسف(2007) "تقليل حمل التبريد بتطبيق منظومة الغلاف المبنى الذكي" الجامعة التكنلوجية , بغداد.

4- حسن فتحي(1988)," كتاب الطاقات الطبيعية والعمارة التقليدية", جامعة الأمم المتحدة- طوكيو,الموسسة العربية للدراسات والنشر,الطبعة الاولى سنة.

5- Matthias Haase,Fleix Wong , Alex Amato (2007),"Double-Skin Facades for Hong Kong", Surveing and Built EnviironmentVola 18(2).

6- Donald Watson, FAIA, and Kenneth labs(1982), ”Energy-Efficient Building Principles and Practices, Climate Design”, Handbook

7- المدونة العراقية للتبريد,2012 وزارة الاسكان والاعمار العراقية, الدائرة الفنية لمشروع المدونات العراقية

8- Yunus A. Cengel(1998),”Heat Transfer A practical approach”, International Edition, WCB McGraw-Hill.

9- American Society of Heating, Refrigeration and Air-condition engineers(2013), ”Fundamentals”, ASHRAE Handbook,\

10- الاستاذ الدكتور علي سليمان الجبوري, "كتاب تكييف الهواء", الكلية الهندسية العسكرية العراقية

11- C.Koranteng, E.G Abaitey(2009),”Simulation Based Analysis on the Effect of Orientation on Energy Performance of Residential Building in Ghana”, Journal of Science and Technology, Vol 29. No.3,pp(86-101).

جدول(1):- الخصائص الحرارية والمواصفات القياسية التي تم ادخالها للبرنامج

الظروف القياسية	حمل التبريد	حمل التدفئة
درجة حرارة الداخلية	24	22
الرطوبة النسبية	50%	40%
مقاومة الملابس	0.3clo	0.6clo
عدد الاشخاص	5	5
معدل الايض	70W/m^2	70W/m^2
مقدار التسريب	0.8ACH	0.8ACH
سرعة الهواء الداخلية	0.15m/s	0.13m/s
الحمل الداخلي المحسوس	5W/m^2	5W/m^2
الحمل الداخلي الكامن	2W/m^2	2W/m^2
مقدار الاضاءة الداخلية	300lux	300lux

KJPS Al-Kitab Journal for Pure Science
Vol.2 (2), ISSN: 2617-1260 (print), 2617-8141(online)
www.kjps.isnra.org

جدول (2):- نتائج احمال التكييف ونسب الادخار السنوي لاستخدام الجدران المزدوجة في الواجهات الاربعة

اتجاه الجدار المزدوج	حمل التبريد Whالسنوي	حمل التدفئة Whالسنوي	حمل الاجمالي Whالسنوي	ادخار حمل التبريد السنوي%	ادخار حمل التدفئة السنوي%	ادخار حمل التكييف السنوي%
بدون جدار مزدوج	55443237	42472130	97915367	0	0	0
شمال	54481176	42470065	96951241	1.735217949	0.004862012	0.984652389
شرق	53963863	41384100	95347963	2.668267728	2.561750494	2.62206442
غرب	53532800	41619190	95151990	3.445752996	2.008234576	2.822209715
جنوب	55369588	42488908	97858496	0.132836761	-0.039503552	0.058081792
المجموع	-----	-----	-----	7.98207543	4.53534353	6.487008316

جدول (3):–نتائج احمال التكييف ونسب الادخار لاستخدام الارضية المزدوجة مع اتجاه الفتحات خلال محاكاة احمال التكييف السنوية.

اتجاه الفتحات	حمل التبريد Whالسنوي	حمل التدفئة Whالسنوي	حمل التكييف Whالسنوي	ادخار حمل التبريد السنوي%	ادخار حمل التدفئة السنوي%	ادخار حمل التكييف السنوي%
بدون رفع الارضية	55443237	42472130	97915367	0	0	0
رفع الارضيةذو فتحات اه الشمال /الجنوب	54373492	42359038	96732530	1.929441818	0.266273436	1.208019779
رفع الارضية ذو فتحات الشرق /الغرب	54142325	42359038	96501363	2.346385367	0.266273436	1.444108359

KJPS Al-Kitab Journal for Pure Science
Vol.2 (2), ISSN: 2617-1260 (print), 2617-8141(online)
www.kjps.isnra.org

جدول (4):-نتائج احمال التكييف ونسب الادخار في حالة اضافة السقف الثانوي من الداخل على بعد 20سم من السقف.

حالة اضافة السقف الكاذب	حمل التبريد السنوي Wh	حمل التدفئة السنوي Wh	حمل التكييف السنوي Wh	ادخار حمل التبريد السنوي %	ادخار حمل التدفئة السنوي %	ادخار طاقة التكييف السنوي%
بدون السقف الكاذب	72187789	33076037	105263826	0	0	0
اضافةالسقف كاذب	71387450	32359769	103747219	1.10869028	2.165519406	1.440767505

شكل(1):- يبين استخدام الجدران المزدوج كممرات في المباني القديمة

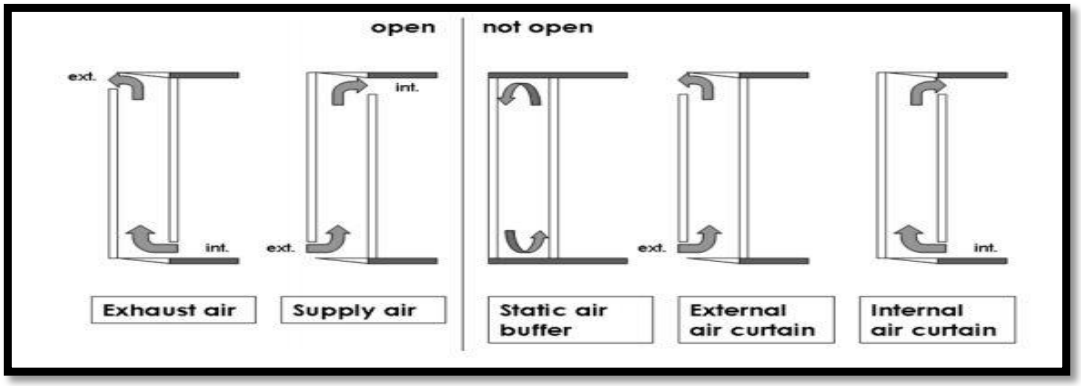

الشكل(2):- تصاميم الجدران المزدوج

KJPS Al-Kitab Journal for Pure Science
Vol.2 (2), ISSN: 2617-1260 (print), 2617-8141(online)
www.kjps.isnra.org

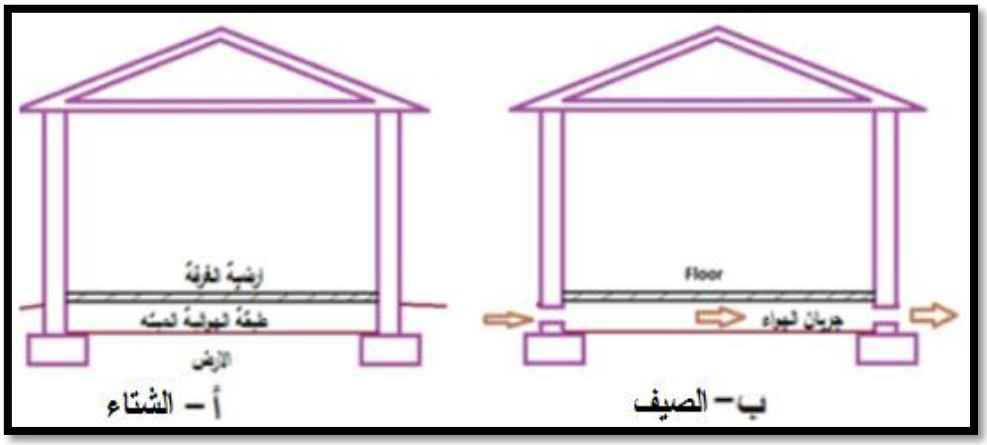

شكل(3):– الية استخدام الارضية المزدوجة في فصل الصيف والشتاء

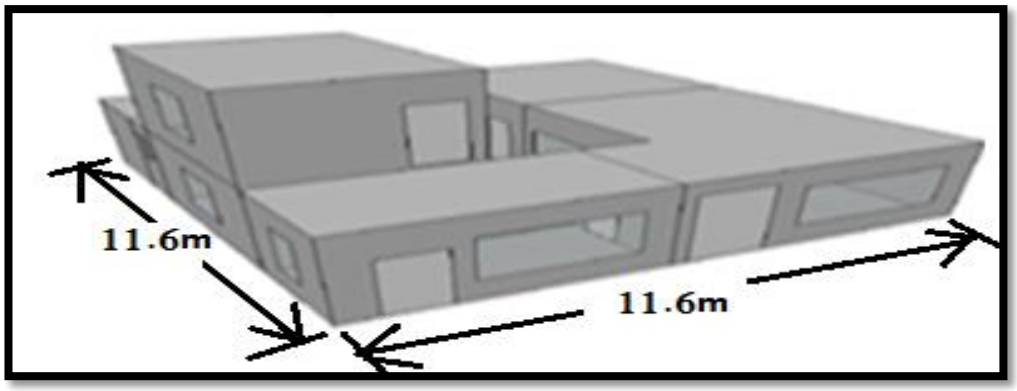

الشكل(4):- نموذج البناية المستخدمة في عمليات الاختبار.

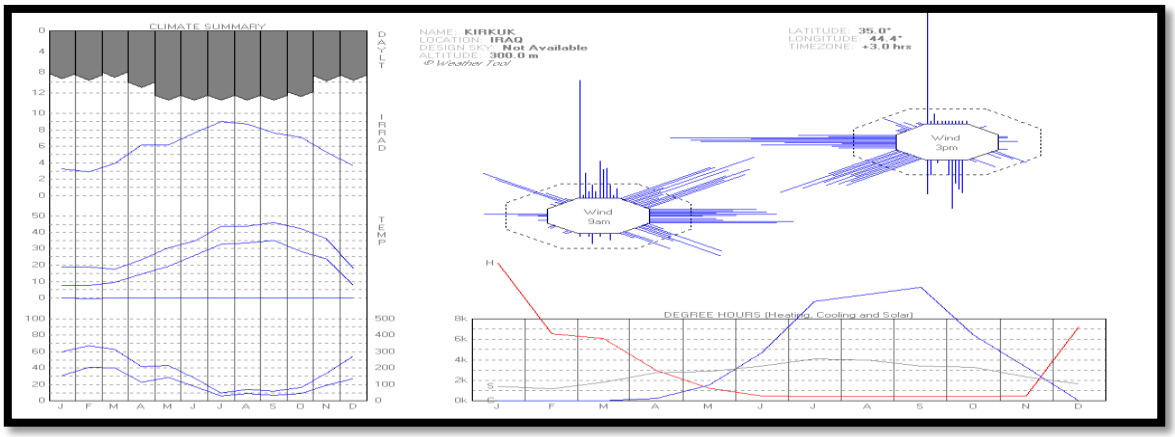

شكل(5):–بين مخططات عوامل الطقس بعد عملية التحويل في مربع حوار محول المناخ في برنامج Ecotect

KJPS Al-Kitab Journal for Pure Science
Vol.2 (2), ISSN: 2617-1260 (print), 2617-8141(online)
www.kjps.isnra.org

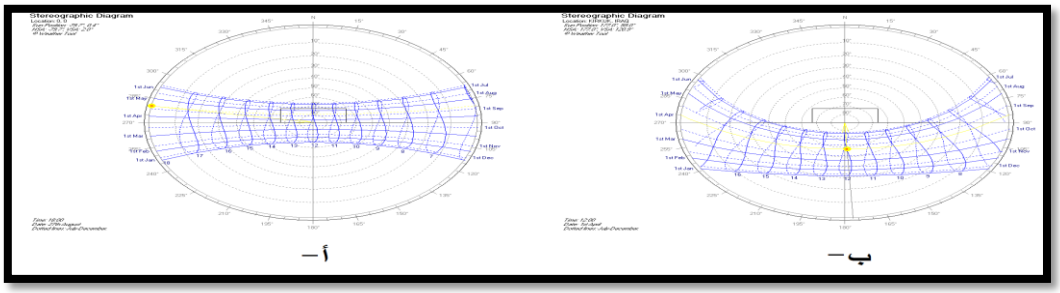

الشكل (6):– أ– مسار الشمس قبل ادخال خطوط الطول والعرض لمدينة كركوك
ب–مسار الشمس بعد ادخال خطوط الطول والعرض لمدينة كركوك.

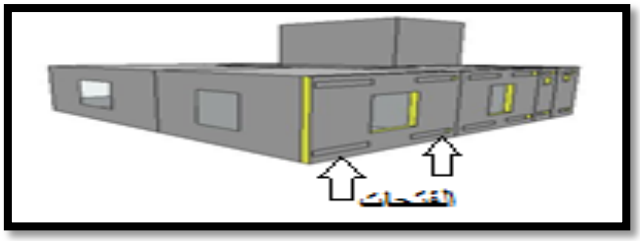

شكل(7):– اضافة الجدران المزدوجة من الخارج

شكل(8):- طريقة رفع الارضية المزدوجة لتكوين الحيز الهوائي السفلي وبالحالتين المغلفة والمفتوحة وبالطريقتين الجنوب/الشمال و الشرق/الغرب لتوجيه الفتحات.

KJPS Al-Kitab Journal for Pure Science
Vol.2 (2), ISSN: 2617-1260 (print), 2617-8141(online)
www.kjps.isnra.org

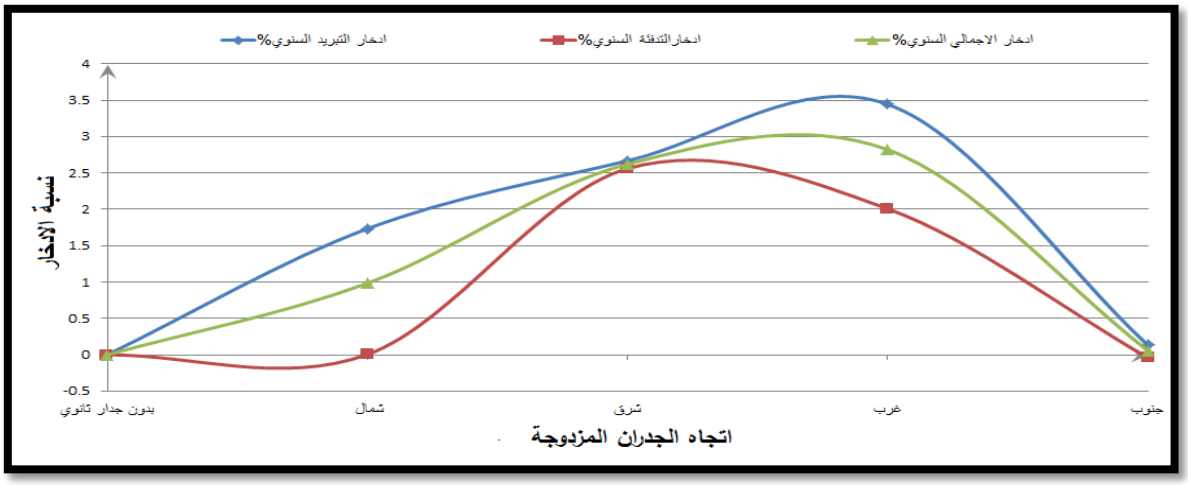

شكل(9):- العلاقة بين الجدران المزدوجة المستخدمة في الواجهات الاربعة مع نسبة الادخار السنوي في حمل التكييف السنوي.

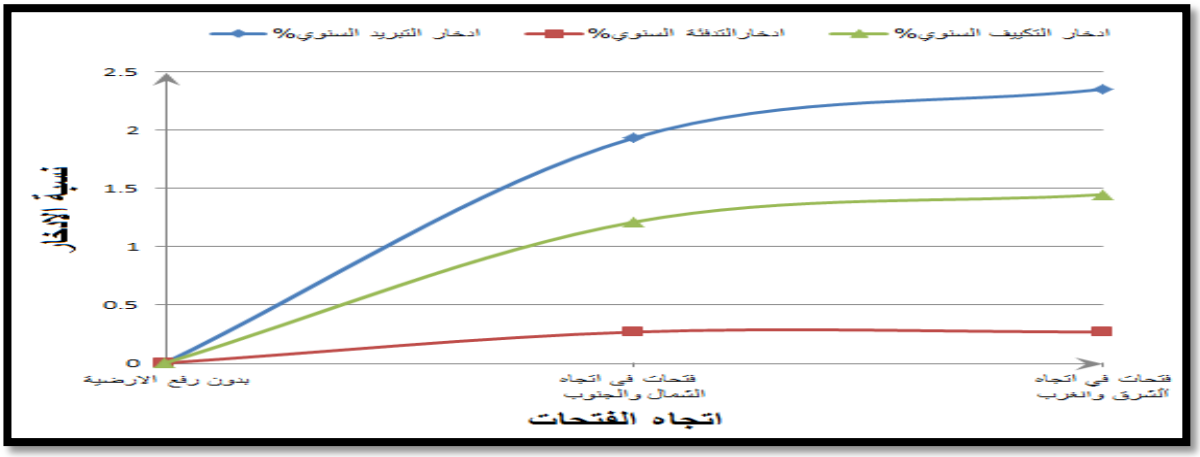

شكل(10):- العلاقة بين نسبة الادخار السنوي مع اتجاه الفتحات الارضية المزدوجة

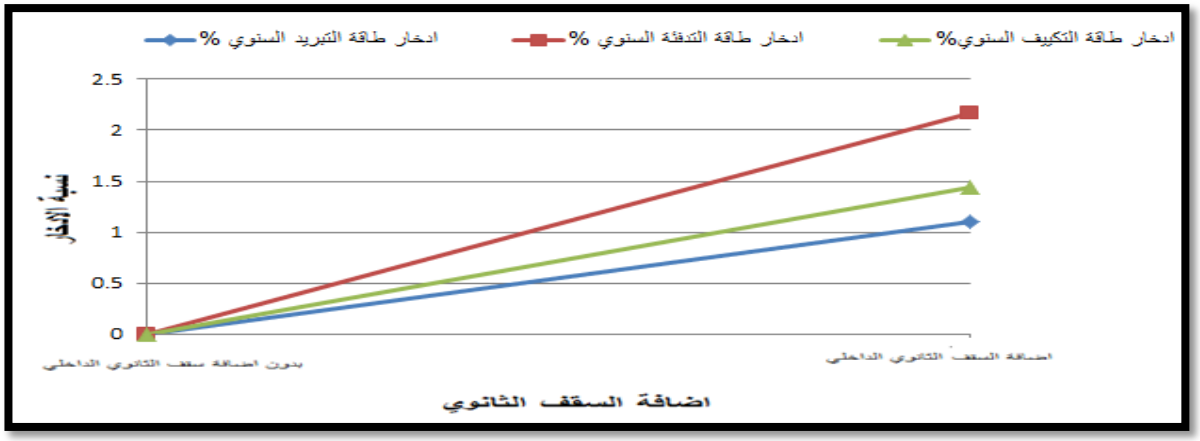

شكل(11):- العلاقة بين نسبة الادخار السنوي مع استخدام وعدم استخدام السقف الثانوي.

KJPS Al-Kitab Journal for Pure Science
Vol.2 (2), ISSN: 2617-1260 (print), 2617-8141(online)
www.kjps.isnra.org

DOI: http://10.32441/kjps.02.02.p18

تأثير عرض الفجوة الهوائية على الحمل الحراري الحر في جدار ترومب يحتوي على مادة متغيرة الطور

احسان فاضل عباس[1]، شيماء عدنان عزيز[2]
[1،2] قسم هندسة تقنيات التبريد والتكييف، الكلية التقنية /كركوك – الجامعة التقنية الشمالية، كركوك، العرارق
[1]ehsanfadhil@ntu.edu.iq

الخلاصة

تهدف الدراسة الحالية مدى تاثير عرض الفجوة الهوائية لمنظومة حرارية تحتوي على جدار ترومب على كل من تدفق الكتلي للهواء ونسبة الخزن الحراري، وذلك من خلال اجراء اختبارات على غرفة بأبعاد (1.5×1×1.5)م^3 مصنوع من الواح بلاستيكية محشوة بمادة عازلة، ويحتوي على جدار خازن للحرارة بابعاد (0.96×1.44×0.1)م^3 مصنوع من هيكل خشب ويحتوي 99 كبسولة من مادة الشمع الصناعي وبقطر (6) سم و طول(9.6)سم، موزعة داخل الهيكل على شكل مصفوفة (9×11)، حيث ثبت الجدار داخل الغرفة على سكلة حديدية من الجانبين ليتحرك بسهولة مسافة (10 الى 35)سم من الغطاء الزجاجي في جهة الجنوب. اجريت الاختبارات على هذه المنظومة في ظروف بيئية حقيقية خلال شهر كانون الاول 2016 لمدينة كركوك، حيث تضمنت الدراسة اختبار ست قياسات لعرض الفجوة الهوائية من (35 الى 10)سم بفرق 5 سم لكل مسافة عرض، وخصص لكل اختبار فترة خمسة ايام. واظهرت النتائج بان عرض الفجوة الهوائية له تاثير كبير على كمية التدفق الهواء خلاله و كمية دخول الطاقة الحرارية الى المنظومة، حيث كانت افضل حالة لعاملين عند العرض(35)سم. اما اعلى نسبة خزن للطاقة الحرارية خلال النهار حصلت عند العرض (15) وبلغت 45% من كمية الطاقة الداخلة الى المنظومة في الاختبارات التى في الايام المشمسة.

الكلمات الدالة: جدار ترومب، مواد متغيرة الطور، جدار خزن حراري

KJPS Al-Kitab Journal for Pure Science
Vol.2 (2), ISSN: 2617-1260 (print), 2617-8141(online)
www.kjps.isnra.org

The Impact of Air Gap Width on the Free Thermal Load in the Trombe Wall Contains a Phase Change Material

Ehsan F. Abbas1, Shayma A. Aziz2
Refrigeration & Air Conditioning Technical Eng. Dept., Kirkuk Technical College, Northern 1,2 Technical University, Kirkuk, Iraq
ehsanfadhil@ntu.edu.iq1

ABSTRACT

The objective of the present study is to investigate the effect of the air gap on the amount of mass flow rate and the ratio of energy storage in the thermal storage system containing a Trombe wall and that is through conducting experiments inside a room with dimensions of (1.5*1*1.5) m3, made of PVC sandwich insulation panel. The room contains a thermal wall of a dimension of (0.96*1.44*0.1) m3 made from a wood frame and contains 99 capsules of industrial wax of (6) cm diameter and (9.6) cm length, distributed by matrix form of (11*9). The wall is supported by four iron guides from both sides to move it easily in a distance of (10 to 35) cm from the glass cover in the south direction. The experiments have been conducted under real weather conditions of December 2016 for Kirkuk city, and this study included six widths of the air gap, arranged from (35 to 10) cm with steps of 5cm each. the results showed that the width of the air gap has a great effect on the mass flow rate through the air gap and energy incoming to the thermal system, where the best case for both factors was obtained at (b=35cm), and the max energy storage has been obtained at (b=15cm) and is about 45% of energy incoming to the system at the experiments of sunny days.

Keywords: **Trombe wall, Phase change materials, Thermal storage system.**

الرموز

A: مساحة m^2

b:عرض الفجوة الهوائية m

C: الحرارة النوعية $J/kg.^oC$

Cd: معامل احتكاك للنوافذ =0.6

KJPS Al-Kitab Journal for Pure Science
Vol.2 (2), ISSN: 2617-1260 (print), 2617-8141(online)
www.kjps.isnra.org

G: شدة اشعة الشمس W/m^2

H: البعد بين النافذتين m

h: معامل انتقال حرارة بالحمل $W/m^2.^oC$

k:الموصلية الحرارية $W/m.^oC$

$\dot{m}$: تدفق كتلي kg/s

Q: الطاقة الحرارية W. Hr

R: المقاومة الحرارية $^oC/W$

T: درجة الحرارة ^oC

U: معامل انتقال الحرارة الاجمالي $W/m^2.^oC$

u: سرعة الرياح m/s

x: السمك m

الرموز اللاتينية

α: الامتصاصية

ε: الانبعاثية

σ: ثابت ستيفان بولتزمان $5.669 \times 10^{-8} W/m^2.K^4$

1. المقدمة

تعد الطاقة من احدى المقومات الرئيسية للمجتمعات المتحضرة، وإن مجالات إستخدامها متنوعة ومتعددة، وزادت طلب عليها في السنوات الأخيرة، نتيجة الإرتفاع المتزايد في تكاليف إنتاج الوقود الأحفوري (النفط ، الغاز ، الفحم)، بسبب اسهام هذه المصادر بشكل فعال في تشكيل نمط حياتنا الحالية فضلا" عن محدودية هذه المصادر ومشكلات التلوث المرافقة لاستعمالها تتزايد يوما بعد يوم. لذلك إتفقت العلماء بأن الطاقة المتجددة هي الخيار الأفضل على الإطلاق، لأنها طاقة لاتستنفذ ويمكن ان تكون متاحة محليا" وإن مصادرها متعددة ومنها الطاقة الشمسية. حيث احد اهم استخدامات الطاقة الشمسية أنظمة التسخين الشمسي وهي عبارة عن أنظمة التدفئة الشمسية السلبية، حيث يتم جمع وتخزين الطاقة الشمسية

KJPS Al-Kitab Journal for Pure Science
Vol.2 (2), ISSN: 2617-1260 (print), 2617-8141(online)
www.kjps.isnra.org

بصورة طبيعية بدون تدخل الأجهزة ميكانيكية أو كهربائية في نقل الطاقة الحرارية، وتصنيف الى نظام الكسب الحراري المباشر ونظام الكسب الحراري غير مباشر. حيث ان جدار ترومب كما يعرف بالجدران التخزين أو التسخين بالطاقة الشمسية من أهم تطبيقات منظومة الكسب الحراري الغير مباشر، اذ يساهم هذا الجدار في تخفيض إستهلاك الطاقة في المباني الى حوالي 30%[1]. تصميم جدار ترومب يعود الى القرن التاسع الذي إبتكره مهندس امريكي (إدوارد مورس) الذي سجل براءة اختراع له في عام1881، تم تطويره بالكامل من قبل المهندس الفرنسي (Felix Trombe) والمهندس المعماري (Jacques Michel) في عام 1960 [2]. يتكون جدار ترومب الاعتيادي من مواد بناء الاعتيادي او من مواد متغيرة الاطوار و يغطى من الخارج بطبقة او طبقتين من الزجاج، يتم طلاء السطح الموجه الى الزجاج بلون أسود لزيادة معدل الإمتصاص وتحسين الأداء الحراري للجدار، ويفصل الجدار والزجاج مسافة لاتتجاوز30 سم لتدوير الهواء خلال النوافذ الموجودة اسفل و اعلى الجدار.اجريت عديد من الدراسات العلمية والتي تضمنت تطوير وتحسين الاداء الحراري لجدار ترومب من قبل الباحثين في عدد من الدول وبالاخص في الدول التي تكون الطقس فيها باردة، ومنهم الباحث (Bear 1973) [3] حيث قام ببناء منزل إستخدم فيه جدار ترومب يحتوي على مائة حاوية سعة الواحدة منها 55gal من الماء لغرض التدفئة. حيث اظهرت النتائج بان جدار ترومب المائي مناسب جدا" في تدفئة المنزل وبكفاءة عالية. اما الباحث (جمال حميد وهيب 2004)[4] فقد قدم دراسة نظرية على جدار ترومب يحتوي على نوعين من مواد متغيرة الطور الملح المائي ($Na_2HPO_4.12H_2O$) والشمع البرافين لغرض التدفئة في اجواء العراق. وأظهرت النتائج العملية بان المادتين قداعطت نتائج جيدة ومقاربة في عمليات التدفئة وساهما بنسبة 40% في ترشيد الطاقة المستهلكة. كما تمكن الباحث (عدنان محمد حسين 2008)[5] من تقديم دراسة نظرية على جدار ترومب مسامي يحتوي على حاويات معدنية مملوءة بالحجر كمستودع حراري مع احتوائه على فتحات في الجدار لتدوير الهواء وقرن نتائجة بنتائج بجدار ترومب مبني بالكونكريت وفي ظل الظروف البيئية لفصل الشتاء، استنتجت من الدراسة بأن الخزن الحراري في جدار المسامي أفضل من جدار كونكريتي. حيث تمكن الباحثان(Dehmani & Dimassi 2012)[6] من تقديم دراسة تطبيقية عن توزيع درجات الحرارة داخل الفجوة الهوائية لمنظومة الكسب الغير مباشر، اظهرت النتائج العملية بان درجات الحرارة في منطقة الفجوة الهوائية كانت مختلفة، والسبب يعود الى عدة عوامل منها الظروف المناخية، تأثير الإرتفاع الجدار ترومب والإشعاع الشمسي، تأثير طول فجوة الهواء، اضافتا"الى نمط تدفق الهواء فجوة الهواء. اما الباحث(Whaib 2001)[7] فقد قدم دراسة نظرية للمقارنة بين المنظومات التدفئة التي تعمل بالإسلوب السلبي من خلال استخدام ثلاثة انواع مختلفة من المواد البناء هذا جدار ترومب وهي (الكونكريت ، جدار مائي و(ماء وكونكريت)).من النتائج التي حصلت عليها، إستنتجت بأن جدار (الماء + الكونكريت) تعطي نتائج أفضل للخزن الحراري من الجدارين الاخرين. في حين قام الباحثان (Khalifa.& Abbas 2009)[8] بإجراء دراسة نظرية لمقارنة الاداء الحراري لتخزين مواد المستخدمة في التدفئة وذلك من خلال استخدام ثلاثة انواع مختلفة من مواد لبناء جدار ترومب وهي الكونكريت بسمك 20 سم والملح المائي($CaCl_2.6H_2O$) بسمك 8 سم والاخير من الشمع بسمك 5 سم. بينت من النتائج التي حصلت عليها، ان جدار الملح المائي قد اعطى درجات الحرارة قريبة من درجة حرارة الراحة وتراوحت بين °C (18-22) بالمقارنة مع النوعين الآخرين، حيث تراوحت درجات الحرارة الغرفة °C (15-25). الباحثان (Ajib & Jaber 2011)[9] قدما دراسة لتحسين الاداء الحراري لمبنى استخدم فيه جدار ترومب من الكونكريت بسمك 20 سم، واستخداما برنامج TRNSYS

KJPS Al-Kitab Journal for Pure Science
Vol.2 (2), ISSN: 2617-1260 (print), 2617-8141(online)
www.kjps.isnra.org

لمحاكاة ولتحليل اداء الحراري لجدار ترومب . حيث استنتج من الدراسة بان جدار ترومب يساهم بخفض إستهلاك الطاقة في المباني الى 32.1% من احتياجات المبنى الى التدفئة سنويا . اما الباحثان (Abbas & Chaichan 2015)[10] تمكنا من تقديم دراسة تطبيقية على جدار ترومب لتحسين الادائه الحراري باستخدام مادة الشمع وضعت داخل أنابيب من الالمنيوم و طليت سطحه الخارجي باللون الاسود وغطيت الانابيب من الخارج بطبقة من الزجاج بسمك 3 ملم بالإضافة الى وضع مروحة صغيرة في فتحة العلوية لزيادة دوران الهواء في المنظومة ، اظهرت من النتائج بان استخدام شمع البرافين يعطي نتائج جيدة من حيث الاداء الحراري للمنظومة.

الهدف من الدراسة الحلية هو تاثير عرض الفجوة الهوائية على كمية تدفق الهواء فيها، وألاداء الحراري لجدار ترومب الذي يحتوي على كبسولات من الشمع الصناعي في ست عروض للفجوة الهوائية حيث تراوحت من (35 الى 10)سم بفرق 5 سم لكل عرض، في غرفة بأبعاد (1.5*1.5*1)م^3 وفي ظل ظروف مناخية لمدينة كركوك كانون الاول2016.

2. الجزء النظري

لتحليل الطاقات الحرارية داخل المنظومة والناتجة من سقوط اشعة الشمس على جدار ترومب والتي تحولت الى طاقة حرارية وتنقل بمختلف طرق انتقال الحرارة (التوصيل ، الحمل و الاشعاع) داخل المنظومة، لذا فقد اجريت اتزان حراري لانتقال الحرارة داخل وخارج المنظومة وذلك لحساب كمية الطاقة الحرارية التي تم خزنها من قبل جدار الترومب في مادة المتغيرة الطور(الشمع الصناعي)، وكما في ادناه

$$Q_s = Q_{in} - (Q_{ven} + Q_l + Q_{con}) \quad \text{.....(1)}$$

حيث ان كمية الطاقة الداخلة الى المنظومة من خلال كمية الاشعاع العابر من الزجاج وممتص من جدار ترومب و الممتص من قبل الزجاج نفسه يساوي:

$$Q_{in} = GA(\alpha + \varepsilon_w \tau) \quad \text{.....(2)}$$

اما كمية الطاقة الحرارية التي تكتسب من الفجوة الهوائية والتي يؤدي الى دوران الهواء بالحمل الحر وتسمى بطاقة التهوية وتحسب كما في ادناه:

$$Q_{ven} = \dot{m}C(T_o - T_i) \quad \text{.....(3)}$$

ولحساب كمية الطاقة الحرارية المفقودة من المنظومة الى المحيط من جهة الجنوب فانها تحسب كما في ادناه:

$$Q_l = UA(\bar{T}_w - T_\infty) \quad \text{.....(4)}$$

$$U = \frac{1}{\sum R_{th}} \quad \text{.....(5)}$$

$$\sum R_{th} = \frac{1}{h_o} + \left(\frac{x}{k}\right)_g + \frac{(h_g + h_w)\cdot h_r}{h_g + h_w + h_r} \quad \text{.....(6)}$$

KJPS Al-Kitab Journal for Pure Science
Vol.2 (2), ISSN: 2617-1260 (print), 2617-8141(online)
www.kjps.isnra.org

$$h_r = \left[\frac{\sigma\left(T_{w,ga}^4 - T_{g,ga}^4\right)}{\frac{1}{\varepsilon g}+\frac{1}{\varepsilon w}-1}\right] \Big/ \left(T_{w,ga} - T_{g,ga}\right) \quad \text{.....(7)}$$

وكمية الطاقة الحرارية التي تنقل بالحمل الحر من السطح الداخلى الى داخل المنظومة ، فانها تساوي:

$$Q_{con} = h_{ro} A\left(T_{w,ro} - T_{ro}\right) \quad \text{.....(8)}$$

حيث ان كمية التدفق الكتلي داخل الفجوة الهوائية تحسب على اساس المصدر [11]

$$\dot{m} = \frac{C d \rho A_c}{\sqrt{1+\left(\frac{Ag}{Av}\right)^2}} \cdot \sqrt{\frac{2gH(T_m - T_{ro})}{T_m}} \quad \text{.....(9)}$$

اما لحساب معامل انتقال الحرارة على سطحي جدار ترومب من الداخل وجهة الفجوة الهوائية والزجاج فقد تم وفقا" للعلاقة التجريبية[12] في حساب معدل عدد النسلت وهي مناسبة لحالة المنظومة:

$$\overline{Nu}^{1/2} = 0.825 + \frac{0.387 Ra^{\frac{1}{6}}}{\left[1+\left(\frac{0.492}{Pr}\right)^{\frac{9}{16}}\right]^{\frac{8}{27}}} \quad \text{.....(10)}$$

حيث ان معدل معامل انتقال الحرارة يساوي:

$$h = \frac{\overline{Nu} \cdot k_a}{H} \quad \text{.....(11)}$$

معامل انتقال الحرارة خارج المنظومة احتسبت من العلاقة الرياضية الاتية [13]:

$$h_o = 5.2 + 4.1u \quad \text{.....(12)}$$

3. الجانب العملي

تم بناء غرفة الاختبار بأبعاد (1.5×1.0×1.5) م^3 من الالواح البلاستكية محشوة بعازل الفوم من جميع الاتجاهات عدا الاتجاه الجنوبي، حيث تم تثبيت طبقة من الزجاج بسمك 6 ملم بابعاد (1.4×0.9) م^2 لتغطية جدار ترومب، وكما مبين في الشكلين(1 و2). الجدارعبارة عن هيكل خشبي بأبعاد (9.6 × 94 × 143) سم^3 ويحتوي على 99 ثقب بقطر 63 ملم لحشر الكبسولات فيه و موزعة على شكل مصفوفة (9*11)، وكذلك يحتوي على اربع نوافذ مستطيلة الشكل بابعاد (7 × 25) سم وزعت بواقع نافذتين في اعلى واخريتين في الاسفل. وغلف وجهي الجدار بلوحين من الالمنيوم بابعاد (94 × 114) سم وسمك 2 ملم مع طلاء سطح الجدار باللون الاسود لغرض زيادة معدل الإمتصاص وتحسين أداء الحراري للجدار من

KJPS Al-Kitab Journal for Pure Science
Vol.2 (2), ISSN: 2617-1260 (print), 2617-8141(online)
www.kjps.isnra.org

جهة الفجوة الهوائية. حيث ثبت جدار ترومب على اربع سكك حديدية من جانبين لتسهيل حركته والحصول على قياس عرض للفجوة الهوائية بدقة. فقد تم استخدام مسجل بيانات درجات الحرارة ذي 32 قناة لتسجيل وخزن درجات الحرارة الياً" لداخل وخارج المنظومة الحرارية طلية فترة الاختبارات. اما بالنسبة لبيانات عن ظروف الطقس فقد اعتمد على بيانات محطة الانواء الجوية نوع HP2000 والقريبة من موقع الاختبار. حيث اجريت اختبارات على المنظومة الحرارية بست قياسات لعرض الفجوة الهوائية وهي (35، 30، 25، 20، 15، 10) سم، وقد خصصت فترة خمسة ايام لكل اختبار وسجلت درجات الحرارة للمنظومة و ظروف الطقس بشكل مستمر خلال فترات الاختبارات، وقد صادفت هذه الفترات ظروف بيئية مختلفة من حيث ايام مشمسة وغائمة وممطرة وكانت درجات الحرارة طلية فترة الاختبارات تقريبا" 15^oC في النهار ودون 5^oC في الليل.

4. النتائج والمناقشة

النتائج التي تم الحصول عليها من جراء الاختبارات على المنظومة الحرارية وتحت ظروف الطقس حقيقية خلال شهر كانون الاول 2016 في مدينة كركوك كما موضح في الشكل (3)، حيث يلاحظ فيه بان شدة اشعة الشمس خلال ذلك الشهر لم يتجاوز في معظم ايامه اكثر من ($400W/m^2$) عدا يومي (22 و29) منه، اذ بلغت شدة اشعة الشمس اعلى قيمة لها بحدود ($600W/m^2$)، اما ادنى شدة اشعة الشمس حصلت في يومي (23 و 24) منه وكانت اقل من ($100W/m^2$). و مدى درجات الحرارة لذلك الشهر تراوحت تقريبا" بين 5^oC) الى 15) لمعظم الايام فيه عدا الايام من الفترة (15 الى 21) من الشهر حيث صادفت فيها درجات حرارة متدنية مقارنتا" بالايام الاخرى في ذلك الشهر و تراوحت درجات الحرارة فيها ^oC (3 الى 9)، وكذلك الايام (22، 25، 29، 30) كانت فيها درجات الحرارة اعلى من 15^oC) خلال النهار، في حين سرعة الرياح خلال فترة الاختبارات لمعظم ايام الشهر لم يتجاوز km/Hr (15)، عدا الايام (1، 2، 4، 14، 24) حيث تجاوزت فيها تلك السرعة. بما ان فترة الاختبارات صادفت فيها تقلبلات جوية ، لذا فقد تم تحليل النتائج العملية على اساس يوم صحو جدا و يوم غائم كليا" او ممطرا"، وتاثيرها على كل من كمية تفق الهواء وكسب الطاقة الحرية للمنظومة.

أ- تاثير عرض الفجوة الهوائية على تدفق الهواء.

الشكلين(3 و4) يوضحان علاقة تدفق الهواء مع فرق درجات الحرارة بين طرفي الفجوة الهوائية لكل عرض للفجوة الهوائية للايام الصحوة والغائمة على التوالي، حيث لوحظ فيهما تاثير كبير للعاملين (b و ($T_{w,ga}$-$T_{g,ga}$)) على كمية تدفق الهواء في الحالتين، حيث كانت هنالك فرق كبير لكمية ($\dot{m}$) بين الايام المشمسة والغائمة لـ(b) والسبب يعود الى الفرق الكبير لـ($T_{w,ga}$-$T_{g,ga}$) فيهما. عند مقارنة كمية ($\dot{m}$) في الاختبارات ايام المشمسة وكما مبين في الشكل (3)، حيث اعظم مدى تدفق لـ($\dot{m}$) حصلت عند (b=35cm) وانخفضت تدريجيا" مع تصغير قياس(b). يلاحظ في الشكل (4) مدى-($T_{w,ga}$-$T_{g,ga}$) لم تكن متساوية لكل الاختبارات، لذا فقد تم اختيار اعلى قيمة مشتركة لفرق ($T_{w,ga}$-$T_{g,ga}$) لجميع الاختبارات وتقدرب(20^oC)، وكانت كمية ($\dot{m}$) لهم(0.0105، 0.0091، 0.0082، 0.0074، 0.006، 0.004) Kg/s لكل من (b=35cm الى b=10cm) وعلى التوالي. بينما كمية ($\dot{m}$) بالنسبة للأيام الغائمة كانت تقريبا" محدودة في الاختبارات وكما مبين في الشكل (**4**) والسبب يعود الى انخفاض شدة اشعة الشمس في هذه الايام حيث لم تتجاوز فيها ($100W/m^2$) مما ادت تقليل في مدي فرق درجات الحرارة ($T_{w,ga}$-$T_{g,ga}$) وهذا ما جعل من درجات الحرارة تكون متقاربة داخل

KJPS Al-Kitab Journal for Pure Science
Vol.2 (2), ISSN: 2617-1260 (print), 2617-8141(online)
www.kjps.isnra.org

المنظومة وخارجها. بالنظر لعدم شمول جميع الاختبارات بنفس مدى لـ($T_{w,ga}$-$T_{g,ga}$) ولاجل المقارنة بين كمية ($\dot{m}$) لجميع الاختبارات وللاسباب التي ذكرت انفا"، فقد تم اختيار قيمة مشتركة لفرق ($T_{w,ga}$-$T_{g,ga}$) بينهما وهي بحدود (4^oC) وكانت كمية ($\dot{m}$) لكل (b) هي (0.00445kg/s، 0.0045، 0.0034، 0.0045) لكل (20،25،30،35cm) على التوالي. حيث لم تظهر قيم لـ($\dot{m}$) عند (b=15cm) وذلك بسبب ظروف الطقس في يومي (22 و23) حيث كانت باردة جدا، وكذلك لم تظهر ايضا"عند (b=10cm) بسبب عدم مصادفة فترة الاختبار ايام غائمة.

ب- تحليل الطاقات الحرارية في المنظومة الخزن الحراري.

التحليل الاحصائي للطاقات الحرارية في المنظومة شملت يومين لكل اختبار على اساس ظرف الطقس أي يوم صحو جدا" و يوم غائم جدا" او ممطر، وعلى ضوء ذلك فقد تم اختيار الايام المشمسة لكل اختبار (4، 7، 12، 16، 23، 27) و الايام الغائمة (3، 8، 15، 19، 24،--) من شهر كانون الاول 2016 للقياسات (b) من (35cm الى 10cm) على التوالي. حيث يلاحظ في الشكل (5) بان اعلى كمية من الطاقة الحرارية قد دخلت الى المنظومة (Q_{in}) خلال النهار كانت عند (b=35cm) والتي بلغت (2845W.Hr)، بينما اقل كمية من (Q_{in}) خلال النهار قد دخلت الى المنظومة الحرارية كانت عند(b=10cm) والتي بلغت (1471.3W.Hr)، وهذه الكمية من الطاقة الحرارية تشكل حوالي 51.7% مما وصلت الى المنظومة في الحالة السابقة بالرغم من ظروف الطقس كانت تقريبا متقاربة فيهما، في حين كمية (Q_{in}) للحالات الاربعة كانت (2359.4W.Hr، 2012، 2067.3، 2234.2) للقياسات (b) من (30cm الى 15) على التوالي، حيث تحولت هذه الطاقة الى مجموعة من الطاقات في المنظومة ولكن بنسب مختلفة في كل اختبار وكما موضح في الجدول (1). واما بالنسبة الاختبارات التي اجريت في الايام الغائمة او الممطرة فان مستوى (Q_{in}) بشكل عام كانت متدنية كما مبين في الشكل (6)، حيث اعلى كمية من (Q_{in}) قد دخلت الى المنظومة كانت عند (b=35 cm) والتي بلغت بحدود (1593W.Hr)، في حين اقل كمية لها دخلت المنظومة كانت عند(b=15cm) والتي بلغت (428.3W.Hr)،في حين لم تظهر كمية (Q_{in}) عند عرض (b=10cm) وذلك لعدم مصادفة ايام غائمة في فترة اختبار عليه. حيث معظم كمية (Q_{in})قد تحولت الى(Q_s) وذلك بسبب ظروف الطقس والتي جعلت من بيئة المنظومة نوع من تقارب في درجات الحرارة فيها مع درجة حرارة الجو، اما بالنسبة تحويل (Q_{in}) الى طاقات حرارية اخرى داخل المنظومة فانها موضحة في الجول (2).

5. الاستنتاجات

من خلال استعراض النتائج التي تم الحصول عليها من المنظومة الحرارية التي تحتوي على جدار ترومب من مادة متغيرة الطور (الشمع الصناعي)، وفي ست قياسات مختلفة لعرض الفجوة الهوائية وتحت ظروف طقس حصو وغائم. حيث تلخصت اهم استنتاجات بمايلي:

أ- كمية $\dot{m}$ خلال الفجوة الهوائية في الايام المشمشة اعتمدت على عاملين وهما b و($T_{w,ga}$-$T_{g,ga}$) في حالة المسافة بين نوافذ التهوية تكون ثابتة، ولم يطابق هذا الاستنتاج على حالات الاختبار في الايام الغائمة وفي ($T_{w,ga}$-$T_{g,ga}$) اقل من (4^oC) فقط.

KJPS
Al-Kitab Journal for Pure Science
Vol.2 (2), ISSN: 2617-1260 (print), 2617-8141(online)
www.kjps.isnra.org

ب- كمية (Q_{in}) اعتمدت على المسافة (b) في ظرفين للطقس (الصحو و الغائم) حيث اكبر كمية من (Q_{in}) دخلت الى المظومة الحرارية في الظرفين عند(b=35cm)، كما اعلى كمية من (Q_s) حصلت عند (b=20cm) في في الايام المشمسة، ولكن في الايام الغائمة كانت معظم (Q_{in}) تتحول الى (Q_s) بسبب تقارب درجات الحرارة داخل المنظومة مع خارجها.

شكل (1) الصورة الف وتوغرافية يوضح الشكل الخارجي للمنظومة الحرارية و جدار ترومب من

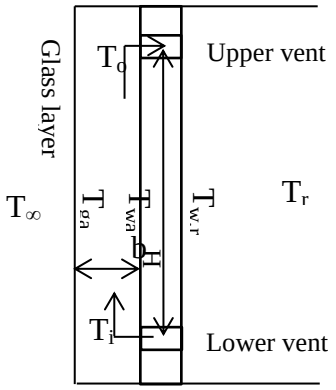

شكل (2) مخطط توضيحي لجدار ترومب في منظومة حرارية

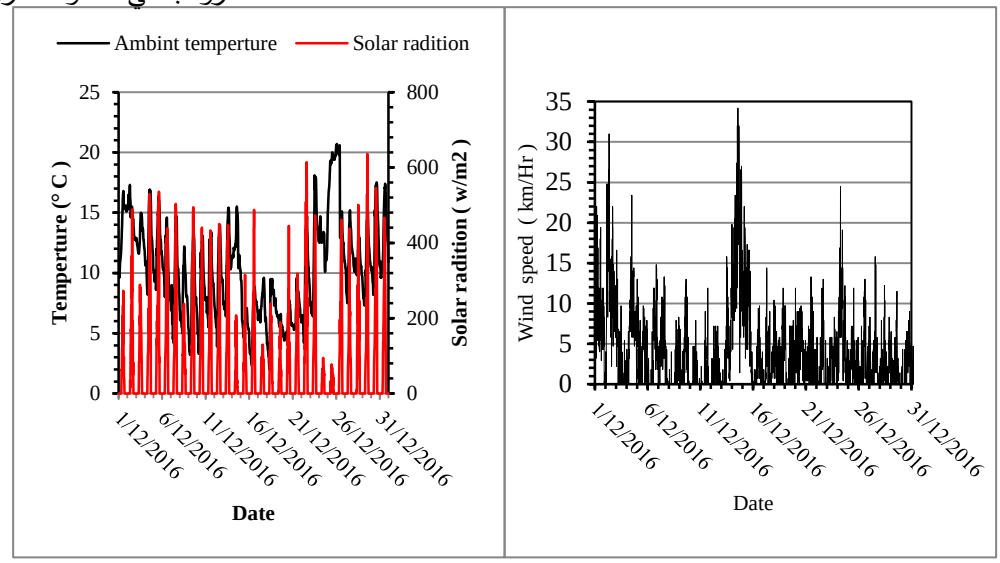

شكل(3) ظروف الطقس مدينة كركوك لشهر كانون الاول 2016

KJPS Al-Kitab Journal for Pure Science
Vol.2 (2), ISSN: 2617-1260 (print), 2617-8141(online)
www.kjps.isnra.org

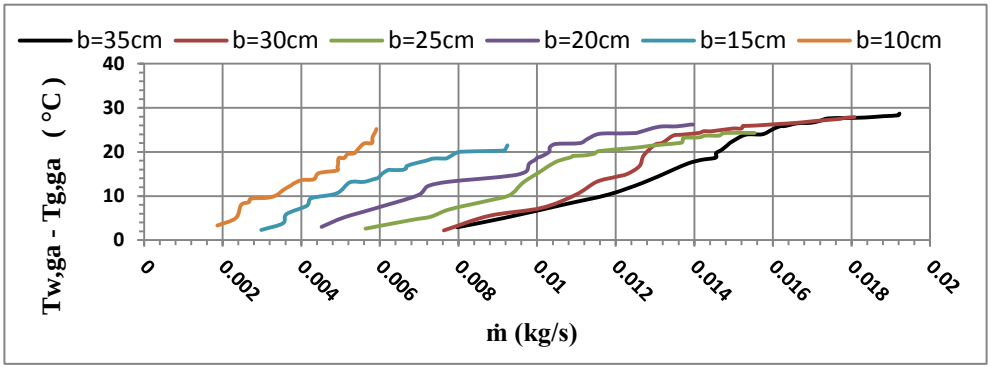

شكل(4) علاقة تدفق الهواء بدرجات الحرارة لسطحي الفجوة الهوائية لجدار ترومب في الايام المشمسة

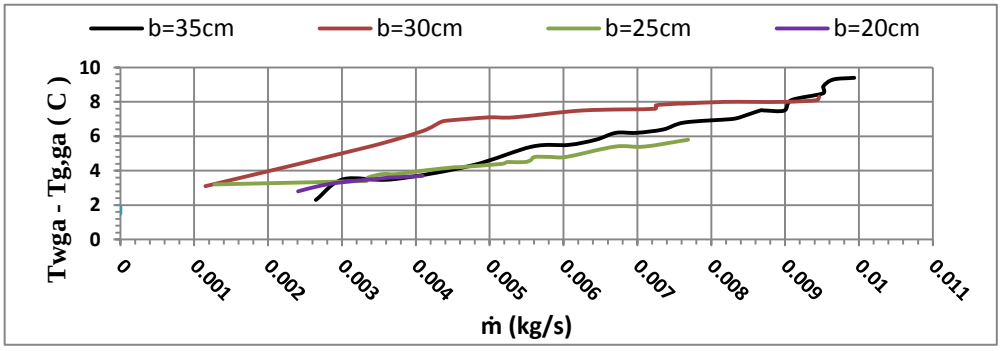

شكل(5) علاقة تدفق الهواء بدرجات الحرارة لسطحي الفجوة الهوائية لجدار ترومب في الايام الغائمة

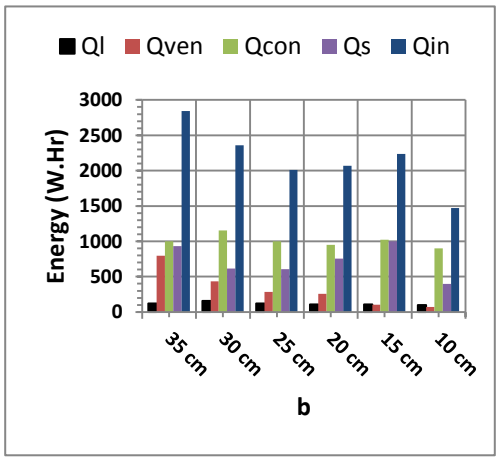

شكل(6) تمثل تحليل الأحصائي للطاقة داخل المنظومة الحرارية خلال النهار ليوم مشمس

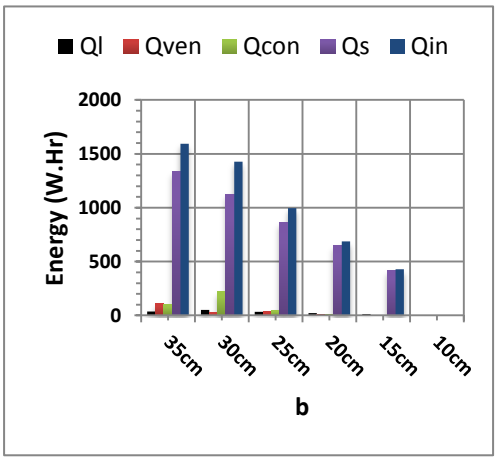

شكل(7) تمثل تحليل الأحصائي للطاقة داخل المنظومة الحرارية خلال النهار ليوم غائم

KJPS Al-Kitab Journal for Pure Science
Vol.2 (2), ISSN: 2617-1260 (print), 2617-8141(online)
www.kjps.isnra.org

جدول (1) نسب توزيع (Q_{in})- الى طاقات اخرى داخل المنظومة الحرارية في الايام المشمسة

Energu Type	Width of Air Gap (b cm)					
	35	30	25	20	15	10
Q_s	33%	26%	30%	37%	27%	27%
Q_{con}	35%	49%	50%	46%	61%	61%
Q_{ven}	28%	18%	14%	12%	5%	5%
Q_l	4%	7%	6%	5%	7%	7%

جدول (2) نسب توزيع (Q_{in})- الى طاقات اخرى داخل المنظومة الحرارية في الايام الغائمة و الممطرة

Energu Type	Width of Air Gap (b cm)					
	35	30	25	20	15	10
Q_s	84%	79%	87%	95%	97%	-
Q_{con}	7%	15%	5%	1%	0	-
Q_{ven}	7%	2%	3%	1%	0	-
Q_l	2%	4%	5%	3%	3%	-

المصادر

[1] Fang X, and Yang T.,"***Regression Methodology for Sensitivity Analysis of Solar Heating Walls***", Applied Thermal Engineering, vol. 28,(17-18), pp. 2289-2294 (2008).

[2] Duffie J. and Beckman W., ***"Solar Engineering of Thermal Processes "***, 4th edition, John Wiley and Sons, Inc. (2006).

[3] Bare,S., ***"The Drum wall In proceedings of the Solar Heating and Cooling for Buildings Workshop***", National Science Foundation, Washington, DC, pp.186-187 (1973).

[4] جمال حميد وهيب، " ***استخدام الأملاح والشمع كمواد خزن الحراري في جدار ترومب*** " مجلة التقني، المجلد (17) ، العدد (1) ص 110-117(2004) .

[5] عدنان محمد حسين،"***دراسة نظرية للحمل الحر الطباقي خلال جدار ترومب مسامي بإستخدام الطاقة الشمسية السلبية***" مجلة التقني، المجلد(21)، العدد 1، ص 140-150 (2008) .

[6] Dimassi N. and Dehmani L., ***"Natural Convection of a Solar wall in a Test Room Under Tunisian Climate"***, ISRN Renewable Energy Volume 2012, Article ID 573176, 9 pages doi:10.5402/2012/573176 (2012).

[7] Whaib J.H., ***"Comparative Study of Thermal Performance For Various Heating System Which are Acting Passively"***, Journal of the Iraqi Eng. Research, serial-148, (4), pp.(50-66) (2001).

[8] Khalifa A.J.N. and Abbas E.F., ***"A Compartive Performance Study of Some Thermal Storage Materials Used for Solar Space Heating"***, Energy and Building, Vol 41,(4),pp.407-415. (2009).

[9] Jaber S.and Ajib S., ***"Optimum technical and energy efficiency design of Residential building in Mediterranean region"***, Energy and Buildings, Vol.43 (8), pp.1891-1834 (2011).

[10] Chaichan M. T. and Abbas K. I., ***"Performance Amelioration of a Trombe Wall by Using Phase Change Material (PCM)"***, Engineering and Technology Vol.2, (4), pp 1-6 (2015).

[11] Bansal N. K., Mathur R., Bhandari M.S., ***"Solar chimney for enhanced stack ventilation***", Building and Environment, Vol.28,(3), pp.373-377. (1993).

[12] Churchill S.W. and Chu H.H.S., ***"Correlating equations for laminar and turbulent free convection from a vertical plate"***, International Journal of Heat and Transfer, Vol. 18,(11), pp.1323-1329 (1975).

[13] Abbas E. F. "***A Comparative Performance Study of Some Thermal Storage Materials Used for Solar Space Heating***", (Master's thesis, University of Technology, Baghdad, Iraq). (1999).

KJPS Al-Kitab Journal for Pure Science
Vol.2 (2), ISSN: 2617-1260 (print), 2617-8141(online)
www.kjps.isnra.org

DOI: http://10.32441/kjps.02.02.p19

حساب خسائر الطاقة المتاحة في محطة قدرة غازية وبيان تأثير تغير درجة حرارة المحيط عليها

الدكتور سعاد حسن دانوك
استاذ مساعد
الكلية التقنية/كركوك
telebshebab@yahoo.com

يحيى حمد الله حسين
طالب ماجستير
الكلية التقنية/كركوك
almuntezer92@gmail.com

الخلاصة: لغرض تحديد كمية ونوعية الخسائر في الطاقة الممكن الاستفادة منها في انتاج الشغل, اجري هذا التحليل لحساب الطاقة والطاقة المتاحة بالاستناد للقانون الاول والثاني للديناميكا الحرارية. حيث تم دراسة تأثير تغير درجة حرارة المحيط على اداء التوربين. بينت النتائج زيادة في خسائر الطاقة المتاحة في التوربين ككل وفي كل جزء من اجزائه الثلاثة(ضاغط الهواء, غرف الاحتراق والتوربين الغازي) مع زيادة درجة حرارة المحيط. كما بينت النتائج انه وبثبوت الحمل للمحطة, فان خسائر الطاقة المتاحة تكون اكبر في درجات الحرارة العالية منها في درجات الحرارة الواطئة. تركزت خسائر الطاقة المتاحة في غرف الاحتراق حيث كانت نسبة الخسائر في غرف الاحتراق الى الخسائر الكلية في التوربين(87%) يليها ضاغط الهواء بنسبة(9%) بينما كانت خسائر الطاقة المتاحة في التوربين الغازي هي الاقل(4%).

الكلمات الدالة: الطاقة المتاحة, خسائر الطاقة المتاحة, اداء التوربين الغازي

KJPS Al-Kitab Journal for Pure Science
Vol.2 (2), ISSN: 2617-1260 (print), 2617-8141(online)
www.kjps.isnra.org

Exergy destruction calculation in gas turbine power plant and showing the effect of ambient temperature on it

Dr.Suad Hassan Danook
Assistant Professor
Technical College/Kirkuk

Yahya H. Hussein
MSc student
Technical College/Kirkuk

telebshebab@yahoo.comalmuntezer92@gmail.com

Abstract: The purpose of this paper is to estimate the quantity and quality of the useful energy that could be converted to work, this analysis was carried out based on the energy and exergy analysis by using the first and second laws of thermodynamics. This paper study the effect of varying the ambient temperature on the performance of the turbine. Results showed increasing in exergy destruction in the turbine solely and in each of its three components(Air compressor, Combustion chambers and the gas turbine) with increasing in ambient temperature. Also results showed by keeping the load unchanged, the exergy destruction are bigger in higher ambient temperatures than in lower ones. The exergy destruction concentrated in the combustion chambers, where the percent of exergy destruction in the combustion chambers to the total exergy destruction in the plant was(87%) followed by the air compressor(9%) and the lower exergy destruction was in the gas turbine(4%).

Key words: Exergy, Exergy Destruction, Gas Turbine Performance

KJPS Al-Kitab Journal for Pure Science
Vol.2 (2), ISSN: 2617-1260 (print), 2617-8141(online)
www.kjps.isnra.org

1) المقدمة(Introduction):

1_1)**الغرض من البحث**: يعتبر قطاع انتاج الطاقة الكهربائية من القطاعات المهمة والحساسة جدا خصوصا في البلدان النامية ومنها العراق. حيث انه وعلى الرغم من شحة تزويد الطاقة الكهربائية في معظم محافظات البلد, فان زيادة التضخم السكاني يزيد العبء على محطات القدرة الكهربائية.

ان نوعية الطاقة المفيدة هي الطاقة الممكن تحويلها الى شغل لأجل انتاج الطاقة الكهربائية. وهذه الطاقة التي من الممكن الاستفادة منها وتحويلها الى شغل ميكانيكي يطلق عليها اسم الطاقة المتاحة(Availability) او الاكسيرجي(Exergy). ان هذه الطاقة المتاحة في اغلب العمليات الحقيقة(غير النظرية) قد تعاني بعض الانحلال نتيجة وجود عدة اسباب التي تؤدي لذلك وتجعل العملية غير انعكاسية وبهذا تتولد الانتروبيا(Entropy) والتي تمثل مقياس للطاقة الغير منتظمة والتي فقدت حضها في انتاج الشغل. وتسمى الاسباب التي تؤدي لهذا الانحلال في الطاقة باللاانعكاسيات. وهي عبارة عن عوامل تشتيت للطاقة المتاحة تؤدي الى ضياع فرصت تحول هذا الجزء من الطاقة الضائعة الى شغل. ولغرض تشخيص مواقع الخسائر في الطاقة المتاحة لزيادة الانتاج وبخسائر اقل وبالتالي زيادة كفاءتها وتحسين اداء المحطة, تم اجراء هذا التحليل. ان اجراء تحليل الطاقة المتاحة وخسائرها هو عبارة عن مزج للقانون الاول والثاني للديناميكا الحرارية, لكون القانون الاول لا يعطي اشارة لنوعية الطاقة المفقودة وانما فقط كمية الطاقة المتحولة, في حين يعطي القانون الثاني مؤشر على نوعية الطاقة وهو مهم جدا لغرض الوقوع على اسباب الخسائر التي تحصل وبحث مسبباتها واعطاء التوصيات لغرض تقليلها[16,15,14,13,11,5,4,3,1]. ومن اجل تحديد كمية ونوعية الخسائر في الطاقة المتاحة وتأثرها بدرجة حرارة المحيط, ومعرفة اسبابها وكيفية التقليل منها اجري هذا البحث.

1_2)ادبيات البحوث السابقة: هنالك العديد من البحوث التي درست تأثير تغير درجة حرارة المحيط على خسائر الطاقة المتاحة. ففي البحث[9] وجد الباحثون ان زيادة درجة حرارة المحيط تؤدي الى زيادة خسائر الطاقة المتاحة في كل جزء من اجزاء دورة التوربين الثلاثة(ضاغط الهواء, غرفة الاحتراق والتوربين الغازي). في البحث[7] وجد الباحث انه وبزيادة درجة حرارة المحيط تزداد خسائر الطاقة المتاحة في التوربين الغازي وتقل في ضاغط الهواء. اما في بحث[12] فان تأثير تغير

KJPS Al-Kitab Journal for Pure Science
Vol.2 (2), ISSN: 2617-1260 (print), 2617-8141(online)
www.kjps.isnra.org

درجة الحرارة للمحيط لم يكن ذو اهمية. اما في بحث[2] فقد وجد الباحثان زيادة في خسائر الطاقة المتاحة في كل من ضاغط الهواء والتوربين الغازي, وفي نفس الوقت انخفاض في خسائر الطاقة المتاحة في غرفة الاحتراق. في بحث[10] وجد الباحث انخفاض في خسائر الطاقة المتاحة في كل جزء من اجزاء التوربين الثلاثة(ضاغط الهواء, غرفة الاحتراق والتوربين الغازي) بارتفاع درجة الحرارة من(0_50) درجة مئوية عند حمل 100%. بحث[6] وجد الباحثان ان خسائر الطاقة المتاحة عندما تكون درجة حرارة المحيط منخفضة اقل من خسائر الطاقة المتاحة في درجات الحرارة العالية للمحيط. واخيرا, فبين البحث[17] ان بزيادة درجة حرارة المحيط تزداد خسائر التوربين الغازي بشكل صغير, وتقل في ضاغط الهواء.

ملخص ادبيات البحوث السابقة: نلاحظ من خلال استعراض نتائج البحوث السابقة اختلافات في النتائج. بالمجموع فان عدد البحوث التي وجدت ارتفاع في خسائر الطاقة المتاحة في ضاغط الهواء مع زيادة درجة حرارة المحيط هي ثلاثة[9,6,2] والتي وجدت انخفاض في خسائر الطاقة المتاحة ايضا ثلاثة[17,10,7], اما بالنسبة لخسائر الطاقة المتاحة في غرفة الاحتراق فقد وجدت البحوث[9,6] زيادة فيها بزيادة درجة حرارة المحيط بينما وجدت البحوث[10,2] انخفاضها. واخيرا, فان اغلب البحوث[17,9,7,6,2] وجدت ارتفاع في خسائر الطاقة المتاحة في التوربين الغازي مع زيادة درجة حرارة المحيط.

2) وصف المحطة والبيانات المأخوذة منها:

2_1) وصف المحطة(Plant Description):

تتكون محطة القدرة الغازية التي تقع في محافظة كركوك في شركة نفط الشمال من توربين متكون من ثلاثة اجزاء رئيسية(ضاغط الهواء, غرف الاحتراق والتوربين الغازي) والمبينة في الشكل رقم(1) وهو من نوع MS5001 من انتاج شركة GE والقدرة التصميمية لأعلى حمل ممكن الوصول اليه تحت ظروف قياسية هي(23.75 ميكا واط) المحطة تتمثل بدورة برايتون مفتوحة ذات عمود ادارة واحد يربط كل من ضاغط الهواء مع التوربين الغازي مع علبة التروس(والتي ترتبط بدورها بالمولد الكهربائي)ووظيفة علبة التروس تعمل على تخفيض سرعة دوران عمود الادارة من (5000 دورة بالدقيقة) الى (3000 دورة بالدقيقة) لكي يتناسب مع السرعة التصميمية للمولد الكهربائي.

KJPS Al-Kitab Journal for Pure Science
Vol.2 (2), ISSN: 2617-1260 (print), 2617-8141(online)
www.kjps.isnra.org

2_2) جمع البيانات(Data Collection):

ان محطة القدرة الغازية التي تم دراستها لا تحتوي على جميع البيانات التي يمكن من خلالها اجراء تحليل للطاقة المتاحة بشكل مباشر, لذلك برزت الحاجة لفرض بعض الفرضيات لتقريب التحليل من الواقع. حيث سوف يتم فرض كل من التالي:

1_ضغط الهواء الداخل لضاغط الهواء ونواتج الاحتراق عند مخرج التوربين الغازي يساوي ضغط الهواء الجوي(1.01325 بار).

2_الكفاءة الكهربائية للمولد الكهربائي والميكانيكية للتوربين تساوي 98% لكل منهما.

اما بخصوص درجة الحرارة لنواتج الاحتراق عند مدخل التوربين الغازي فيحصل عليها من خلال اجراء موازنة للطاقة على غرف الاحتراق بعد فرض كمية الوقود المتدفق.

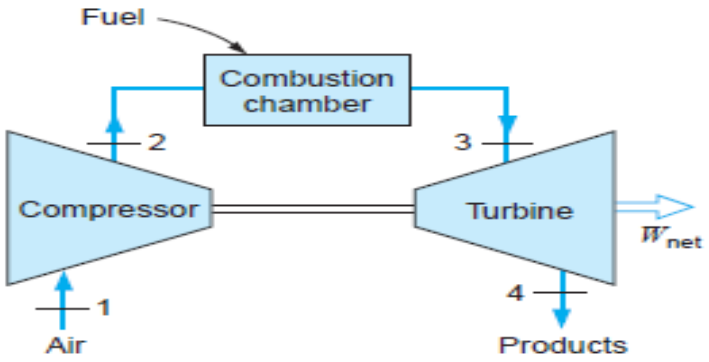

شكل(1): يبين الدورة مفتوحة والاجزاء الرئيسية الثلاثة للتوربين[5]

3) تحليل الطاقة المتاحة(Exergy Analysis):

1_3) المعادلات العامة(General Equations):

KJPS Al-Kitab Journal for Pure Science
Vol.2 (2), ISSN: 2617-1260 (print), 2617-8141(online)
www.kjps.isnra.org

تتكون الطاقة المتاحة من عدة مكونات وهي الطاقة المتاحة الفيزيائية, الطاقة المتاحة الكيميائية, الطاقة المتاحة الحركية والطاقة المتاحة الكامنة. وتعطى بالقانون التالي[11,8]:

$$\dot{E}_X = \dot{E}_X^{PH} + \dot{E}_X^{CH} + \dot{E}_X^{KN} + \dot{E}_X^{PT} \dots (1)$$

اما بالنسبة للطاقة المتاحة الكامنة والحركية فغالبا ما تكون قيمتها صغيرة جدا ولذلك يمكن اهمالها.

يمكن تمثيل الطاقة المتاحة الفيزيائية بالعلاقة التالية[11,5]:

$$\dot{E_X}^{PH} = \dot{m}[(h - h_0) - T_0(s - s_0)] = \dot{m}[C_{p,av}(T - T_0) - T_0(s - s_0)] \dots (2)$$

الحد الاخير من المعادلة يمثل التغير في الانتروبيا ويمكن حسابه من المعادلة التالية[10,7]:

$$s - s_0 = C_{p,av} \ln\frac{T}{T_0} - R\ln(\frac{P}{P_o}) \dots (3)$$

تحسب الحرارة النوعية عند متوسط درجة الحرارة بين الحالتين ومعادلتها عبارة عن دالة لدرجة الحرارة متعددة الحدود[5].

اما بالنسبة للطاقة المتاحة الكيميائية للوقود في غرفة الاحتراق فهنالك علاقة تقريبية تربط كل من الطاقة المتاحة الكيميائية مع القيمة الحرارية الصغرى(Lower heating value) مع عدد ذرات الكاربون والهيدروجين في المركب, وللطور الغازي فإنها تكون بالصيغة التالية[3]:

$$\frac{\bar{e}_{x_i}^{ch}}{LHV_i} = 1.033 + 0.0169\frac{b}{a} - \frac{0.0698}{a} \dots (4)$$

حيث يمثل(a) عدد ذرات الكاربون في المركب و(b) عدد ذرات الهيدروجين في المركب.

لا يوجد هنالك طاقة متاحة كيميائية في ضاغط الهواء كون تركيب الهواء فيه مشابه لتركيبه في الهواء الجوي. اما بالنسبة للتوربين الغازي فسيكون هنالك جزء صغير من الاختلاف نتيجة احتراق الوقود واستهلاك جزء من الاوكسجين وانتاج ثنائي اوكسيد الكاربون وبخار الماء, وتحسب الطاقة المتاحة الكيميائية لنواتج الاحتراق من المعادلة التالي[11]:

KJPS Al-Kitab Journal for Pure Science
Vol.2 (2), ISSN: 2617-1260 (print), 2617-8141(online)
www.kjps.isnra.org

$$\bar{e}_{x_3}{}^{ch} = \sum_{i=1}^{j} y_i \, \bar{e}_{x_i}{}^{ch} + \bar{R}T_0 \sum_{i=1}^{j} y_i \ln y_i \ldots (5)$$

2_3) موازنة الطاقة المتاحة وحساب خسائرها(Exergy Balance and Destroyed):

لحساب خسائر الطاقة المتاحة, نجري موازنة الطاقة المتاحة على كل جزء من اجزاء التوربين. تتمثل المعادلة العامة لموازنة الطاقة المتاحة بالمعادلة التالية[15,13,11,8,5,3,1]:

$$\frac{dE_{X,cv}}{dt} = \sum_{j} (1 - \frac{T_0}{T_j}) \dot{Q}_j - \dot{W}_{cv} + \sum_{i} \dot{m}_i \, e_{x,i} - \sum_{e} \dot{m}_e \, e_{x,e} - \dot{E}_{X,D} \ldots (6)$$

وبفرضية الحالة المستقرة(steady state) فلن يكون هنالك تراكم للطاقة المتاحة في النظام, وايضا بفرض ان جميع العمليات التي تتم في اجزاء التوربين الثلاثة تكون اديباتية(Adiabatic), وبعد اعادة ترتيب المعادلة اعلاه نحصل على المعادلة العامة التالية:

$$\dot{W}_{cv} = \sum_{i} \dot{m}_i \, e_{x,i} - \sum_{e} \dot{m}_e \, e_{x,e} - \dot{E}_{X,D} \ldots (7)$$

الان, سوف نقوم بتطبيق هذه المعادلة على الاجزاء الثلاثة للتوربين وكالتالي:

1_موازنة الطاقة المتاحة لضاغط الهواء:

ان اشارة الشغل لحجم السيطرة في معادلة(7) وضعت بفرضية كون الشغل ينتج من النظام, اما في حالة كون الشغل ينتج على النظام فيكون بالإشارة السالبة, وبهذا بعد تغيير اشارة الشغل في الحد الايسر الى الاشارة السالبة ومن ضرب المعادلة في سالب واحد نحصل على معادلة موازنة الطاقة المتاحة لغرفة الاحتراق التالية:

$$\dot{W}_c = \dot{E}_{X,2} - \dot{E}_{X,1} + \dot{E}_{X,D,c} \ldots (8)$$

ولحساب خسائر الطاقة المتاحة نطبق القانون التالي:

$$\dot{E}_{X,D,c} = \dot{m}_a * T_0 * (s_2 - s_1) \ldots (9)$$

KJPS Al-Kitab Journal for Pure Science
Vol.2 (2), ISSN: 2617-1260 (print), 2617-8141(online)
www.kjps.isnra.org

2_موازنة الطاقة المتاحة للتوربين الغازي:

بالاستعانة بمعادلة(7) مع تعويض ما يماثل كل حد نحصل على معادلة موازنة الطاقة المتاحة للتوربين الغازي كالتالي:

$$\dot{W}_t = \dot{E}_{X,3} - \dot{E}_{X,4} - \dot{E}_{X,D,t} \dots (10)$$

ولحساب خسائر الطاقة المتاحة نطبق القانون التالي:

$$\dot{E}_{X,D,t} = \dot{m}_g * T_0 * (s_4 - s_3) \dots (11)$$

3_موازنة الطاقة المتاحة لغرف الاحتراق:

باستعمال معادلة (7) مع التعويض عن الحد الايسر من المعادلة بقيمة صفر لعدم وجود شغل منتج او مستهلك في غرف الاحتراق, وتعويض عن مدخلات الطاقة المتاحة ومخرجاتها بما يساويها, نحصل على المعادلة التالي لخسائر الطاقة المتاحة في غرفة الاحتراق:

$$\dot{E}_{X,D,cc} = \dot{E}_{X,2} + \dot{E}_{X,f} - \dot{E}_{X,3} \dots (12)$$

4) النتائج والمناقشة(Results and Discussion):

تم اجراء حسابات خسائر الطاقة المتاحة وقوانين الديناميكا الحرارية الاول والثاني بواسطة استخدام برنامج الماتلاب عن طريق كتابة برنامج بالاستناد الى القوانين التي ذكرت. في التحليل كانت درجة حرارة المحيط هي نفسها درجة حرارة الهواء الداخل لضاغط الهواء.

KJPS Al-Kitab Journal for Pure Science
Vol.2 (2), ISSN: 2617-1260 (print), 2617-8141(online)
www.kjps.isnra.org

جدول رقم(1):بيانات التحليل للطاقة

No.	T_1 °C	T_2 °C	T_3 °C	T_4 °C	T_f °C	P_2 Bar	P_f Bar	$\dot{m}_a$ kg/s	$\dot{m}_f$ kg/s
1	32.6	338	880.95	443	49.2	7.8	8.7	91.3524	1.4244
2	38.2	345	894.35	460	50.3	7.6	8.7	93.2977	1.4785
3	45.8	356	902.35	479	52.5	7.5	8.7	101.5832	1.6066
4	47	358	898.15	483	52.9	7.4	8.7	108.1819	1.6902

في جدول رقم(1) يوجد نوعين من البيانات, النوع الاول هو البيانات المحصول عليها مباشرة من المحطة والتي تشمل جميع البيانات عدا درجة حرارة نواتج الاحتراق عند مدخل التوربين المولد(T_3) والتدفق الكتلي للوقود($\dot{m}_f$) والتان تم الحصول عليهما من خلال فرضية نسبة الوقود وايجاد درجة الحرارة من خلال موازنة الطاقة المتاحة على غرفة الاحتراق.

جدول رقم(2):قيم انواع الطاقة المتاحة

No.	$\dot{E}_{X,1}^{PH}$ kW	$\dot{E}_{X,2}^{PH}$ MW	$\dot{E}_{X,f}^{PH}$ MW	$\dot{E}_{X,f}^{CH}$ MW	$\dot{E}_{X,3}^{PH}$ MW	$\dot{E}_{X,3}^{CH}$ MW	$\dot{E}_{X,4}^{PH}$ MW	$\dot{E}_{X,4}^{CH}$ MW
1	0	25.299	0.4312944	72.524	63.144	1.0295	15.033	1.0295
2	0	25.901	0.4551911	75.278	64.978	0.9609344	15.91	0.9609344
3	0	28.569	0.5061238	81.801	70.672	0.8734793	17.862	0.8734793
4	0	30.388	0.5344042	86.057	74.571	0.8812952	19.174	0.8812952

اما جدول رقم(2) فيبين الطاقة المتاحة بنوعيها الكيميائية والفيزيائية عند كل مدخل ومخرج في التوربين. حيث يبين الجدول كما تم ذكره سابقا نوعين من الطاقة المتاحة, ونلاحظ وجود نوع واحد للطاقة المتاحة وهو الطاقة المتاحة الفيزيائية في

KJPS Al-Kitab Journal for Pure Science
Vol.2 (2), ISSN: 2617-1260 (print), 2617-8141(online)
www.kjps.isnra.org

نقطة 1 و2 اي في مدخل ومخرج ضاغط الهواء لعدم وجود طاقة متاحة كيميائية نتيجة لعدم وجود اختلاف في التركيب لكل من النقطتين مع الهواء الجوي.

الان سوف نضع القيم التي تم الحصول عليها لخسائر الطاقة المتاحة في كل حالة للنظام. يبين الجدول رقم(3) خسائر الطاقة المتاحة في كل من ضاغط الهواء وغرف الاحتراق والتوربين الغازي بالإضافة الى الخسائر الكلية في المحطة.

جدول رقم(3):خسائر الطاقة المتاحة

No.	$\dot{E}_{X,D,c}(MW)$	$\dot{E}_{x,D,cc}(MW)$	$\dot{E}_{X,D,t}(MW)$	$\dot{E}_{X,D,T}(MW)$
1	3.6273	34.081	0.9636285	38.672
2	3.8087	35.696	1.1381	40.643
3	4.191	39.331	1.8279	45.35
4	4.5999	41.527	2.1913	48.318
Total	16.2269	150.635	6.1209285	-
Average	4.056725	37.65875	1.5302321	-

تم اخذ قيم متوسط خسائر الطاقة المتاحة في كل جزء لتبيان نسبة خسائر الطاقة المتاحة في كل جزء من هذه الاجزاء كمعدل للقراءات الاربعة.

تمت دراسة تأثير تغير درجات الحرارة للمحيط عند حمل عالي(17,5ميكا واط) اي ما يشكل نسبة(74%) تقريبا من الحمل الاقصى للمحطة.

في الشكل رقم(1) الذي يبين علاقة خسائر الطاقة المتاحة بدرجة حرارة المحيط نلاحظ زيادة خسائر الطاقة المتاحة في ضاغط العواء مع زيادة درجة الحرارة للمحيط. ان من اسباب الزيادة هو زيادة كمية الهواء الداخلة الى ضاغط الهواء

KJPS Al-Kitab Journal for Pure Science
Vol.2 (2), ISSN: 2617-1260 (print), 2617-8141(online)
www.kjps.isnra.org

وكذلك زيادة درجة حرارة الهواء الخارج من التوربين وانخفاض ضغط الهواء الخارج والذي يؤدي الى تحول جزء الطاقة الميكانيكية الى درجة حرارة اعلى وبالتالي زيادة الانتروبيا للهواء وبالتالي زيادة خسائر الطاقة المتاحة .

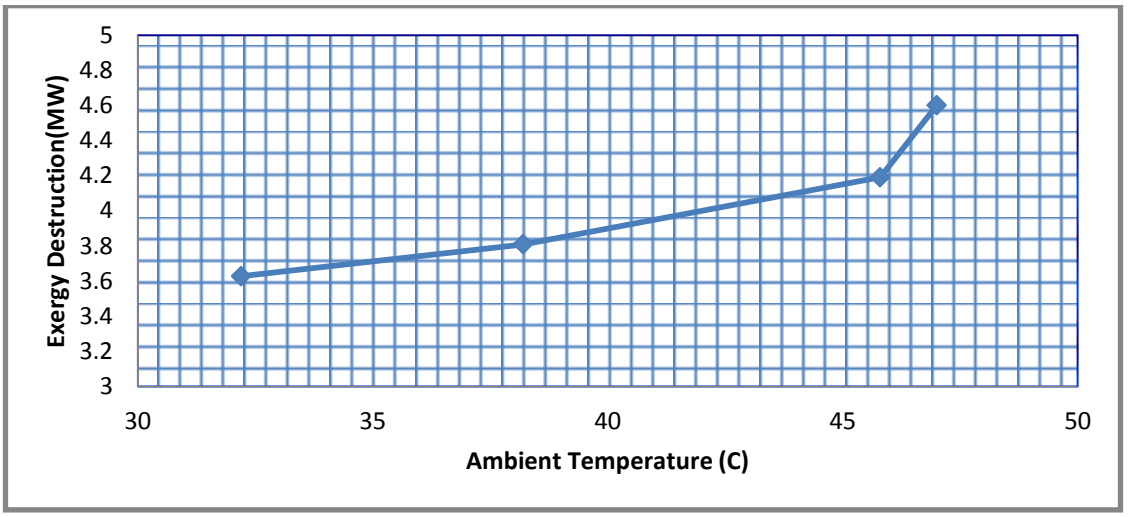

الشكل(2): يبين خسائر الطاقة المتاحة في ضاغط الهواء

حيث لوحظ ان الزيادة تكون اكبر في درجات الحرارة العالية. فبين القراءتين 1و2 فان زيادة درجة الحرارة درجة مئوية واحدة يؤدي الى زيادة خسائر الطاقة المتاحة بقيمة تقريبا 0,03 ميكا واط كمعدل, اما بين القراءتين 2 و3 فكانت القيمة اكبر من 0,05 ميكا واط واخيرا فكانت القيمة بين القراءتين 3 و4 اكبر من 0,34 ميكا واط لكل ارتفاع في درجة الحرارة درجة مئوية واحدة. الشكل رقم(2) الذي يبين علاقة خسائر الطاقة المتاحة بدرجة حرارة المحيط في غرف الاحتراق نلاحظ زيادة خسائر الطاقة المتاحة مع زيادة درجة الحرارة للمحيط. من التحليل الطاقة والطاقة المتاحة اللذان يظهران زيادة في معدل احتراق الوقود, وبسبب كون عملية الاحتراق غير انعكاسية وينتج عن هذه اللاانعكاسية انتروبيا والتي تقلل من الطاقة المفيدة والتي يمكن تحولها الى شغل, فان زيادة استهلاك الوقود سوف يتسبب بزيادة كمية الانتروبيا المتولدة وبالتالي زيادة خسائر الطاقة المتاحة بالإضافة الى انخفاض الضغط للهواء القادم من ضاغط الهواء وزيادة كمية الهواء المتدفق لغرف

KJPS Al-Kitab Journal for Pure Science
Vol.2 (2), ISSN: 2617-1260 (print), 2617-8141(online)
www.kjps.isnra.org

الاحتراق.

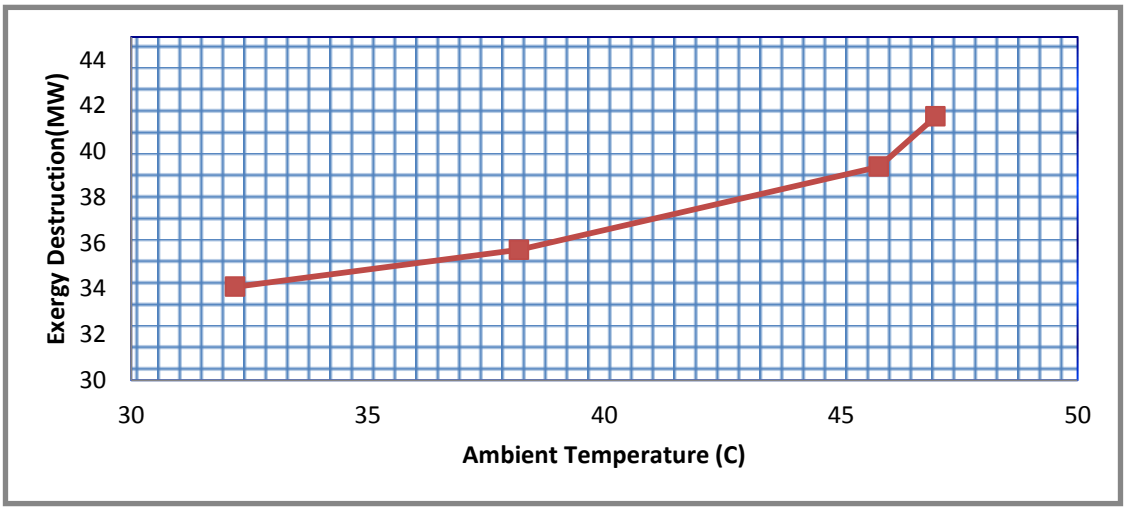

الشكل(3): يبين خسائر الطاقة المتاحة في غرف الاحتراق

كما في ضاغط الهواء, فان خسائر الطاقة المتاحة في غرف الاحتراق تكون في درجات الحرارة العليا اعلى منها في درجات الحرارة الصغرى. حيث بين القراءتين 1و2 كانت الخسائر تقريبا 0,29 ميكا واط, وكانت بين القراءتين 2و3 الخسائر 0,5 ميكا واط تقريبا واخيرا كانت 1,8 ميكا واط تقريبا بالمعدل بين القراءتين 3و4(طبعا لكل درجة حرارة مئوية وبالمعدل). الشكل رقم(3) يبين علاقة خسائر الطاقة المتاحة بدرجة حرارة المحيط في التوربين الغازي وكما في ضاغط الهواء وغرفة الاحتراق فان خسائر الطاقة المتاحة تزداد بزيادة درجة حرارة المحيط.

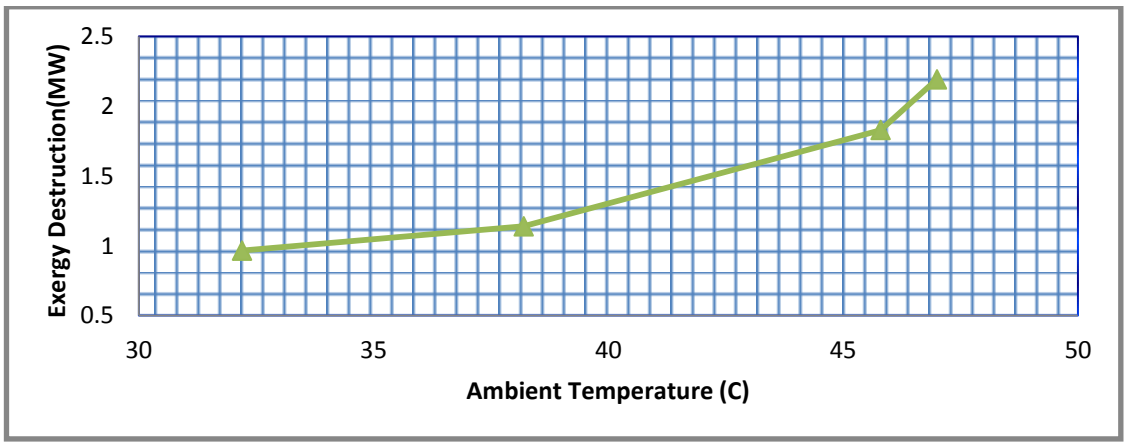

الشكل(4): يبين خسائر الطاقة المتاحة في التوربين الغازي

KJPS Al-Kitab Journal for Pure Science
Vol.2 (2), ISSN: 2617-1260 (print), 2617-8141(online)
www.kjps.isnra.org

كانت خسائر الطاقة المتاحة بين القراءات 1و2 وبعدها 2و3 واخيرا 3و4 لكل درجة حرارة مئوية تقريبا(0,03, 0,09 و0,3) ميكا واط بالمعدل على التوالي. كما هو الحال في كل جزء من اجزاء التوربين فان مجموع ذلك هو ايضا له نفس العلاقة بزيادة درجة الحرارة. حيث الشكل(4) يمثل هذه العلاقة وكانت الخسائر بين القراءات لكل درجة حرارة مئوية تقريبا(0,35, 0,6 و2,5) ميكا واط بالمعدل على التوالي.

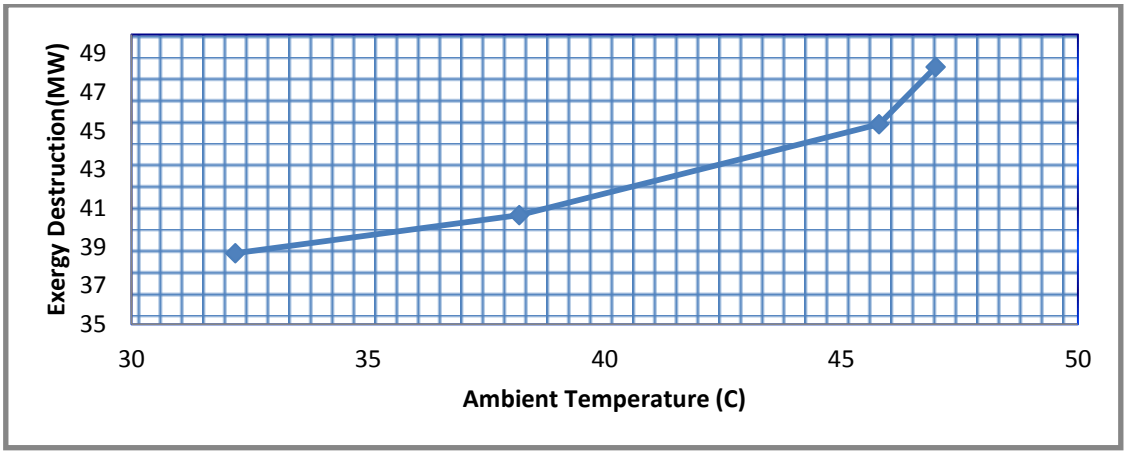

الشكل(5): يبن خسائر الطاقة المتاحة الكلية في التوربين

الشكل الذي يلي يمثل الخسائر في كل جزء من اجزاء التوربين بالإضافة للخسائر الكلية في التوربين.

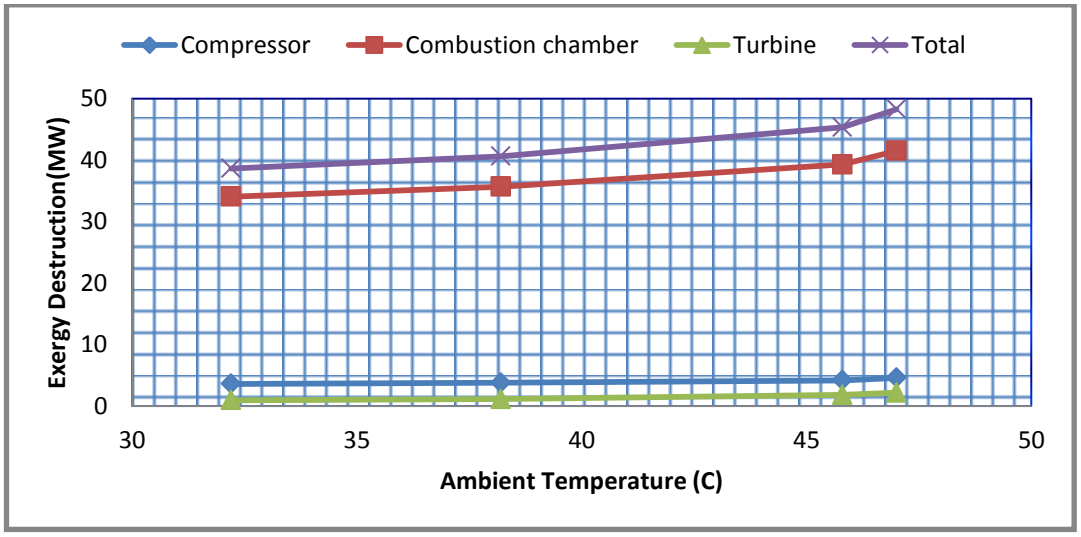

الشكل(6): العلاقة بين خسائر الطاقة المتاحة ودرجة الحرارة

KJPS Al-Kitab Journal for Pure Science
Vol.2 (2), ISSN: 2617-1260 (print), 2617-8141(online)
www.kjps.isnra.org

5) الاستنتاج(Conclusions):

تم اجراء تحليل للطاقة المتاحة لبيان اداء التوربين في محطة قدرة غازية لإنتاج الطاقة الكهربائية وبيان تأثير تغيرات درجة حرارة هواء المحيط. بينت النتائج ان الجزء الاعظم من خسائر الطاقة المتاحة تحدث في غرفة الاحتراق يليها ضاغط الهواء واقلها التوربين الغازي كمعدل للقراءات الاربعة. كما بينت النتائج ان زيادة درجة حرارة المحيط يزيد من خسائر الطاقة المتاحة في التوربين ككل وفي كل جزء من اجزائه وان هذه الزيادة تكون في درجات الحرارة العالية اكبر منها في درجات الحرارة الواطئة.

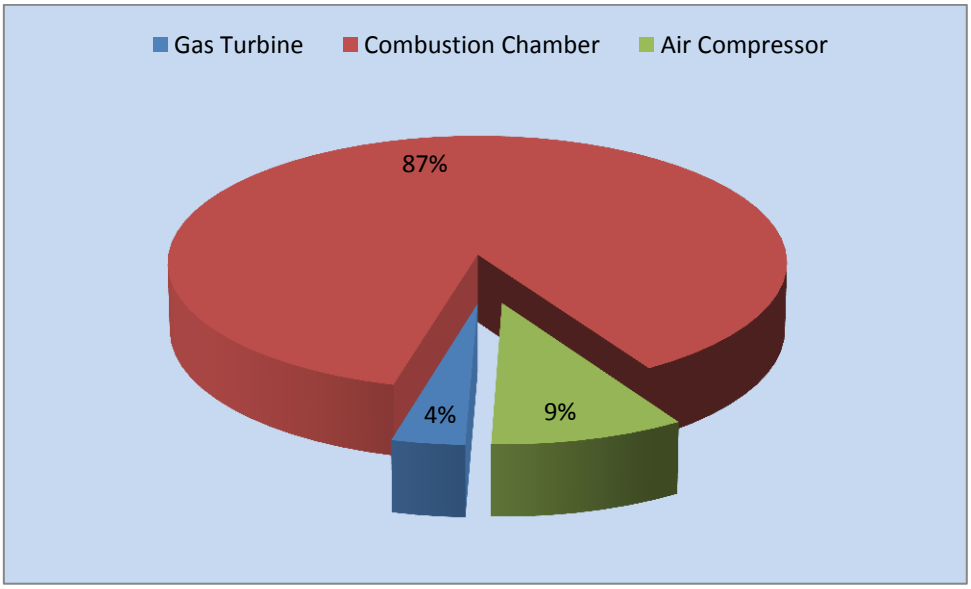

الشكل(7): يبين نسب متوسط خسائر الطاقة المتاحة في كل جزء من اجزاء التوربين

ان جزء صغير من الطاقة المتاحة في الوقود يتحول الى طاقة كهربائية. الشكل ادناه يبين النسبة الصافية لتحول الطاقة المتاحة الكلية الداخلة للتوربين عن طريق الوقود الغازي كمعدل للقراءات الاربعة الى طاقة كهربائية مستفاد منها.

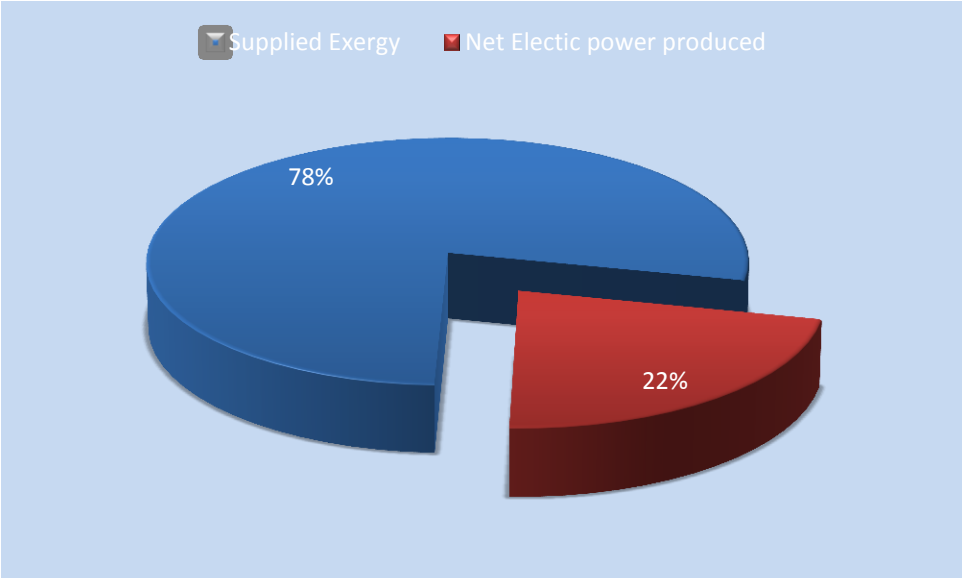

الشكل(8): يبين نسبة تحول الطاقة المتاحة للوقود الى طاقة كهربائية

ولهذا يتطلب وضع تقنيات لتقليل درجة حرارة الهواء الداخل للتوربين من خلال تصميم مبرد هوائي في مدخل ضاغط الهواء.

6) المصادر (References):

[1] Annamalai, Kalyan, Ishwar K. Puri, and Milind A. Jog. ***Advanced thermodynamics engineering***. CRC press, 2010.

[2] A. Mousafarash and M. Ameri, "***Exergy and exergo-economic based analysis of a gas turbine power generation system***," Open Access J. J. Power Technol., vol. 93, no. 1, pp. 44–51, 2013.

[3] Bejan, Adrian. ***Advanced engineering thermodynamics***. John Wiley & Sons, 2016.

[4] C. Borgnakke and R. E. Sonntag, ***Fundamentas of Thermodynamics***. 2009.

[5] Cengel, Yunus A., and Michael A. Boles. "***Thermodynamics: An Engineering Approach***, Seventh edition, Mc. Graw-Hill, New York, 2013.

[6] E. Henry Okechukwu and O. Albert Imuentinyan, "***Exergy analysis of Omotosho phase 1 gas thermal power plant***," Int. J. Energy Power Eng., vol. 2, no. 5, pp. 197–203, 2013.

[7] F. F. Hatem, "***Exergy Losses Calculation for a 125 MW Combined Power Plant***," Journal, vol. 27, 2009.

[8] I. Dincer and M. A. Rosen, ***Exergy: Energy, Environment and Sustainable Development***, 2013.

[9] Ibrahim, Thamir K., et al. "***Thermal performance of gas turbine power plant based on exergy analysis***." Applied Thermal Engineering 115 (2017): 977-985.

[10] L. Pattanayak, "***Thermodynamic modeling and Exergy Analysis of Gas Turbine Cycle for Different Boundary conditions***," Int. J. Power Electron. Drive Syst. J., vol. 6, no. 2, pp. 2088–8694, 2015.

[11] Moran, Michael J., et al. ***Fundamentals of engineering thermodynamics***. John Wiley & Sons, 2010.

[12]M. N. Parth, "***Exergy Analysis of Gas Turbine Power Plant***," Int. J. Sci. Eng. Res., vol. 5, no. 2, 2014.

[13]P. K. Nag, "***Basic and applied thernodynamics***." p. 985, 2002.

[14]Rajput, R. K. ***Engineering Thermodynamics: A Computer Approach***. Jones & Bartlett Publishers, 2009.

[15]S. Klein and G. Nellis, ***Thermodynamics***. 2011.

[16]Singh, Onkar. ***Applied thermodynamics***. New Age International, 2009.

[17]حميد حيدر هاشم, د.ابو بكر اعويدات سالم, "***حساب خسائر الاكسيرجي لمحطة قوى مشتركة***", الطاقة والحياة– العدد(الثالث والعشرون) الصيف(يونيو)2006.

KJPS Al-Kitab Journal for Pure Science
Vol.2 (2), ISSN: 2617-1260 (print), 2617-8141(online)
www.kjps.isnra.org

DOI: http://10.32441/kjps.02.02.p20

دراسة تأثير أنواع مختلفة من الزيوت وعوامل الشد السطحي على قابلية إنتاج الكاروتينويدات من خميرة *Rhodotorula glutinis*

احمد إبراهيم صالح
كلية الزراعة / الحويجة، جامعة كركوك، كركوك، العراق.
ahmed_abc111@yahoo.com

الملخص

هدفت الدراسة لمعرفة تأثير أنواع مختلفة من الزيوت وعوامل الشد السطحي على قابلية إنتاج الكاروتينويدات من خميرة *Rhodotorula glutinis*. بينت النتائج أن أعلى نسبة كاروتينويدات كانت مع عامل الشد السطحي Tween 80 اذ بلغت 2056.53 مايكروغرام/ لتر ثم تبعها كل من زيت الزيتون وزيت جوز الهند اذ بلغت الكمية 1956.51 و 1947.45 مايكروغرام/ لتر على التوالي أما اقل القيم فكانت مع زيت الحبة السوداء اذا بلغت 1057.75 مايكروغرام/ لتر.

أما فيما يخص كمية السكر المستهلك فكانت أعلى القيم مع زيت الزيتون إذ بلغت 24.475 غم/لتر واقلها مع زيت الخروع اذ بلغت 23.9672 غم / لتر. أما من ناحية كفاءة الإنتاج فكانت اعلى كفاءة إنتاج باستخدام زيت جوز الهند اذ بلغت القيمة 89.285 مايكروغرام /غرام والتي تبعتها المعاملة المحتوية على Tween 80 والبالغة 86.725 مايكروغرام /غرام. أما اقل نسبة كاروتينويدات إلى السكر المستهلك فكانت مع استخدام زيت الحبة السوداء اذ بلغت 44.322 مايكروغرام/غرام، أما فيما يخص الكتلة الحيوية فسجلت اعلى القيم لزيوت جوز الهند وزهرة الشمس واللوز الحلو اذ بلغت 10.60 غم / لتر، واقلها كانت مع استخدام زيت الحبة السوداء اذ بلغت 8.60 غم / لتر، أما قيم الأس الهيدروجيني فقد شهدت انخفاضاً حاداً لجميع المعاملات فكانت بأعلى مستوى لها مع زيت الحبة السوداء اذ بلغت 2.62 واقلها مع زيت الزيتون اذ بلغت 2.55 وتراوحت قيمة الأس الهيدروجيني لبقية المعاملات ما بين تلك القيم.

الكلمات الدالة: تأثير الزيوت، عوامل الشد السطحي، الكاروتينويدات، *Rhodotorula glutinis*

KJPS Al-Kitab Journal for Pure Science
Vol.2 (2), ISSN: 2617-1260 (print), 2617-8141(online)
www.kjps.isnra.org

Effect of some types of oils and Surfactant factors on the production of carotenoids from the yeast of *Rhodotorula glutinis*.

Ahmed Ibrahim salih
College of Agriculture, hawija, Kirkuk University , Kirkuk, IRAQ.

ABSTRACT

The study aimed to investigate the effect of some types of oils and Surfactant factors on the production of carotenoids from the yeast of *Rhodotorula glutinis*. The results showed that the highest carotenoids were with Tween 80 with 2056. 53 micrograms / l followed by olive oil and coconut oil with a quantity of 1956.51 and 1947.45 µg / L respectively. The lowest values were with black seed oil at 1057.75 µg / L. As for sugar consumed was the highest values with olive oil as it was 24.475 g / l and the least with castor oil at 23.9672 g / l. In terms of efficiency of production was the highest production efficiency using coconut oil with a value of 89.285 µg / g followed by the treatment containing Tween 80, amounting to 86.725 microgram / g. The lowest percentage of carotenoids to the sugar consumed was with the use of black seed oil as it was 44.322 micrograms / gram. As for biomass, the highest values of coconut oil, sunflower and sweet almond were recorded at 10.60 g / l and the lowest was with

the use of black seed oil as it reached 8.60 g / l. The pH values showed a sharp decrease in all treatments. The highest level was with black seed oil 2.62 and the lowest with olive oil 2.55. The pH value of the other treatments ranged between these values.

Key words: Effect of oils, Surfactant factors, carotenoids, *Rhodotorula glutinis*.

1. المقدمة:

في السنوات الأخيرة اصبح التوجه نحو استخدام الصبغات المنتجة من مصادر طبيعية في الغذاء ذو أهمية متزايدة كبديل عن تلك الأصباغ الصناعية الغير مرغوب فيها إذ يزداد الطلب في الأسواق وبشكل كبير على المركبات ذات الأصل الطبيعي يوم بعد يوم بسبب الوعي بالفوائد الصحية الإيجابية للمركبات الطبيعية، وتلعب المكونات الميكروبية دوراً أساسياً كعامل تلوين للعديد من الأغذية [1] .

تعد الكاروتينويدات ذات أهمية كبيرة للإنسان والحيوانات على حد سواء وذلك لقابليتها على تعزيز الاستجابة المناعية والتحول إلى فيتامين A وتنظيف الجسم من الجذور الحرة للأوكسجين [2]. لقد جذب الإنتاج الميكروبي للكاروتينويدات اهتماما واسعا، فعلى الرغم من توفر مختلف الكاروتينويدات الصناعية والطبيعية إلى ان هناك اهتماما متزايدا بالإنتاج من المصادر الميكروبية بالمقارنة مع الاستخلاص من الخضراوات أو الصناعات الكيميائية [3]. والسبب الرئيسي للتوجه نحو الإنتاج الميكروبي للكاروتينويدات هو المشاكل الفصلية والجغرافية المتنوعة المؤثرة في إنتاج الملونات العديدة ذات الأصل النباتي فضلا عن الجدوى الاقتصادية للتصنيع الميكروبي خصوصا عند استعمال مواد طبيعية منخفضة الكلفة كمصادر للكربون[4] . ومن بين الأحياء المجهرية المهمة المنتجة للكاروتينويدات فان سلالة الخمائر *Rhodotorula spp.* هي السلالة الأكثر إنتاجية للكميات الكبيرة من البيتا كاروتين[5] . أن معدلات تكوين الكاروتينويدات للخميرة قد ازداد بشكل كبير مع إضافة Tween 80 1% حجم/حجم وكذلك مع إضافة زيت بذرة القطن [6] . وتشير البحوث الأولية على الإنتاج الميكروبي للكاروتين بان إضافة عامل منشط سطحي غير أيوني كـ Tritone x – 100 كان فعالاً بصورة إيجابية

KJPS Al-Kitab Journal for Pure Science
Vol.2 (2), ISSN: 2617-1260 (print), 2617-8141(online)
www.kjps.isnra.org

في التأثير على إنتاج البيتا الكاروتين بفعل الزرع المدمج للعفن *Blakeslea trispora* ، وذكر الباحثون بان إضافة زيت فول الصويا إلى الوسط الصناعي قد حسن من قابلية الإنتاج [7] . ان أضافة بعض العوامل لوسط التنمية كإضافة المنظفات والزيوت تزيد من القابلية التنافذيه للخلية مما يزيد من إنتاج الكاروتينويدات[8] . وقد درس تأثير العوامل السطحية المختلفة مثل (tritone x100,tween85,tween80,tween60,span40,span20) وبتركيز 0.1 % على إنتاج البيتا كاروتين باستخدام المزارع المتزاوجة للعفن *B. Trispora* NRRL 2895 (+) و NRRL2896 (-)، فقد تبين أن Span 20 هو الأكثر أهمية من بقية العوامل التي تم اختبارها، وقد زاد من حاصل الكاروتين من 1.5 ملغم/لتر إلى 2 ملغم / لتر. أما العوامل السطحية الأخرى فلم تزيد الحاصل بشكل كبير، ان تركيز span 20 كان بحده الأمثل عند تركيز 0.2% والذي أدى إلى إنتاج 2ملغم / لتر من البيتا كاروتين و 12.36 غم/ لتر من وزن الخلية الجاف. أما التراكيز اعلى من 0.2% لهذا العامل قد خفضت الاستفادة من سكر الكلوكوز المتواجد في الوسط وبالتالي التخفيض في إنتاج البيتا كاروتين ويمكن التكهن بأن الزيادة في إنتاج البيتا كاروتين يمكن ان ينتج عن تصنيع حوامض trisporic. كما وأوضحوا بان الزيوت الطبيعية كزيت فول الصويا وزيت زهرة الشمس وزيت الزيتون وزيت الذرة وزيت النخيل قد تم اختبارها في وسط الإنتاج عند تركيز 3% حجم/حجم لتحديد تأثيرها على إنتاج البيتا كاروتين بواسطة مزارع متزاوجة من *B. trispora* فتبين بأن زيت فول الصويا قد زاد من إنتاجية البيتا كاروتين بينما زيت الزيتون وزيت زهرة الشمس دعم النمو ولكنه خفض من إنتاج البيتا كاروتين. أما زيت النخيل وزيت الزيتون وزيت الذرة فقد أعطت نموا جيدا ولكنه حصل انخفاض في كمية البيتا كاروتين المنتج[9] .

2. المواد وطرائق العمل:

جمع العينات:

تم الحصول على الزيوت المستخدمة في الدراسة من الأسواق المحلية وهي من إنتاج معمل عماد لصناعة الزيوت النباتية. أما مادة Tween 80 فكانت مجهزة من شركة SCRC الصينية.

مصدر الخميرة:

KJPS Al-Kitab Journal for Pure Science
Vol.2 (2), ISSN: 2617-1260 (print), 2617-8141(online)
www.kjps.isnra.org

تم الحصول على خميرة *Rhodotorula glutinis* var. *glutinis* من البنك الوطني لجمع الخمائر (إنكلترا) National collection yeast Culture (NCYC) ، نشطت العزلة بوسط yeast extract-malt extract agar (YMA) ثم جددت شهريا وحفظت على موائل من الوسط المذكور لحين الاستعمال.

وسط التخمر:

استخدم في التجربة وسط التخمر (25 غم / لتر سكروز، 2.2 غم / لتر كبريتات الأمونيوم $(NH_4)_2SO_4$، 2غم فوسفات البوتاسيوم أحادية الهيدروجين K_2HPO_4، 2 غم / لتر فوسفات البوتاسيوم ثنائية الهيدروجين KH_2PO_4 و 0.1 غم / لتر كبريتات المغنيسيوم $MgSO_4.7H_2O$ مع قيمة اس هيدروجيني أولي PH=7 وحرارة 30م باستخدام الحاضنة الهزازة على سرعة دوران 150 دورة / دقيقة وحددت نسبة الزيت المضاف بنسبة 2% من حجم التخمر المستخدم.

تحضير اللقاح:

تم إعداد اللقاح في الوسط yeast extract-malt extract Broth (YMB) بالنسب التالية محسوبة على أساس غم / لتر من وسط التخمر (خلاصة الخميرة 3، خلاصة المالت3، الببتون5، وسكر الكلوكوز10)، وقيمة اس هيدروجيني 5–5.5 والتلقيح لهذا الوسط من الوسط المائل الصلب بواسطة إبرة التلقيح بعشر مرات لـ 50 مل من الوسط السابق ثم التحضين على حرارة 28م واستخدام الحاضنة الهزازة على 100 دورة بالدقيقة لمدة 24 ساعة لحين وصول قيمة الامتصاصية إلى 570 نانوميتر [10] ليستخدم بعدها كلقاح لوسط التخمر في عملية الإنتاج.

تقدير وزن الخلايا الجاف (الكتلة الحيوية):

استخدم 50 مل من مزرعة التخمر لتقدير وزن الخلايا الجاف اذ اجري عليها عملية النبذ المركزي بسرعة 3500 دورة / دقيقة لفترة زمنية مقدارها 15 دقيقة بعد ذلك غسل الراسب بالماء المقطر وعلى دفعتين وتم التخلص من ماء الغسل

KJPS Al-Kitab Journal for Pure Science
Vol.2 (2), ISSN: 2617-1260 (print), 2617-8141(online)
www.kjps.isnra.org

بعد كل غسلة وتعاد عملية النبذ المركزي ثم بعد ذلك أجريت عملية تجفيف العينات على حرارة 85 م لحين ثبات الوزن. قدر الوزن الجاف للخلايا بصيغة غرام / لتر من حجم الوسط الزرعي [11] .

استخلاص وتقدير صبغة الكاروتينويد:

أجريت عملية النبذ المركزي لـ (50) مل من مزرعة التخمر على 3500 دورة / دقيقة وبزمن مقداره 15 دقيقة. فصل الراشح عن الراسب لغرض تقدير الكربوهيدرات المتبقية في الراشح. أجريت عملية غسل الراسب ولمرتين مع إجراء النبذ المركزي مع كل مرة غسل والتخلص من ماء الغسل بعد كل عملية نبذ مركزي. أضيف بعدها 10 مل حامض الهيدروكلوريك (0.5 عياري) للخلايا المترسبة في أنبوبة الفصل وأجريت له عملية تسخين على 100م ولمدة 10 دقائق. ثم التبريد بالماء البارد لمدة 10 دقائق أضيف بعد ذلك كمية من الأسيتون إلى عالق الخلايا التحريك واستخدام الهاون والمدقة في عملية الاستخلاص لضمان التحطيم الكامل للخلايا والهدف هو استخلاص الصبغة من الخلايا المحطمة مع الاستمرار بإضافة الأسيتون في كل مرة وتحويل المستخلص إلى دورق سعة 250 مل ثم تكرار العملية مع الخلايا المتبقية مع إضافة كمية أخرى من الأسيتون لحين الحصول على خلايا عديمة اللون وبذلك نكون قد اتممنا عملية الحصول على الصبغة. ينقل الأسيتون والصبغة بعد ذلك إلى قمع الفصل بعد ان يقدر حجم الأسيتون المستخدم في عملية الاستخلاص وذلك لاستخدام نفس الكمية من الهكسان في قمع الفصل مع التحريك بهدوء بوجود 15%من محلول كلوريد الصوديوم البارد لزيادة قابلية استخلاص الصبغة، تمزج المكونات مع بعضها بهدوء وتثبيت القمع عموديا لحين استخلاص كامل الصبغة من الأسيتون وانتقالها إلى الطبقة العلوية وهي طبقة الهكسان مع الصبغة. قدرت الامتصاصية باستخدام جهاز المطياف الضوئي على طول موجي 450 نانوميتر [12] . ثم قدرت كمية الكاروتينويدات باستخدام المنحنى القياسي للبيتا كاروتين القياسي المجهز من شركة (sigma Aldrid).

تقدير كمية الكربوهيدرات المتبقية:

قدرت الكربوهيدرات الكلية المتبقية في راشح وسط التخمر بطريقة (الفينول– حامض الكبريتيك) وذلك بأخذ 1 مل من راشح المزرعة الخالي من خلايا الخميرة وأجريت له التخافيف المطلوبة بالماء المقطر. ثم اخذ من التخفيف الأخير

KJPS Al-Kitab Journal for Pure Science
Vol.2 (2), ISSN: 2617-1260 (print), 2617-8141(online)
www.kjps.isnra.org

1 مل من المحلول واضيف اليه 1 مل من محلول الفينول (5%) ثم رج الأنابيب جيدا لإتمام عملية الامتزاج واضيف بعدها 5 مل من حامض الكبريتيك المركز لكل أنبوبة مزجت الأنابيب بصورة جيدة ثم وضعت بعدها في حمام مائي على حرارة 30 م لمدة نصف ساعة استخدم الطول الموجي 490 نانوميتر لقياس الكثافة الضوئية باستعمال جهاز المطياف الضوئي وفقا لطريقة [13] . اعتمد المنحني القياسي لسكر الكلوكوز النقي لحساب تراكيز السكر المتبقي. حظر المحلول القياسي لسكر الكلوكوز بتراكيز تراوحت بين (32–192 مايكروغرام / مل) واستعملت نفس الطريقة المذكورة أعلاه لقياس الكثافة الضوئية لسكر الكلوكوز القياسي.

التحليل الاحصائي:

حللت النتائج باستخدام برنامج التحليل الإحصائي الجاهز [14] لدراسة تأثير العوامل وفقا للتصميم العشوائي الكامل CRD. وحددت معنوية الفروقات ما بين متوسطات العوامل المدروسة بأجراء اختبار دنكن [15] عند مستوى احتمالية 0.05.

النتائج والمناقشة:

بينت نتائج التحليل الإحصائي الموضحة في الجدول (1) اثر بعض الزيوت وعوامل الشد السطحي على إنتاج الكاروتينويدات وكمية السكر المستهلك وكفاءة الإنتاج لخميرة *R. glutinis*.

جدول (1): تأثير إضافة بعض انواع الزيوت وعوامل الشد السطحي على إنتاج الكاروتينويدات والكتلة الحيوية من خميرة *Rhodotorula glutinis* .

الصفات المدروسة / المعاملة	الكاروتينويدات (مايكرو غرام/لتر)	السكر المستهلك (غم / لتر)	الكاروتينويدات/ السكر المستهلك (مايكرو غرام /غم)
عينة المقارنة	1764.10 D	24.441 a	72.177 Cd

KJPS Al-Kitab Journal for Pure Science
Vol.2 (2), ISSN: 2617-1260 (print), 2617-8141(online)
www.kjps.isnra.org

زيت الخروع	1771.10 D	23.967 ab	73.893 Cd
زيت جوز الهند	1947.45 B	24.257 ab	89.285 A
زيت السمسم	1757.18 D	24.287 ab	72.353 cd
زيت زهرة الشمس	1902.24 C	24.432 a	77.854 c
زيت الزيتون	1956.51 B	24.475 a	79.994 bc
Tween 80	2056.53 A	24.059 ab	86.725 ab
زيت الحية السوداء	1057.75 G	23.865 b	44.322 e
زيت الكتان	1572.98 F	24.109 ab	65.245 d
زيت الذرة الصفراء	1912.33 C	24.432 a	78.270 bc
زيت اللوز الحلو	1647.35 E	24.346 ab	67.717 d

a-f: الأحرف المتشابهة في العمود الواحد تشير إلى عدم وجود اختلافات معنوية عند مستوى احتمالية 0.05.

إذ أشارت النتائج إلى ان إضافة عامل الشد السطحي Tween 80 قد عزز من إنتاج الكاروتينويدات من 1764.10 مايكروغرام / لتر لعينة المقارنة غير المحتوية على المنشطات (المحفزات) كالزيوت وعوامل الشد السطحي إلى 2056.53 مايكروغرام / لتر كما ازداد إنتاج الكاروتينويدات باستعمال زيت الزيتون وزيت جوز الهند وزيت الذرة الصفراء وزيت زهرة الشمس بصورة ملحوظة اذ بلغت الكميات 1956.51 و 1947.45 و 1912.33 و 1902.24 مايكروغرام / لتر على التوالي. واتفقت النتيجة مع ما توصل اليه [6] الذين أشاروا إلى أن معدلات تكوين الكاروتينويدات

KJPS Al-Kitab Journal for Pure Science
Vol.2 (2), ISSN: 2617-1260 (print), 2617-8141(online)
www.kjps.isnra.org

للخميرة قد ازداد بشكل ملحوظ مع إضافة Tween 80 1% حجم/حجم وكذلك مع إضافة زيت بذرة القطن قد ازداد إنتاج الكاروتينويدات بشكل كبير بالمقارنة مع الوسط الزرعي الغير حاوي على منشط لتنمية خميرة *R. glutinis* اذ أنتجت 52 ملغم / لتر من الكاروتين الكلي مع زيت بذرة القطن 1% حجم/حجم بينما كانت الكمية 35 ملغم /لتر كاروتينويدات قد تكونت بفعل الخميرة بدون استخدام منشط. وقد انخفض إنتاج الكاروتينويدات بشكل كبير عند إضافة زيت الحبة السوداء. اتفقت النتيجة مع ما توصل اليه [16] اذ أشاروا إلى التأثير المثبط للمستخلص الزيتي للحبة السوداء لنمو العديد من الأحياء المجهرية بضمنها الخمائر قيد الدراسة، .أما كمية السكر المستهلك فقد ارتبطت بشكل وثيق مع ارتفاع أو انخفاض إنتاج الكاروتينويدات والكتلة الحيوية إذ سجلت انخفاضا كبيرا ولجميع المعاملات وذلك لحاجة خلايا الخميرة لمصدر الطاقة والكربون بشكل كبير للفعاليات الحيوية والبناء الخلوي فكانت اكبر كمية سكر مستهلك بوجود زيت الزيتون اذ بلغت 24.475 غم /لتر والتي لم تختلف معنويا عن عينة المقارنة وزيت زهرة الشمس وزيت الذرة الصفراء. أما اقل نسبة سكر مستهلكة فقد كانت مع زيت الحبة السوداء اذ بلغت 23.865 غم/لتر وذلك لتثبيط العديد من الفعاليات الأيضية لخلايا الخميرة لوجود المواد الفعالة في هذا الزيت والمثبطة للنمو الميكروبي [17] . أما كفاءة الإنتاج والمحسوبة على أساس نسبة الكاروتينويدات الكلية مقسومة على نسبة السكر المستهلك والمقدرة (مايكروغرام / غرام) فكانت اعلى كفاءة إنتاج باستخدام زيت جوز الهند اذ بلغت القيمة 89.285 مايكروغرام /غرام والتي لم تختلف معنويا مع المعاملة المحتوية على Tween 80 والبالغة 86.725 مايكروغرام /غرام. واتفقت هذه النتيجة مع ما توصل اليه [8] . الذين أشاروا إلى ان أضافة بعض العوامل لوسط التنمية كإضافة المنظفات والزيوت تزيد من القابلية التنافذيه للخلية مما يزيد من إنتاج الكاروتينويدات. أما اقل نسبة كاروتينويدات إلى السكر المستهلك كانت مع زيت الحبة السوداء اذ بلغت 44.322 مايكروغرام/غرام والذي يعود إلى قلة كمية الكاروتينويدات المنتجة وقلة السكر المستهلك بالمقارنة مع بقية المعاملات. واتفقت النتيجة مع ما توصل اليه [17] الذين أشاروا إلى احتواء زيت الحبة السوداء على مواد قلويدية وكلايكوسيدية مثبطة للنمو الميكروبي.

يتضح من الشكل رقم (1) بأن الوزن الجاف للخلية قد ارتفع بشكل واضح مع استخدام زيت جوز الهند وزيت زهرة الشمس وزيت اللوز الحلو اذ بلغت الكتلة الحيوية 10.60 غم /لتر واقل قيمة للكتلة الحيوية سجلت مع زيت الحبة السوداء

KJPS Al-Kitab Journal for Pure Science
Vol.2 (2), ISSN: 2617-1260 (print), 2617-8141(online)
www.kjps.isnra.org

اذ بلغت 8.60 غم/لتر وقد يعود السبب في ذلك إلى ان بذور الحبة السوداء تحتوي على قلويدات وكلوسيدات خاصة بها والتي لا توجد في غيرها من النباتات الطبية ومنها Nigellicine و Nigllidine فضلا عن القلويدات الأخرى ذات التأثير المثبط للعديد الأحياء المجهرية ومنها الفطريات[17].

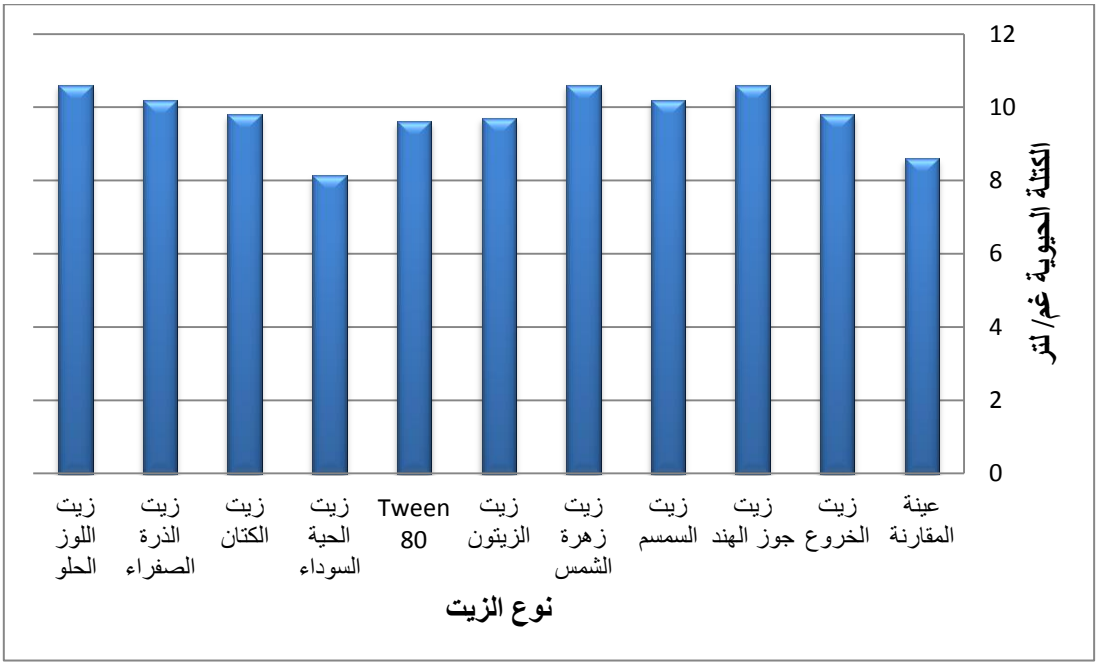

شكل (1): تأثير إضافة بعض أنواع الزيوت وعوامل الشد السطحي على إنتاج الكتلة الحيوية لخميرة *R. glutinis*

أما قيمة الأس الهيدروجيني والموضحة في الشكل (2) فقد سجلت انخفاضا شديدا لجميع المعاملات بالمقارنة مع قيمة الأس الهيدروجيني لوسط التخمر الأصلي والذي ضبط على اس هيدروجيني 7 .

KJPS Al-Kitab Journal for Pure Science
Vol.2 (2), ISSN: 2617-1260 (print), 2617-8141(online)
www.kjps.isnra.org

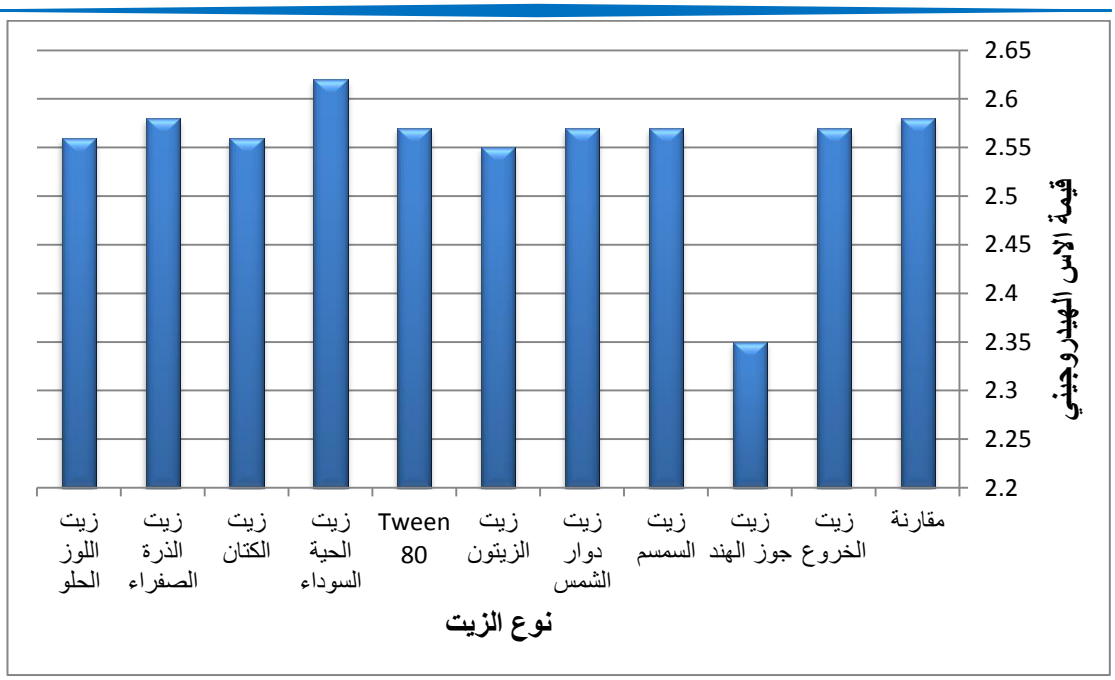

شكل (2): تأثير إضافة بعض أنواع الزيوت وعوامل الشد السطحي على قيمة الأس الهيدروجيني النهائي لوسط التنمية لخميرة *R. glutinis*

اذ انخفضت القيمة من 7 إلى أدنى مستوى لها مع جميع المعاملات اذ وصلت إلى 2.35 عند استخدام زيت جوز الهند، أما اقل القيم تأثرا هي مع استخدام زيت الحبة السوداء والتي سجلت اعلى اس هيدروجيني فقد بلغ 2.62 وقد يعود السبب في انخفاض قيم الأس الهيدروجيني لجميع المعاملات إلى النشاط الحيوي للخميرة اذ ان إنتاج الأحماض العضوية مثل حامض الخليك وحامض البايروفيك وحامض اللاكتيك تعمل على خفض قيمة الأس الهيدروجيني نتيجة لزيادة تركيز أيونات الهيدروجين في الوسط. واتفقت النتيجة مع ما توصل اليه [18] الذي أشار إلى ان العديد من الخمائر تثبط نتيجة انخفاض الأس الهيدروجيني بفعل الأحماض العضوية وخصوصا حامض البايروفيك الناتج من العمليات التمثيلية لهذه الخمائر وقد يعزى السبب إلى تحرر أيونات الكبريتات اذ ان الخميرة عند استخدامها لكبريتات الأمونيوم كمصدر للنتروجين ستستهلك أيونات الأمونيوم لغرض البناء الحيوي للبروتينات والأحماض الأمينية مما يؤدي بالنتيجة إلى تحرر أيون الكبريتات في الوسط وتكوين حامض الكبريتوز الذي يعمل على انخفاض قيم الأس الهيدروجيني لجميع المعاملات وفقا لما أشار اليه [19] . النتائج المتحققة من الدراسة تشير إلى الدور الإيجابي لإضافة بعض المنشطات وعوامل الشد السطحي

KJPS Al-Kitab Journal for Pure Science
Vol.2 (2), ISSN: 2617-1260 (print), 2617-8141(online)
www.kjps.isnra.org

في زيادة إنتاج الكاروتينويدات من خميرة *R. glutinis* والتي تطابقت مع ما حصل عليه [6] .الذين وجدا ان زيت بذور القطن قد زاد من إنتاج الكاروتينويدات الكلي بواسطة خميرة *R. glutinis* مقارنة بالوسط الغير محتوي على المنشطات.

3. المصادر:

[1] Tibor, C. ,"**Liquid Chromatography of Natural pigments and synthetic dyes**", J. Chromatography Library, 71, 11-19 (2007).

[2] Kiokias, S. and Gordon, M. H.**,"Antioxidant properties of carotenoids *in vitro* and *in vivo*",** Food Rev. Int., 20, 99 – 121(2004).

[3] Ausich, R. L. **"Commercial opportunities for carotenoid production by biotechnology**", Pure and App. Chem., 69(10), 2169-2173 (1997).

[4] Frengova, G. I. and Beshkova, D. M., "**Carotenoids from *Rhodotorula* and *Phaffia*: yeasts of biotechnological importance**", J. Ind. Microbiol.Biotechnol., 36 ,163–180 (2009**).**

[5] Buzzini, P. and Martini, A. , **"Production of carotenoids by strains of *Rhodotorula glutinis* cultured in raw materials of agro-industrial origin**". Bioresour. Technol., 71 , 41–44 (2000).

[6] Aksu, Z. and Tugba Eren, A., **"Production of carotenoids by the isolated yeast of *Rhodotorula glutinis***", Biochem. Eng. J., 35 , 107–113, (2007).

[7] Ciegler, A.; Arnold, M. and Anderson, R. F., " **Microbiological production of carotenoids. IV. Effect of various grains on production of carotene by mated strains of *Blakeslea trispora***" , Appl. Microbiol., 7, 94–98 (1959).

[8] Kim, S.; Seo, W. and Park, Y., **"Enhanced synthesis of trisporic acid and β- carotene production in *Blakeslea trispora* by addition of a non-ionic surfactant Span 20"**, J. Ferment. Bioeng., 4 ,330–332(1997).

[9] Choudhari, S. M.; Ananthanarayan, L. and Singhal, R.S. , **"Use of metabolic stimulators and inhibitors for enhanced production of β-carotene and lycopene by *Blakeslea trispora* NRRL 2895 and 2896**", BioresourceTechnol., 99 , 3166–3173 (2008).

[10] El-Banna, A. A.; Abd El-Razek, Amal M. and El-Mahdy, A. R.,**"Some factors affecting the production of carotenoids by *Rhodotorula glutinis* var. *glutinis*"** .Food and Nutr. Sci., 3, 64-71(2012).

[11] Ali, D. F., **Studies on carotenoids production from some yeasts**. Ph.D. Thesis, Faculty of Agriculture, Mansoura University, (2013).

[12] Park, P. K.; Cho, D. H.; Kim, E. Y. and Chu, K. H.," **Optimization of carotenoid production by *Rhodotorula glutinis* using statistical experimental design**" , World Journal of Microbiology and Biotechnology, 21(4), 429-434 (2005**).**

[13] Dubois, M.; Gilles, K. A.; Hamilton, J. K.; Rebers, P. and Smith, F., **"Colorimetric method for determination of sugars and related substances**. Analytical chemistry, 28(3), 350-356(1956).

[14] SAS , **"SAS Users-Guide. SAS Institute Inc"**, Cary NC. USA, (2001)

[15] Duncan, D. B. ,"**Multiple range and F. test**", Biometric, 11, 42 (1955**).**

[16] Mashhadian N. V. and Rakhshandeh H. **"Antibacterial and antifungal effects of Nigella sativa extracts against *S. aureus, P.aeroginosa and C. albicans***", J Med Sci . 21(1), 47-52(2005**).**

[17] Atta, U. R. and Malik, S.O. , "**Nigellidine, a new indazole alkaloid from seeds of *Nigella sativa***" , J. Res Iinst; 36 , 1993-1996 , (1995**).**

[18] Walt, J.P. Vander, "**Criteria and methods used in classification in "The yeast, ataxonomic study"** Chap. II (Lodder, J. ed) North-Holland publishing company.Amsterdam-London, (1970).

[19] Abd El-Razek, A. M. , "**Isolation, classification and mutagenesis of yeast carotenoids and optimizing factors affecting its production**", Ph.D. Thesis, Faculty of Agriculture, Alexandria University, (2004).

KJPS Al-Kitab Journal for Pure Science
Vol.2 (2), ISSN: 2617-1260 (print), 2617-8141(online)
www.kjps.isnra.org

DOI: http://10.32441/kjps.02.02.p21

تقييم فعالية بعض المستخلصات النباتية كبديل للمبيدات الكيميائية في مكافحة دغل السعد Cyperus rotundus L النامي تحت ظروف البيت النباتي

غسان فارس عطية عبد الحميد محمد حمودي السامرائي
احمد عبد الحكيم توفيق السامرائي رنا ابراهيم خليل
قسم علوم الحياة ، كلية التربية، جامعة سامراء, سامراء قسم علوم الحياة ، كلية التربية , قسم علوم الحياة ، كلية التربية
قسم علوم الحياة ، كلية التربية، جامعة سامراء, سامراء قسم العمارة, كلية الهندسة, جامعة سامراء, سامراء,
ahmed.alhasoon@gmail.com drranaibrahim6@gmail.com ghfaat76@gmail.com hamed56@yahoo.com

الخلاصة:

نفذت تجربتين باستخدام الأصص في البيت النباتي في قسم علوم الحياة /كلية التربية– جامعة سامراء خلال للموسم الصيفي للعام 2016 لتقييم فعالية ثلاث من المستخلصات المائية لأوراق نبات الدفل (Nerium oleander.L) ,الزيتون (Olea europaea L.) و الخروع (Ricinus communis L), في السيطرة على انبات درنات ونمو باردات دغل السعد بطريقة الري المباشر كبدائل للمبيدات الكيميائية المستخدمة. طبقت التجارب وفق القطاعات العشوائية CRD وبواقع اربع مكررات . اشتملت التجارب على عاملين، الاول النوع النباتي (ثلاث انواع نباتية) والثاني عامل التراكيز (2.5% ,5% و 10 %) وتأثيرهما على صفتي نسبة الانبات وتثبيط نمو البادرات . اشتملت التجربة الاولى على دراسة نسبة انبات درنات السعد بعد الزراعة في الأصص بالري المباشر المنتظم بالمستخلصات النباتية عند تراكيز مختلفة. فيما اشتملت التجربة الثانية على تقييم فعالية المستخلصات قيد الدراسة في تثبيط نمو بادرات السعد بعد 30 يوما من تاريخ الانبات. سجلت نتائج التجربة الاولى لصفة نسبة الانبات لدرنات السعد المروية بمستخلص اوراق الدفلة نسبة تثبيط بلغت 90% عند تركيز 5 و 10 % مقارنة مع نفس التراكيز لنبات الزيتون والخروع التي سجلت نسبة تثبيط تراوحت ما بين 30 و 40 % على التوالي . فيما سجل التركيز 2.5% اقل المعدلات التثبيط لصفة نسبة الانبات لجميع المستخلصات النباتيه . اظهرت تجارب الاداء لصفة تثبيط نمو باردات السعد في التجربة الثانية تفوق معنوي للمستخلص المائي لنبات الدفلة عند تركيز 10% بتسجيل نسبة تثبيط بلغت 100% بالمقارنة مع نفس التراكيز لنبات الزيتون ، تلاها التركيز 50% ومن ثم 25% الذي سجل اقل المتوسطات لصفة تثبيط النمو لجميع المستخلصات قيد الدراسة .اشارات نتائج الدراسة الحالية الى

KJPS Al-Kitab Journal for Pure Science
Vol.2 (2), ISSN: 2617-1260 (print), 2617-8141(online)
www.kjps.isnra.org

امكانية استخدام المنتجات الطبيعية من اصل نباتي كبدائل للمبيدات الكيميائية كأحدى وسائل المكافحة الحيوية في ادارة برامج مكافحة الادغال في القطاع الزراعي مع مزيد من الدراسات المستقبلية المستفيضة.

الكلمات الدالة: دغل السعد , تضاد بايوكيميائي، مستخلصات نباتية، مكافحة حيوية.

"Evaluation of the Efficacy of Some Plant Extracts as an Alternative to Chemical Weedicides in Controlling on *Cyperus rotundus L* "

Rana.I Khaleel, Ahmad.H.Al-Samarrai, Abdul-Hameed.M. Hamoody,
Department of Biology, College of Education, University of Samarra, Samarra, Iraq
Corresponding author: Ghassan.F. Al-Samarai
E-mail:ghfaat76@gmail.com

Abstract:

Two experiments were carried out during the summer season, 2016, in the green house / Department of Biology/Collage of Education, Samarra University, to evaluate the activity of three aqueous extract of leaves of Nerium (Nerium oleander L.),olives (Olea europaea .L) and castor (Ricinus communis.L), on control of tuber germination and growth of seedling of Cyperus rotundus L as an alternative for chemical pesticides. Experiments applied according to the complete randomized design (CRD) with four replicates. The experiments included two factors: the first factor plant species (three plant species),and the second factor concentration of plant extracts (2.5%, 5% and 10%) and their impact on germination rate and inhibition of seedling growth. The results of the first experiment recorded inhibition percentage reached (90%) at 5% and 10% from Nerium extracts compared with the same concentrations from Olive and Castor which, recorded inhibitory rate reached (30-40%) respectively. While the concentration of 2.5% was the lowest inhibition rates for germination ratio of all plant extracts under study. The second experiment showed effect of the Nerium extract at a concentration (10%) by recording completely inhibition ratio (100%), compared with the same concentrations of Castor and Olive extracts, which recorded the lowest mean growth inhibitory for all extracts. The results of the current study indicate the possibility of using

KJPS Al-Kitab Journal for Pure Science
Vol.2 (2), ISSN: 2617-1260 (print), 2617-8141(online)
www.kjps.isnra.org

natural products of plant origin as alternatives to chemical pesticides as one of the means of biological control in the management program agricultural sector with further studies of the future.

Keywords: *Cyperus rotundus* L, Biochemistry, Plant Extract, Allelopathy

6. المقدمة

الادغال هي واحدة من العوامل المهمة التي توثر في انتاج المحاصيل و تحد من أهمية الاقطاع الزراعي من خلال منافسة النباتات على الموارد البيئية وتسبب خسائر فادحة بالإنتاج **Jafari et al [1]** . حسب تقارير وردت من قبل منظمة الزراعة العالمية **FAO [2]** فان الخسائر الناتجة عن الادغال قد تصل الى حوالي (14%) من الانتاج الكلي للمحاصيل الزراعية. نبات السعد يعد واحدا من أسوأ الادغال العشبية انتشارا في العالم واكثرها مقاومة للبقاء وطرق المكافحة التقليدية بسب قدرتها على البقاء تحت الظروف البيئة الحرجة والتكاثر السريع من خلال البصيلات ودرنات القاعدية **Nishimoto [3]** . بارتفاع الطلب على الغذاء والزيادة الهائلة في النمو السكاني في جميع انحاء العالم وخصوصا المحاصيل الزراعية كانت هناك ضرورة ملحة واهتمام كبير لايجاد طرق ووسائل سريعة ومجدية للسيطرة على الادغال التي تنافس المحاصيل على الضوء والماء ومغذيات التربة وتحد من نموها وانتاجها. واحدة من طرق المكافحة المجدية والسريعة تمثلت باستخدام مبيدات الادغال الكيميائية للحد من انتشارها واظهرت نتائج مذهلة تتماشى مع الطلب المتزايد على المنتجات الزراعية الطازجة لسد حاجة السوق والمستهلك **Hawver et al [4]** . النتائج باستخدام المبيدات المصنعة زاد الطلب على استخدامها واصبحت واحدة من اهم طرق مكافحة الادغال العشبية بما فيها نبات السعد **Md et al [5])**

ومع ذلك، هناك تزايد في الاهتمام العالمي حول الحد من استخدام مبيدات الادغال الاصطناعية في القطاع الزراعي بسبب خطر التعرض المستمر للإنسان للحد الادنى من المستويات المتراكمة في الفواكه والخضر من مبيدات من خلال نظامه الغذائي **Japans MRL's, [6]** . حيث افادت تقارير من قبل **FAOMRL's [71** بان هناك العديد من المبيدات الكيميائية قد تجاوزت الحد الادنى المسموح به (A maximum residue limit (MRL للتراكم في الثمار الطازجة وفق المعايير العالمية. وبالإضافة إلى ذلك التأثير السلبي للمبيدات على صحة الانسان و البيئة من خلال تراكمها في التربة والمياه والتأثير على التنوع البيولوجي **Lofts, [8]** . كما ان الاستخدام المفرط لمبيدات الادغال قاد الى ظهور سلالات جديدة مقاومة لمبيدات الادغال الكيميائية؛ وفقا لتقرير **Kebede,[9]** فقد سجل ظهور 189 نوع من ادغال الحشائش المقاوم للمكافحة الكيميائية. وقد تم الإبلاغ عن بعض محاولات لتطبيق المستخلصات المائية للنباتات لقمع الاعشاب. وقد أدى السيناريو أعلاه إلى البحث عن بدائل آمنة للمبيدات الاصطناعية للسيطرة على الادغال في القطاع الزراعي لتقليل الخسائر وتجنب الآثار السلبية لاستخدام المبيدات المصنعة. الأبحاث الحالية تركز على استخدام طرق المكافحة الحيوية كبديل جدي ونافع عن مبيدات الادغال الكيمائية في السيطرة على الادغال. الاحتياجات البيئية والزراعية اقتضت الى تطوير تكنلوجيا بديلة لمكافحة الحشائش. احد الحلول المقترحة هو استخدام تقنية التضاد البايو كيميائي (Allelopathy)

KJPS Al-Kitab Journal for Pure Science
Vol.2 (2), ISSN: 2617-1260 (print), 2617-8141(online)
www.kjps.isnra.org

كأحدي طرق المكافحة الطبيعية المتوافقة والصديقة للبيئة , التي يمكن ان تستخدم لتكون البديل الفعال في ادارة الاعشاب الضارة وزيادة انتاج القطاع الزراعي.

2. المواد وطرائق العمل

2.1 اختيار وجمع العينات النباتية

جمعت درنات نبات السعد من قرية العباسية / قضاء سامراء من الاراضي الزراعية الواقعة على ضفاف نهر دجلة حيث ينمو دغل السعد بشكل كثيف وغزير في الاراضي المزروعة بالمحاصيل. اختيرت الدرنات النامية بشكل جيد وكبيرة الحجم والخالية من الاصابة المرضية . جلبت الدرنات بعد الجمع الى المختبر وغسلت بالماء جيدا لإزالة الاتربة والاوساخ العالقة. تركت حتى الجفاف ومن ثم حفظت في علب بلاستكية حتى الاستعمال. تم اختيار ثلاث نباتات لتحضير المستخلصات النباتية لتقييم ادائها في مكافحة دغل السعد كما موضح جدول رقم (1) , وهي نباتات محلية يشاع زراعتها في جميع انحاء العراق تقريبا.

جدول (1) الانواع النباتية قيد الدراسة

	الاسم الشائع	الاسم الانكليزي	الاسم العلمي
1	دفلة	Nerium	*Nerium oleander*.L
2	زيتون	Olive	*Olea europaea* . L
3	خروع	Castor	*Ricinus communis*. L

بعد اختيار النباتات جمعت اوراقها الطازجة مباشرة من الاشجار المنتشرة في ضواحي مدينة سامراء, جلبت الى المختبر وغسلت بماء الحنفية بعناية لإزالة الاتربة والاوساخ ومن ثم غسلت بالماء المقطر. تركت في المختبر مع التقليب اليومي المستمر لتجنب التعفن حتى وصلها الى الجفاف التام. جمعت العينات بعد التجفيف بالمختبر ووضعت في اكياس ورقية مثقبة ومن ثم وضعت بالفرن الكهربائي على درجة حرارة 60 مئوية لمدة 48 ساعة لضمان الوصول الى الجفاف التام **Ruch [10]** . سحقت عينات الاوراق المجففة يدويا باستخدام المنخل لاستبعاد الاجزاء الصلبة الغير قابلة للطحن ومن ثم اتبعت بطحن العينات باستخدام الخلاط الكهربائي للحصول على مسحوق جاف. حفظت عينات المسحوق النباتي في علب زجاجية نظيفة ومقفلة بأحكام ودون عليها اسم العينة لسهولة الحفظ والتخزين.

2.2 تحظير المستخلصات المائية بتراكيز محتفلة

باستخدام المسحوق المخزن تم تحضير المستخلص المائي للنباتات قيد الدراسة بطريق النقع وفقا لطريقة عمل **Francisco et al [11]** . تم وزن مقادير معلومة من المسحوق الجاف وفقا للتراكيزالمراد تحظيرها (10%) لكل نبات ونقعت بالماء مع التحريك المستمر وصولا الى حالة التجانس ومن ثم تركت لمدة 48 على درجة حرارة 4 مئوية في الثلاجة. رشحت العينات باستخدام القماش الناعم(الململ) لإزالة الشوائب كبيرة الحجم . حضرت سلسلة تخافيف (7.5% و 5%) من الراشح الاصلي (10%) وحفظت في اوعية بلاستيكية لحين الاستخدام. تم تحضير المستخلصات تباعا وحسب الحاجة تجنبا للتلف او اي تغير قد يطرا اثناء الخزن.

KJPS Al-Kitab Journal for Pure Science
Vol.2 (2), ISSN: 2617-1260 (print), 2617-8141(online)
www.kjps.isnra.org

2.3 تصميم التجارب

اجريت التجارب وفق تصميم القطاعات العشوائية (CRD) وبواقع عاملين, الاول النوع النباتي(3 نباتات) والعامل الثاني التراكيز واشتملت ثلاث تراكيز(5% , 7.5% و 10%) جدول رقم (2) وبواقع 4 مكررات تحت ظروف البيت النباتي باستخدام السنادين البلاستيكية.

جدول رقم 2. المعاملات المستخدمة في التجربة

T0	معاملة سيطرة باستخدام الماء	T6	تركيز 7.5% نبات زيتون
T1	معاملة سيطرة باستخدام المبيد	T7	تركيز 5% نبات زيتون
T2	تركيز 10% نبات دفلة	T8	تركيز 10% نبات خروع
T3	تركيز 7.5% نبات دفلة	T9	تركيز 7.5% نبات خروع
T4	تركيز 5% نبات دفلة	T10	تركيز 5% نبات خروع
T5	تركيز 10% نبات زيتون		

واشتملت التجارب على :

1.تجربة نسبة الانبات

جهزت السنادين الزراعية قبل الزراعة وملئت بالتربة الزراعية المهيئة مسبقا للزراعة في البيت النباتي . رويت السنادين قيل الزراعة للوصول الى حالة الامتلاء المثلى والتخلص من الفراغات . وزعت السنادين وفق تصميم التجربة بواقع (11 معاملة) 9 معاملات (3 نباتات3× 3 تراكيز) + 2 معاملة سيطرة . زرعت درنات السعد في السنادين بواقع 4 درنات لكل سندانه ورويت بشكل منتظم(رية لكل يومين) بالمستخلصات المائية . روقبت التجربة يوميا وسجلت نسبة الانبات لجميع المعاملات على مدة اسبوعين. تم احتساب نسبة انبات الدرنات تبعا لطريقة عمل **Singh and Bhati [12]** وفقا للمعادلة أدناه:

$$\text{معدل نسبة الانبات} = \frac{\text{نسبة انبات الدر نات لمعاملة السيطرة – نسبة انبات الدرنات (المروية بالمستخلصات)}}{\text{نسبة انبات الدرنات لمعاملة السيطرة}} \times 100$$

2. .تثبيط نمو البادرات

بعد تهيئة السنادين للزراعة زرعت الدرنات وتركت حتى النمو والوصول الى طور البادرة بارتفاع ما بين (10-15 سم) . يعد وصول النباتات الى مرحلة البادرة سقيت النباتات بالمستخلصات النباتية المحضرة بانتظام (رية لكل يومين) لمدة شهر ومن ثم اخذت البيانات بالاعتماد على نسبة الضرر او القتل التي لحقت بالنباتات المروية بالمقارنة بمعاملة السيطرة التي رويت بالماء فقط. تم احتساب معدل التثبيط وفقا للمعادلة أدناه:

KJPS Al-Kitab Journal for Pure Science
Vol.2 (2), ISSN: 2617-1260 (print), 2617-8141(online)
www.kjps.isnra.org

عدد النباتات في معاملة السيطرة – عدد النباتات المعاملة (المروية بالمستخلصات)

النسبة المئوية للتثبيط = ---------- × 100

عدد النباتات في معاملة السيطرة

2.4 التحليل الاحصائي

اجري التحليل الإحصائي للصفات المدروسة وفق تحليل التباين ((ANOVA باستخدام البرنامج الاحصائي الجاهز SPPS . استخدم اختبار دنكن المتعدد الحدود **Duncan Multiple Range Test [13]** للمقارنة بين المتوسطات على مستوى معنوية ($P \leq 0.05$).

4 .النتائج والمناقشة

4.1 تأثير النوع النباتي والتراكيز على نسبة انبات

سجلت نتائج التجربة الاولى لصفة نسبة الانبات لدرنات السعد المروية بالمستخلصات المائية لأوراق النباتات قيد الدراسة فروق معنوية مابين المعاملات ومعاملتا السيطرة من جهة والمعاملات فيما بينها من جهة اخرى من حيث نوع المستخلص النباتي و التركيز المستخدم في كبح نمو درنات دغل السعد شكل1 و 2 . النسبة الاعلى لتثبيط نمو بادرات السعد المروية بالمستخلصات النباتية سجلت مع الري بمستخلص اوراق نبات الدفلة مع معدل تنبط بلغ 80 % تلاها مستخلص اوراق الخروع 35 % بينما سجل مستخلص نبات الزيتون اقل النسب للتثبيط 23% شكل (1).

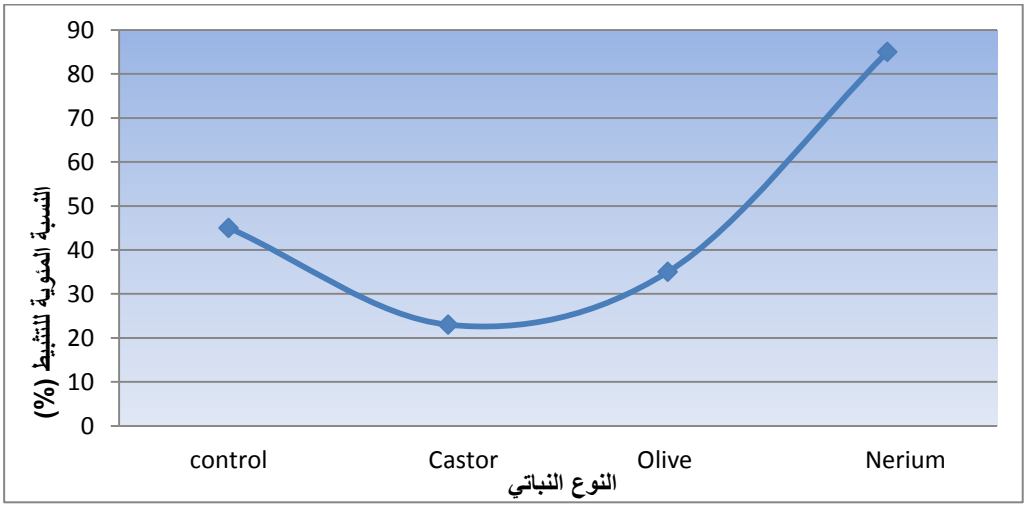

شكل (1). النسبة المئوية لتثبيط نمو درنات دغل السعد *Cyperus rotundus* L. المروية بالمستخلصات المائية لأوراق نبات الدفلة (Nerium), والزيتون Olive والخروع (Castor) .

KJPS Al-Kitab Journal for Pure Science
Vol.2 (2), ISSN: 2617-1260 (print), 2617-8141(online)
www.kjps.isnra.org

شكل (2) بين تأثير استخدام تراكيز مختلفة من المستخلص المائي للنباتات قيد الدراسة على نسبة كبح وتثبيط نمو درنات السعد المروية. اظهرت النتائج الى تفوق معنوي لتركيز 10% و 7.5% لمستخلص نبات الدفلة في نسبة التثبيط لانبات درنات السعد مع قيم بلغت (90%) لكلا التركيزين على جميع التراكيز قيد الدراسة لنفس النبات و النباتات الاخرة ومعاملة السيطرة لمبيد الادغال. فيما سجلت اقل نسب للتثبيط ولجميع التراكيز(10%, 7.5% و 5 %) باستخدام المستخلص المائي لأوراق نبات الزيتون مع نسب وصلت الى (25%, 25% و15%) على التوالى. من جانب اخر كان هناك زيادة طردية في نسب التثبيط مع زيادة تركيز المستخلص حيث سجل ارتفاع في نسب التثبيط مع التراكيز 10% و 70% بالمقارنة مع التركيز 5% لجميع النباتات المدروسة .

T0 معاملة بطرة ستخدام الماء	T1معاملة بطرة ستخدام المبيد	T2 تركيز 10% نبات دفلة	T3تركيز 7.5% ات دفلة	T4تركيز 5% ات دفلة	T5 تركيز 10% نبات زيتون
T6 تركيز 7.% نبات يتون	T7 تركيز % نبات يتون	T8تركيز 10% نبات روع	T9تركيز 7.5% ات خروع	T10 تركيز % نبات خروع	

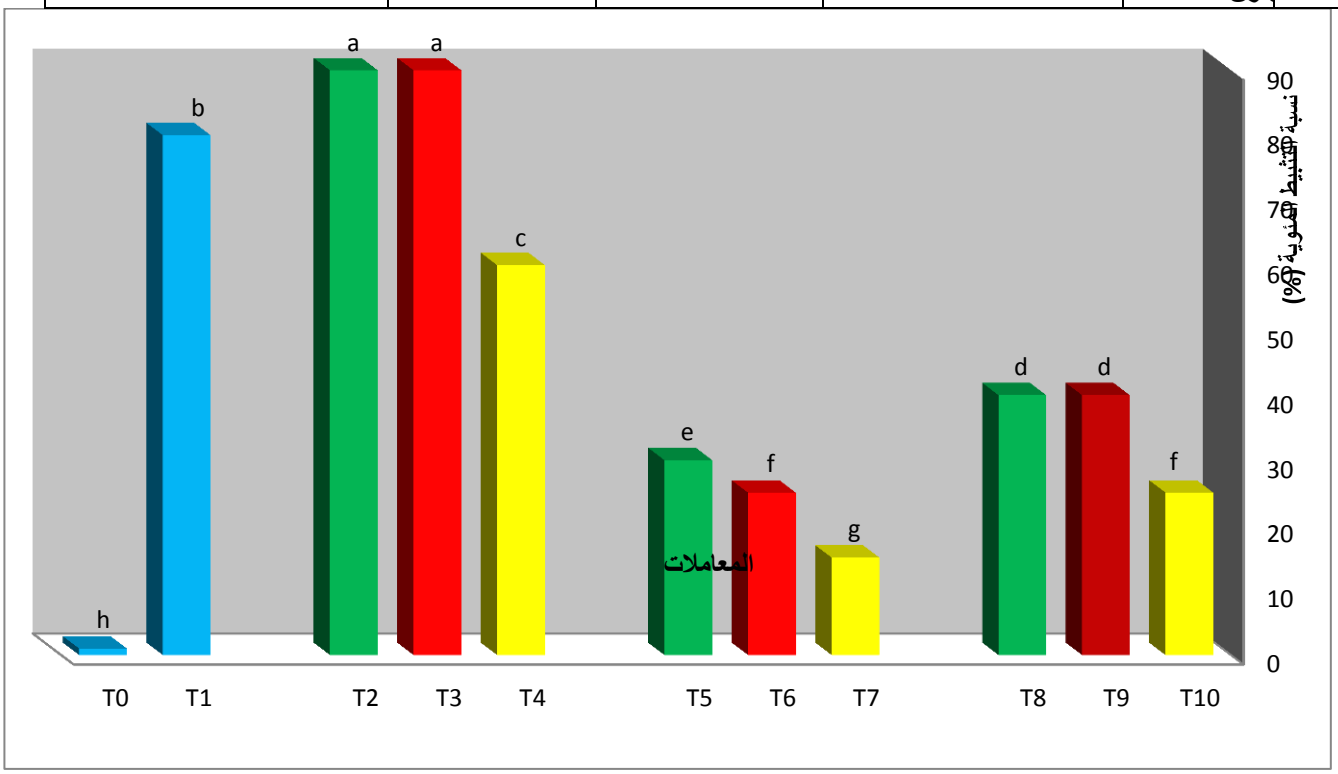

*اختلاف الأحرف لنسب التثبيط المئوي دلالة على وجود فرق معنوي بين المعاملات , فيما التشابه بين الأحرف دلالة على عدم وجود اختلافات معنوي عند مستوى معنوية 0.05

شكل (2) .النسبة المئوية (%) لتثبيط انبات درنات السعد Cyperus rotundus L باستخدام تراكيز (10% , 7.% و 5%) من المستخلصات المائية لنبات الدفلة (Nerium), والزيتون (Olive والخروع (Castor) .

مما سبق يلاحظ ان مستخلص نبات الدفلة المائي اظهر تأثيرا تثبيطا اعلى من مستخلصي الخروع والزيتون في تثبيط انبات الدرنات. وقد يعزى سبب هذا التثبيط في الانبات.الى التأثيرات الأليلوباثيه لاحتواء النبات على. مواد قابلة للذوبان. في الماء ، كما قد يعود هذا .الى التأثير في عملية التشرب كأول عملية. في الانبات. وهذا بدوره يؤثر. على استمرار العمليات الفسلجية. الأخرى. من جانب اخر فقد يعزى الاختلاف في نسبة كبح وتثبيط انبات درنات السعد باختلاف الانواع النباتية

KJPS Al-Kitab Journal for Pure Science
Vol.2 (2), ISSN: 2617-1260 (print), 2617-8141(online)
www.kjps.isnra.org

الى طبيعة اختلاف التركيب الكيميائي لهذه النبات من حيث احتوائها على مجاميع فعالة من المركبات الكيمائية مما قاد الى الاختلاف في تأثيرها. التثبيط الأليلوباثي معقد ويمكن أن ينطوي على التفاعل بين فئات مختلفة من المواد الكيميائية، مثل phenolic compounds, flavonoids, terpenoids, alkaloids, steroids, carbohydrates, amino acids او خليط من مركبات كيميائية مختلفة لها أحيانا تأثير سمي أكبر من المركبات الفردية وحدها **Bangarwa et al. [14]**. جاءت نتائج الدراسة الحالية بالاتفاق مع نتائج **السعيد والدوس [15]** بأن لراشح الحرمل تأثيرًا مثبطًا لإنبات البذور وكان ذلك أشد عند استخدام راشح الأوراق الغضة. ولقد كان هناك تثبيط كامل لإنبات بذور الجربة *Farsetia aegyptia* والثيموم *Pennisetum divisum* , كما أظهرت النتائج أن لراشح الحرمل تأثيرًا مثبطًا لسرعة الإنبات. كما اشارات دراسة اجريت من قبل **Bangarwa al et [14]** بان المركبات النباتية المستخلصة يمكن أن تشمل مجموعة واسعة من آليات المثبطة للعمل من خلال تأثيرها على الحمض النووي (قلويدات)، التمثيل الضوئي ,وظيفة الميتوكوندريا (Quinines)، عمل الهرمونات النباتية، امتصاص الأيونات والتوازن المائي (الفينول) .كما اشارات دراسة من قبل **حسن [16]** بان استخدم الدفله بشكل واسع لدواعي طبيه وحتى مبيدات فطرية وحشريه لما تمتلكه من تأثير سام في تركيبتها الكيميائية . قد يكون التأثير المثبط للدفلى ناجمة عن منتجات التحلل من glucosinolate التي تتراكم بكميات كبيرة في الأجزاء الخضرية من وخاصة اوراق الدفلة . حيث اثبتت العديد من الدراسات الى وجود كميات كبيرة من (Oleandrin Neriine) وهي تصنف ضمن مجموعة الكلاكوسيدات السامة.

4.2 تايير نوع المستخلص وتركيزه على بادرات دغل السعد

بعد ري البادرات النامية بطول 10- 15 سم بالمستخلصات النباتية عند تراكيز مختلفة تم تقييم نتائج التأثير على اساس نسبة تثبيط وقتل البادرات. سجلت المستخلصات المائية لنباتي الدفلة والخروع اعلى تأثير من حيث نسبة التثبيط وقتل البادرات مع قيم بلغت معدلاتها (87 و 85.5%) على التوالي والتي تفوقت عن نبات الزيتون ومعاملة السيطرة. فيما سجل اقل مستوى كبح للنمو من ري بادرات دغل السعد بمستخلص نبات الزيتون مع معدل قيم بلغت نسبتها (55%) شكل 3 .

KJPS
Al-Kitab Journal for Pure Science
Vol.2 (2), ISSN: 2617-1260 (print), 2617-8141(online)
www.kjps.isnra.org

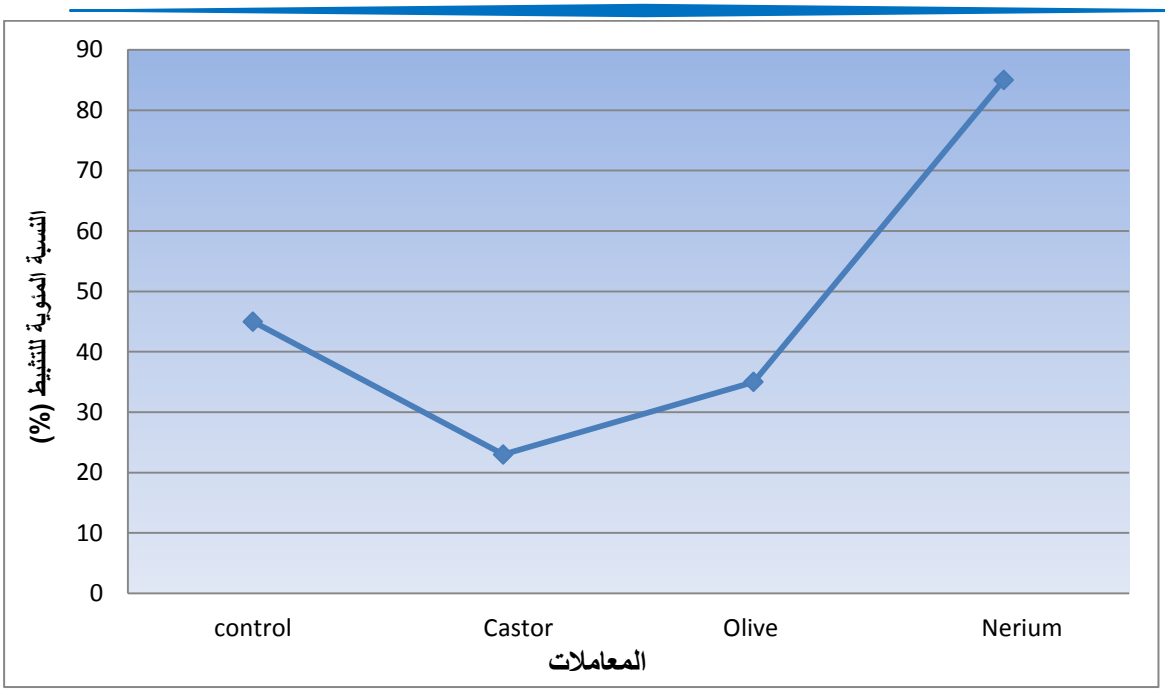

1. شكل (3). النسبة المئوية لتثبيط نمو بادرات دغل السعد .Cyperus rotundus L المروية بالمستخلصات المائية لأوراق نبات الدفلة (Nerium), و الزيتون (Olive) والخروع (Castor)

تأثير تراكيز المستخلصات المختلفة (5% , 7.5% و 10%) المحضرة من نبات الدفله والخروع والزيتون في كبح نمو بادرات السعد وضحت في الشكل.4. اعلى نسبة تثبيط سجلت مع التركيز 10% مع قيم تثبيط بلغت (82%) الذي سجل اختلاف معنوي بسيط عن التركيز 7.5 % مع قيم تثبيط وصلت الى (77%) لنبات الدفلة. في نفس الوقت سجل التركيزيين اختلاف معنوي عن جميع التراكيز الاخرى لنفس النبات والنباتات الاخرى. ومن الشكل 4. يلاحظ ان معامله السيطرة باستخدام المبيد الكيميائي سجلت مستويات عالية من كبح النمو لدغل السعد بلغت (74%) بالمقارنة مع مستخلصي نبات الخروع والزيتون وعند جميع التراكيز. واظهر مستخلص نبات الخروع تأثير متوسط لجميع التراكيز (40, 48 و 50 %) , فيما سجل مستخلص نبات الزيتون اقل النسب في كبح وتثبيط بادرات دغل السعد مع قيم بلغت (20 %, 32% و34 %) لتراكيز 5 , 7.5 و10% على التوالي .

T0 معاملة سيطرة باستخدام الماء	T1معاملة سيطرة بتخدام المبيد	T2 تركيز 10% نبات دفلة	T3تركيز 7.5% ت دفلة	T4تركيز 5% نبات دفلة	T5 تركيز 10% نبات زيتون
T6 تركيز 7.5% نبات زيتون	T7 تركيز 5% نبات ون	T8تركيز 10% نبات وع	T9تركيز 7.5% ت خروع	T10 تركيز 5% نبات وع	

KJPS Al-Kitab Journal for Pure Science
Vol.2 (2), ISSN: 2617-1260 (print), 2617-8141(online)
www.kjps.isnra.org

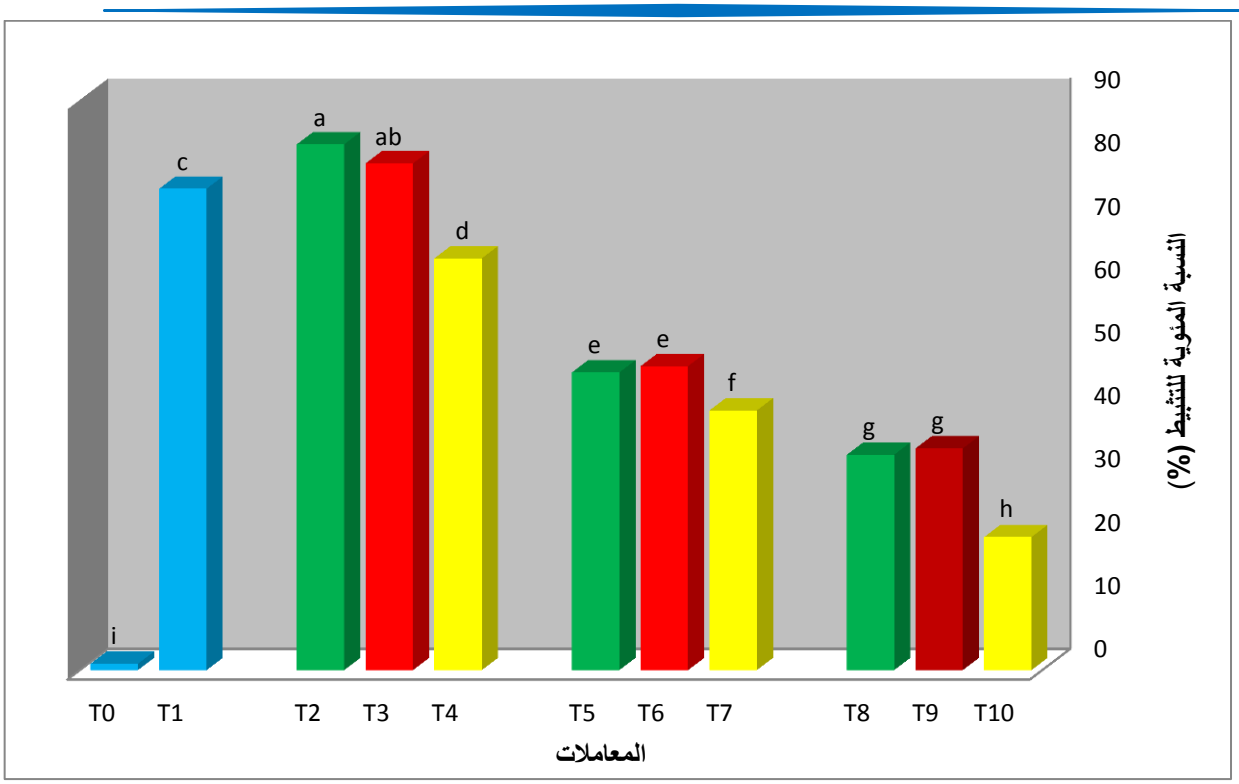

*اختلاف الأحرف لنسب التثبيط المئوي دلالة على وجود فرق معنوي بين المعاملات , فيما التشابه بين الأحرف دلالة على عدم وجود اختلافات معنوي عند مستوى معنوية 0.05

شكل (4) .النسبة المئوية (%) لتثبيط انبات بادرات السعد Cyperus rotundus L باستخدام تراكيز (10% , 7.% و 5%) من المستخلصات المائية لنبات الدفلة (Nerium), والزيتون (Olive) والخروع (Castor) .

من النتائج يلاحظ وجود اختلاف في التأثير الأليلوباثي باختلاف المستخلص النباتي ما بين قوي وضعيف وهذا يتفق مع ما توصل اليه **الجبوري** [17] بأن بعض المستخلصات المائية للأدغال الحولية كان لها تـأثيراتً مختلفة على إنبات بعض الادغال وان تأثيرات هذه المستخلصات تراوحت مابين سلبي أو إيجابي على النباتات الأخرى. كما بينت النتائج بان التأثير النتائج من المركبات الأليلوباثيه على انبات ونمو النبات وتطوره ممكن ان تعتمد على النوع النباتي والتركيز وان هذه المركبات قد تسبب تـأثيرات فسجليه مختلفة على النبات المستقبل **Reigosa et al [18]**.

كما جاءت نتائج الدراسة الحالية متفقه مع نتائج دراسات اجريت من قبل **Olofsdotter et al [20] , El-Rokiek et al [19]** **Duke et al [21]**، بتسجيل نسبه تثبيط عالية لنمو الأعشاب الضارة باستخدام المستخلصات النباتية المختلفة . ولكن لا توجد تقارير بشأن الاستخدام المحتمل الأنواع النباتية من الدفلة والخروع من الفورما النباتية العراقية . حيت تم الكشف عن إمكانية وكفاءة هذه المستخلصات النباتية الكبيرة في هذه الدراسة لأن المستخلصات اظهرت كفاءة وسميه عالية في مكافحة الادغال مشابه لاستخدام مبيدات الادغال المصنعة. نتائج الدراسة الحالية تتفق مع نتائج توصلت اليها دراسة **Turk et al [22]** بان المستخلص المائي لأورق نبات *Palmaris minor* اظهر تأثير ايجابي فعال في كبح وتثبيط معدل إنباب البذور ، طول البادرات والشتلات الوزن الجاف من الساق على جميع الأعشاب الضارة التي شملتها الدراسة.

KJPS Al-Kitab Journal for Pure Science
Vol.2 (2), ISSN: 2617-1260 (print), 2617-8141(online)
www.kjps.isnra.org

5. الاستنتاجات

اشارات نتائج الدراسة الحالية الى امكانية استخدام المستخلصات النباتية للنباتات المحلية (الدفله , الخروع) بكفاءة عالية كبدائل للمبيدات الكيميائية المصنعة في السيطره على نمو دغل السعد ويمكن ان تشكل احدى طرق المكافحة المتكاملة في برامج أداره الادغال الزراعيه .

المصادر

[1] Jafari R, Rezai S, Shakarami J, "***Evaluating effects of some herbicides on weeds in field bean"*** International Research Journal of Applied and Basic Sciences, 6 (8): 1150-1152. (2013).

[2] Food and Agriculture Organization .FAO, "***Implications of Maximum Residue Levels (MRLs) on tea trade*** " (2011).

[3] Nishimoto, R. (2001)"Purple nutsedge tubersprouting. Weed Biol. Manag. 1 (4),203,

[4] Hawver, C. A S. B. Gifford, and J. Hecht"***Comparison of methods to control invasive plant species in the Albany Pine Bush Preserve***" Albany Pine Bush. (2000).

[5] Md. Wasim Aktar, Dwaipayan Sengupta, and Ashim Chowdhury "***Impact of pesticides use in agriculture: their benefits and hazards***",, *Interdiscip Toxicol*, 2(1): 1-12,(2009***).***

[6] Food and Agriculture Organization FAO,"***Weed management for developing countries" (Addendum 1),(2011).***

[7] Japan Food Chemical Research Foundation" Maximum Residue Limits (MRLs) of Agricultural Chemicals in Foods,"(2011).

[8] Lofts, S "***Prediction of accumulation and leaching of fungicide copper in agricultural soils"*** NERC/Centre for Ecology and Hydrology, 58pp. (2011).

[9] Kebede, Z.,"**Review articles Chemical Ecology" Colorado State** University,http://www.colostate.edu/Depts/Entomology/courses/en570/papers_1994/kebede.html. (1994).

[10] Ruch, B. "***Processing of neem for plant protection simple and sophisticated standardized extracts" Abstracts of the Work shop, Neem and Pheromones***, University of Uberaba, Brazil, March 29-30 Augusts, P.499,(2001).

[11] Francisco, D. H., Francisco Castillo-Reyes, G., Raul. R" ***Lippia graveolens and Carya illinoensis Organic Extracts and there in vitro Effect against Rhizoctonia Solani Kuhn"*** American Journal of Agricultural and Biological Sciences,5(3):380-384. (2010).

[12] Singh, G. and M. Bhati"***Mineral Accumulation, Growth, and Physiological functions in Dalbergia sissoo Seedlings Irrigated with Different Wastewaters***" J. Environ. Sci. Health Part A-Toxic/Hazardous Substances & Environmental Engineering, 38:2679–2695 (2003).

[13] Majeed A, Chaudhry Z and Muhammad Z," ***Allelopathic assessment of fresh aqueous extracts of Chenopodium album L. for growth and yield of wheat (Triticum aestivum*** L.)" . Pak. J. Bot. 44(1): 165-167(2012).

[14] Bangarwa, S. K., J. K. Norsworthy, and E. E. Gbur "***Effect of Turnip Soil Amendment and Yellow Nutsedge (Cyperus esculentus) Tuber Densities on Interference in Polyethylene-Mulched Tomato***." Weed Technology 26: 364-370. 2012.

[15]السعيد,عبد العزيز بن محمد و الدوس عبد الله بن عبد العزيز"***التأثير الاليلو باثي لنبات الحرمل Rhazya stricta علي انبات بذو بعض النباتات المراعي***" المجلة الزراعية السنوية 42 (1), 159- 167(199).

[16]حسن فوزي طه "النباتات الطبية زراعتها ومكوناتها" دار المريخ للنشر, الرياض. ص356. (1981).

[17]الجبوري، باقر عبد خلف" علم الأدغال" وزارة التعليم العالي والبحث العلمي،الجمهورية العراقية.2002.

[18] Reigosa, M. J.; Gonzales, L. souto; X.C.; pastoriza , J.E "***Allelopathy in forest ecosystems Kluwer Acadmic publisher***s" , 184-193(2000).

[19] El-Rokiek, K. G.; El-Din, S. A. S.; Sharara, F. A.A "***Allelopathic behaviour of Cyperus rotundus L. on both Chorchorus olitorius (broad leaved weed) and Echinochloa crus-galli (grassy weed) associated with soybean***" Journal of Plant Protection Research,50(3) ,274-279,(2010) .

[20] Olofsdotter, M.; Jensen, L. B.; Courtois, B" ***Improving crop competitive ability using allelopathy - an example from rice***" Plant Breeding, 121(1), 1-9(2002)..

[21] Duke, S. O.; Dayan, F. E.; Rimando, A. M" ***Natural products as tools for weed management"*** *Weed Research***,** 40 (1) :99-111, 1998.

KJPS Al-Kitab Journal for Pure Science
Vol.2 (2), ISSN: 2617-1260 (print), 2617-8141(online)
www.kjps.isnra.org

DOI: http://10.32441/kjps.02.02.p22

خوارزمية مهجنة بين الشبكة المناعية الاصطناعية وتقنيةANFIS مع التطبيق

أ.م.د.عمر صابر قاسم م.م. اسراء رستم الخياط

كلية علوم الحاسوب والرياضيات، جامعة الموصل، الموصل، العراق.

[1] omarsaber79.os@gmail.com, [2]israaru.alkhayyat@gmail.com

الملخص

تم في هذا البحث تطوير إحدى خوارزميات الذكاء المناعي الاصطناعي وتحديدا الشبكة المناعية الاصطناعية (Artificial Immune Network) باستخدام تقنية نظام الاستدلال الضبابي العصبي التكيفي (Adaptive Neuro Fuzzy Inference System) والتي يرمز لها اختصارا ANFIS وذلك من خلال استخدام الذاكرة المناعية (Immune Memory)الناتجة من الشبكة المناعية كمدخلات لتقنية ANFIS لأجل زيادة فرصة تدريب نموذج يعتمد على أسلوب محاكاة أنماط البيانات, إذ أن الذاكرة المناعية الناتجة من الشبكة المناعية تقوم بعمل نسخ للبيانات بخصائص مشابهة للبيانات الأصلية, وقد أثبتت الخوارزمية المقترحة أنها ذات نتائج أفضل وأكفئ في التعرف على الأنماط مقارنة مع النظام المناعي الاصطناعي الاعتيادي.

الكلمات الدالة: الشبكة المناعية الاصطناعية, نظام الاستدلال الضبابي العصبي التكيفي.

KJPS Al-Kitab Journal for Pure Science
Vol.2 (2), ISSN: 2617-1260 (print), 2617-8141(online)
www.kjps.isnra.org

A Hybrid Algorithm Between the Artificial Immunological Network and the ANFIS Technique with Application

Omar S.Kasim[1] **Israa Ru.Alkhayyat[2]**

[1,2] **College of Computer Science & Mathematics, Mosul University, Mosul, Iraq.**

[1] **omarsaber79.os@gmail.com**,[2]**israaru.alkhayyat@gmail.com**

ABSTRACT

In this research, we have taken one of the artificial immune intelligence algorithms, namely the Artificial Immune Network, was developed using the Adaptive Neuro Fuzzy Inference System (ANFIS) by using the Immune Memory, The immunological network as an input to ANFIS technology to increase the chance of training a model based on the pattern of simulation of data patterns, as the immune memory resulting from the immunological network makes copies of data with characteristics similar to the original data. The proposed algorithm proved to have better and more efficient results rack on the patterns compared with the usual artificial immune system.

Keywords: Artificial Immune Network, Adaptive Neuro Fuzzy Inference System.

1. المقدمة Introduction

النظر إلى المستقبل البعيد قد يكون من اختصاص كتاب الخيال العلمي أما النظر إلى ما سيأتي بعد سنوات فهو توقع يدعمه الكثير إلى ما توصلنا إليه في مجالات البحث العلمي بشكل عام وبحوث الذكاء الاصطناعي بشكل خاص. إذ تعد تقنيات الذكاء الاصطناعي بإمكاناتها المذهلة وتطبيقاتها الواسعة في مختلف جوانب الحياة الأثر الواضح في خدمة العلوم المختلفة بكافة تخصصاته بما فيها التعرف على الأنماط.

ومن هذا المنطلق أصبحت هذه التقنيات مفتاح التطور الأساس لما تمتلكه من ميزات معالجة ولأسلوب بناءها المتوازي, إذ تم بناء نظام خبير يستطيع إن يصنف البيانات اعتمادا على معلومات المعطاة وأدلة العلمية المعتمدة وهذا يتطلب تعاونا كبير بين علماء الذكاء الاصطناعي وعلماء العلوم المختلفة. فالعلم لم يعد مقتصراً على الوسائل الكلاسيكية بل أمتد وتطور في الكثير من الدول المتقدمة وأصبح يعتمد بشكل كبير على تكنولوجيا المعلومات ووسائل الاتصالات لتصنيف الكثير من الحالات.

KJPS Al-Kitab Journal for Pure Science
Vol.2 (2), ISSN: 2617-1260 (print), 2617-8141(online)
www.kjps.isnra.org

إذ تم في هذا البحث دراسة إحدى احدث تقنيات الذكاء الاصطناعي وهي الشبكة المناعية الاصطناعية والتي تعتمد في عملها بشكل أساسي على مفهوم الذاكرة المناعية مع تقنية نظام الاستدلال الضبابي العصبي التكيفي, وذلك من خلال اخذ الصفات الايجابية لكلا التقنيتين لبناء نظام مهجن بين التقنيتين للتعرف على أنماط البيانات النباتية وتحديدا بيانات نبات زهرة السوسن والمعروفة بالاسم اللاتيني Iris .

حيث أثبتت التقنية المقترحة أنها ذات نتائج أفضل وأكفأ في التعرف على أنماط البيانات وتحديد نوع كل حالة وذلك من خلال مقارنة نتائج كل من التقنية المقترحة مع تقنية الشبكة المناعية الاصطناعية في التعرف على أنماط نبات زهرة السوسنIris وذلك بالاعتماد على عاملي الزمن(Time) ونسبة متوسط معدل مربع الخطأ(Mean Square Error) والذي من خلالهما يتم حساب كفاءة الطريقة المقترحة بالنسبة لطريقة الشبكة المناعية الاصطناعية.

2.الدراسات السابقة The Previous Studies

تعد الأنظمة المهجنة فرع من فروع الذكاء الاصطناعي والذي يعتمد في عمله على دمج تقنتين أو أكثر حسب طبيعة المسالة المراد حلها, إذ قدمت العديد من الدراسات في هذا المجال نستعرض بعضا منها.

في عام(2005) قدم كل من(Kemal Polat, Seral Şahan, Halife Kodazand Salih Güneş) بحثاً وظفا فيه استخدام خوارزميات النظام المناعي الاصطناعي مع المنطق المضبب في تصنيف الصور الرقمية[13].

وفي عام (2007) قدم كل (Salam A.Ismaeel, Ahmed M.Hassan, and Ali Farouq) دراسة تضمنت نظام الاستدلال الضبابي العصبي التكيفي على منظومة الملاحة حيث تم اخذ الصفات كلا من منظومة تحديد الموقع العالمي ومنظومة الملاحة بعزم القصور الذاتي ذوات الخواص المتناقضة فيما بينهما من اجل الحصول على منظومة متكاملة في عملها للحصول على ملاحة دقيقة في سرعة إعطاء المعلومة إذ يجب أن تحل قبل إعطاء أي تكامل بينهما[5].

KJPS Al-Kitab Journal for Pure Science
Vol.2 (2), ISSN: 2617-1260 (print), 2617-8141(online)
www.kjps.isnra.org

وفي عام (2010) قدم الباحث (Ibrahim F.Jasim) دراسة تضمنت استخدام نظام الاستدلال الضبابي العصبي التكيفي لمثبتات أنظمة القدرة إذ تم استخدام الدوائر المتكيفة للحصول على مثبت أنظمة قدرة يمكن هذا للنظام تجنب الصفات السلبية كلا من التقنيتين المنطق المضبب والشبكات العصبية الاصطناعية[6]. وفي عام (2015) قدم كل من الباحثين (Mahmoud Reza Saybani1, Shahaboddin Shamshirband, Shahram Golzari, Teh Ying Wah, Aghabozorgi Saeed, Miss Laiha Mat Kiah,Valentina Emilia Balas) بحثا لتشخيص مرض السل من خلال نظام طبي خبير يعتمد على النظام المناعي الاصطناعي وتضمنت هذه الدراسة 175 عينة منها 114 عينة للذين كانوا مصابين بمرض السل و 61 للذين لم يصابوا بالمرض[14].

3. التعرف على الأنماط Pattern Recognition

يعد نظام التعرف على الأنماط أو تمييز الأنماط هو علم وصف (تمييز) أو تصنيف المعايير, إذ يعرف النمط(Pattern) بأنه أي شيء(Object) يمتلك عدة صفات, كما تعرف صفة النمط (Pattern Feature) بأنها مجموعة من المعايير التي يمتلكها ذلك النمط (كاللون,التردد...الخ)[12].

يتم التعرف على الأنماط من خلال تقسيم البيانات إلى مجموعات معينة مبنية على صفات موحدة تعرف بصنف النمط (Pattern Class)ويفترض بالأصناف (Classes) أن تعطي تصنيف جميع أنماط البيانات المطلوب التعرف عليها, وذلك من خلال الحد الفاصل (Decision Boundary) المحيط بمنطقة التصنيف[19].

4. النظام المناعي الاصطناعي Artificial Immune System

تعد تقنية الأنظمة المناعية الاصطناعية (Artificial Immune Systems) والتي تكتب اختصارا (AIS) من أهم أصناف علوم الحاسوب الحديثة في مجال علم الذكاء الاصطناعي والتي يتم من خلالها محاكاة النظام المناعة الطبيعي إذ تعتمد هذه التقنية على مبادئ وعمليات مستوحاة من آليات العمل الطبيعية التي يقوم بها النظام المناعي في جسم الإنسان[4][21].

KJPS Al-Kitab Journal for Pure Science
Vol.2 (2), ISSN: 2617-1260 (print), 2617-8141(online)
www.kjps.isnra.org

تم في هذا البحث التطرق إلى إحدى هذه التقنيات وهي الشبكة المناعية الاصطناعية والمستوحاة من نظرية الشبكة المناعية الطبيعية (Idiotypic) إذ تعتمد في عملها على الخلايا المناعية نوع B-Cell التي يحفزها النمط الغريب (المستضدAg) لتكون شبكة مترابطة من الأجسام المضادةAb والتي من خلالها يتم التعرف على النمط الغريبAg ويتم ذلك من خلال مرحلتين:

الأولى: تحفيز الشبكة (Activation Network): إذ يتم ربط مستقبل الجسم المضاد(Paratope) مع مستقبل المستضد (Epitope) بقوة اتصال معينة تعرف بقوة التطابق(Matching).

الثانية: إخماد الشبكة(Suppression Network): يتم ربط مستقبل جسم مضاد(Idiotope) مع مستقبل جسم مضاد آخر(Idiotope),وبذلك فأن الجسم المضادAb2 يمتلك صورة ذاكرة داخلية(Internal Memory Image)عن الجسم المضادAb1[15].الموضحة في الشكل الأتي:

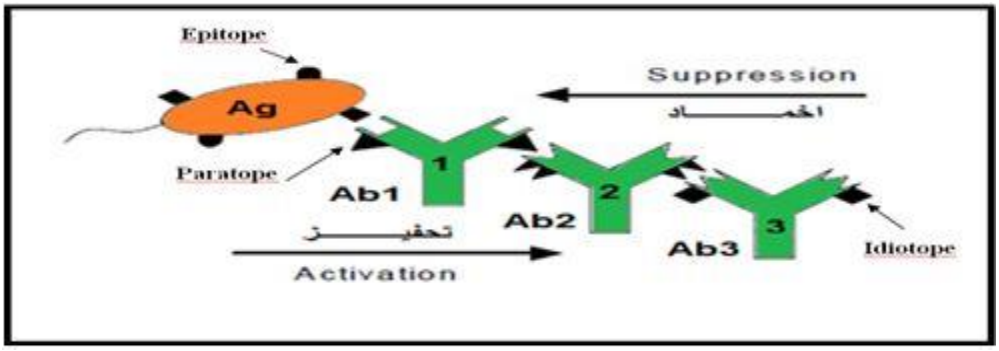

الشكل(1): يوضح آلية عمل نظرية الشبكة المناعية.

5. معمارية الشبكة المناعية الاصطناعية (AIN)

اقترحت خوارزمية AIN من قبل (De Castro and Von Zuben) عام 2001, إذ تتكون من الخطوات الآتية: [1]

الخطوة الأولى: التهيئة(Initialization): إنشاء مجتمع ابتدائي عشوائي من مجموعة الكاشفات (الأجسام المضادةAb), ولتكن M تمثل الذاكرة المناعية (Memory Immune),M=Ø.

الخطوة الثانية: التمثيل (Representation): لكل نمط غريب مدخل (i) الذي يمثل (المستضد Ag) الاستمرار في إجراء الخطوات الآتية :

KJPS Al-Kitab Journal for Pure Science
Vol.2 (2), ISSN: 2617-1260 (print), 2617-8141(online)
www.kjps.isnra.org

- الاختيار النسيلي(Clonal Selection): لكل نمط غريب مدخل (المستضدAg) يتم إيجاد درجة صلته(Affinity Degree) مع مجموعة الكاشفات (الاجسام المضادة Ab) ويتم ذلك من خلال تطبيق إحدى دوال درجة الصلة فمثلاً تطبيق دالة المسافة الاقليدية.
- يتم اختيار (n) من الكاشفات (الأجسام المضادةAb) التي تمتلك درجة الصلة عالية (High Affinity) مع النمط الغريب (المستضد Ag)ويتم استنساخها(Clone) بشكل يتناسب مع صلتها (أي التي تملك صلة عالية لها نسبة اختيار اكبر) أي أن عدد النسخ يتناسب طردياً مع مقدار درجة الصلة.
- تغير الصلة (Affinity Mutation): يتم تطبيق عملية الطفرة (التغير) إذ يتم تغير نسخ الكاشفات(الأجسام المضادة Ab) بصورة تتناسب عكسيا مع درجة صلته أي التي تمتلك أعلى مقدار للصلة تكون نسبة التغير صغيرة والعكس بالعكس.
- يتم حساب درجة صلة مجموعة الكاشفات (الأجسام المضادة Ab) المحسنة مع النمط الغريب المدخل (المستضدAg) (i), ويتم اضافتها إلى مجموعة الذاكرة المناعية.
- الموت الطبيعي (Natural Death): إزالة مجموعة الكاشفات (الأجسام المضادةAb) المحسنة التي لها درجة صلة أقل من حد العتبة (Pruning Threshold) مع النمط الغريب (المستضدAg) وتكتب اختصارا (tp).
- الإخماد النسيلي(Clonal Suppression): حساب درجة الصلة بين مجموعة الكاشفات (الأجسام المضادة Ab) المحسنة (Ab-Ab) وإزالة منها مجموعة الكاشفات (الأجسام المضادة Ab) التي لها درجة صلة أقل من حد العتبة الإخماد(Suppression Threshold) وتكتب اختصارا (ts).
- دمج مجموعة الكاشفات (الأجسام المضادةAb) المتبقية من الذاكرة مع مجموعة الكاشفات (الأجسام المضادةAb) للشبكة.

الخطوة الثالثة:إخماد الشبكة (Network Suppression) : حدد درجة الصلة بين مجموعة الكاشفات (الأجسام المضادة Ab) للشبكة وإزالة الكاشفات (الأجسام المضادة) التي لها درجة صلة بالبقية أقل من عتبة الإخماد (ts).

KJPS Al-Kitab Journal for Pure Science
Vol.2 (2), ISSN: 2617-1260 (print), 2617-8141(online)
www.kjps.isnra.org

الخطـــوة الرابعـــة: اســتبدال الكاشــفات (الأجســام المضــادةAb) التــي تكــون درجــة صــلتهم قليلــة بــآخرين يــتم توليدهم بشكل عشوائي .

الخطوة الخامسة: تكرار الخطوات من (2-4) إلى أن يتحقق مقياس التوقف.

6. نظام الاستدلال الضبابي العصبي التكيفي Adaptive Neuro Fuzzy Inference System

هـو نظـام حاسـوبي ذكـي يعتمـد فـي عملـه علـى تهجـين بـين تقنيتـين المنطـق المضـبب والشـبكات العصـبية الاصطناعية, ويتم ذلك من خلال اخذ الصفات الايجابية لكلا التقنيتين و التغلب على الصفات السلبية من اجل تصميم نظام ذو كفاءة أعلى لمعالجة البيانات واتخاذ القرار, إذ تعتمد كلا التقنيتين في عملهما على محاكاة آلية معالجة المعلومات بطريقة أكثر شبهاً للعقل البشري. فإذا دمجت كلا التقنيتين باعتبار أن احدهما مكمل للأخر تتحقق نتائج أفضل مما لو طبقت لوحدها[5][8].

1.6المنطق المضبب Fuzzy Logic

إن منطق الغموض لا يعني التفكير المضبب بل هو أسلوب لمعالجة حالات الغموض واللادقة في حياتنا إذ تعد نظرية المنطق المضبب توسيع للمنطق التقليدي والتي اقترحها العالم لطفي زاده من جامعة كاليفورنيا عام 1965. والتي تعتمد في عملها على المجموعة المضببة(Fuzzy Set)التي تتميز عن المجموعة الاعتيادية(Ordinary Set) وتسمى أيضا المجموعة الهشة(Crisp Set) بان حدودها مرنة وليست قطعية ولا يمكن تعريف حدودها بشكل دقيق, إذ يمكن تمثيل ذلك بالفرضية الآتية لنفترض لدينا عنصر ما ولنتعرف على درجة انتماء ذلك العنصر للمجموعة الاعتيادية فان ذلك العنصر قد ينتمي أو لا ينتمي لمجموعة ويمكن تمثيلها بالمعادلة الآتية:

$$M_A(x) = \begin{cases} 1 & \Leftrightarrow \quad x \in A \\ 0 & \Leftrightarrow \quad x \notin A \end{cases} \qquad \dots (1)$$

أما في المنطق المضبب يكون للعنصر له انتماء جزئي ودرجة انتماءه يطلق عليها درجة العضوية وتكون درجة عضوية مجموعة جزئية من مجموعة شاملة. فلو كانت X تمثل المجموعة الشاملة (Universal Set) فان المجموعة المضببةA من X هي عبارة عن مجموعة الأزواج المرتبة(Ordered Pairs) والموضحة بالشكل الأتي[9][11]:

KJPS Al-Kitab Journal for Pure Science
Vol.2 (2), ISSN: 2617-1260 (print), 2617-8141(online)
www.kjps.isnra.org

$$A=\{x, M_A(x)\} \qquad ...(2)$$

حيث أن:
x:هو عنصر في المجموعة **X**.
$M_A(x)$: تمثل درجة العضوية العنصر **x** في **A** .
ودرجة العضوية $M_A(x)$ تقع بين 0 و 1.

بما أن مفهوم المنطق المضبب يعتمد بشكل أساسي على مبدأ انه لايوجد انتماء كلي للمجموعات، فهناك ثمة انتماء أو انتماء جزئي بمستوى يتحدد من خلال معالجة المعلومات وقد أطلق على هذه المستويات دالة العضوية(Membership Function) التي يتم من خلالها تحديد نسبة الانتماء إلى خصائص المجموعة,وان هذه الدالة يقع مداها بين الصفر والواحد كما أن لها أشكالاً متعددة منها[7]:

1) دالة كاوس(Gaussian Function):

$$\mu(x) = e^{-\frac{(x-c)^2}{2\sigma^2}} \ldots\ldots(3)$$

إذ تمثل c وσتمثلان على التوالي الرأس العلوي للشكل وبعد الأطراف عن مركز الشكل.

2) دالة العضوية ذات الشكل المثلثي(Triangular Function):

$$\mu(x) = \begin{cases} 0 & x \le a \\ \frac{x-a}{b-a} & a \le x \le b \\ \frac{c-x}{c-b} & b \le x \le c \\ 0 & c \le x \end{cases} \quad \ldots..(4)$$

حيث أن a و b و c هي معلمات الدالة,a و c تمثلان قوائم الدالة المثلثية وقيمة b تمثل رأس المثلث.

3) دالة العضويه ذات الشكل شبه المنحرف(Trapezoidal Function):

$$\mu(x) = \begin{cases} 0 & x \le a \\ \frac{x-a}{b-a} & a \le x \le b \\ 1 & b \le x \le c \\ \frac{d-x}{d-c} & c \le x \le d \\ 0 & d \le x \end{cases} \quad \ldots.(5)$$

KJPS Al-Kitab Journal for Pure Science
Vol.2 (2), ISSN: 2617-1260 (print), 2617-8141(online)
www.kjps.isnra.org

حيث أن كل من a و b و c و d هي معلمات للدالة وأن a و d تمثلان الرؤوس السفلى للشكل في حين b و c تمثلان الرؤوس العليا.

إن أهم ما يميز النظام المضبب هو قدرته على التعامل مع البيانات اللغوية والتي تختلف عن البيانات الرياضية بأنها تأخذ من الكلمات كقيم للإدخال البيانات للنظام المضبب وهذا مايميزه عن الأنظمة الذكائية الأخرى التي تتعامل مع الأرقام كقيم للإدخال. ولتصميم أي نموذج مضبب لابد من أن يمر بالمراحل المعالجة الموضحة بالمخطط الأتي[18]:

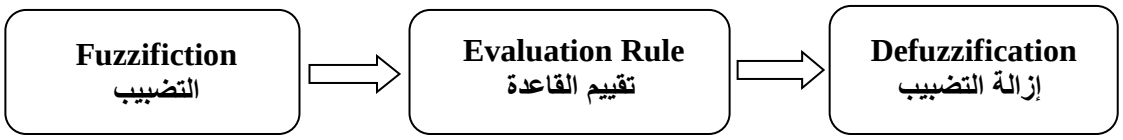

2.6 أنظمة الاستدلال المضببة Fuzzy Inference System

إن نظام الاستدلال المضبب بشكل عام هو أسلوب الذي يستخدم التفكير المضبب لتحويل فضاء الإدخال إلى فضاء الناتج بالاعتماد على قاعدة (If…Then), إذ يوجد نوعان من أنظمة الاستدلال المضببة الأساسية لأجل عمل القواعد المضببة لاتخاذ القرار المناسب في معالجة البيانات:

1) نظام الاستدلال الضبابي مامداني Mamdani.

2) نظام الاستدلال الضبابي تاكاجي–سوجينو Takagi-Sugeno.

يعد نظام الاستدلال من نوع مامداني من أكثر الأنظمة انتشارا وملائم لكثير من الإدخالات البشرية,إذ يستخدم أسلوب عكس التضبيب (Defuzzification) على المجموعة المضببة الناتجة من حاصل جمع المجموعات المضببة لكل قاعدة في جزء تابع (Consequent),إذ يتم تمثيل الإخراج فيه بشكل مجاميع مضببة بالاعتماد على قاعدة (If…Then) ويمكن توضيح ذلك بالصيغة الآتية:

يعد نظام الاستدلال من نوع مامداني من أكثر الأنظمة انتشارا وملائم لكثير من الإدخالات البشرية,إذ يستخدم أسلوب عكس التضبيب (Defuzzification) على المجموعة المضببة الناتجة من حاصل جمع المجموعات المضببة لكل قاعدة

KJPS Al-Kitab Journal for Pure Science
Vol.2 (2), ISSN: 2617-1260 (print), 2617-8141(online)
www.kjps.isnra.org

في جزء تابع (Consequent)إذ يتم تمثيل الإخراج فيه بشكل مجاميع مضببة بالاعتماد على قاعدة (If…Then)

ويمكن توضيح ذلك بالصيغة الآتية:

$$R_i : IF\ x\ is\ A_i\ THEN\ \ y\ is\ B_i \qquad i = 1, 2, \ldots\ldots, K$$

A_i: تمثل معلمات الأسبقية(Antecedent).

B_i: تمثل مجموعة النواتج التابعة(Consequent).

أما نظام الاستدلال من نوع تاكاجي_سوجينو يقوم هذا النظام بتوليد القواعد المضببة بالاعتماد على نوع بيانات الإدخال والإخراج وأما الناتج (Y) فيحسب بأخذ معدل الأوزان للقواعد, إذ يتم تمثيل الاخراج فيه بشكل قيم ثابتة ويمكن توضيح ذلك كما يأتي[20][18][10]:

$$R_i: IF\ x\ is\ A_i\ \ THEN\ \ Y_i\ =\ a_i^T x + b_i \qquad i = 1, 2, \ldots\ldots, K$$

a_i: متجه معلمات التابع,b_i: مقياس تعديل.

كما أن المعدل الموزون للقواعد يحسب من خلال المعادلة الآتية :

$$Y = \frac{\sum_{i=1}^{K} \beta_i(x) y_i}{\sum_{i=1}^{K} \beta_i(x)} = \frac{\sum_{i=1}^{K} \beta_i(x)\left(a_i^T x + b_i\right)}{\sum_{i=1}^{K} \beta_i(x)} \qquad \ldots (6)$$

$\beta_i(x)$: تمثل دالة العضوية.

وكحالة خاصة عندما يكون من الرتبة صفر (Zero-Order Polynomials) فان التابع يكون بالشكل الآتي:

$$Ri: IF\ x\ is\ A_i\ \ THEN\ \ Y =\ b_i \qquad i = 1, 2, \ldots . k$$

7.معمارية نظام الاستدلال الضبابي التكيفي (ANFIS)

تتكون معمارية هذا النظام من خمسة طبقات, والتي تعتمد على التهجين بشكل أساسي لتمثيل معلمات أنظمة الاستدلال من نوع (تاكاجي-سوجينوTakagi-Sugeno), إن أهم الصفات التي يمتلكها نظام المنطق المضبب انه يعتمد على قواعد لغوية (If… Then) لذلك فهو يحتاج إلى أن تكون بيانات التدريب متغيرات لغوية لذلك فان النظام يوصف بشكل لغوي.

KJPS Al-Kitab Journal for Pure Science
Vol.2 (2), ISSN: 2617-1260 (print), 2617-8141(online)
www.kjps.isnra.org

أما ما يميز الشبكات العصبية الاصطناعية فإنها تملك أمثلة تدريب كافية بدون معرفة البيانات المدخلة, وتتم عملية معالجة المعلومات من خلال استخدام طريقتي المربعات الصغرى (LS)بالاتجاه الأمامي وتطبيق شبكة الانتشار الخلفي (BP) بالاتجاه العكسي وهذا النظام بأكمله يسمى معمارية نظام الاستدلال الضبابي العصبي التكيفي(ANFIS)[17] .

الطبقة الأولى :تسمى طبقة التضبيب(Fuzzification layer), إذ يتم فيها تضبيب المدخلات من خلال دوال العضوية والموضحة بالمعادلة الآتية:

$$O_i^1 = \mu_{A_i}(x) \dots (7)$$

$\mu_{A_i}(x)$: تمثل دالة العضوية.

O_i^1: الإخراج للطبقة الأولى.

الطبقة الثانية : تمثل طبقة القواعد (Rules), إذ أن كل خلية عصبية في هذه الطبقة تقابل قاعدة مضببة وحيدة من نوع تاكاجي–سوجينو, وكل خلية قاعدة تستلم الإدخالات من خلايا التضبيب وتحسب قوة إثارة القاعدة (Firing Strength) التي تمثلها.في تقنية (ANFIS), ارتباط أسبقيات القاعدة يقدر من خلال حاصل الضرب (Product),وحساب ناتج الخلية العصبية (i) في الطبقة الثانية يتم من خلال المعادلة الآتية:

$$O_i^2 = w_i = \Pi \mu_{A_i}(x) \dots (8)$$

الطبقة الثالثة :الخلية العصبية فهذه الطبقة تستلم الإدخالات من كل الخلايا العصبية في طبقة القاعدة،إذ يتم فيها إجراء عملية التطبيع (Normalization) على الخلايا العصبية لحساب قوة الإثارة. كما أن حساب ناتج الخلية العصبية (i) في الطبقة الثالثة يتم من خلال المعادلة الآتية:

KJPS Al-Kitab Journal for Pure Science
Vol.2 (2), ISSN: 2617-1260 (print), 2617-8141(online)
www.kjps.isnra.org

$$O_i^3 = \overline{w_i} = \frac{w_i}{\sum w_i} \dots (9)$$

الطبقة الرابعة : تتم في هذه الطبقة عملية عكس التضبيب (Defuzzification), إذ أن كل خلية عصبية في هذه الطبقة تتصل بخلية التطبيع الخاصة وأيضا تستلم الإدخالات الأولية (Initial Inputs) مثل (x1 and x2).

إن كل خلية في هذه الطبقة تحسب قيمة الإخراج للقاعدة المستند على معلمات التوابع:

$$O_i^4 = y_i = \overline{w_i} f_i = \overline{w_i}(p_i x_1 + q_i x_2 + r_i) \quad \dots (10)$$

حيث تمثل p_i و q_i و r_i معلمات التوابع للقاعدة (i).

الطبقة الخامسة: تتكون من خلية عصبية وحيدة تمثل حاصل جمع النواتج للخلايا العصبية في الطبقة السابقة (طبقة عكس التضبيب), ويتم من خلالها حساب الإخراج النهائي لنظام الاستدلال الضبابي العصبي التكيفي(ANFIS)[2].

$$O_i^5 = \sum_i y_i = \sum_i \overline{w_i} f_i = \sum_i \overline{w_i}(p_i x_1 + q_i x_2 + r_i) \dots (11)$$

8.الخوارزمية المقترحة (AIN_ANFIS)

الخوارزمية المقترحة تتألف من مرحلتين أساسيتين من مراحل معالجة البيانات, إذ يتم في المرحلة الأولى استخدام تقنية الشبكة المناعية الاصطناعية من اجل الحصول على أنماط بيانات كافية (حالات جديدة) من خلال اعتماد مفهوم مصفوفة الخزن في الشبكة المناعية والتي تحاكي البيانات الأصلية من خلال الصفات الموجودة في هذه البيانات, إذ إن الآلية التي يعتمدها النظام المناعي الاصطناعي (AIS) في تكوين مصفوفة الذاكرة (M) يساهم بشكل مباشر في إيجاد

KJPS Al-Kitab Journal for Pure Science
Vol.2 (2), ISSN: 2617-1260 (print), 2617-8141(online)
www.kjps.isnra.org

حالات جديدة بالاعتماد على دراسة سلوك الحالات المدخلة بشكل أنماط بيانات التدريب, إلا أن هذه الزيادة في عدد الحالات قد تحتاج إلى وقت اكبر في عملية التصنيف المتبعة في الشبكة المناعية الاعتيادية من خلال سلوك المقارنة بين النمط المدخل والأنماط المخزونة في مصفوفة الذاكرة, لذلك تم تطبيق تقنية (ANFIS) في المرحلة الثانية لأجل تصنيف بيانات الاختبار بدلا من استخدام عملية المقارنة المتبعة في الشبكة المناعية الاعتيادية, حيث أن الخطوات الآتية تبين آلية عمل الخوارزمية المقترحة (AIN_ANFIS) في هذه الدراسة:

1- تهيئة أنماط بيانات الإدخال بشكل مصفوفة (X) صفوفها تمثل عدد الحالات للبيانات وأعمدتها تمثل عدد الميزات التي تم قياسها في كل من هذه الحالات.
2- تقسيم أنماط بيانات الإدخال إلى مجموعتين أساسيتين، تمثل الأولى مجموعة أنماط بيانات التدريب(x_{Train}) ويكون عددها (70%) من البيانات في حين تمثل المجموعة الثانية بيانات الاختبار (x_{Test}) ويكون عددها (30%)من البيانات، أي بواقع ثلثين بالمئة من الحالات للتدريب وثلث منها للاختبار.
3- استخدام مجموعة بيانات التدريب (x_{Train}) في النظام المناعي لبناء مصفوفة الخزن (Memory Matrix) وذلك من خلال تطبيق مفاهيم الشبكة المناعية الاصطناعية.
4- استخدام مصفوفة الخزن (Memory Matrix) الناتجة من الشبكة المناعية كمجموعة بيانات تستخدم في تدريب نموذج (ANFIS).
5- استخدام تقنية(ANFIS) في تصنيف حالات الاختبار، بعد أن يتم تدريبها باستخدام البيانات الناتجة من مصفوفة الخزن.
6- مقارنة نتائج مجموعة بيانات الاختبار (x_{Test})مع النتائج الحقيقية، بعد تطبيقها على الخوارزمية المقترحة لمعرفة مدى كفاءتها.

9.تطبيق الخوارزمية المقترحة على بيانات (Iris)

تم تطبيق الخوارزمية المقترحة على بيانات زهرة السوسن(Iris) والمأخوذة من موقع البيانات العالمي (UCI Machine Learning Repository)، حيث أن عدد الحالات للبيانات هي 150 حالة والتي تصنف إلى ثلاث أنواع (النوع الأول يسمى Setosa, والنوع الثاني يسمى Versicolor أما النوع الأخير فيكون من نوع Virginica) حيث يتوزع عددها بنسبة 50 حالة لكل صنف.

KJPS Al-Kitab Journal for Pure Science
Vol.2 (2), ISSN: 2617-1260 (print), 2617-8141(online)
www.kjps.isnra.org

Iris_Virginica Iris_Vericolor Iris_Setosa

إن مجموعة معلومات زهرة السوسن أو آيريس أو آيريس فيشر قدمت من قبل الخبير الإحصائي والإحيائي البريطاني رونالد فيشر عام 1935 إذ عرفت البيانات باسمه (Fisher Iris Data) ومن خلال دراسته لأنواع الثلاث إذ تتكون البيانات من قراءات تمثل مقياسي الطول والعرض للأوراق التويجية (Petal) وكذلك مقياسي الطول والعرض للأوراق الكاسية(Sepal)[3].

إن الخوارزمية المقترحة نموذجا حاسوبيا يعتمد مبادئ علم الأنظمة الذكائية القادرة على معالجة البيانات بإسلوب يحاكي الأنظمة الحيوية الطبيعية، حيث تم في هذه الخوارزمية المقترحة تطوير تقنية الشبكة المناعية الاصطناعية وذلك من خلال تقنية (ANFIS)، من اجل الحصول على طريقة قادرة على تصنيف البيانات بأسلوب أكثر ايجابية من حيث تقليل نسبة الخطأ والوقت المستغرق في معالجة البيانات.

لقد تم تطبيق الخوارزمية المقترحة (AIN_ANFIS) على بيانات الاختبار (Data Test) الخاصة بزهرة السوسن والمعروفة بالاسم العلمي اللاتيني (Iris) ومقارنتها مع الشبكة المناعية الاصطناعية (AIN) القياسية، وتم الاعتماد على عدد من المقاييس منها مقياس الزمن (Time) بالثواني (Seconds) ومقياس متوسط مربع الخطأ (Mean Square Error) والذي يكتب اختصارا (MSE)، حيث يتم حسابه بالشكل الآتي:

$$\boldsymbol{MSE = \frac{1}{N}\sum_{i=1}^{N}(t_i - Actual_i)^2} \qquad \dots\dots\dots(12)$$

حيث أن:
N: عدد الحالات.
t_i: يمثل الإخراج المطلوب (Target Output) للبيانات.
$Actual_i$: يمثل الإخراج الحقيقي (Actual Output) للشبكة.

KJPS Al-Kitab Journal for Pure Science
Vol.2 (2), ISSN: 2617-1260 (print), 2617-8141(online)
www.kjps.isnra.org

الجدول (1): مقارنة بين الشبكة المناعية الاعتيادية (AIN) والخوارزمية المقترحة (AIN_ANFIS) في تصنيف أوراق نبات السوسنIris

نوع التقنية المستخدمة *(Type of Technique)*	معدل مربع الخطأ *(MSE)*	الزمن بالثانية *(Time)*	مقياس الكفاءة *(EFF)*
الشبكة المناعية المهجنة (AIN_ANFIS)	0.01944	18.54	2.7723
الشبكة المناعية الاعتيادية (AIN)	0.44444	324.64	0.0406

نلاحظ من خلال الجدول(1) أن الطريقة المقترحة (AIN_ANFIS) باستخدام الشبكة المناعية (AIN) وتقنية (ANFIS) أعطت نتائج أفضل من الشبكة المناعية الاصطناعية (AIN) القياسية في تصنيف بيانات (Iris), وذلك من خلال مقياس معدل مربع الخطأ (MSE).

كما نلاحظ أن الزمن المستغرق في معالجة أنماط بيانات باستخدام التقنية المقترحة (AIN_ANFIS) هو أقل من الزمن المستغرق في معالجة البيانات باستخدام الشبكة المناعية الاصطناعية(AIN)القياسية, ومن خلال ذلك يمكن التأكيد بان التقنية المقترحة (AIN_ANFIS)هي الأفضل في تصنيف أنماط بيانات (Iris), من الشبكة المناعية الاصطناعية القياسية. إذ تم حساب مقياس الكفاءة (Efficiency Scale) والذي يكتب اختصارا (EFF) ويمثل المحصلة النهائية لكل من عاملي الزمن(Time) ومتوسط مربع الخطأ(MSE), حيث يتم احتسابه بالشكل الآتي[16].

$$EFF = 1/(MSE * Time) \quad \ldots\ldots\ldots (13)$$

10.الاستنتاجات والتوصيات Conclusions and Recommendations

تضمنت هذه الدراسة خوارزمية مقترحة بين كل من الشبكة المناعية الاصطناعية (AIN)الاعتيادية وتقنية(ANFIS) واستخدامها في تصنيف بيانات زهرة السوسن (Iris). ومن خلال التطبيق العملي تبين بان نسبة التصنيف للخوارزمية المقترحة(AIN_ANFIS) تفوق نسبة التصنيف في خوارزمية الشبكة المناعية

الاصطناعية(AIN)القياسية وذلك من خلال مؤشر متوسط مربع الخطأ (MSE)، كما أن الزمن (Time) المستغرق في انجاز الخوارزمية المقترحة اقل نسبيا بكثير من الزمن المستغرق في انجاز خوارزمية الشبكة المناعية الاصطناعية، مما يدل على كفاءة الخوارزمية المقترحة(AIN_ANFIS) مقارنة بالخوارزمية الشبكة المناعية الاصطناعية الاعتيادية.

كما نوصي بدراسة تطوير الشبكة المناعية الاصطناعية (AIN) باستخدام التقنيات الذكائية الأخرى وعمليات تحسينها من خلال عملية التهجين، لتطوير آلية تصنيف الأنماط المختلفة من البيانات ومنها (Iris)، كما يمكن اعتماد الطريقة المقترحة في تصنيف الحالات للبيانات المختلفة بدلا من الطريقة الاعتيادية التي تستغرق وقتا طويلا في اختبار الأنماط من خلال مقارنتها مع الأنماط الموجودة في مصفوفة الخزن (Memory Matrix).

11. المصادر References

[1]الخياط, إسراء رستم محمد, (2013), "**ملاءمة نموذج لنظام مناعي حاسوبي مهجّن في التشخيص الطبي**", رسالة ماجستير غير منشورة, كلية علوم الحاسوب والرياضيات, جامعة الموصل.

[2] قاسم, عمر صابر,(2010)"**تطبيق التقنيات الذكائية في المعلوماتية الحياتية** " اطروحة دكتوراه, غير منشورة, كلية علوم الحاسوب والرياضيات, جامعة الموصل.

[3] ويكيبيديا الموسوعة الحرة,(2017), على الرابط https://en.wikipedia.org/wiki/Iris_flower_data_set.

[4] Ertel Wolfgang,(2011)," **Introduction to Artificial Intelligence**", Translated by Nathanael Black With illustrations by Florian Mast, Springer-Verlag London Limited 2011, www.springer.com /series/7592.

[5] Ismaeel Salam A., Ahmed M.Hassan, and Ali Farouq,(2007),"**ADAPTIVE FUZZY SYSTEM FOR GPS DATA PREDICTION** ",IJCCCE, VOL.7, NO.2.

[6] Jasim Ibrahim F.,(2010)," Fuzzy Neural Design of Power Systems Stabilizers", Journal of Kerbala University , Vol. 8 No.1 Scientific.

[7] klir George J. and Yuan Bo,(1995),"FUZZY SETS AND FUZZY LOGIC" Theory and Applications,ISBN 0-13-101171.

[8] Klir George J.,(2006), "UNCERTAINTY AND INFORMATION" Foundations of Generalized Information Theory, ISBN-13:978-0-471-74867-0 ,ISBN-10:0-471-74867-6, Printed in the United States of America 10987654321.

[9] Konar A., (2000), **" Artificial Intelligence and Soft Computing Behavioral and Cognitive Modeling of the Human Brain"**, Department of Electronics and Tele-communication Engineering Jadavpur University, Calcutta, India, © by CRC Press LLC.

[10] Majeed Rasha Ilham,(2009),” Design and FPGA Implementation of Takagi- Sugeno Fuzzy Controller Based on LUTs”, Al-Rafidain Engineering Vol.18 No.6 December 2010.

[11] Negnevitsky M., (2005), **" Artificial Intelligence A Guide to Intelligent Systems"**, Second Edition ,ISBN 0321204662.

[12]Obinata G. and Dutta A., (2007), **" Vision Systems: Segmentation and Pattern Recognition"**, ISBN 978-3-902613-05-9.

[13] Polat K. ,Sahan S.,Kodaz H. and Güneş S., (2005), **" Outdoor Image Classification Using Artificial Immune Recognition System (AIRS) with Performance Evaluation by Fuzzy Resource Allocation Mechanism"**, A. Gagalowicz and W. Philips (Eds.): CAIP, LNCS 3691, pp. 81 – 87, © Springer-Verlag Berlin Heidelberg .

[14] Saybani1 Mahmoud Reza, Shamshirb and Shahaboddin, Golzari Shahram, WahTeh Ying, Saeed Aghabozorgi, Kiah Miss Laiha Mat, and Balas Valentina Emilia,(2015**),”RAIRS2 a new expert system for diagnosing tuberculosis with real-world tournament selection mechanism inside artificial immune recognition system**” DOI 10./1007/s11517_015_1323_6,springer.

[15] Slocket J., (2011), **" Dynamic Strategy Generation in computer games using Artificial Immune Systems"**, A Thesis presented to The University of Guelph In partial fulfilment of requirements for the degree of Master of Science in Computer Science.

[16] Steel R.G.D. and Torrie J.H., (1980), **"Principles and Procedures of Statistics a Biometrical Approach"**, Mc Graw-Hill, Inc.

[17] Suliman Mohammed Yahya,(2016),” A Proposal Technique of High Impedance Fault Detection Using Adaptive Neuro- Fuzzy Logic Control”,Eng.&Tech.Journal,vol.34,part(A),NO.11.

[18] Sumathi S. and Surekha p., (2010), **" Computational Intelligence Paradigms Theory and Applications Using MATLAB "**,by Taylor and Francis Group, LLC CRC Press is an imprint of Taylor & Francis Group, an Informa business**.**

[19] Theodoridis S. and Koutroum K., (2010), " **Introduction to Pattern Recogition a Matlab Approach** ",www.elsevier.com/permissions.

[20] Ying Hao,(2000),"Fuzzy Control and Modeling" Anlytical Foundations and Application ISBN 0-7803-34973.

[21] Yang H., Guo J. and Deng F., (2011), " **Collaborative RFID Intrusion Detection with an Artificial Immune System**", J IntellInfSyst 36:1–26,DOI 10.1007/s10844-010-0118-3.